

Regulation of HCV Cell-to-Cell Spread by ADP-ribosylation factor 1-Dependent  
Regulation of Cytosolic Lipid Droplet Homeostasis

by

Abdullah Awadh

A thesis submitted in partial fulfillment of the requirements for the degree of

Doctor of Philosophy

in

Virology

Department of Medical Microbiology and Immunology

University of Alberta

© Abdullah Awadh, 2018

## **ABSTRACT**

Hepatitis C virus (HCV) infects cells via cell-free virions by direct cell-to-cell transmission. Entry of cell-free HCV virions has been fairly well-characterized. Several host factors involved in this process have been identified, including the cell surface receptors, tight junction molecules, and lipid transport proteins. HCV cell-to-cell spread has not been equally characterized, beyond the identification of the involvement of a subset of the host factors involved. The relative importance of infection via cell-free virions or by direct cell-to-cell transmission remained unaddressed. Similarly, whether the release of virions into the extracellular space and the direct cell to cell transmission followed the same pathways or not was unknown.

In collaboration with Dr. Novikov, we identified and characterized the mechanism of action of small molecule derivatives of a substituted uracil. An optimized derivative, Z390, inhibited HCV foci formation with no effect on a panel of related or unrelated viruses. Z390 inhibited HCV cell-to-cell spread without affecting HCV replication, assembly, or release of infectious virions, or susceptibility or permissivity of cells to HCV infection. Z390 altered the intracellular distribution of HCV core and NS5A proteins and the homeostasis of the cellular cytosolic lipid droplets (cLDs). Oleic acid (OA), which has the same effect as Z390 on cLDs homeostasis, also reproduced the effect of Z390 on HCV protein localization and HCV cell-to-cell spread. Knockdown of Arf1 had been shown before to mimic the phenotype of Z390 and OA on HCV proteins and cLDs. Knockdown of Arf1 inhibited HCV cell-to-cell spread, and expression of Arf1 non-cycling mutants mimicked the effects of Z390 on NS5A and core colocalization, on cLDs size and

distribution and on cell-to-cell spread.

Using Z390, we identified a mechanism of direct HCV cell-to-cell spread involving cellular cLDs and Arf1. We propose that regulation of cLD homeostasis by Arf1 cycling determines the preferred pathway of HCV spread, either via the release of cell-free virions or by direct cell-to-cell spread.

## TABLE OF CONTENTS

<b>ABSTRACT .....</b>	<b>ii</b>
<b>LIST OF TABLES.....</b>	<b>vii</b>
<b>LIST OF FIGURES.....</b>	<b>viii</b>
<b>LIST OF ABBREVIATIONS .....</b>	<b>xii</b>
<b>CHAPTER ONE: INTRODUCTION .....</b>	<b>1</b>
1.1 HEPATITIS C VIRUS .....	1
1.1.1 Structure and replication .....	1
1.1.2 Infection and pathogenesis .....	25
1.1.3 Lipid droplets .....	37
1.1.4 Lipid droplets and microbial infections .....	51
1.2 ADP-RIBOSYLATION FACTOR IN HCV LIFE CYCLE AND LIPID DROPLET HOMEOSTASIS .....	60
1.2.1 ADP-ribosylation factors (Arfs).....	60
1.2.2 Arf and microbial infections.....	64
1.2.3 Arf and lipid droplets .....	67
1.3 DIRECT CELL-TO-CELL HCV SPREAD .....	71
1.3.1 Evidence .....	71
1.3.2 Experimental approaches .....	75
1.3.3 Mechanisms.....	78
1.3.4 Roles of cell-to-cell spread.....	80
1.4 Model and hypothesis .....	88
<b>CHAPTER TWO: MATERIALS AND METHODS .....</b>	<b>91</b>
2.1 Materials .....	91
2.1.1 Compounds .....	91
2.1.2 Chemical and general reagents .....	91
2.1.3 Fluorescence microscopy reagents .....	93
2.1.4 Molecular biology reagents .....	93
2.1.5 Antibodies .....	94
2.1.6 Plasmids .....	95
2.1.7 siRNA .....	99
2.1.8 Cell culture reagents.....	99
2.1.9 Cells.....	100
2.1.10 Viruses .....	100
2.2 methods .....	103
2.2.1 Preparation of viral stocks.....	103
2.2.2 Virus titrations.....	105
2.2.3 Transfections .....	106
2.2.4 Plaque formation assay .....	108
2.2.5 Foci formation assay.....	108
2.2.6 Antiviral activity .....	109
2.2.7 Single-step replication assays .....	109
2.2.8 Quantitation of HCV RNA .....	111
2.2.9 Pre-treatment of HCV virions or Huh7.5 cells before infection.....	113
2.2.10 Serum neutralization.....	113

2.2.11 Co-culture assay.....	114
2.2.12 Lipid droplets synthesis stimulation with oleic acid .....	115
2.2.13 Transwell infection .....	115
2.2.14 Serial passaging of HCV infection .....	119
2.2.15 Western blots.....	122
2.2.16 Cytotoxicity .....	122
2.2.17 Immunofluorescence and fluorescence labelling .....	124
<b>CHAPTER THREE: IDENTIFICATION OF A SMALL MOLECULE INHIBITOR OF HCV CELL-TO-CELL SPREAD .....</b>	<b>126</b>
3.1 INTRODUCTION .....	126
3.2 qRESULTS .....	131
3.2.1 1,5-substituted pyrimidines inhibit HCV foci formation .....	131
3.2.2 Optimization of Z390.....	141
3.2.3 Specificity of Z390 against flaviviruses .....	141
3.2.4 Z390 does not inhibit HCV replication.....	145
3.2.5 Z390 does not inhibit HCV virion infectivity, or cell susceptibility or permissiveness to infection.....	149
3.2.6 Z390 inhibits cell-to-cell spread of HCV in co-culture assays .....	154
3.3 DISCUSSION.....	160
3.4 Summary .....	165
<b>CHAPTER FOUR: HCV SPREADS PREFERENTIALLY BY CELL-TO-CELL TRANSMISSION .....</b>	<b>166</b>
4.1 INTRODUCTION .....	166
4.1.1 Spread of viral infections.....	166
4.1.2 Spread of HCV infection .....	168
4.2 RESULTS .....	173
4.2.1 Spread of HCV infection by cell-free or cell-associated infectivity in transwell plates .....	173
4.2.2 Cell-free or cell-associated passaging of HCV infection .....	177
4.3 DISCUSSION.....	181
4.4 Summary .....	187
<b>CHAPTER FIVE: Z390 AFFECTS THE LOCALIZATION OF HCV CORE AND NS5A PROTEINS AND CLD METABOLISM.....</b>	<b>188</b>
5.1 INTRODUCTION .....	188
5.1.1 Cellular distribution of HCV proteins .....	188
5.1.2 Association of HCV core with cLD .....	189
5.1.3 Association of NS5A with cLD .....	194
5.1.4 Role of cLD in HCV.....	197
5.1.5 Role of LDAPs in cLD and HCV.....	199
5.1.6 Role of ADRP in cLD .....	200
5.1.7 Role of ADRP in HCV .....	201
5.1.8 Role of TIP47 in cLD.....	202
5.1.9 Roles of TIP47 in HCV replication .....	204
5.2 RESULTS .....	206
5.2.1 Treatment with Z390 results in HCV core protein more efficient localization to the surface of enlarged cLD.....	206

5.2.2	Z390 redistributes HCV NS5A protein from ER to the surface of enlarged cLD	211
5.2.3	Effect of Z390 on other HCV proteins	212
5.2.4	Z390 treatment induces the formation of mature cLDs	212
5.2.5	The number of small cLD decreases in cells treated with Z390	216
5.2.6	Oleic acid also enriches core on enlarged cLD	219
5.2.7	Oleic acid induces redistribution of HCV NS5A from the ER to the surface of enlarged cLD	224
5.2.8	Oleic acid inhibits cell-to-cell HCV spread	224
5.3	DISCUSSION	230
5.3.1	Z390 effect on HCV core	230
5.3.2	Z390 effect on HCV NS5A	232
5.3.3	Z390 effect on cLD and ADRP	232
5.3.4	Z390 effect on TIP47	234
5.3.5	Effect of oleic acid on HCV core, NS5A, and cLD	235
5.3.6	Effect of oleic acid on HCV cell-to-cell spread	236
5.4	Summary	237
<b>CHAPTER SIX: ARF1 IS REQUIRED FOR CLD METABOLISM AND CELL-TO-CELL HCV SPREAD</b>		<b>239</b>
6.1	INTRODUCTION	239
6.1.1	Role of Arf1 in vesicular trafficking	239
6.1.2	Role of Arf1 in HCV life cycle	241
6.1.3	Role of Arf1 in cLD homeostasis	243
6.2	RESULTS	248
6.2.1	Arf1 knockdown affect core and NS5A association with cLD	248
6.2.2	Knockdown of Arf1 inhibits cell-to-cell spread	251
6.2.3	Arf1 non-cycling mutants enrich core and NS5A around enlarged cLD	256
6.3	DISCUSSION	264
6.3.1	Knockdown of Arf1 redistributed NS5A onto enlarged cLD	264
6.3.2	Knockdown of Arf1 affected cLD homeostasis and core distribution	265
6.3.3	Knockdown of Arf1 inhibit HCV cell-to-cell spread	265
6.4	Summary	271
<b>CHAPTER SEVEN: DISCUSSION AND FUTURE DIRECTIONS</b>		<b>272</b>
7.1	Identification of a small molecule inhibitor of HCV cell-to-cell spread	272
7.2	HCV spreads preferentially by direct cell-to-cell transmission	275
7.3	The role of cLDs homeostasis in cell-to-cell spread	280
7.4	Role of Arf1 in HCV infection and cLDs homeostasis	287
7.5	FUTURE DIRECTIONS	298
7.5.1	Evaluating the role of cLD in HCV virion release and cell-to-cell spread	298
7.5.2	In vitro studies of Arf1 and Z390	301
7.5.3	Evaluating the role of Arf1 in HCV entry	302
<b>REFERENCES</b>		<b>303</b>

## LIST OF TABLES

<b>Table 2.1 List of primary antibodies .....</b>	<b>96</b>
<b>Table 2.2 List of secondary antibodies .....</b>	<b>97</b>
<b>Table 2.3 List of viruses used in the testing for antiviral activity of the initial derivatives of the small molecule scaffold shown in Figure 2.1.....</b>	<b>102</b>
<b>Table 3.2 Chemical structures and anti-HCV activity and cytotoxicity profile of the 1,5-diarylpyrimidines. ....</b>	<b>133</b>

## LIST OF FIGURES

Figure 1.1. A schematic representation of HCV virion.....	4
Figure 1.2. HCV genome, and proteins.....	5
Figure 1.2. A schematic representation of spread of HCV infection.....	11
Figure 1.3 A schematic representation of HCV replication.....	14
Figure 1.4. Proposed mechanism of HCV assembly .....	16
Figure 1.5. Synthesis of cytosolic lipid droplets .....	39
Figure 1.6 A schematic representation of growth and expansion of cLDs. ....	41
Figure 1.8. Exchange of Arf1-GDP and hydrolysis of Arf1-GTP.....	62
Figure 1.8. A schematic presentation of the role of Arf1 on proteins trafficking to and from cLD. ....	70
Figure 1.9. Spread of HCV infection.....	74
Figure 2.1. Small molecule scaffold diaryl-substituted uracil to test for antiviral activity. ....	92
Figure 2.2. Testing the candidate small molecules for antiviral activity.....	110
Figure 2.3. Single-step replication assay for HCV.....	112
Figure 2.4. Co-culture assay.....	116
Figure 2.5. Co-culture assay for oleic acid-treated donor cells.....	117
Figure 2.6. Co-culture assay for Arf1-knocked down donor cells.....	118
Figure 2.7. Spread of HCV infection by cell-free or cell-associated virions.....	120
Figure 2.8. Passaging of HCV cell-associated virions.....	121
Figure 2.9. Passaging of HCV cell-free virions. ....	123



<b>Figure 3.1. Z197 and Z214 inhibit HCV foci formation.</b>	<b>132</b>
<b>Figure 3.2. Z390 inhibits HCV foci formation at non-cytotoxic concentrations. ..</b>	<b>142</b>
<b>Figure 3.3. Z390 inhibits HCV foci formation. ....</b>	<b>143</b>
<b>Figure 3.4. Z390 reduces the number of cells per focus but not that of foci per well.</b>	
<b>.....</b>	<b>144</b>
<b>Figure 3.5. Z390 does not inhibit replication of Zika virus.</b>	<b>146</b>
<b>Figure 3.6. Z390 does not inhibit replication of DV.</b>	<b>147</b>
<b>Figure 3.7. Z390 does not inhibit RSV foci formation.</b>	<b>148</b>
<b>Figure 3.8. Z390 does not inhibit HCV replication. ....</b>	<b>151</b>
<b>Figure 3.9. Z390 does not inhibit HCV replication. ....</b>	<b>152</b>
<b>Figure 3.10. Proposed mechanisms of action of Z390.</b>	<b>153</b>
<b>Figure 3.11. Z390 does not affect virion infectivity or cell permissiveness to infection.</b>	<b>156</b>
<b>Figure 3.12. Anti-HCV neutralizing antibodies inhibit secondary infections but not foci formation.</b>	<b>157</b>
<b>Figure 3.13. Z390 inhibits HCV cell-to-cell spread.</b>	<b>159</b>
<b>Figure 4.1 HCV spreads primarily by cell-to-cell transmission. ....</b>	<b>175</b>
<b>Figure 4.2 Quantitation of HCV, Zika, or RSV spreads on inserts or in wells .....</b>	<b>176</b>
<b>Figure 4.3 HCV spreads primarily by cell-to-cell transmission. ....</b>	<b>179</b>
<b>Figure 4.4 HCV spreads primarily by cell-to-cell transmission .....</b>	<b>180</b>
<b>Figure 5.1 HCVcc-JFH1 core localizes in ring-like structures around enlarged cLD in the presence of Z390.</b>	<b>207</b>

<b>Figure 5.2 Quantitation of Z390 effect on HCV core and cLD in HCV-infected cells.</b>	
.....	208
<b>Figure 5.3 HCV-Jc1 core localizes in ring-like structures around enlarged cLD in the presence of Z390.</b>	
.....	209
<b>Figure 5.4 HCVcc-H77 core localizes in ring-like structures around enlarged cLD in the presence of Z390.</b>	
.....	210
<b>Figure 5.5 HCV NS5A redistributes from the ER to enlarged cLD in the presence of Z390.</b>	
.....	213
<b>Figure 5.6 Quantitation of Z390 effect on HCV NS5A localization in HCV-infected cells.</b>	
.....	214
<b>Figure 5.7 Effect of Z390 on NS3 distribution.</b>	
.....	215
<b>Figure 5.8 Z390 results in more ADRP localized around mature cLD.</b>	
.....	217
<b>Figure 5.9 Quantitation of Z390 effect on the size of cLD).</b>	
.....	218
<b>Figure 5.10 Z390 decreases small nascent cLD.</b>	
.....	220
<b>Figure 5.11 Quantitation of Z390 effect on enrichment of TIP47 at sites of nascent cLD.</b>	
.....	221
<b>Figure 5.12 HCV core associates with enlarged cLD in cell treated with OA. HCV core associates with enlarged cLD in cell treated with OA.</b>	
.....	222
<b>Figure 5.13 Quantitation of OA effect on HCV core and cLD in HCV-infected cells.</b>	
.....	223
<b>Figure 5.14 HCV NS5A associates with enlarged cLD in cell treated with OA. HCV core associates with enlarged cLD in cell treated with OA.</b>	
.....	225

<b>Figure 5.15 Quantitation of OA effect on HCV NS5A and cLD in HCV-infected cells.</b>	226
<b>Figure 5.16 Oleic acid inhibits HCV cell-to-cell spread.</b>	228
<b>Figure 5.17 Quantitation of OA effect HCV cell-to-cell spread.</b>	229
<b>Figure 6.1 Knockdown of Arf1 affects the distribution of HCV core and cLD.</b>	249
<b>Figure 6.2 Quantitation of Arf1 knockdown effect on HCV core and cLD in HCV-infected cells.</b>	250
<b>Figure 6.3 Knockdown of Arf1 affects the distribution of HCV NS5A and cLD.</b>	252
<b>Figure 6.4 Quantitation of Arf1 knockdown effect on HCV NS5A and cLD in HCV-infected cells.</b>	253
<b>Figure 6.5 Knockdown of Arf1 inhibits HCV cell-to-cell spread.</b>	254
<b>Figure 6.6 Quantitation of Arf1 knockdown effect on HCV cell-to-cell spread.</b>	255
<b>Figure 6.7 Knockdown of Arf1 does not inhibit HCV replication in donor cells.</b>	257
<b>Figure 6.8 Experiment design of the effect of Arf1 mutants on the localization of HCV core and NS5A and cLD.</b>	259
<b>Figure 6.9 Expression of non-cycling mutants of Arf1 affects the localization of HCV core and cLD.</b>	260
<b>Figure 6.10 Quantitation of localization of HCV core and cLD in the presence of non-cycling mutants of Arf1.</b>	261
<b>Figure 6.11 Expression of non-cycling mutants of Arf1 affects localization of HCV NS5A and cLD.</b>	262
<b>Figure 6.12 Quantitation of non-cycling mutants of Arf1 affects localization of HCV NS5A and cLD.</b>	263

## LIST OF ABBREVIATIONS

ADRP	Adipocyte differentiation factor
ApoB	Apolipoprotein B
ApoC	Apolipoprotein C
ApoE	Apolipoprotein E
Arf1	ADP-ribosylation factor
ATLG	Adipose triglycerol lipase
BFA	Brefeldin
BIG	Brefeldin A-inhibited guanine nucleotide-exchange factors
CD81	Cluster of differentiation 81
CE	Cholesterol ester
cLD	cytosolic lipid droplet
CLDN	Claudin
DAG	Diacylglycerol
DGAT1	Diacylglycerol O-acyltransferase 1
DGAT2	Diacylglycerol O-acyltransferase 2
DV	Dengue virus
EGFR	Epidermal growth factor receptor
ER	endoplasmic reticulum
ERES	ER exit site
ERGIC	ER Golgi intermediate complex
FAA	Free fatty acid
FH	Fulminant hepatitis
GAG	Glycosaminoglycan
GAP	GTPase activation factor
GBF	Golgi-specific brefeldin A-resistance guanine nucleotide exchange factor
GCA	Golgicide A
GDP	Guanine diphosphate
GEF	Guanine exchange factor
GPAT4	Glycerol-3-phosphate acyltransferase 4
GTP	Guanine triphosphate
HAV	Hepatitis A virus
HBV	Hepatitis B virus
HCV	Hepatitis C virus
JFH	Japanese fulminant hepatitis

HI	Helix I
HII	Helix II
HL	Helix lope
HSL	Hormone sensitive lipase
HSV1-KOS	Herpes simplex virus 1 strain KOS
IAV	Influenza A virus
LDAP	Lipid droplet associated protein
LDL	Low-density lipoprotein
LDLR	Low-density lipoprotein receptor
LVP	Lipoviroparticle
MAG	Monoacylglycerol
OA	Oleic acid
OCLN	Occludin
PV	Polio virus
RC	Replication complex
RSV	respiratory syncytial virus
SAR	Structure-activity relationship
SP	signal peptidase
SPP	signal peptide peptidase
SR-BI	Scavenger receptor BI
TG	Triglycerol
TGN	Trans-Golgi network
TIP47	Tail-interacting protein
VACV	Vaccinia virus
VLDL	Very-low-density lipoprotein
VSV	Vesicular stomatitis virus

## **CHAPTER ONE: INTRODUCTION**

### **1.1 HEPATITIS C VIRUS**

#### **1.1.1 Structure and replication**

##### **1.1.1.1 Brief history of the discovery of HCV**

Hepatitis B virus (HBV) and hepatitis A virus (HAV) were discovered in 1968 (M. E. Bayer, Blumberg, & Werner, 1968) and 1973 (Feinstone, Kapikian, & Purceli, 1973), respectively. As a result of the development of serological tests for HBV and HAV, it became apparent in the following years that most transfusion-related hepatitis cases were not caused by HBV or HAV (Feinstone et al., 1973; Prince et al., 1974). These cases were named non-A, non-B hepatitis (NANBH). The risk of acquiring NANBH from transfusion was as high as 10% (Alter, 1980). NANBH was described as starting as mild hepatitis but mostly turning into a chronic form that extended over many years with poor prognosis and most often resulting in serious liver diseases such cirrhosis (Dienstag & Alter, 1986) or hepatocellular carcinoma (HCC) (Kiyosawa, Akahane, Nagata, & Furuta, 1984).

Conventional methods of virus discovery had failed to isolate or identify the etiological agent of NANBH (Shih, Mur, & Alter, 1986), because of its low titer and poor infectivity in culture. The breakthrough came after seven years of intensive work starting in 1982 and culminating in the public report of the discovery of hepatitis C virus (HCV) in 1989 (Choo et al., 1989). The research team applied molecular cloning for the first time to identify the causative agent of a viral disease. Chimpanzees were infected with human serum. Nucleic acids from infectious chimpanzee plasma were cloned into bacteriophage

expression vectors, generating expression libraries. These libraries were screened against patient sera, eventually leading to the identification of a clone containing a small insert not derived from the chimpanzee genome. The clone hybridized with RNA purified from the plasma of infected chimpanzee or human patients carrying antibodies to the cloned protein. Eventually, PCR sequence identified the NANBH agent as a novel virus related to the flaviviruses, which was called HCV.

#### **1.1.1.2 Virion, genome, and proteins**

Initially, the newly identified virus was classified as *Flavivirus* under the *Flaviviridae* family, based on sequence similarity to members of *Flavivirus* and *Pestivirus*, the two genera comprising the *Flaviviridae* family. Subsequently, HCV was classified as the founding member of the new genus *Hepacivirus* (R. H. Miller & Purcell, 1990). Structurally, the HCV virion displays heterogeneity in size and morphology. The diameter of HCV virions ranges from 30 to 100 nm (Lindenbach et al., 2005; Wakita et al., 2005). Unlike most of the enveloped viruses, HCV virions from patient sera or cell-culture display a broad range of buoyant density (1.03-1.25 g/ml) (Kanto et al., 1994). In contrast, intracellular virions have higher and a narrower range of higher buoyant density, 1.15-1.2 g/ml (Gastaminza, Kapadia, & Chisari, 2006). This difference in biophysical properties of intracellular versus released virions is thought to result from the acquisition of structural components from host cell during egress. Indeed, it was later found that HCV virions isolated from patients or cell culture contain components of lipoproteins. The infectivity of HCV virions inversely correlates with density. Accordingly, only HCV virions with density < 1.10 g/ml transmit infection (Bradley et al., 1991; Carrick, Schlauder, Peterson, & Mushahwar, 1992). Immunoprecipitation studies showed that HCV virions in the higher density fractions were

precipitated by neutralizing sera, whereas virions in the lower density fractions co-eluted with very-low-density lipoproteins (VLDL) (Prince, Huima-Byron, Parker, & Levine, 1996; Thomssen, Bonk, & Thiele, 1993). The association of HCV virions with VLDL is supported by their size similarity, ~30-60 or 30-80 nm for HCV and VLDL, respectively (He et al., 1987). The HCV virion was termed as “lipovirparticle” (LVP) because of the presence of triglyceride (TG), apolipoproteins B (ApoB) and E (ApoE), HCV RNA, and capsid protein (Andre et al., 2002) (**Figure 1.1**). The correlation between the association of HCV virions with lipoproteins and infectivity is further supported by comparing the infectivity profile of HCV from chimpanzee or chimeric humanized liver mice with that of HCV derived from Huh7.5 cell culture. Peak infectivity of Huh7.5-derived HCV is at 1.14 g/ml, compared to <1.10 g/ml for HCV from chimpanzee or chimeric mice. Huh7.5 cells are defective in producing authentic VLDL particles. The specific infectivity, defined as the number of infectious particles per genome copy, is ~1 in 1,000 for virions produced in Huh7.5 cell culture, compared or 1 in 10 for virions recovered from chimpanzee or chimeric mice sera (Lindenbach et al., 2006).

The HCV genome is a 9.6 kb positive-sense single-stranded RNA [(+) ssRNA] that encodes a single polyprotein of 3,000 amino acids (Hijikata, Kato, Ootsuyama, Nakagawa, & Shimotohno, 1991). The polyprotein is proteolytically cleaved by host and viral proteases to produce 10 individual mature proteins (Harada et al., 1991). From the N-terminal end, they are the envelope glycoproteins E1 and E2, nucleocapsid, viroporin p7, the non-structural proteins NS2, NS3, NS4A, NS4B, NS5A, and NS5B (Grakoui, Wychowski, Lin, Feinstone, & Rice, 1993) (**Figure 1.2**).



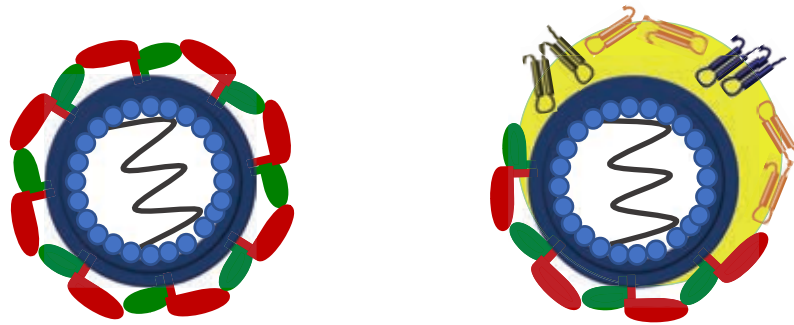
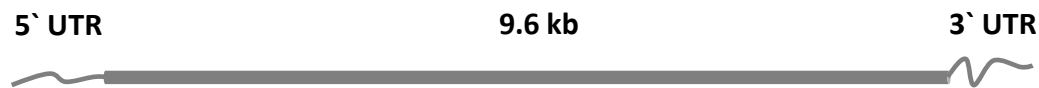


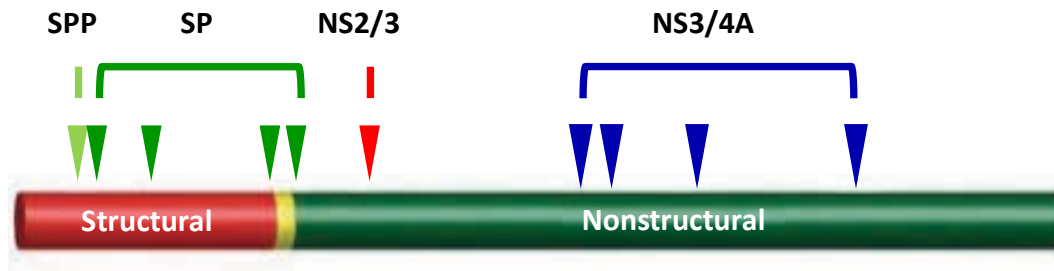
**Figure 1.1. A schematic representation of HCV virion.**

HCV is an enveloped virion containing heterodimers of envelope glycoproteins E1 and E2 enclosing a nucleocapsid of monomer capsid protein and RNA genome. HCV virions display heterogeneity in size, with a diameter between 40 and 100 nm. Smaller (~50 nm) and higher and narrower buoyant density (1.15-1.2 g/ml) virions are the predominant populations recovered from cell lysate while (left). Larger (~80 nm) and lower and broader buoyant density (1.03-1.25 g/ml) are those found in the extracellular environment. (right). The difference in the biophysical characteristics between the two forms of the virions is due the association of the extracellular HCV virions with low-density lipoproteins LDL or VLDL (right).

(A)



(B)



(C)

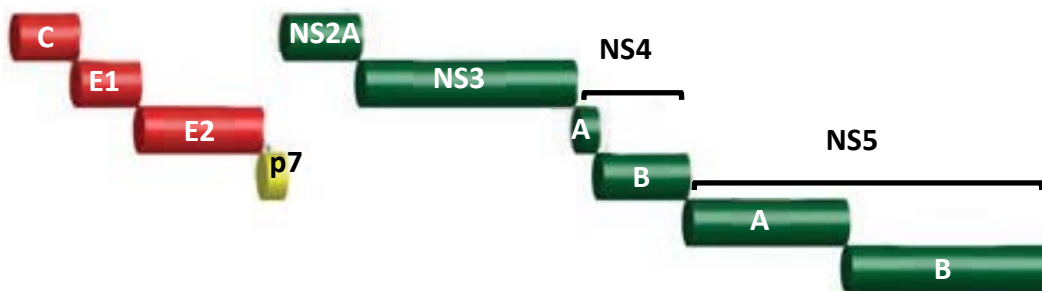


**Figure 1.2. HCV genome, and proteins.**

HCV genome is a ~ 9.6 kb positive-sense single-stranded RNA containing an internal ribosomal entry site (IRES) element in both the 5' and 3'-nontranslated region which recruits host-RNA binding proteins that stimulate translation (A). Translation of HCV RNA produces ~3000 amino acid polyprotein (B) which is cleaved by cellular and viral proteases to produce ten individual proteins. Three structural proteins, capsid and envelope glycoproteins E1 and E2, an ion channel p7, and six non-structural, NS2-NS5B (C).

The capsid protein of HCV is first cleaved from the polyprotein by signal peptidase-dependent processing. Then, a second cleavage by signal peptide peptidase (SPP) produces the mature capsid protein (McLauchlan, Lemberg, Hope, & Martoglio, 2002; Targett-Adams et al., 2006). HCV core includes three domains, based on hydrophobicity, domain I, aa 2-18; domain II, aa 119-174; and domain III, aa 175-191 (Hope & McLauchlan, 2000; Okamoto, Moriishi, Miyamura, & Matsuura, 2004). Domain II contains a helix-loop-helix structure essential for its association with cytosolic lipid droplets (cLDs) (Hope, Murphy, & McLauchlan, 2002). This association is essential for the assembly of progeny virions (Okamoto et al., 2008). Three amino acid residues in domain II, Leu 139, Val140, and Leu144 are required for SPP-dependent cleavage. The envelope glycoproteins E1 and E2 are cleaved from the polyprotein by the signal peptidases (Hijikata et al., 1991). E1 and E2 are type I glycoproteins consisting of ectodomains projecting into the lumen of the endoplasmic reticulum (ER) membrane, or outside the virion, and a C-terminal transmembrane region (Deleersnyder et al., 1997). E1 and E2 form non-covalent heterodimers and are highly glycosylated at 11 sites (Goffard & Dubuisson, 2003). Although the core region of E2 resembles class II fusion protein (Khan et al., 2014; Kong et al., 2013), its role in membrane fusion along with E1 has not been fully defined. Nonetheless, the aa 262-290 region of E1 is known to be required for membrane fusion whereas E2 is required for the initiation of entry (H. F. Li, Huang, Ai, Chuang, & Chen, 2009).

#### **1.1.1.3 Genotypes and evolution**

Phylogenetic analysis of isolates from across the globe demonstrates the extent of genetic diversity in HCV (H. Li et al., 2011; Simmonds, 2004). The variations in HCV

genomes are generated as consequence of the error-prone, non-proofreading RNA-dependent RNA polymerase. The estimated HCV mutation rate is amongst the highest, at  $10^{-4}$  substitutions per site in each round of replication (Lu, Nakano, Orito, Mizokami, & Robertson, 2001; Thimme et al., 2002). The high error rate of the HCV RNA-dependent RNA polymerase and the host selective pressure have driven the virus to diverge into seven genotypes that differ by 31-33% in whole genome nucleotide sequence (Simmonds, 1995). Genotypes 1 to 6 include at least 67 subtypes that differ by at least 15% in nucleic acid sequence (Bukh, Miller, & Purcell, 1995). The genetic diversity is not equally distributed across the HCV genome. For example, the 5'-UTR is highly conserved at 90% sequence similarity across all strains (Bukh, Purcell, & Miller, 1992; Pineiro & Martinez-Salas, 2012). The gene encoding capsid protein comes as the second highest conserved region with 81-88% sequence similarity. The coding region for the envelope glycoproteins E2 hypervariable regions 1 (HVR1), and 2 (HVR2) is the most variable with only 50% sequence similarity (Argentini, Genovese, Dettori, & Rapicetta, 2009; Le Guillou-Guillemette et al., 2007).

The HCV genotypes differ in heterogeneity and geographical distribution. Genetically distant HCV strains are likely to have risen from far apart geographic areas. In contrast, strains that are genetically closer are likely to have been disseminating in confined geographical regions (Messina et al., 2015). Subtypes 1a, 1b, 3a, and to lesser extent 2a, 2b, and 2c are globally distributed (Gower, Estes, Blach, Razavi-Shearer, & Razavi, 2014). Genotypes 1 and 2 are endemic in Central and West Africa (Ruggieri et al., 1996; Stuyver et al., 1993), whereas genotype 3 strains are mostly found in South Asia (Wasitthanasem et al., 2015). The Middle East and Central Africa are dominated

by genotype 4 strains, which were recently found to be widespread in the Mediterranean region (Ramia & Eid-Fares, 2006; Ray, Arthur, Carella, Bukh, & Thomas, 2000). Genotype 5 (particularly 5a) is prevalent in South Africa and Belgium (Al Naamani, Al Sinani, & Deschenes, 2013), while genotype 6 is considered the dominant genotype in China and Southeast Asia (Hollederer et al., 2015; Tokita et al., 1995).

#### **1.1.1.4 Entry**

Like most viruses, HCV uses membrane glycoproteins to enter into the host cell. The unique properties of the HCV virion structure, particularly its association with VLDL (Andre et al., 2002), and the involvement of multiple host factors (Lindenbach & Rice, 2013) have hindered a complete characterization of HCV entry. Many host cells factors which act sequentially or simultaneously, are involved in HCV entry (Li et al., 2016; Miao et al., 2017; Ujino et al., 2015). The entry process is initiated by low-affinity attachment to non-specific cell receptors followed by high-affinity binding to specific cell surface receptors. Through interaction with additional host factors, entry is completed by the fusion of the viral and host membranes.

Although attachment of HCV is mediated by the E1 and E2 glycoproteins, E2 plays the major role. Attachment begins with binding of E2 to the glycosaminoglycan heparan sulfate (HS) (Barth et al., 2003). It is enriched in the space of Disse between the endothelial cells and hepatocytes (Cortes & Rigotti, 2007). In addition to HS, other members of the HS proteoglycans (HSPG) family, syndecan 1 (SDC1) and 4 (SDC4), were recently reported to contribute in the initial attachment (Lefevre, Felmlee, Parnot, Baumert, & Schuster, 2014; Q. Shi, Jiang, & Luo, 2013). The lipoprotein components of the HCV virion include ApoE, ApoB, ApoA1, and ApoCII (Merz et al., 2011; Ujino et al.,

2016). Of them, ApoE contains an HSPG-binding domain that attaches to negatively charged sulfated disaccharides. This binding may facilitate the attachment of HCV to HS (Jiang, Wu, Tang, & Luo, 2013). HCV virions circulate as LVP in association with VLDL. The low-density lipoprotein receptor (LDL-R) is involved in HCV attachment through binding to ApoE (Petit et al., 2007; Syed et al., 2014). However, the requirement for LDL-R might vary between different genotypes (Bridge et al., 2015). Although scavenger receptor class B member 1 (SR-B1) was identified as an HCV receptor (Scarselli et al., 2002) that can bind directly to E2, its role in HCV entry is limited to the initial attachment (Bartosch et al., 2003; Dreux et al., 2009). SR-B1 was thought to participate in HCV attachment through binding to the lipoprotein associated with the HCV particle. Supporting this notion, attachment of HCV to SR-B1 was not inhibited by anti-HCV E2 antibodies but it was by saturating level of ApoE, LDL, or VLDL (Voisset et al., 2005; von Hahn et al., 2006).

Spread of HCV infection in hepatocytes proceeds by entry of cell-free virions or direct cell-to-cell transmission. The two processes reportedly employ the HCV envelope glycoproteins E1 and E2 and several host factors, including the tetraspanin CD81 (Pileri et al., 1998), SR-B1, claudin-1 (CLDN) (Evans et al., 2007), occludin (OCLN) (Ploss et al., 2009), and epidermal growth factor receptor (EGFR) (Lupberger et al., 2011). In comparison to the early steps of HCV entry, the late steps, including fusion, remain poorly characterized (Meertens, Bertaux, & Dragic, 2006). The HCV envelope glycoproteins E1 and E2 interact with specific cellular receptors leading to the internalization of HCV particle via clathrin-mediated endocytosis (Bertaux & Dragic, 2006; Blanchard et al., 2006; Farquhar et al., 2012; Tan et al., 2003). Endocytosed vesicles containing HCV are

is transported to the early endosome (Meertens et al., 2006). Exposure of HCV E1 and E2 to the low pH of the endosome triggers conformational changes in the glycoproteins, leading to fusion (Op De Beeck et al., 2004; Sharma, 2011). It is not clear yet which glycoprotein is mainly responsible for fusion and both appear to participate in it. Based on its crystal structure E2 was thought not likely to function as the fusion protein (Krey et al., 2010; Yagnik et al., 2000). However, the crystallized structure lacks the ectodomain that could contain the fusion peptide (El Omari et al., 2014; Khan et al., 2014; Kong et al., 2013). The fusion process may in fact involve E1/E2 heterodimer.

In addition to entry of cell-free virions, HCV infection also spreads by direct transmission between adjacent cells, which is referred to as cell-to-cell spread. It was proposed that HCV persistence in human liver is facilitated by cell-to-cell spread (Agnello, Abel, Knight, & Muchmore, 1998; Chang et al., 2003; Gosalvez et al., 1998). Cell-to-cell transmission appears to be relevant for HCV spread in the infected liver. Sera from HCV infected individuals neutralize HCV infectivity of in vitro and in vivo (de Jong et al., 2014; Giang et al., 2012; Law et al., 2008). Neutralizing sera inhibit cell-free infectivity of HCV virions but not the spread of infection between adjacent cells (de Jong et al., 2014; Edwards, Tarr, Urbanowicz, & Ball, 2012; Sabo et al., 2011) (**Figure 1.3**).

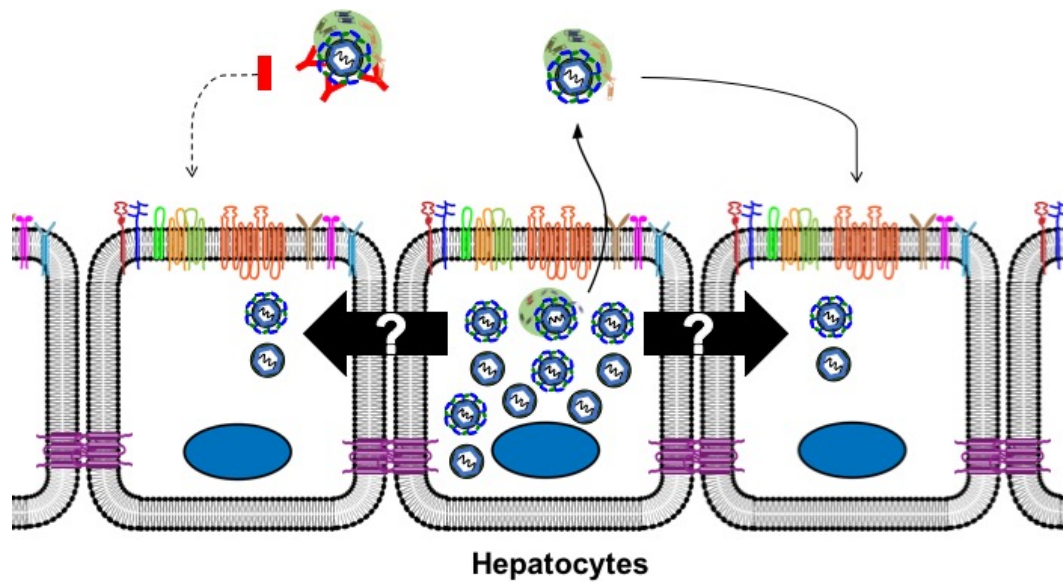


**Figure 1.3. A schematic representation of spread of HCV infection.**

It is proposed that progeny virions released from infected cells spread the infection by cell-free entry route of transmission (virion infecting the cell at the right). Anti-HCV neutralizing antibodies in the sera of HCV-infected individuals or post-immune of recombinant E1E2 blocks infectivity of cell-free virions (virion infecting the cell at the left). Inhibition of infectivity of cell-free virions does not inhibit the spread of infection. Consequently, it was proposed that HCV could also spread by direct cell-to-cell route of transmission.



#### **1.1.1.5 Translation and replication**

The HCV RNA genome consists of a single open reading frame (ORF) that encode for a polyprotein of 3,000 amino acids (V. Lohmann et al., 1999). The ORF is flanked by UTRs at the 5' and 3' ends which are critical for translation initiation and replication of HCV RNA (Kolykhalov, Feinstone, & Rice, 1996; Song et al., 2006). The stem loops I and II within the 5'-UTR contribute to genome replication (Qi et al., 2003). The 5'-UTR sequence, and secondary structures within the core coding region, that are required for HCV genome replication (Friebe, Lohmann, Krieger, & Bartenschlager, 2001; Luo, Xin, & Cai, 2003). Cap-independent initiation of translation of the HCV RNA genome is facilitated stem loops II-IV. These loops comprise the internal ribosome entry site (IRES) (Jubin et al., 2000; Otto & Puglisi, 2004). Several regions within the 3'-UTR, along with two other cis-acting replicative elements at the NS5B coding sequence are required for replication (Romero-Lopez & Berzal-Herranz, 2009) (Yi & Lemon, 2003). The ER resident signal peptidase and the signal peptide peptidase facilitate proteolytic cleavage of the structural proteins, core, E1, E2, and p7 from the remaining non-structural proteins (Hussy, Langen, Mous, & Jacobsen, 1996; Okamoto et al., 2004; Suzuki et al., 1996). NS3 proteolytic activity then mediates the cleavage between NS3, NS4A, and NS4B. NS4A forms a complex with NS3 that cleaves between NS4B and 5A and between NS5A and 5B (Bartenschlager, Ahlborn-Laake, Mous, & Jacobsen, 1994; Grakoui et al., 1993).

RNA synthesis begins by the generation of negative sense strands from the positive HCV genomic RNA. The negative strands in turn function as a template for the synthesis of nascent positive RNA strands (Binder et al., 2007; Iacovacci et al., 1997; Mora et al., 2010). The newly synthesized positive sense RNA is translated to produce

more viral proteins or used as a template to synthesize negative sense RNA. At certain stage, The genomic RNA associate with the nucleocapsid protein for packaging into progeny virions (Bartenschlager, Kaul, & Sparacio, 2003; Iacovacci et al., 1997; Lindenbach & Rice, 2005; V. Lohmann, Hoffmann, Herian, Penin, & Bartenschlager, 2003; Moradpour, Penin, & Rice, 2007). Replication of HCV induces massive rearrangement of the ER membrane creating what is known as “membranous web” (Aizaki, Lee, Sung, Ishiko, & Lai, 2004; Gosert et al., 2003; Quinkert, Bartenschlager, & Lohmann, 2005). Initially, the membranous web is primarily composed of double membranous vesicles (DMV) which coincide with the peak of RNA synthesis (Blanchard & Roingeard, 2015; Ferraris, Blanchard, & Roingeard, 2010). Later, the DMVs extend into tubular structure coupled with the appearance of multi membrane vesicles (MMV) (D. Paul, Hoppe, Saher, Krijnse-Locker, & Bartenschlager, 2013; Romero-Brey et al., 2012). While individual expression of non-structural proteins NS3/4A, NS4B, NS5A, and NS5B could induce remodeling of the ER membrane, DMVs form only when NS5A is expressed (Romero-Brey et al., 2015). Initiation of the membrane remodeling of ER requires the expression of NS4B (Aligo, Jia, Manna, & Konan, 2009; Egger et al., 2002; D. Paul et al., 2011). However, the formation of various forms of HCV-induced vesicular structures requires the expression of all non-structural proteins, suggesting that unique interaction of each protein with host factors collectively mediate the extensive remodeling of ER membrane. These viral-induced membranous structures are thought to generate sites for optimal genome replication (Blight, 2011; D. Paul et al., 2011). In fact, the induction of unique membraneous structures is a common feature of all (+) ssRNA viruses (Miller & Krijnse-Locker, 2008; Romero-Brey & Bartenschlager, 2014) (**Figure 1.4**).

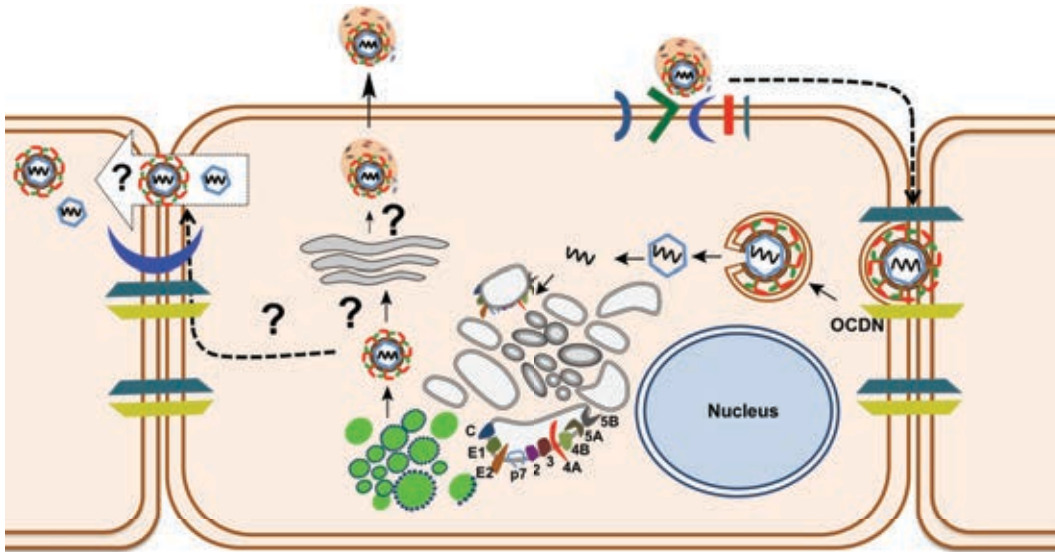


**Figure 1.4 A schematic representation of HCV replication.**

HCV enters hepatocyte by binding to several host cell factors including surface receptors such as CD81, SR-BI, and EGRF, and tight junction molecules such as CLDN1 and OCLN leading to the internalization via clathrin-mediated endocytosis. Viral and cellular membranes fuse leading to the release of the nucleocapsid which uncoats to release the RNA genome into the cytoplasm. The (+) SS-RNA genome is translated into a polyprotein precursor which attaches to the ER membrane. The polyprotein precursor is proteolytically cleaved to produce three structural proteins, the capsid, and the envelope glycoproteins E1 and E2 which form the virion, and six non-structural proteins, NS2-NS5B which replicate the virus. E1 and E2 remained attached to the ER, mature capsid associates with cytosolic lipid droplets (cLD) (dark blue dots surrounding bright green round structures), and the non-structural proteins localize to the replication complexes (irregularly-shaped, ER-derived membranous structures). Capsid, NS5A, E1, and E2 are the minimal requirement for virion assembly. It is thought that assembled virions are released to the extracellular environment via the secretory pathway. Question marks indicate that lack of direct evidence in the respective steps of assembly, release, or the proposed direct cell-to-cell transmission.

#### 1.1.1.6 Assembly and egress

Formation of HCV progeny virions requires the localization of the structural components of the virion, the nucleocapsid protein and the envelope glycoproteins E1 and E2 near the sites of RNA replication. As other members of the family Flaviviridae, assembly of progeny virions of HCV requires the participation of most of the non-structural proteins, too (Apte-Sengupta, Sirohi, & Kuhn, 2014; Murray, Jones, & Rice, 2008). Assembly of HCV virions is tightly regulated to cLDs (Gastaminza et al., 2008; D. M. Jones & McLauchlan, 2010; David Paul, Madan, & Bartenschlager, 2014; Shavinskaya, Boulant, Penin, McLauchlan, & Bartenschlager, 2007). The release of virions from infected cells is the least characterized step of HCV replication cycle. HCV virions components at stages of budding, assembly, or egress was proven difficult to detect (Badia-Martinez et al., 2012; Prince et al., 1996). However, the acquisition of various apolipoprotein components suggested that HCV egresses through the ER-to-Golgi secretory pathway (Syed, Khan, Yang, & Siddiqui, 2017; Triyatni, Berger, & Saunier, 2016). Trafficking through the secretory pathway gives HCV virions the low buoyant density through the acquisition of lipids primarily in the form of cholesterol ester (CE) (Merz et al., 2011). The source of lipids in HCV virions is from the VLDL or LDL particles (Bassendine et al., 2011). Finally, envelope glycoproteins are glycosylated by complex glycans at Golgi before trafficking through the endosomal pathway (Goffard & Dubuisson, 2003; Iacob, Perdivara, Przybylski, & Tomer, 2008) (**Figure 1.5**).

HCV core protein interacts with HCV genomic RNA to form the nucleocapsid at sites of replication complexes (Mamiya & Worman, 1999; Shimoike, Mimori, Tani, Matsuura, & Miyamura, 1999). Proteolytic cleavages of core protein by SP and SPP at

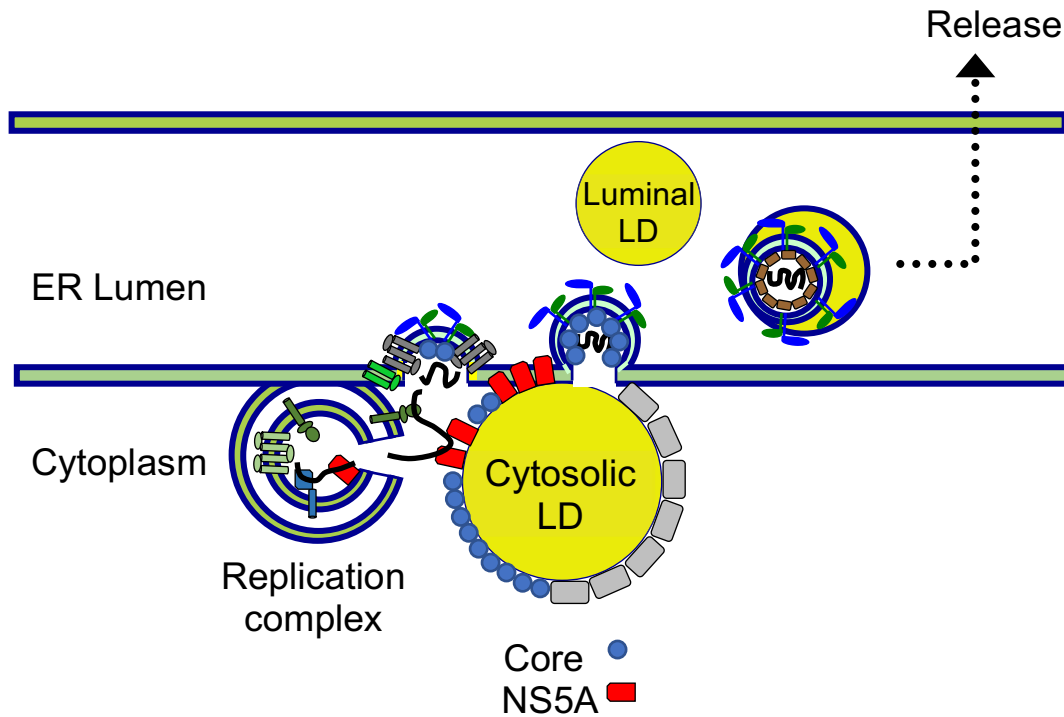


### Figure 1.5. Proposed mechanism of HCV assembly

Assembly of HCV virions requires retrieval of RNA genome from the replication complexes and capsid from the cLDs into ER-embedded E1E2 heterodimers. This step is facilitated by an interaction of capsid, NS5A, and RNA molecules. It is thought that assembled virions bud into the ER lumen where they interact and associate with luminal lipid droplets in the form of low-density and very low-density lipoproteins (LDL and VLDL). The lipoviral particles (LPVs) traffic through the ER-to-Golgi secretory pathway to egress the infected cells. Direct evidence is lacking; the mechanism was proposed primarily based on the association of HCV virions with lipoproteins.

ER, first from the polyprotein, then within itself, produces the mature 21 kD protein which homodimerizes and associates with cLDs (Hope & McLauchlan, 2000; Hope et al., 2002; McLauchlan et al., 2002). The association of core with cLDs is mediated via its cLD-binding domain which consists of two amphipathic helices at the C-terminus (Boulant et al., 2006). The association of core to cLDs is critical for the assembly, mutations in the cLD-binding domain that inhibit the association of core to cLDs abolish assembly (Boulant, Targett-Adams, & McLauchlan, 2007; Miyanari et al., 2007; Shavinskaya et al., 2007). Accumulation of HCV core protein on cLDs induces upregulation of lipogenesis demonstrated by an increase in the cellular content of lipids such as the number and size of cLDs (Clement et al., 2011; Harris, Herker, Farese, & Ott, 2011; Yamaguchi et al., 2005). The increase in cellular contents of cLDs could enhance the platforms for HCV assembly by increasing the surface area available for core association. Transient accumulation of HCV core protein on cLDs is a prerequisite for efficient assembly of progeny virions and does not appear to be regulated by the rate of assembly (Counihan, Rawlinson, & Lindenbach, 2011). Thus, a defect in assembly would result in further accumulation of core on the surface of cLDs. For example, HCV p7 mutants (Gentzsch et al., 2013) and D88 variants (Noppornpanth et al., 2007) are defective in assembly; they showed intensified accumulation of core protein on enlarged cLDs.

HCV envelope glycoproteins, E1 and E2, are critical for the formation of progeny virus. E1 and E2 are associated with ER membrane as heterodimer by covalent interaction via disulfide bridges (Choukhi, Ung, Wychowski, & Dubuisson, 1998; Deleersnyder et al., 1997; Dubuisson & Rice, 1996). Core and E1E2 glycoproteins are not localized in proximity to initiate assembly of progeny virions. Therefore, since core

proteins are stationed on cLDs, it was suggested that E1E2 translocate to core-decorated cLDs by trafficking on ER membrane. In fact, an interaction involving NS2, p7, and E1E2 is required for the translocation of E1E2 to the site of assembly near the core and cLD (C. T. Jones, Murray, Eastman, Tassello, & Rice, 2007; Stapleford & Lindenbach, 2011).

A critical step in virion assembly is mediated by the interaction of NS5A C-terminal domain with cLD-embedded core protein (Galli et al., 2013; Gawlik et al., 2014; Masaki et al., 2008). NS3 interacts with core protein through its helicase domain, and this interaction is involved in assembly of HCV virions (D. M. Jones, Atoom, Zhang, Kottlil, & Russell, 2011). Assembly of HCV virion has also been shown to involve an interaction between the C-terminus of NS4A and core protein (Pietschmann et al., 2009). Mutation in either the NS3 helicase or the C-terminus of NS4A results in defective assembly (Mousseau, Kota, Takahashi, Frick, & Strosberg, 2011). Moreover, recent data implicated an uncharacterized role for NS4B and NS5B in virion assembly (Aligeti, Roder, & Horner, 2015; Blight, 2011; Han, Manna, Belton, Cole, & Konan, 2013).

Several host factors interact with the core to facilitate virion assembly. Diacylglycerol acyltransferase-1 (DGAT1), an enzyme essential for the formation of cLDs is also required for efficient particle assembly by interacting directly with HCV core to mediate core association with cLDs (Herker et al., 2010). Accordingly, knockdown of DGAT1 inhibits core association with cLDs and leading to a reduction in virion assembly (Lange & Zeuzem, 2011). DGAT1 along with the Rab18, small GTPase with multiple roles in membrane traffic, is involved in the recruitment of NS5A to cLD-bound core protein (Camus et al., 2013; Salloum, Wang, Ferguson, Parton, & Tai, 2013). At the level of gene regulation, HCV infection activates transcription factor sterol regulatory element binding

proteins (SREBPs) through the transcription coactivator CBP/p300 (Kim et al., 2007; Li, Pene, Krishnamurthy, Cha, & Liang, 2013). Activation of SREBP-mediated gene transcription induces lipogenesis which in turn enhance the formation of cLDs (Douglas, Esmaili, & George, 2014). Mature core on cLDs is the source of the nucleocapsid of the progeny virions (Ait-Goughoulte et al., 2006). Therefore, the formation of progeny virions requires the retrieval of the core from cLDs into assembling virions near ER-embedded glycoproteins E1 and E2 on one side and the replication complex harboring genomic RNA molecules on the other side. HCV core protein contains a conserved tyrosine-based YXXØ targeting motif that is required for retrieval of core protein from cLDs (Boulant et al., 2006; Neveu et al., 2012).

Biogenesis of HCV virion is tightly linked to assembly and maturation pathway of VLDL (Huang et al., 2007). Inhibitors targeting host factors involved in the VLDL synthesis greatly block the formation of HCV virions (Bassendine et al., 2011). Examples include the microsomal triglyceride transfer protein (MTP) (Jones & McLauchlan, 2010) and the long chain acyl-CoA synthetase 3 (ACSL3) (Yao et al., 2008). Despite that HCV virion contains several species of apolipoproteins such as ApoB, ApoA1, and ApoCII, II, and III, ApoE appears to be the most essential for the production of infectious HCV virions (Yang et al., 2016). This is because ectopic expression of the only ApoE in non-hepatic cells rescued the infectivity of HCV virions (Hueging et al., 2014).

Besides VLDL biogenesis and maturation pathway, the endosomal-sorting complex required for transport (ESCRT) which is a complex of cytosolic proteins involved in membrane remodeling for budding of vesicles, also contributes to the assembly of HCV virion (Ariumi et al., 2011; Corless, Crump, Griffin, & Harris, 2010). Although several



enveloped viruses use this pathway for budding and egress, the role of ESCRT in HCV assembly and budding is not completely understood. Nevertheless, infectious HCV virions have been shown to egress in exosomes which are mediated by ESCRT (Bukong, Momen-Heravi, Kodys, Bala, & Szabo, 2014). Hence, ESCRT could cooperate with VLDL assembly and egress pathway or provide an alternative pathway for HCV release from infected cells.

#### **1.1.1.7 Experimental systems to study HCV**

Interferon (IFN)-based regimens have been the treatment of chronic HCV infection for the past two decades, and its introduction was a major step in the milestone of drug development for the treatment of chronic HCV infections (Chevaliez & Pawlotsky, 2009; Hayashi & Takehara, 2006). However, IFN-based regimens are not specific and were associated with serious side effects and a success rate of less than 50% (Flisiak, Jaroszewicz, & Parfieniuk-Kowerda, 2013). The first breakthrough in the treatment of chronic HCV infections was the approval of the first direct acting antivirals (DAAs) in 2011, the NS3/4A protease inhibitors telaprevir and boceprevir (Chevaliez, 2011; Fontaine & Pol, 2011; Ilyas & Vierling, 2011). Soon after, further DAAs against NS5A (Belema et al., 2014) or NS5B (Asselah, 2014) have been developed and approved in combination with other DAAs or on their own. This progress in the development of HCV DAAs has improved the success rate of treatment of chronic HCV infection to as high as 90% (Falade-Nwulia et al., 2017). This remarkable improvement in the treatment of chronic HCV infections has resulted from intensive research spanning over twenty years, which led to the development of several in vitro and in vivo experimental systems to study HCV infection (Catanese & Dorner, 2015; V. Lohmann & Bartenschlager, 2014). These systems were

not only crucial for the development of DAAs but also were instrumental in understanding HCV-host interactions for the characterization of the immune response, pathogenesis, and resistance to DAAs. Several examples of the widely-used models are described.

Since the discovery of HCV in 1989, it took nearly seven years for the first model to be developed in the form of an infectious clone. Despite the fact that it was a remarkable progress in the development of HCV experimental system, the clones that were infectious in chimpanzee failed to produce viral particles in cell culture (Kolykhalov et al., 1997; Yanagi, Purcell, Emerson, & Bukh, 1997). Subsequently, the first model of HCV replication was developed in the form of a subgenomic replicon containing the minimal set of HCV proteins required for replication in cell culture. The indispensable part of the HCV clone for replication encodes the non-structural HCV proteins, NS3/4A, NS4B, NS5A, and NS5B. The clone is a bicistronic RNA construct that has an antibiotic resistance gene under the control of HCV internal ribosomal entry site (IRES), and the HCV proteins are under the control of encephalomyocarditis virus (EMCV) IRES. The construct is transcribed in vitro and then transfected into Huh-7 cells, and then a cell line stably replicating HCV is selected by the emergence of the antibiotic resistance cell line clones. Like the first clone developed, no virus particles were produced from the stably transfected cell line clones (V. Lohmann et al., 1999).

The second recognizable step in the development of HCV in vitro experimental models was the improvement of HCV replicon systems by the selection of replicon variant containing culture adaptive mutations (Abe, Ikeda, Dansako, Naka, & Kato, 2007; Bartenschlager, Penin, Lohmann, & Andre, 2011; Blight, Kolykhalov, & Rice, 2000). These mutations were scattered along the region encoding the HCV proteins NS3 to 5B

but could cluster in certain areas within each protein coding sequence (Krieger, Lohmann, & Bartenschlager, 2001; Welker et al., 2012). The identified adaptive mutations resulted in an increase of HCV replication by several orders of magnitude. Combination of certain mutations leads to synergistic increases in HCV replication. (Ikeda, Yi, Li, & Lemon, 2002; Targett-Adams & McLauchlan, 2005). The increase in HCV replication differs greatly between mutations. For example, mutations within NS5A (Shimakami et al., 2004) and NS4B (Welker et al., 2012) enhance HCV replication stronger than mutations in NS3 (Liefhebber, Hensbergen, Deelder, Spaan, & van Leeuwen, 2010). The mechanisms whereby the compensatory mutations enhance HCV replication remains unknown. However, mutations that affect the phosphorylation degree of NS5A which exist as basal or hyperphosphorylated correlated inversely with HCV replication.

Apart from enhancing HCV replication through cell culture adaptive mutations, further improvement was achieved by identifying more permissive cell lines. Cells which supported higher replication of HCV from the transfection pool were selected then the replicons within these cells were removed by treatment with interferon or with HCV DAAs after becoming available. The cured cells supported a higher level of HCV replication through higher or lower level of expression of supporting or restricting host factors, respectively (Blight, McKeating, & Rice, 2002; Sumpter et al., 2005). The establishment of HCV replicon systems has provided the foundation for further developments that have ensued and resulted in more efficient systems. For example, the insertion of cell culture adapted mutations into none or very low replication isolates such as Con1 (genotype 1b) or H77 (genotype 1a) allowed for efficient replication (Blight, McKeating, Marcotrigiano, & Rice, 2003).

Another important phase in the development of in vitro HCV experimental models was the discovery of an isolate that replicates in cell lines without acquisition of cell culture adaptive mutations. The isolate was cloned from the serum of a Japanese patient presented with acute fulminant hepatitis, and hence it was designated JFH1. This clone not only replicates to a very high level compared to all the replicons developed before, but is also capable of replication in otherwise non-permissive cell lines such as HepG2, HeLa, and 293T cells (Lindenbach et al., 2005; Wakita et al., 2005; J. Zhong et al., 2005). Other than the faster kinetic of HCV RNA synthesis (Binder et al., 2007; Koutsoudakis et al., 2006), the mechanism responsible for the exceptionally high replication of JFH1 has not been entirely elucidated. However, the HCV polymerase NS5B appears to have a different conformational structure which allows for faster kinetic of HCV RNA replication (Schmitt et al., 2011; Simister et al., 2009). The introduction of JFH1 has enabled the generation of chimeras of other genotypes. They are based on the genome region encoding the replicase proteins of JFH1 including the NS3, NS5B, and 3'-UTR and the genome region structural proteins of the non-replicating isolates (Bartenschlager & Sparacio, 2007) (Gottwein et al., 2009). The addition of JFH1 to the existing replicon systems broadened the range of the cell lines that can be used to support efficient replication. Besides, several chimeras were developed to contain luciferase reporter genes which allow for high throughput analyses such as screening for antiviral compounds (Pietschmann et al., 2006). Live-cell imaging of HCV replication has been possible by the insertion of GFP in NS5A without affecting replication (Moradpour, Evans, et al., 2004). Similarly, fluorescent labeling of HCV core protein for live-cell imaging was possible by insertion of small tetra-cysteine peptide tag at the N-terminus of the core of

HCV-Jc1 (a chimera of genotype 2a isolates, JFH1 and Jc6) clone with minimal effects on the production of infectious particles compared to the untagged-Jc1 core. Labeling of the core is mediated by tetra-cysteine-based protein detection using the reagents FIAsh (green) or ReAsH (red) which are added just before the imaging of the infection (Counihan et al., 2011).

The discovery of the in vitro subgenomic replicons and the full-cycle replicating JFH1 isolate provided critical tools for the discovery and development of anti-HCV drugs. However, primary HCV isolates replicate inefficiently in cell culture, and on the other hand, primary hepatocytes do not support robust replication. Genetic manipulation of mouse either via knockdown of factors that restrict productive HCV infection or complementation with human factors required for HCV replication has been used to generate a mouse model for HCV infection. For example, transient expression of the human HCV entry receptors CD81 and OCLN by adenoviruses allowed entry of HCVcc-JFH1 into mouse hepatocytes (Dorner & Ploss, 2011). Therefore, providing a model to test entry inhibitors or vaccine candidates (Giang et al., 2012). Further development of this approach, which was to the generation of mice transgenic for multiple HCV entry factors and deficient in several innate immunity signaling pathways, allowed low-level replication and production of infectious virions in the serum (L. Chen, Zhao, Yang, Gao, & Cheng, 2014; Dorner, Rice, & Ploss, 2013).

The development of the mouse with human liver is a considerable step in the advancement of experimental models for HCV infection. The so called chimeric mice with humanized liver are generated by infusion of primary human hepatocytes into an injured liver of immunodeficient mouse. Due to their high regenerative capacity, the xenografted

human hepatocytes could repopulate the entire of the mouse liver (Mercer et al., 2001). This model allows productive infection of both primary or cell culture derived HCV isolates, and therefore, provided a tool to characterize the HCV life cycle, the assessment of passive immunization strategies (Law et al., 2008; Meuleman et al., 2011), and testing antiviral agents (Yang & Huang, 2010).

Since this model is immunodeficient, the immune response aspects of HCV infection are not possible to characterize. Thus, immunocompetent human liver chimeric mouse models were later generated by intrahepatic engraftment of human hepatoblasts (hepatocyte progenitor cells) and CD34 hematopoietic stem cells (HSCs) from a single fetal donor. Upon challenge with HCV, the mice could produce human anti-HCV T cell response and develop liver fibrosis. Despite the presence of HCV RNA in the mice liver, viremia was not detected (Gutti et al., 2014; Levin et al., 2014; Washburn et al., 2011).

### **1.1.2 Infection and pathogenesis**

#### **1.1.2.1 Anatomy of the liver**

The liver is a roughly triangular organ that extends horizontally throughout the abdominal cavity from the right side and it descends toward the left end. It is composed of two large lobes, right and left, and two small “accessory” lobes, caudate and quadrate. It contains approximately  $1 \times 10^5$  functional anatomical units, the acini. Acini are individually vascularized and separated by a connective tissue. The acinus is a hexagonal unit consisting of a central vein and six peripheral portal triads, which contain the portal arterioles and venules and the bile ductules. The portal blood vessels open into sinusoids, structures that resembles leaky capillaries. The sinusoids are lined by two types of cells, the fenestrated endothelial cells through which the exchange between the hepatocytes

and blood is mediated through the space of Disse, and the phagocytic Kupffer cells, resident liver macrophages which engulf pathogens and damaged cells. Hepatocytes are the parenchymal cells, occupying 70-85% of the liver volume. They are cuboidal epithelial cells arranged in cords one or two cells thick separated by the sinusoids. The basolateral surface of cell membrane of the hepatocyte faces the sinusoid, has and the apical surface faces the biliary canaliculi.

Blood enters the liver sinusoids from the small branches of the hepatic portal vein and hepatic artery. As blood flows through the liver sinusoids, hepatocytes adjacent to them regulate solute and nutrient levels and absorb or secrete molecules such as plasma proteins. The central veins collect the blood from the sinusoids of the acini and ultimately merge into the hepatic veins, which empty into the inferior vena cava. The bile canaliculi merge to form bile ductules, carrying bile to the bile ducts in the nearest portal area. Bile plays an important role in the digestion of fats in the small intestine.

#### **1.1.2.2 Natural course of infection**

HCV infection represents a global health burden on 71 million people. If untreated, HCV infection often leads to serious hepatic diseases such as liver cirrhosis, which consequently increase the risk of HCC. HCV is a blood-borne virus transmitted through contacts with contaminated blood, mostly by transfusion before the implementation of the screening tests for transfusion products in 1992 (Koerner, Cardoso, Dengler, Kerowgan, & Kubanek, 1998). Other important routes of infection are intravenous drug use and accidents at health care places (Hansurabhanon et al., 2002) (Danielsson et al., 2014) (Henderson, 2003) (Yazdanpanah et al., 2005). Although sexual transmission is

considered rare, there has been a noticeable increase in the cases of acute HCV infections among men who have sex with men (van de Laar et al., 2007).

Although the incubation period of HCV infection significantly varies, HCV RNA could be generally detected in the sera of infected individuals approximately one to three weeks after infection (Chevaliez, 2011; Hajarizadeh et al., 2014). The incubation period is followed by a rapid increase in the HCV RNA, and liver injury manifested by an increase in alanine aminotransferase (ALT) and bilirubin could ensue. However, most of the acute phase of HCV infections remain asymptomatic, which contributes to the difficulties in early diagnosis. Besides jaundice, over 80% of patients present with non-specific symptoms during the acute HCV infection (Maasoumy & Wedemeyer, 2012; Tillmann & Thursz, 2007; Westbrook & Dusheiko, 2014). Although it occurs only rarely, the development of acute HCV infection into what is so called “fulminant hepatitis” represents a most serious complication (Farci et al., 1996; Younis et al., 2015).

Acute HCV infection could resolve spontaneously. However, 50 to 85% of infected individuals progress to the chronic phase of the infection, defined as detection of HCV RNA in serum after six months of acquiring the infection (Kwon, Ray, & Ray, 2014). Despite the identification of several correlates, the precise mechanisms for the spontaneous clearance of acute HCV infection, as opposed to the progression into the chronic phase, have not been determined (Missiha, Ostrowski, & Heathcote, 2008; Rueger et al., 2015). Gender is among prominent correlation observed. Twice as many women as men clear the infection in the acute phase. The higher estrogen level in women could account for the difference, as premenopausal women respond to interferon/ribavirin therapy better than post-menopausal women do (Narciso-Schiavon et al., 2010; Paladino



et al., 2006; Rigamonti et al., 2005). Despite experiencing symptoms of acute HCV infection, individuals who mount robust T cell responses have better chances to clear the acute infection than asymptomatic ones (E. C. Shin et al., 2008). Several single-nucleotide polymorphisms (SNPs) have been found in association studies to play a role in the clearance of acute HCV infections. The first locus identified was near the interleukin 28B (IL28B) gene region, rs12979860 CC on chromosome 19. This locus encodes for interferon-lambda-3, but a subsequent study could not reproduce the association (Kaczor, Seczynska, Szczeklik, & Sanak, 2015). Soon after, SNP rs8099917 TT has been shown to have the strongest association with spontaneous clearance of acute HCV infection (Grebely et al., 2010; Melis et al., 2011).

Individuals who fail to clear the acute HCV infection spontaneously progress to develop chronic HCV infection, a long-term persistent infection that leads to severe liver damage (Yamane, McGivern, Masaki, & Lemon, 2013). Chronic HCV may also cause several extrahepatic manifestations (EHM) (Cacoub, Commarmond, Sadoun, & Desbois, 2017; Sherman & Sherman, 2015). More than 50% of chronic HCV patients present with one or more EHM (Galossi, Guarisco, Bellis, & Puoti, 2007). Twenty to 50% of chronic HCV infection patients present with mixed cryoglobulinemia (MC), which is characterized by the presence of cryoglobulins in the blood (Abrahamian et al., 2000). Cryoglobulins are immunoglobulins that precipitate below 37°C. Cryoglobulinemia is classified into three types based on the composition of immunoglobulins. Type I are composed of monoclonal immunoglobulin (mostly IgM). Type II and III are composed of polyclonal and monoclonal components and hence “mixed.” HCV infections are associated with 60-95% of the cases of type II and III cryoglobulinemia. Most patients might not experience symptoms, but up

to 30% of patients develop MC syndrome manifestations, such as peripheral neuropathy or systemic vasculitis (Lidove et al., 2001). Other frequent manifestations of MC syndrome include membranoproliferative glomerulonephritis (R. J. Johnson et al., 1993; Ozkok & Yildiz, 2014) and B-cell lymphoma (Visco & Finotto, 2014) in 30-36% or 7.5-10% of chronic HCV patients, respectively. Patients with chronic HCV infection are also at risk of developing insulin resistance and type 2 diabetes (Torres et al., 2008). The acquisition of diabetes is accompanied by poor prognosis and faster progression into liver cirrhosis (Foxton et al., 2006; Witteveldt et al., 2009). Approximately 20-80% of chronic HCV patients may present with central nervous system symptoms, which include fatigue, mood disorders, or cognitive impairments (Forton, Thomas, & Taylor-Robinson, 2004; Hoftberger et al., 2007).

Liver cirrhosis is one of the most serious complications of chronic HCV infection. It increases mortality, as a consequence to the development of decompensated liver disease and subsequently HCC. Progression to liver cirrhosis from chronic HCV infection has been estimated to be as high as 70%. The current worldwide estimate of progression to liver cirrhosis varies considerably from the statistics originated from hospitals compared to those from research studies. At any point during chronic HCV infection, the likelihood of progression into liver cirrhosis ranges from 15 to 56% (Freeman et al., 2001) (Thein, Yi, Dore, & Krahn, 2008). Many studies have reported an average of 16% chronic HCV patients develop liver cirrhosis within 20 years (Lawson & Ryder, 2006; Marcellin, Asselah, & Boyer, 2002). It has been estimated that approximately 25% of HCC cases are due to chronic HCV infections. The likelihood of developing non-HCV-related HCC is estimated to be 1.4 to 4.9% per year after the onset of liver cirrhosis, whereas HCV-

induced cirrhosis progression to HCC is as high as 30% in five years (Chayanupatkul et al., 2017; El-Serag, 2012).

### **1.1.2.3 Immune responses**

The induction of IFN- $\alpha$  and IFN- $\beta$  (type I), IFN- $\gamma$  (type II), and IL-28A/IFN-I2, IL-28B/IFN-I3, IL-29/IFN-I1, and IFN-I4 (type III) is essential for the host to control invading pathogens. These three types of interferons bind to their designated receptors IFNAR, IFNGR, IFNLR, respectively, leading to phosphorylation of STAT-1 and STAT-2, which then form the transcription factor ISGF3 complex comprised of phosphorylated STAT-1 and 2 and the Interferon Response Factor (IRF) 3 (Stetson & Medzhitov, 2006). Nuclear translocation of ISGF3 regulates the production of IFN-stimulated antiviral genes (ISGs), which in turn results in the inhibition of viral replication and the apoptosis of infected cells (Metz et al., 2012).

The hepatocytes initiate induction of type I and III interferons in response to HCV infection, through the toll-like (TLRs) and retinoic-acid-inducible gene-like receptors, including the retinoic acid-inducible gene I (RIG-I) and the melanoma differentiation-associated gene 5 (MDA-5) (Foy et al., 2005; Saito, Owen, Jiang, Marcotrigiano, & Gale, 2008). TLR3 sense membranous or endosomal dsRNA replication intermediates resulting in activation of Toll/interleukin-1 receptor-domain-containing adapter-inducing interferon- $\beta$  (TRIF) (Terczynska-Dyla et al., 2014; Thomas et al., 2012). RIG-I and MDA-5 sense viral dsRNA or ssRNA and trigger a signaling cascade through mitochondrial antiviral signaling protein (MAVS) (Israelow, Narbus, Sourisseau, & Evans, 2014; Saito & Gale, 2008). Activation of either TRIF or MAVS leads to the activation of IKK-related kinases IKK $\epsilon$  and TBK-1 which phosphorylates the transcription factors IRF3 or IRF7 which then

translocate into the nucleus to produce type I and II interferons (Loo et al., 2006). Infection of chimpanzee rapidly induces the production of type I IFN and ISGs (Su et al., 2002) whereas infection of the humans induces human IFN- $\gamma$ 4 (type III), which induces ISGs that could inhibit primary translation and, therefore, replication (Amanzada et al., 2013).

HCV counteracts several arms of the innate response by multiple mechanisms. HCV E2 (Taylor, Shi, Romano, Barber, & Lai, 1999) and NS5A (Gale et al., 1998) proteins suppress cellular mRNA translation by phosphorylation of protein kinase R (PKR) and elongation initiation factor 2a, with no effect on translation of HCV RNA. HCV NS3/4A protease target TRIF for degradation and thereby block TLR3 signaling (K. Li et al., 2005). NS3/4A protease cleaves MAVS, leading to disassociation from mitochondrial membranes, thus, inhibition of the MAVS-IKK $\epsilon$ -IRF3 signaling cascade, and as a result interruption of type I interferon production is inhibited (Lin, Chang, Yu, Liao, & Lin, 2006). Inactivation of MAVS interferes with the recruitment of inflammatory cells by reducing the production of the essential chemokines (Ding, Huang, Lu, Liu, & Zhong, 2012). HCV core prevents cell response to type I and III interferons indirectly by negatively regulating the phosphorylation of STAT and the activity of ISGF3 (Lin et al., 2006). The chronic upregulation of ISGs in chronic HCV infection is made ineffective by a concurrent upregulation of the inhibitory ISGs. IFN- $\alpha$  therapy cannot further upregulate ISGs which are already maximally upregulated. Induction of STAT1 phosphorylation by type III interferon does not appear to be impaired by the inhibitory ISGs induced by type I interferon. This lack of impairment had led to interest in the use of IFN- $\gamma$  as an alternative therapeutic approach (Makowska, Duong, Trincucci, Tough, & Heim, 2011; Sarasin-Filipowicz et al., 2008).

The primary cellular response to HCV infection is the recruitment of natural killer (NK) and T cells (Ahmad & Alvarez, 2004). Induction of type I and III interferons from infected hepatocytes activates resident dendritic cells (DCs), hepatic stellate cells (HSCs), and Kupffer cells (KCs). These activated cells, in turn, produce several cytokines, including IL-12, IL-15 and IL-18 (Velazquez et al., 2012), which recruit IFN- $\gamma$ -producing NK cells to the liver. Induction of type I and III interferons triggers liver sinusoidal endothelial cells (LSEC) to produce chemokines to recruit T cells.

Tissue resident DCs are the primary detectors of invading pathogen producing inflammatory cytokines to activate effector and regulatory immune cells. DCs are activated by detection of pathogen then mature and migrate to the lymphoid tissue to present the foreign antigens to B and T cell. There are three subtypes of DCs in human, myeloid DC 1 (mDC1), mDC2, and plasmacytoid DC (pDC). mDCs and pDCs recognize pathogens through pattern-recognition receptor such as TLRs whereby they enhance expression of class I and II human leukocyte antigen (HLA), upregulate co-stimulation ligands and produce immunostimulatory cytokines IL-12, IFN- $\gamma$ , or IFN- $\alpha$  and - $\gamma$ , respectively. DCs function is impaired in HCV infection, too (Auffermann-Gretzinger, Keefe, & Levy, 2001; Saito et al., 2008). Although the mechanisms of impairment are not defined, several studies have indicated that may result from defects in maturation and antigen presentation or in phagocytosis and expression of co-stimulation ligands (Dolganiuc, Garcia, Kodys, & Szabo, 2006; O'Beirne, Mitchell, Farzaneh, & Harrison, 2009). The critical consequences of DCs impairment in HCV infection are reduced maturation of cytokine-dependent NK cells and defects in priming of CD4<sup>+</sup> and CD8<sup>+</sup> T cells.

NK cells are critical antiviral effectors that kill infected target cells via several effector and stimulatory functions. NK cells secrete perforin which damages the membrane of the target cells or engages death receptor ligands, such as FasL or TRAIL. These receptors, which are members of the tumor necrosis factor (TNF) family, induce apoptosis (Kaser, Vogel, & Tilg, 1999) (Kokordelis et al., 2014). NK cells produce IFN- $\gamma$  and several chemokines that recruit T and B cells to the site of infection (Pelletier et al., 2010). The role of NK cells on the outcome of HCV infection remains poorly defined. On the one hand, highly active and cytotoxic NK cells were found among active injection drug users with no HCV infection, but NK cell effector and stimulatory activities were not among the determinants of the outcome of acute HCV infections (Golden-Mason, Cox, Randall, Cheng, & Rosen, 2010).

In chronic HCV infections, the frequency of peripheral NK cells may decrease without affecting the cytotoxic functions (Morishima et al., 2006). HCV core indirectly inhibits receptor expression and cytokine production by NK cells required to activate DCs (Nattermann et al., 2005). NK cells also produce immunosuppressive cytokines such as IL-10, which negatively impact maturation of DCs (De Maria et al., 2007). NK cells may contribute to the exacerbation of liver injury due to chronic HCV infection or acute fulminant hepatitis. The balance between the cytolytic and cytokine-producing NK cells in the liver may be associated with the progression of liver fibrosis (Oliviero et al., 2009). Thus, highly cytotoxic NK cells producing less IFN $\gamma$  may be detrimental to the liver during chronic HCV infection or acute fulminant hepatitis.

Activated mDCs and pDCs migrate to lymphoid tissue to stimulate the production of antigen-specific B and T cells. CD8<sup>+</sup> T cells are the immune effectors that directly kill

virus-infected cells by cytolytic or non-cytolytic mechanisms. CD4<sup>+</sup> T cells are key regulators of the activity of CD8<sup>+</sup> T and B cells. The robustness of the HCV-specific T cell response is a critical determinant for the outcome of acute HCV infection (Thimme, Chang, Pemberton, Sette, & Chisari, 2001). Induction of robust and sustained multi-specific CD4<sup>+</sup> and CD8<sup>+</sup> IFN- $\gamma$ <sup>+</sup> T cell responses to HCV correlates with clearance of acute infection. Weak or transient responses correlates with persistent infection (Diepolder et al., 1995; Gerlach, Diepolder, & Pape, 1999; Gruner et al., 2000; Missale et al., 1996). These correlations have been reproduced experimentally in chimpanzees depleted of CD4<sup>+</sup> and CD8<sup>+</sup> T cells. This depletion resulted in persistence of HCV infection (Kato et al., 1992; Thomson et al., 2003). The proliferation of CD4<sup>+</sup> T cells, in response to acute HCV infection, stimulates HCV-specific CD8<sup>+</sup> T cells into anti-HCV effectors targeting infected hepatocytes (Chemello et al., 1986; Shoukry et al., 2003).

The role of HCV-specific effector T cells in chronic HCV infection is not yet clearly understood. The presence of peripheral HCV-specific CD4<sup>+</sup> T-cell IFN- $\gamma$  response correlated with less severe outcomes of chronic HCV infection (Hoffmann et al., 1995). However, correlations between intrahepatic HCV-specific CD4<sup>+</sup> and CD8<sup>+</sup> T cell IFN- $\gamma$  and the progression of chronic HCV infection have not been evaluated (K. M. Chang et al., 1997; Kamal et al., 2004). In conditions of a global defect in T cell, such as in HIV/HCV co-infections or immunosuppressed individuals, infection results in high viral titers, which are often associated with severe and accelerated progression (McCaughan & Zekry, 2000). Failure to generate effective anti-HCV T cells prevents the resolution of the acute HCV infection, leading to the chronic infection. Other causes of the failure of T-cell response include altered priming of T-cell by intrahepatic antigen-presenting cells

(Wuensch, Pierce, & Crispe, 2006), viral escape mutations (Bull et al., 2015), induction of immunosuppressive responses by regulatory T cell (T-reg), and T cell anergy (Boettler et al., 2005; Ulsenheimer et al., 2003). Treg cells are identified by the expression of the transcription factor foxp3 and high expression of the IL-2 receptor  $\alpha$  chain (CD25) (S. Li et al., 2009). Activated T-regs suppress effector T cells within target tissues in a contact-dependent manner (Cabrera et al., 2004). In vitro, CD4<sup>+</sup> T cells co-cultured with HCV-infected hepatocyte cell lines develop a T-reg phenotype with increased expression of foxp3 and CD25 (A. J. Hall, 2010).

HCV-specific IL-10-producing T cells, typically not expressing foxp3 or high-levels of CD25, comprise an additional regulatory cell population involved in HCV pathogenesis (Levings, Sangregorio, & Roncarolo, 2001). Although many cell types produce IL-10, including DCs, macrophages, monocytes, and NK cells, IL-10<sup>+</sup> foxp3<sup>-</sup> CD4<sup>+</sup> T cells appear to be a major source of IL-10. These cells directly inhibit effector T cell function in h IL-10-dependent and IL-10-independent manners (Sundstedt, O'Neill, Nicolson, & Wraith, 2003). HCV proteins directly induce virus-specific production of IL-10 by CD4<sup>+</sup> and CD8<sup>+</sup> T cells (MacDonald et al., 2002).

Prolonged antigenic stimulation in chronic infection leads to the upregulation of several inhibitory co-receptors on antigen-specific CD8 T cells. This upregulation generates a state of functional CD8<sup>+</sup> hyporeactivity (Barber et al., 2006). The best characterized inhibitory receptors included in this regulation include programmed death-1 (PD-1), cytotoxic T-lymphocyte associated protein-4 (CTLA-4), NK cell receptor 2B4 (CD244), lymphocyte associated gene-3, and Killer cell lectin-like receptor subfamily G member 1. PD-1, a 55-kDa glycoprotein member of the CD28 superfamily, that contains



an immunoreceptor tyrosine-based inhibitory motif and immunoreceptor switch motif that phosphorylate the kinase SHP-2. Phosphorylated SHP-2 dephosphorylates various signal transduction kinases involved in T-cell receptor induced and proliferation and production. The PD-1 ligand PD-L1 is expressed on intrahepatic mDC, LSEC, and KC. CTLA-4, an immunoglobulin-like receptor, competes with CD28 for binding to CD80 and CD86, thereby blocking T cell co-stimulation (Q. Zhang et al., 2012). PD-1 and CTLA-4 are expressed to high levels HCV-specific CD8<sup>+</sup> and CD4<sup>+</sup> T cells early in acute HCV infection. They are expressed to high level through the persistent infection but are normalized after viral clearance (Urbani et al., 2006). HCV-specific memory CD8<sup>+</sup> T cells, particularly within the liver, express high levels of PD-1, impaired effector cytokines production, and low levels of cytolytic granules during chronic HCV infection (Radziewicz et al., 2007).

The B-cell-mediated antibody response to HCV is first detected within 6 to 8 weeks of infection (McHutchison, Kuo, Houghton, Choo, & Redeker, 1991; Peters et al., 1994). Neutralizing antibodies, which interfere with viral envelope binding to targets such as LDLR, SRBI, CD81 and claudin-1 in early acute infection, are associated with resolution in some, but not all, studies (Netski et al., 2005; Pestka et al., 2007). Lack of antibody-mediated protection may result from several causes. Firstly, the quasispecies nature of HCV allows for rapid selection of antibody escape variants (Netski et al., 2005). Secondly, the intrinsic sequence-specific E1E2 have variability to their sensitivity to neutralization (Tarr et al., 2011). HCV antibody titers may wane after 2 to 3 decades in up to 40% of patients with spontaneous viral clearance. In persistent infection however, novel B-cell clones are continuously stimulated to respond to evolving viral populations (Dowd, Netski,

Wang, Cox, & Ray, 2009 Cox, & Ray, 2009; Takaki et al., 2000). The interactions between the HCV E2 envelope protein and B-cell CD81, an activating tetraspanin co-receptor, drive antigen-independent polyclonal B-cell stimulation, thus predisposing to B-cell lymphoproliferative disorders. Despite chronic activation of virus-specific and non-virus-specific B cells, memory B cells do not accumulate in chronically infected patients (Visentini et al., 2012). Role of lipid droplet metabolism in HCV replication.

### **1.1.3 Lipid droplets**

#### **1.1.1.1 Structure**

Cytosolic lipid droplets (cLDs) are spherical structures with typical diameters ranging from 0.1 to 5  $\mu\text{m}$  in non-adipocytes, or up to more than 100  $\mu\text{m}$  in white adipocytes. cLDs are composed of an organic core of neutral lipids, mostly in the forms of TG and CE, surrounded by a phospholipid monolayer (Bartz, Li, et al., 2007). The major components of this monolayer are phosphatidylcholine (PC), phosphatidylethanolamine (PE), and phosphatidylinositol (PI) (Bartz, Li, et al., 2007; Tauchi-Sato, Ozeki, Houjou, Taguchi, & Fujimoto, 2002). Several types of proteins, classified as structural, enzymatic, or small GTPases involved in the endomembrane trafficking, decorate the surface of cLDs (Brown, Rozelle, Yin, Balla, & Donaldson, 2001). The association of proteins with cLDs is dynamic. Even within an individual cell, several populations of cLDs have different sets of associated proteins (Ducharme & Bickel, 2008).

#### **1.1.1.2 Synthesis**

The widely-accepted model of cLDs synthesis postulates budding of the neutral lipid globule from the cytoplasmic leaflet of the ER membrane (Murphy & Vance, 1999). The neutral lipids of the cLDs are synthesized by enzymes residing primarily in the ER (Wilfling

et al., 2013). TG synthesis is catalyzed by DGAT1 and DGAT2, where CE synthesis is catalyzed by the acyl CoA:cholesterol acyltransferase (ACAT) enzymes ACAT1 and ACAT2 (also known as sterol O-acyl- transferase 1 and 2, respectively) (Villanueva et al., 2009; Wendel, Cooper, Ilkayeva, Muoio, & Coleman, 2013). Current evidence suggests that DGAT1, an ER-resident enzyme, is responsible for esterifying excess fatty acids, which otherwise would cause ER membrane toxicity. DGAT2, by contrast, appears to be closely linked to de novo lipogenesis and to have a primary role in triglyceride storage (Wurie, Buckett, & Zammit, 2012).

The current model propose that TG and CE accumulate within the ER bilayer (Mackinnon, May, & Mountford, 1992; van Leeuwen et al., 1994). Once a critical concentration of neutral lipids is reached, a phase separation takes place which may generate lipid lenses. The lenses are blister-like inflations of the ER bilayer, approximately 17 nm in diameter. They grow and deform the ER bilayer membrane until they reach a critical size that triggers budding of nascent cLDs into the cytoplasm (Hansen, Falconer, Hamilton, & Herpok, 1981; Khandelia, Duelund, Pakkanen, & Ipsen, 2010) (**Figure 1.6**). During this process, the nascent cLDs acquire several proteins, particularly, members of the perilipin family, which are integral cLD-associated proteins. In addition to the perilipins, several other proteins associate with cLDs transiently under certain cellular conditions. Seipin, a homo-oligomeric integral ER membrane protein localizes to the ER-cLD contact sites.

Seipin is required for the early steps of cLD formation and has been shown be involved in the maturation of nascent to mature cLDs in multiple cell lines (Szymanski et

al., 2007). Fat storage-inducing transmembrane protein 2 (FITM2, also known as FIT2) (Gross, Zhan, & Silver, 2011), an ER-residing six-transmembrane-domain containing

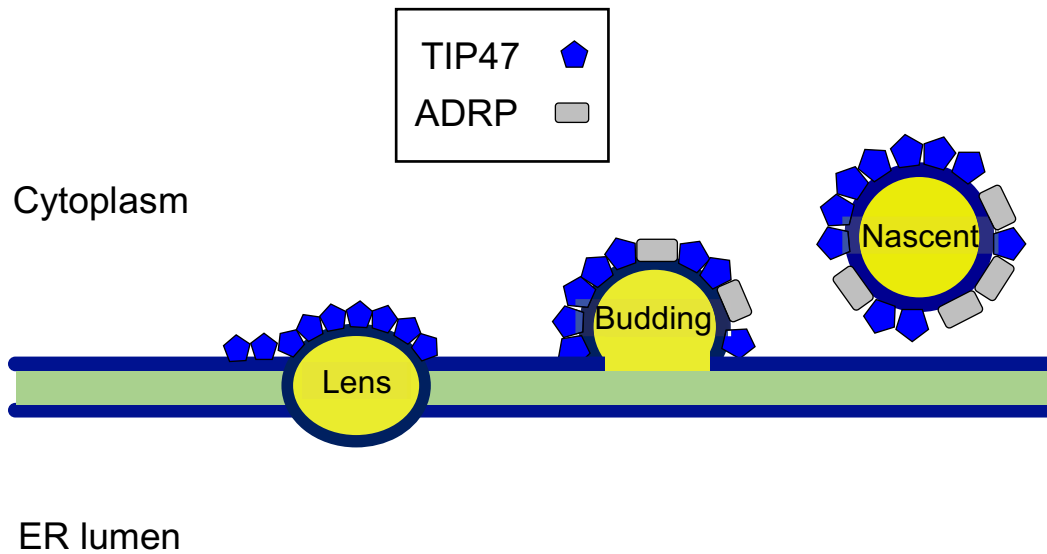


### Figure 1.6. Synthesis of cytosolic lipid droplets

Formation of cLD begins by accumulation of neutral lipids, TG and CE, between the leaflets of the ER membrane forming lenses of inflated bilayer by a TIP47 (lipid droplet-binding protein) -dependent mechanism. TIP47 translocate from the cytoplasm into sites of neutral lipid accumulation on ER. Further incorporation of neutral lipids into forming nascent cLD increases the inflation of the ER leaflet facing the cytoplasm. Another lipid droplet-binding protein, ADRP, begins to bind to forming droplets at this stage. Budding droplets are eventually excised into the cytoplasm forming nascent cLD which has more TIP47 than ADRP.

protein, has also been implicated in cLD formation. FITM2 has been implicated in the budding of cLDs toward the cytosol.

### **1.1.1.3 Growth**

Once nascent cLDs are formed and released from the ER membrane as physically separate entities, they continue to mature by accumulating more neutral lipids, expanding their size. Population of nascent and mature cLDs reflects the normal physiological balance based on the metabolic status of the organism. However, expansion into an enlarged population of cLDs is associated with pathological conditions which can be transient such as response to an ER stress or chronic such as persistence infections (**Figure 1.7**). Several models have been proposed for the mechanism of cLDs growth. The growth of cLD requires increases in the production of the internal neutral lipids and the phospholipids making the monolayer membrane. Both types of lipids may be synthesized in the ER and then delivered to growing cLD through ER-cLD contact sites (Skinner et al., 2009; Soni et al., 2009) or directly on the surface of growing mature cLDs (Poppelreuther et al., 2012; Wilfling et al., 2013). The localization of several enzymes essential for synthesis of both types of lipids on the surface of cLDs supported the local synthesis model. The third model of cLD growth is via fusion of existing cLDs. This fusion is considered a rare event under normal condition, but it becomes obvious under certain conditions such as treatment of adipocytes with insulin and fatty acid.

The size of cLDs is controlled by the neutral lipid core, the monolayer membrane, and the associated proteins. Neutral lipids, TG and CE, are essential in the formation of cLDs (Gross, Zhan, & Silver, 2011). Yeast strains lack diacylglycerol (DAG) and sterol acyltransferases are void of cLDs (Ferreira, Regnacq, Alimardani, Moreau-Vauzelle, &

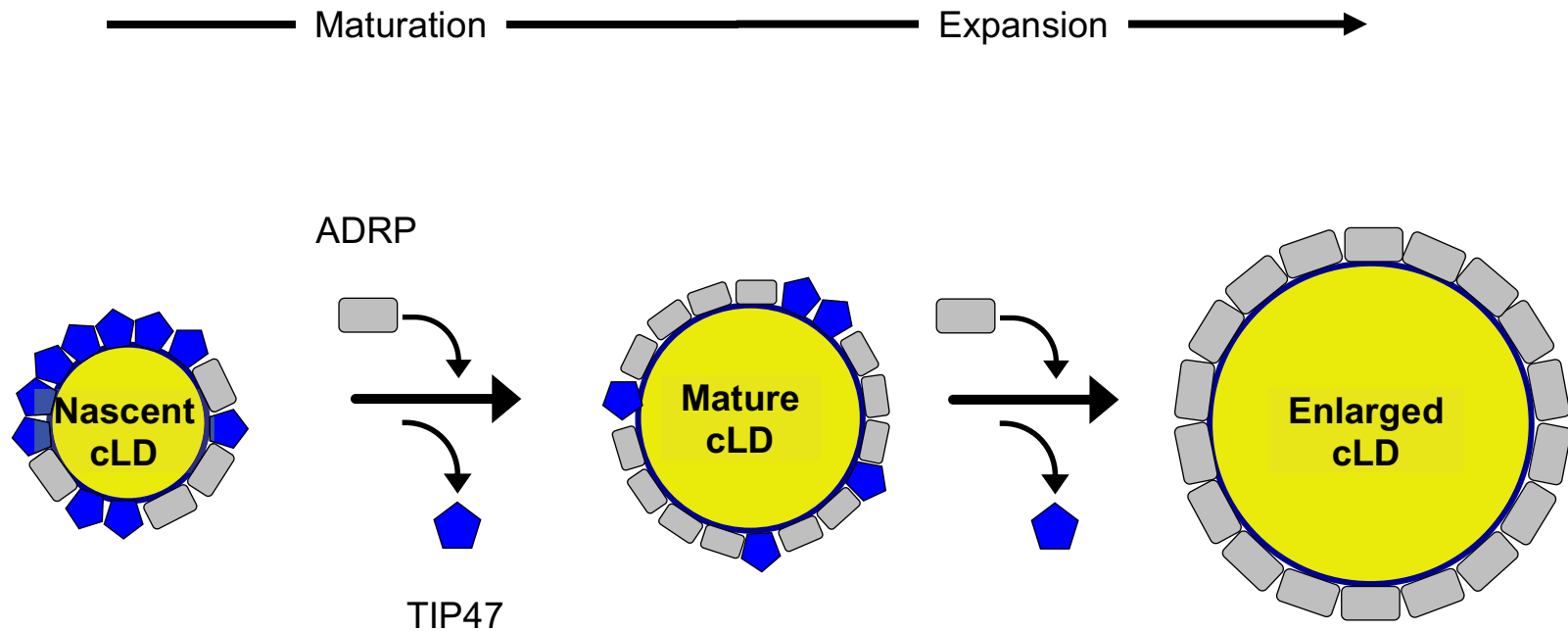


**Figure 1.7 A schematic representation of growth and expansion of cLDs.**

Steady-state incorporation of neutral lipids into nascent cLDs promotes maturation which increases in size and gradual replacement of TIP47 by ADRP. ADRP stabilizes mature cLDs by mechanisms that limit lipolysis. Further enlargement of cLDs could indicate a pathological process related to the metabolism of cLDs.

Berges, 2004), although these yeast strains possess other forms of neutral lipids such as squalene (Valachovic, Garaiova, Holic, & Hapala, 2016). Conversely, TG and SE are sufficient to promote the cLDs growth. Treatment of hepatoma cells with oleic acid for 24 h promotes enlargement of cLDs by several-fold (Rohwedder, Zhang, Rudge, & Wakelam, 2014 & Wakelam, 2014).

Although there is variation between organisms, the major phospholipid components of the cLDs monolayer are PC and PE (Tauchi-Sato et al., 2002 Taguchi, & Fujimoto, 2002). The rate limiting enzyme in PC synthesis is CTP: phosphocholine cytidyltransferase (CCT). CCT translocates to the surface of growing cLDs to provide sufficient PC to meet the demand of the cLDs expansion (Krahmer et al., 2011). PC is critical for the stabilization of cLDs. Lack of PC in S2 cells leads to the coalescence of cLDs (Guo et al., 2008). Subsequent studies have also implicated the fusogenic phosphatidic acid (PA) in the cLDs stability. Increasing the ratio of PA to PC in the cLDs monolayer membrane may trigger cLD coalescence in vitro (Fei et al., 2011).

In addition to the TG and CE synthesizing enzymes, several other proteins contribute to the regulation of the cLDs growth. CIDEA, CIDEB, and CIDECD, members of the Cell death-inducing DFF45-like effector (CIDE) protein family, associate with cLDs (Nishimoto & Tamori, 2017; Xu et al., 2016). The CIDE proteins participate in the regulation of cLDs homeostasis. cLDs appears as large unilocular in white adipocytes. Deficiency of CIDECD results in numerous small cLDs, whereas ectopic CIDECD expression results in fewer and larger cLDs (Y. Li, Han, Hu, Sommerfeld, & Hu, 2010). CIDE proteins expression are upregulated in hepatic steatosis (A. M. Hall et al., 2010). CIDE proteins could thus play a major role in the regulation of cLDs metabolism. In contrast to the clear

evidence of the participation of CIDEc and CIDEA in the cLDs growth, their molecular mechanisms remain elusive. A recent study demonstrated that CIDEc, and to lesser extent CIDEA, might facilitate the transfer of lipids from small to large cLDs. This model of CIDE proteins-mediated lipid transfer was supported by the enrichment of CIDEc or CIDEA at cLDs contact sites (Xu et al., 2016).

A screen of the yeast gene deletion library revealed that FLD1 (yeast orthologue to mammalian Seipin) deletion resulted in 20-fold larger cLDs (Grippa et al., 2015). Seipin is known for its implication in a severe recessive disorder called “Berardinelli-Seip congenital lipodystrophy type 2” (BSCL2), which manifests as near complete loss of adipose tissue, severe insulin resistance, and fatty liver (Simha & Garg, 2003). While cLDs present as small and aggregated in seipin-deficient A431 (human epidermoid carcinoma) cells in vitro (Salo et al., 2016), the salivary glands of seipin deficient drosophila contain giant cLDs (Mahnert et al., 2015). It is thus evident that seipin is involved in regulating the size and cellular distribution of cLDs although the precise mechanisms remain unknown. PA level were increased in cLDs membrane in seipin-deficient cells (Boutet et al., 2009; Pagac et al., 2016). Seipin may thus regulate the size of cLDs indirectly through increasing the level of PA in the cLDs membrane.

FITM2 facilitates budding of nascent cLDs, which appears to contribute to the regulation of mature cLDs growth (De Miranda, Schlater, Green, & Kanatous, 2012). FITM2 knockdown reduces TG levels and its overexpression increases the TG levels and cLDs size in mouse liver and also in cultured cells. FITM2 appears to enhance the transfer of TG into the cLDs, as it directly binds to TG (Miranda et al., 2014).



The number and size of cLDs is a reflection of a dynamic balance between lipogenesis and lipolysis of the neutral lipid core and the biophysical properties of the monolayer membrane. For example, perilipin 1 (Plin1) regulates lipolysis in white adipocyte tissue (WAT) by facilitating the assembly of complex lipolytic proteins on the cLDs surface (Lass, Zimmermann, Oberer, & Zechner, 2011). Under basal conditions, Plin1 is non-phosphorylated, and the major lipases adipose triacylglycerol lipase (ATGL) and hormone-sensitive lipase (HSL) reside in the cytosol (Miyoshi et al., 2007). The ATGL activator CGI-58 [comparative gene identification-58; A/B-hydrolase domain 5 (ABHD5)] binds to Plin1 on the surface of cLDs (Eichmann et al., 2015). Phosphorylation of CGI-58 by protein kinase A (PKA) leads to the recruitment of ATGL, which catalyzes the first step of TG hydrolysis, generating free fatty acids (FFAs) and DAG (Yen & Farese, 2006). Thus, Plin1 is critical for lipolysis in WAT by acting as a barrier against lipases in the basal state.

Plin1 is the master regulator of lipolysis of cLDs in WAT, whereas ADRP (Plin2) and TIP47 (Plin3) are the equivalents in non-adipose tissues. ADRP and TIP47 appear to be less efficient in the protection of cLDs against lipolysis. However, still, ADRP-deficient hepatocytes contain a reduced level of TG due to an elevated rate of lipolysis (Imai et al., 2007). Localization of ATGL and CGI-58 to the cLDs surface increases in ADRP<sup>-/-</sup> cells. Plin1 interacts directly with ATGL and cofactor CGI-58 on the cLDs, whereas ADRP does not. ADRP may exert its effects by competing with the ATGL and CGI-58 binding sites (Listenberger & Brown, 2007). The interactions between ATGL and CGI-58 increase in the absence of ADRP leading to faster/more efficient lipolysis. The neutral lipids in the core of cLDs can also be released by macroautophagy or macrolipophagy via lysosomal degradation pathway (K. Liu & Czaja, 2013). ADRP and

TIP47 prevent fusion of cLDs with autophagosomes under normal conditions (Khaldoun et al., 2014). Under nutrient deprivation conditions however, ADRP and TIP47 are degraded via the chaperone-mediated autophagic degradation resulting in the fusion of cLDs with autophagosomes. Subsequently, autophagosomes fuse with lysosomes to form autolysosomes in which cytoplasmic and lysosomal lipases breakdown TG (Kaushik & Cuervo, 2015).

#### **1.1.1.4 Interactions with other organelles**

The FFAs liberated from TG within the core of the cLDs serve as a substrate for several reactions. They are used in  $\beta$ -oxidation, in mitochondria or peroxisomes, to generate ATP (Bartlett & Eaton, 2004). FFAs are also shuttled to the ER for the biosynthesis of phospholipids or protein lipidation. The FFAs used in cLDs TG synthesis are obtained from endocytosed lipoproteins or the cell surface, via fatty acid transport proteins (Lehner, Lian, & Quiroga, 2012; Sturley & Hussain, 2012). It is thus not unexpected that cLDs interact with cellular organelles involved in the metabolism and transport of FFAs, which include mitochondria, peroxisomes, ER, or endosomes. The proximity between cLDs and mitochondria in adipocytes, increases during stimulation of lipolysis. cLDs are within 10 nm from mitochondria in porcine oocytes (Sturmey, O'Toole, & Leese, 2006). By electron microscopy, ER partially or completely wraps some cLDs (Choudhary, Ojha, Golden, & Prinz, 2015). A single 10 years old report demonstrated also a possible direct contact between cLDs and early endosomes (Bartz, Zehmer, et al., 2007).

Rab is a family of proteins under the Ras superfamily of monomeric G proteins. The primary functions of Rab family proteins include selection, sorting, and budding of cargo as well as transport, tethering, uncoating, and fusion of vesicles (Stenmark, 2009).

As small GTPases, Rab proteins have GDP or GTP-bound forms. Several studies of cLDs proteomics under various conditions of lipid metabolism have identified various members of the Rab family of proteins (Brasaemle, Dolios, Shapiro, & Wang, 2004; Cermelli, Guo, Gross, & Welte, 2006). Overall, more than 15 different Rab proteins were associated with cLD by proteomics. The overlap across the different screens however, was relatively poor. Only four members were consistently identified including Rab1, Rab5, Rab7, and Rab18. Rab18 localizes to mature but not nascent cLDs. Its association with cLDs inversely correlates with that of ADRP. Rab18 appears to have a role in the lipolysis of cLDs. It translocates to the surface of the cLDs in response to lipolytic stimulation (S. Martin, Driessen, Nixon, Zerial, & Parton, 2005). Association of Rab18 with cLD increases the proximity of cLD to the ER, an effect that increases when Rab18 is overexpressed (Ozeki et al., 2005).

#### **1.1.1.5 Motility and distribution**

cLDs exhibit two forms of motility, directionless oscillatory movements within 1  $\mu\text{m}$ , and long-range vectorial movements over several microns (S. W. Martin & Konopka, 2004; Targett-Adams et al., 2003). Movement around the cell on the long-range movement depends on the microtubular network. This movement may facilitate the interactions of cLDs with other organelles (Arora, Tran, Rizzo, Jain, & Welte, 2016). cLDs display plus and minus-end movement on microtubules, involving the plus and minus-end microtubule motor proteins kinesin and dynein, respectively (Bostrom et al., 2005; Shubeita et al., 2008).

The link between the motility and biology of cLD has not been thoroughly investigated. Several observations, mostly from genetic studies in *Drosophila*, supports a

role of the movement in the metabolism of cLDs. Lipid storage droplet 2 (LSD2), the *Drosophila* homolog to mammalian ADRP, is essential for the maintenance of lipid storage (Fauny, Silber, & Zider, 2005). Loss-of-function mutations in LSD2 result in the generation of lean flies, whereas gain-of-function mutation results in obesity (Teixeira, Rabouille, Rorth, Ephrussi, & Vanzo, 2003). In addition to maintaining lipid storage, LSD2 is prominently involved the motility of *Drosophila* cLDs. LSD2 regulate the engagement of the motor proteins dynein and kinesin (Welte et al., 2005). Regulation of motility and lipid storage by the same protein suggests a link between movement and metabolism of cLDs. The enrichment of dominant-negative mutant of caveolins on the surface of cLDs leads to inhibition of cLDs motility and of lipolysis, supporting again a link between movement and metabolism (Ward, Polishchuk, Caplan, Hirschberg, & Lippincott-Schwartz, 2001). The appearance of nascent cLDs at the periphery of adipocytes, and their gradual traffic to the center of the cell as they increase in size also supports this link (Jambunathan, Yin, Khan, Tamori, & Puri, 2011). Conversely, the large juxtanuclear cLDs fragment into numerous small cLDs and appear dispersed throughout the cytoplasm under stimulation of lipolysis (Orlicky, Monks, Stefanski, & McManaman, 2013)

#### **1.1.1.6 Functions**

The main function of cLDs is the storage of neutral lipids, which are hydrolyzed under catabolic conditions such that the products are utilized in several cellular processes, including ATP generation by  $\beta$ -oxidation, membrane phospholipids synthesis, and production of signaling molecules. The TG in the cLDs are hydrolyzed to generate DAG, MAG, FFAs, and CE. Within cLDs in most cells however, they are utilized for the synthesis of steroids and eicosanoids, in the steroidogenic cells and the arachidonic acid esters

within the cLDs of the mast cells, respectively. The fatty acid produced by the catabolism of cLDs neutral lipids are used to synthesize lipoprotein particles in hepatocytes (Gibbons, Lin, Cotter, & Raetz, 2000).

Excess FFAs induces lipotoxicity, leading to severe cellular dysfunction or apoptosis (Schaffer, 2003). Esterification of FFAs into TG and their storage within the cLDs is a mechanism of cell protection mechanism. Unsaturated FAs promote synthesis of TG by acting as ligands for the peroxisome proliferator-activated receptor  $\gamma$  (PPAR  $\gamma$ ), a group of transcription factors that regulate fatty acid storage and glucose metabolism. Unsaturated FAs serve as a favorable substrate for the DGAT enzymes that saturate FAs. Both saturated or unsaturated FAs were toxic in DGAT-deficient fibroblasts (Listenberger et al., 2003).

Besides the lipid metabolism-related functions, cLDs may have other roles related to the degradation of proteins. Lipidated ApoB-100 particles appear to accumulate on the surface of cLDs in crescent-like structures which could represent a partial wrap of the ER membrane in contact with cLDs (Ohsaki, Cheng, Fujita, Tokumoto, & Fujimoto, 2006). The ApoB-100 crescents appear scarcely in Huh hepatoma cells but chemical inhibition of the proteasomal or autophagic degradation pathways results in their being enlarged/more abundant/ more prominent/more frequent. (Ohsaki, Cheng, et al., 2006).  $\alpha$ -Synuclein, a major protein of the Lewy bodies found in Parkinson's disease, showed similar association to cLDs as ApoB-100 (Cole et al., 2002; Webb, de Beer, de Beer, & van der Westhuyzen, 2004). Both proteins contain hydrophobic motifs and could thus form aggregates in aqueous solution. cLDs may provide a hydrophobic environment for

these excess and potentially toxic proteins and may help in their transfer to degradation pathways.

#### **1.1.1.7 Lipid droplet associated proteins**

The perilipins are a family of proteins characterized by sequence homology in the N-terminus, which harbors the hydrophobic PAT domain (100 aa), and a repeating 11-mer helical motif of different lengths (Garcia, Sekowski, Subramanian, & Brasaemle, 2003; McManaman, Zabaronick, Schaack, & Orlicky, 2003). The C-terminal of the plins, in contrast, contains common and unique sequences (Hickenbottom, Kimmel, Londos, & Hurley, 2004). Plin2 (ADRP), plin3 (TIP47), and plin5 proteins are approximately 300–400 aa, plin4 is 1,500 aa, and plin1 has four variants of 522 aa as a result of alternative splicing (Itabe, Yamaguchi, Nimura, & Sasabe, 2017). Individual cells could express different plins, and the tissue distribution of plins varies substantially. For example, plin1 is mostly expressed in WAT and brown adipose tissue (BAT), whereas, ADRP (Brasaemle et al., 1997) and TIP47 (Szigeti et al., 2009) are expressed ubiquitously. Plin4 (Pourteymour et al., 2015) and Plin5 (H. Wang et al., 2011) are expressed mostly in organs where the demand for  $\beta$ -oxidation is high such as the brain, heart, and skeletal muscles (Kuramoto et al., 2014; Laurens et al., 2016; Pourteymour et al., 2015). Thus, the different tissue distribution of plins suggest that each plin contributes uniquely to the metabolism of cLDs.

#### **1.1.1.8 Targeting**

The mechanism of targeting proteins to the surface of cLDs is not fully understood yet. One of the most intriguing questions is how transmembrane proteins can bind to both bilayer and monolayer phospholipid membrane. Several mechanisms have been

proposed. First, the proteins could use an extended hydrophobic domain that embeds through the monolayer and the core of the cLDs while the hydrophilic domains on either side remain outside toward the cytosolic side. This mechanism of cLD targeting appears to be employed by caveolins according to their structure. They are targeted to specialized domains of the plasma membrane and cLDs (Martin and Parton, 2006). The lipid synthesizing enzyme DGAT2 may also attach by similar mechanism (Kuerschner et al., 2008; Stone et al., 2006). Second, proteins may bind to cLDs surface by embedding an amphipathic helix. The examples of such proteins include members of the integral cLD-associated proteins (e.g. perilipin 1, ADRP, or TIP47) (Brasaemle, 2007).

The association of plins with cLDs determine their stability. Under conditions of lipolysis, plin1 and ADRP dissociate and are rapidly degraded by the proteasomal or lysosomal pathway (Marcinkiewicz, Gauthier, Garcia, & Brasaemle, 2006; Miyoshi et al., 2007), providing access for lipases to hydrolyze TG (Lass et al., 2006; Moore, McGarvey, Russell, Cullen, & McClure, 2005). Under lipogenesis conditions conversely, plin1 and ADRP association with cLDs increases, enhancing their stabilities (Imamura et al., 2002; Listenberger, Ostermeyer-Fay, Goldberg, Brown, & Brown, 2007; Mak, Ren, Ponomarenko, Cao, & Lieber, 2008; Y. Takahashi et al., 2013). TIP47 is also subjective to lysosomal degradation (Crossingham et al., 2009), but the mechanisms for the stability and degradation of plin4 and 5 are yet to be determined. Plin1 (Yu Takahashi et al., 2015) and ADRP (Kovsan, Ben-Romano, Souza, Greenberg, & Rudich, 2007) are not stable in the absence of cLDs, TIP47, plin 4, and plin 5 maintain stability by binding to cytosolic components. TIP47, plin 4, and plin 5 exist as high-density, disk-like structures in the cytosol as evaluated by electron micrographs (Wolins et al., 2006).

### **1.1.4 Lipid droplets and microbial infections**

#### **1.1.4.1 cLDs roles in infection**

Studying the interactions between pathogens and their host cells provide invaluable insights into the molecular mechanisms of pathogenesis and also on cell biology. Recent studies of the roles of cLDs in the life cycle and the pathogenesis of a variety of pathogens have uncovered several previously unrecognized roles of cLDs in cell biology. Further studies on the mechanisms of pathogen-cLD interaction may well also reveal novel venues for intervention strategies.

*Chlamydia trachomatis* are intracellular bacteria that infect the genital tract or the eye, causing urethritis or trachoma, respectively. *C. trachomatis* requires TG and CE to grow (van Ooij et al., 2000). *C. trachomatis* is metabolically inert in the environment and become metabolically active only upon infection (Belland, Ojcius, & Byrne, 2004). *C. trachomatis* replicates in membrane-bound vacuoles isolated from the intracellular organelles (Fields & Hackstadt, 2002). *C. trachomatis* acquire during its replication several lipids via exocytotic vesicles, such as glycerophospholipids, sphingolipids, and cholesterol (Carabeo, Mead, & Hackstadt, 2003). cLDs accumulate to the cytosolic side of the vacuoles where *C. trachomatis* replicates. The juxtaposition of cLDs with the vacuoles allows three *C. trachomatis* LD-associated proteins, Lda1 (CT156), Lda2 (CT163), and Lda3 (CT473), to translocate across the vacuoles into the contacting cLDs. The association of these proteins with the cLDs appears to induce cytotoxicity. Ablation of cLDs from yeast confers protection against Lda2-induced cytotoxicity. Consistently with this model, small molecule inhibitor of fatty acid synthase (FAS) inhibits the *C. trachomatis* growth (Kumar, Cocchiaro, & Valdivia, 2006). Moreover, cLDs may be translocate into



the vacuoles in a process mediated by Lda3. ADRP, which protect cLDs from lipolysis, is dissociated from the cLDs as they are translocated into the vacuoles (Cocchiari, Kumar, Fischer, Hackstadt, & Valdivia, 2008), leading to easier access to catabolize the neutral lipids within the core of cLDs.

*Mycobacterium tuberculosis* (MTB) is intracellular bacterium that infect alveolar macrophages, causing tuberculosis. MTB infection in the lung result in the formation of host response-mediated granulomas, composed of infected macrophages and bystander phagocytes and lymphocytes surrounded by a fibrous layer of endothelial cells. MTB stays dormant in the granuloma but becomes active and replicates when the immune system become suppressed (Ishigami, Zhang, Rayhill, Katz, & Stolpen, 2004). MTB encodes for its triacylglycerol synthase 1 to synthesize TG and a lipase to hydrolyzes these TG (Davis et al., 2006) as its largest source of energy (Daniel et al., 2004). TG are stored within bacteria LDs (Becucci, D'Amico, Cinotti, Daniele, & Guidelli, 2011).

*Plasmodium falciparum* is a parasitic pathogen transmitted to humans by the bite of an infected anopheline mosquito and causes a virulent form of malaria. The injected sporozoites first infect hepatocytes, where they propagate. The merozoites are released into the blood-stream where they infect erythrocytes. The infected erythrocytes display a substantial increase in the level of phospholipids and TG (Palacpac et al., 2004). Similar to MTB, *P. falciparum* encodes its DGAT enzyme to synthesize TG (Vielemeyer, McIntosh, Joiner, & Coppens, 2004).

Dengue virus (DENV) is a mosquito-borne flavivirus with (+) ssRNA genome. It is the causative agent of dengue fever, which is acquired by a bite of *Aedes* mosquitos carrying the virus (Rodenhuis-Zybert, Wilschut, & Smit, 2010). The first target cells after

the bites are the skin resident dendritic cells (Langerhans cells). After uncoating of the infecting virions, the RNA is translated into a polyprotein that later cleaved into individual proteins, very much like HCV (Clyde, Kyle, & Harris, 2006). DENV replication also occurs in ER-derived membranous structures. The assembly of progeny virions is facilitated by the encapsidation of the genome RNA at ER sites enriched in envelope glycoproteins (Ishigami et al., 2004). Virions then mature as they traffic through the ER-Golgi secretory pathway (Zybert, van der Ende-Metselaar, Wilschut, & Smit, 2008). Like HCV core protein, DENV core protein also associates with cLDs. DENV infection of baby hamster kidney cells upregulates lipid metabolism, thereby increasing cellular cLDs content (Samsa et al., 2009). DENV NS3 protein may interact with, and enrich, the FAS at the replication sites (Heaton et al., 2010). Mutations in the cLD association hydrophobic motif within DENV core disrupt its association with cLDs, resulting in inhibition of replication. Small molecule inhibitors of FAS inhibit the formation of cLDs and inhibit assembly and egress of progeny virions (Samsa et al., 2009). Despite the differences between DENV and HCV, including the life cycle, tissue tropism, and the spectrum of pathology they cause, both rely on lipid metabolism and utilize cLDs to support replication and assembly. Modification of the cellular content of cLDs by HCV and DENV suggest that cLDs are vital organelles for viral replication.

Rotaviruses (RVs) are another group of viruses that require cLDs. They are non-enveloped dsRNA viruses in the *Reoviridae* family (Patton, Silvestri, Tortorici, Vasquez-Del Carpio, & Taraporewala, 2006). RVs infect intestinal enterocytes, causing acute gastroenteritis in children (Parashar, Gibson, Bresee, & Glass, 2006). The RNA genome comprises 11 segments encoding 6 structural proteins (VP1, 2, 3, 4, 6, and 7) and 6 non-

structural ones (NSP1, 2, 3, 4, 5, and 6). RV infection induces the formation of inclusion bodies known as viroplasms, in which the virus replicates and partially assembles (Pesavento, Crawford, Estes, & Prasad, 2006). Viroplasms colocalize to cLDs in the intestinal carcinoma Caco-2 cells. Using subcellular fractionation, RV dsRNA, NSP5, and ADRP co-fractionate in the low-density fractions where cLDs usually fractionate. Knockdown of NSP5 in Caco-2 cells inhibits the association of viroplasms to cLDs and inhibits replication. Like for DV, an inhibitor of FAS inhibits the formation of cLDs and inhibit virus replication (Cheung et al., 2010).

HBV interacts with cLDs. HBV protein HBx upregulates lipogenic genes such as SREBP-1, FAS, and PPAR $\gamma$  via activation of the transcription factor liver X receptors, major regulators of cholesterol, fatty acid, and glucose homeostasis (Na et al., 2009). The list of viruses known to utilize cLDs at any step of their replication cycle continue to grow, including diverse viruses such the human adenovirus 36, which decreases lipid turnover leading to obesity (Z. Q. Wang, Yu, Zhang, Floyd, & Cefalu, 2010). Further investigation into the interactions of cLDs with intracellular pathogens could potentially reveal underestimated roles of the cLD biology in response to microbial infections.

#### **1.1.4.2 HCV**

The density profile of HCV particles is remarkably low and widely distributed, from 1.03 to 1.20 g/cm (Pumeechockchai et al., 2002). The peak infectivity coincides with the lower-density population (Bradley et al., 1991). These unique biophysical characteristics result from the association of lipoprotein components such as ApoE, ApoB, ApoA1 and several ApoC proteins with HCV particles, both in infected individuals and in cell culture (Catanese, Uryu, et al., 2013; K. S. Chang, Jiang, Cai, & Luo, 2007; Gastaminza et al.,

2008a; Meunier et al., 2008). CE accounts for more than half of the neutral lipids in HCV particles. This enrichment is consistent with that in LDL and VLDL (Merz et al., 2011). ApoE levels are increased by 50-fold in cell culture derived HCV isolates over clinical ones. However, cell culture derived also have higher density than patients isolates (Merz et al., 2011; Tomiyasu, Walsh, Ikewaki, Judge, & Sacks, 2001). The difference between the two sources of HCV particles is attributed to the well-recognized defect in VLDL production by the hepatoma cell lines used to replicate HCV (Jammart et al., 2013). This difference in the biophysical features affects infectivity.

The presence of lipoprotein components in HCV particles contributes for the entry into hepatocytes. The degree of lipidation of the HCV particles appears to influence the kinetics of entry. The first step in HCV entry involves binding of the LDL component of the LVPs to the LDL receptor, binding which induces clathrin-dependent endocytosis (Owen, Huang, Ye, & Gale). The precise mechanism is not known, and the entry of HCV LVP likely does not resemble that of the lipoprotein particles. As a major difference, the entry kinetic of HCV LVP or LDL particles are very different. Another host factor with an established function in lipid metabolism that is also involved in entry of HCV is SR-BI. SR-BI is an integral membrane protein that facilitates the cellular uptake of cholesterol from high-density lipoprotein (HDL) (Shen, Hu, Hu, Kraemer, & Azhar, 2014). SR-BI interacts directly with the HVR 1 of HCV E2 glycoprotein. SR-BI appears to participate in HCV entry at multiple levels, including initial attachment and post-binding events. Very recently, a redundancy between LDLr and SR-BI in HCV entry has been suggested based on LDLr/SR-BI double knockout (Van Eck et al., 2003). The blocked HCV entry in LDLr/SR-BI knockout cells was rescued by the ectopic expression of either LDLr or SR-BI.

Cholesterol transporter NPC1L1 is another factor involved in lipid metabolism, which also participates in HCV entry (Sainz, Barretto, Yu, Corcoran, & Uprichard, 2012). The apical location of NPC1L1, where it resorbs cholesterol from the bile, suggests that its role in HCV entry, which occurs at the basolateral surface, could be secondary to the maintenance of cellular cholesterol levels.

HCV infections induce extensive rearrangement of the ER membrane creating what is known as the "membranous web," in which HCV replication is thought to occur (Egger et al., 2002; Rouille et al., 2006). The membranous web is composed of ER membrane convoluted segments of harboring small vesicles. HCV non-structural proteins NS3/4A, NS4B, NS5A and NS5B, and the genomic RNA associate with the membranous web (Gosert et al., 2003). Compared with HCV genotype 1a or 1b replicons, infection of Huh7.5 with HCVcc-JFH1 produces more prominent alterations to the ER membrane, marked by the presence of numerous single or double membrane vesicles (DMV) (Ferraris, Blanchard, & Roingeard, 2010; D. Paul et al., 2011). HCV NS4B and NS5A proteins are essential for the formation of the membranous web, although the mechanism is not entirely understood. NS4B protein alone results in the formation of membranous webs (Egger et al., 2002), whereas NS5A leads to the formation of (DMV) resembling those during in the infection (D. Paul et al., 2011). The altered membranous structures induced by HCV infections or NS4A or NS5B are richer in cholesterol and sphingolipids than ER membrane. Thus, HCV infection induces physical and chemical changes to at least parts of the ER membrane. These changes likely create an environment that favors HCV RNA efficient replication.

Several host factors with roles in the lipid metabolism are implicated in HCV replication. Phosphatidylinositol-4 kinase-III alpha (PI4KIII $\alpha$ ) is an enzyme that catalyzes the first step in the synthesis of the membrane phospholipid phosphatidylinositol 4,5-bisphosphate (PI(4,5)P<sub>2</sub>), which resides normally in the ER or plasma membrane. During HCV infection however, PI4KIII $\alpha$  is enriched at sites of HCV replication. HCV NS5A directly binds and activates PI4KIII $\alpha$  (Berger, Kelly, Jordan, Tartell, & Randall, 2011; Reiss et al., 2011). Inhibition of PI4KIII $\alpha$  by small molecule inhibitors potently inhibits replication of HCV (Kazmierski et al., 2014). The role of PI4KIII $\alpha$  in HCV replication is likely indirect. Activation of PI4KIII $\alpha$  increases the level of Phosphatidylinositol 4-phosphate (PI4P), a precursor to the end product of PI4KIII $\alpha$ , PI(4,5)P<sub>2</sub> (Berger et al., 2011). PI4P interacts with two lipid transfer proteins, oxysterol-binding protein 1 (OSBP) (H. Wang et al., 2014) and four-phosphate adaptor protein 2 (FAPP2) (Khan et al., 2014). Both were recently shown to participate in HCV replication. OSBP interacts with PI4P in the Golgi membrane where it transfers and exchanges it for cholesterol (Mesmin et al., 2013). OSBP could perhaps also transfer cholesterol to the cholesterol rich HCV replication complexes. A small molecule inhibitor of OSBP inhibits HCV replication (H. Wang et al., 2014). FAPP2 is involved in the transport of glucosylceramide to HCV replication complexes for conversion to more complex sphingolipids. Depletion of FAPP2 or defective FAPP2 mutants inhibit replication of HCV (Khan et al., 2014). Therefore, OSBP and FAPP2 promote HCV replication, most likely by transporting several forms of lipids to the membranous web, thus generating an environment supportive of HCV replication.

The extensive alterations to the ER membrane and the generation of the membranous webs induced by HCV increase phospholipids demand. Expression of phospholipid synthesizing enzymes is consistently upregulated during HCV infections (Diamond et al., 2010). This regulation is controlled, at the transcription level, by the SREBPs that drive uptake and synthesis of fatty acids as well as cholesterol synthesis (Waris, Felmlee, Negro, & Siddiqui, 2007). SREBPs are upregulated in response to HCV infection (Nasheri et al., 2013). The importance of fatty acid in HCV replication is also supported by the differential effect of the degree of saturation of exogenously added fatty acids. Addition of either saturated or mono-unsaturated fatty acids such as palmitic or oleic acids, respectively, enhances replication of HCVcc-JFH1 or HCV-1b(con1). In contrast, addition of poly-unsaturated fatty acids (PUFAs), such as alpha linolenic acid, inhibits HCV replication (Zhong et al., 2005). The inhibitory effect of PUFAs result from increases in lipid peroxidation. The addition of as antioxidant vitamin E rescues the HCV replication (D'Angelo et al., 2007).

Core and NS5A are essential in HCV assembly (Masaki et al., 2008). Both proteins contain a highly basic motif required for binding to HCV RNA (Appel et al., 2008; Boulant, Vanbelle, Ebel, Penin, & Lavergne, 2005). Core and NS5A should not localize to the replication complexes before HCV RNA replication as they would compete with the RNA-replication proteins. Accordingly, HCV core (Boulant et al., 2008) and to lesser extent NS5A (S. T. Shi et al., 2002) localize to the surface of cLDs at initiation of assembly. DGAT1, the enzyme involved in TG synthesis binds to both core and NS5A. It is thought that DGAT1 could facilitate core-NS5A interaction on the cLD surface (Camus et al., 2013). Production of HCV virions is tightly associated to ApoE, ApoB, ApoA1, and ApoC1

(Boyer et al., 2014; Gastaminza et al., 2008a; H. Huang et al., 2007). ApoE is the most determinant of the apolipoproteins for the assembly of HCV. HCV virions are neutralized by anti-ApoE and genetic depletion of ApoE inhibits assembly (Hueging et al., 2014). Although the level of virion ApoB is associated with infectivity, the use of Huh derived cell lines might underestimate the role of ApoB. To date, there is no cell line that can replicate HCV and produce authentic ApoB VLDL particles. The role of any individual lipoprotein in the morphogenesis of HCV virion in cell culture however, may not reflect well its actual involvement in the infected liver. MTP, which mediates the transfer of the neutral lipids from cLDs to assembling ApoB-containing particles, is also proposed to be implicated in HCV-induced steatosis (Perlemuter et al., 2002).



## **1.2 ADP-RIBOSYLATION FACTOR IN HCV LIFE CYCLE AND LIPID DROPLET HOMEOSTASIS**

### **1.2.1 ADP-ribosylation factors (Arfs)**

#### **1.2.1.1 Introduction**

The ADP-ribosylation factor (Arf) family is a group of small GTP-binding proteins essential for fundamental cellular processes. Arf1, the founding member of the Arf family, was initially identified as a host factor required for the ADP-ribosylation of the cholera toxin adenylate cyclase activator (Kahn and Gilman, 1986). Based on sequence homology, there are three classes of Arf proteins in mammals, class I (Arf1 and Arf3), class II (Arf4 and Arf5) and class III (Arf6) (Manolea et al., 2010). Along with Arf3, Arf4, and Arf5, Arf1 is the major Arf protein in the secretory pathways which initiate from the ER membrane through intermediates organelles and Golgi to the plasma membrane (Donaldson and Jackson, 2011). Arf6 primarily functions at the plasma membrane, where it is involved in endocytosis and cell migration (D'Souza-Schorey and Chavrier, 2006).

Arf proteins localize to different membrane in the cell, including the ER membrane, the plasma membrane, endosomes, and lysosomes. Binding of Arfs to GTP allows the insertion of the myristoyl group and the N-terminal amphipathic helix of Arf1 into the membrane (Antonny, Huber, Paris, Chabre, & Cassel, 1997). GTP binding induces also a second conformational change, which allows interactions with effectors proteins (Goldberg, 1998; Y. Liu, Kahn, & Prestegard, 2010). Not all Arfs require the GTP-bound status to bind to the membrane. Arf1 and Arf3 dissociate from membrane upon hydrolysis of GTP to GDP, but Arf6, and likely Arf4 and Arf5, still localize to the membrane in their GDP-bound state (Donaldson & Jackson, 2011). The guanine exchange factors (GEFs)

and GTPase activating proteins (GAPs) protein families of proteins catalyze Arfs GTP exchange or hydrolysis, respectively (Koumandou et al., 2013) (**Error! Reference source not found.**).

The Arf GEFs contain a conserved Sec7 domain which catalyzes the exchange of GDP for GTP (Chardin et al., 1996). The intrinsic GTP-hydrolysis activity of Arfs is negligible, but Arf GAPs contain a conserved zinc-finger domain that triggers the hydrolysis of the GTP-bound Arfs (Cukierman, Huber, Rotman, & Cassel, 1995). The specificity of GEFs and GAPs for Arf proteins is not entirely clear. The activity of small GTPases was evaluated by analyzing their binding to either GDP or GTP. GDP or GTP-bound Arf were considered to be inactive or active, respectively. Similarly, the GEFs and GAPs, which regulate the GTP/GDP exchanges and GTP hydrolysis, respectively, were considered as activators or inactivators, respectively. However, these descriptions may be not accurate.

#### **1.2.1.2 Arf GEF**

There are six subfamilies of Arf GEFs in human, comprising 15 individual GEF. The Golgi-specific brefeldin A-resistance GEF (GBF) subfamily, functions at the cis-Golgi and the brefeldin A-inhibited GEF (BIG) subfamily functions at the trans-Golgi sections of the secretory pathways (Donaldson and Jackson, 2011). The cytohesin subfamily, EFA6 and IQSEC/BRAG, function mainly in the endosome-to-plasma membrane trafficking pathways (Casanova, 2007; Gillingham and Munro, 2007). The FBXO8 GEFs, which is limited to vertebrates, contain an F-box in addition to the Sec7 domain (Gillingham and Munro, 2007). GEFs often are in an auto-inhibited state in the cytosol, to become activated upon recruitment to the respective membranes.

Acceptor membrane

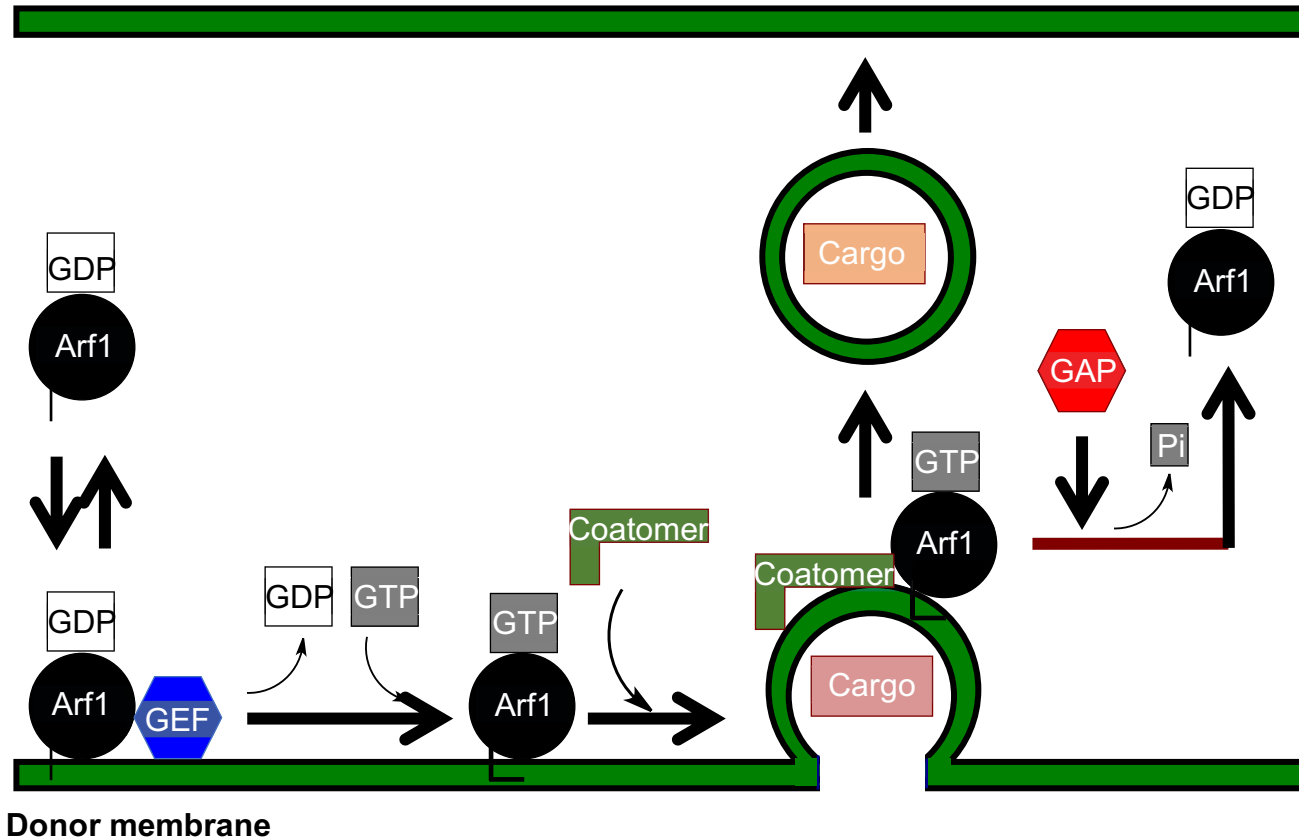


**Figure 1.8. Exchange of Arf1-GDP and hydrolysis of Arf1-GTP.**

Arf1 cycles between GDP and GTP-bound form. Exchange of Arf1-GDP for GTP is mediated by the interaction of GDP-bound Arf1 and guanine nucleotide exchange factor (GEF) leading to the release of GDP which allows binding of GTP. Binding of GTP to Arf1 leads to the firm insertion of the myristoyl-modified N-terminal amphipathic helix into the membrane. Arf1-GTP assembles the factors forming the vesicle coat. Hydrolysis of Arf1-GTP, which is mediated by GTPase activating protein (GAP), initiates events leading to the release of the cargo vesicle from the donor membrane. Arf1-GDP traffic with cargo vesicle to the target membrane where GDP is exchanged for GTP by GEF.

## **Arf GAPs**

There are 9 subfamilies of Arf GAPs in human, comprising 31 GAPs (Schlacht et al., 2013). The ArfGAP1 proteins possess amphipathic lipid packing sensor (ALPS) motifs, which mediate binding to curved membranes (Antonny, 2011). The primary role of ArfGAP1 is the release of the coat protein complex I (COPI) coated vesicles, which are formed by Arf1-mediated recruitment of coat proteins. Arf1-GTP and coat proteins induce membranes to adapt curvatures. When the curvature reaches the budding phase, ArfGAP1 binds to Arf1-GTP to activate hydrolysis of the bound GTP to GDP, stimulating events that lead to budding (Bigay et al., 2003). Besides activating hydrolysis of Arf1-GTP, ArfGAPs have other domains that allow for interactions with proteins in many signaling pathways. (Randazzo, 2007). Certain ArfGAPs containing ankyrin repeats and Src homology-3 (SH3) domains, such as ASAP3 or ARAP2, participate in focal adhesions and membrane ruffles. These ruffles have been proposed to be involved in metastasis (Randazzo et al., 2007; Sabe et al., 2006).

### **1.2.1.3 Arf effectors in vesicle trafficking**

The typical cascade of Arfs activation upon binding to GTP starts with the recruitment of coat proteins, lipid-modifying enzymes, tethers and scaffold proteins that influence membrane structure (D'Souza-Schorey & Chavrier, 2006). For example, GTP-bound Arf1 recruits the cytoplasmic coatomer complex I (COPI) to Golgi membranes, where it facilitates sorting of cargo proteins into transport vesicles. At the trans-Golgi network (TGN), the Arf proteins recruit the clathrin adaptor protein 1 (AP1), AP3 and AP4, and three Golgi-localized  $\gamma$ -ear-containing Arf-binding proteins 1 (GGA1), GGA2, and GGA3. These proteins help to incorporate the cargo proteins into the vesicles for sorting and

transport to destination (Nie et al., 2003). Arfs also recruit and activate several membranes and lipid modifying enzymes, such as the phospholipase D (PLD). PLD hydrolyzes PC to generate PA, a phospholipid that influences membrane curvature (Hong et al., 1998). Arf proteins may also recruit and activate several phosphoinositide kinases such as PI4P5K to generate PIP(4,5)P<sub>2</sub>, which is involved in several signaling pathways (Anna Godi & Cristiano Iurisci, 1999; L. Zhang et al., 2012). Arf1 recruits and activates PI4K to generate PI4P, a Golgi-residing lipid with an important role in Arf1-mediated functions in vesicular transport (De Matteis & Godi, 2004).

### **1.2.2 Arf and microbial infections**

Many intracellular pathogens require coordinated processes involving cellular membranes for their entry, replication, and spread. Entry of many pathogens occur through endocytosis or phagocytosis, therefore requiring membrane curvature and directional mobilization of actin. The creation of membrane curvature needs several small GTPases. Several intracellular pathogens have evolved mechanisms to exploit host factors involved in membranes or cytoskeleton modification of (Dautry-Varsat et al., 2005; Goody and Itzen, 2013; Hsu et al., 2010; Humphreys et al., 2013; Matto et al., 2011). *Legionella pneumophila* and *Rickettsia prowazekii*, human intracellular pathogens causing Legionnaires disease and endemic typhus, respectively, encode proteins known as RalF which act as an Arf1 GEF. RalF recruits and activates Arf1 at vacuolar structures where the bacteria replicate (Amor et al., 2005; Nagai et al., 2002). The activation of Arf6 at the plasma membrane to induce the macropinocytosis that facilitates entry of the enteric bacteria salmonella is another example (Humphreys et al., 2013). Arf1 and its GEF GBF1 have been shown to play roles in many viral infections, including

enteroviruses, HCV, influenza A virus, and coronaviruses (Verheije et al., 2008; Goueslain et al., 2010; Belov et al., 2008; Lanke et al., 2009;). The generation of altered membranous structures derived from the ER membrane to support their replication is a common feature among these viruses. They thus also all required Arf1 and its effectors involved in these membrane modifications.

Several steps of the viral replication occur in the vicinity of cellular organelles, including components of the endocytic or secretory pathways, and It is also very well-known that viruses induce alterations to the cell environment favorable for their replication (Lorizate & Krausslich, 2011; S. Miller & Krijnse-Locker, 2008; Scott, Snitbhan, Bancroft, Alter, & Tingpalapong, 1980). One of the common modification of the cellular environment is the manipulation of the lipid metabolism to create the membraneous structures induced by (+) ssRNA viruses (Stapleford & Miller, 2010). The two major membrane trafficking pathways in eukaryotic cells are the secretory and endocytic pathways (Tokarev et al., 2009). The secretory pathway facilitates the movement of newly synthesized proteins from the ER to the cell surface, either for secretion to the extracellular space or their insertion in the plasma membrane (Le Borgne & Hoflack, 1998; Ward, 2007). This pathway involves trafficking from the ER exit sites (ERES) through the ER-Golgi intermediate compartment (ERGIC) to the Golgi and then to the cell surface (Duden, 2003; Watson & Stephens, 2005). The endocytic pathway, conversely, facilitates the transfer of proteins from the extracellular space into the cells. internalized proteins are then transported to early or late endosomes depending on the fate of the internalized proteins (Grant & Donaldson, 2009). LDL is endocytosed after binding to the LDLr and then transported to the early endosome. In this compartment LDL dissociates, and the

LDLr is recycled back to the cell membrane. The endocytic pathway mediates the transport between endosomal compartments via vesicles that bud from the donor endosome and fuse with the target one.

One of the earliest indications of viral induced membrane alterations was demonstrated in EM micrographs of PV infected cells. It was described as a juxtanuclear clustering of a heterogeneous population of vesicles ranging in size from 70 to 400 nm in diameter (Howes, Melnick, & Reissig, 1956; Robbins, Enders, & Weller, 1950). Many, if not most viruses appear to induce similar effects on the endomembranous system. However, the molecular mechanisms of these membrane alterations have only recently started to be revealed. For instance, several members of the COPII complex colocalize with the PV induced vesicular structures (A. L. Richards, Soares-Martins, Riddell, & Jackson, 2014; Rust et al., 2001; Trahey, Oh, Cameron, & Hay, 2012). COPII vesicles may deliver host factors required for PV replication. Alternatively, COPII vesicles could deliver membrane modifying enzymes to mediate the formation of these vesicle that harbors PV replication.

Arf proteins and their regulators, most likely facilitate the replication of several viruses. Arf proteins localize to the virus-induced membranous structures and their inactivation by small molecule inhibitors or genetic depletion inhibits viral replication (Doyle, Hellard, & Thompson, 2012). Arf proteins are key regulators of membrane transport, they interact with several host factors that initiate vesicle formation by inducing membrane curvature. Arf1 primarily functions in the recruitment of the COPI complex, which mediates the Golgi-to-ER retrograde transport. Viruses modulates Arf proteins indirectly via interactions with the GEF or GAP regulators. The PV non-structural proteins

interact with different GEFs to recruits members of Arf family. While the PV non-structural protein 3A interacts with GBF1, 3CD interacts with the BIG 1 and 2, recruiting Arf5 or Arf1, respectively (Belov, Feng, Nikovics, Jackson, & Ehrenfeld, 2008).

HCV NS5A and NS5B interact with vesicle-associated-membrane (VAP), a multifunctional protein with roles the regulation of the retrograde COPI-mediated transport. VAP is essential for the formation of HCV replication complexes (RCs), and therefore, RNA replication (Hamamoto et al., 2005). VAP interacts with the membrane-associated phosphatidylinositol transfer protein 1 (PITPNM1), an important regulator of cell signaling, phospholipid metabolism, and membrane trafficking. VAP interactions with PITPNM1 contribute to ER alterations, leading to the formation of the HCV-induced membranous web.

The precise mechanisms of virus-induced membranous structure formation are not yet clearly understood. The induction of the heterogeneous vesicles requires phospholipid bilayers and membrane bending. Conical shape or scaffolding proteins, such as COPI/II (Nie et al., 2003) or clathrins (Hinrichsen, Meyerholz, Groos, & Ungewickell, 2006) induce membrane bending. Arf proteins possess an amphipathic helix at the N-terminus that also bends membranes (Beck et al., 2008). Thus, recruitment of Arf proteins by PV to the site of replication may facilitate membrane bending.

### **1.2.3 Arf and lipid droplets**

Arf1 plays a major role in the regulation of the lipid environment within cellular membranes. It facilitates the transfer of lipids between different membranous organelles at the membrane contacts sites. Aside from the vesicular transport mechanisms, Arf1 also recruits proteins that execute the transfer of lipids species, such as cholesterol and



sphingolipid precursors (Levine and Rabouille, 2005; Stefan et al., 2013; Voelker, 2003). Arf1 recruits lipid transfer proteins (LTPs) such as FAPP2 and OSBP at ER-Golgi contact sites to transfer glucosylceramide and sterols, respectively. FAPP2 and OSBP connect with the Golgi membrane, by binding to trans-Golgi-bound Arf1 and PI4P via their PH domain, and to the ER one, by binding to ER-bound VAP (Lev, 2010; Levine and Loewen, 2006; Mesmin et al., 2013). Nearly all members of Arf family participate in the regulation of structural and signaling lipids. Several Arf proteins activate membrane-resident phosphatidylinositol 4-phosphate 5-kinase (PIP5K) (Honda et al., 1999) or PLD (Cockcroft, 2009; Jenkins and Frohman, 2005). Both are essential enzymes in the generation of signaling lipid molecules that regulate many fundamental cellular processes such as rearrangement of cytoskeleton, migration, polarity, and endocytosis (Vicinanza et al., 2008). Arf1 also regulates the intracellular trafficking of sterols. It recruits and activates PI4K to generate PI4P, which in turn initiate the sterol transfer through LTPs (Mesmin et al., 2013). Arf6 is involved in the regulation of cell migration. It recruits and activate PIP5K at the plasma membrane to generate PtdIns(4,5)P<sub>2</sub>, which in turn induces the characteristic formation of plasma membrane ruffling in actively migrating cells (Honda et al., 1999).

The role of Arf family and its regulators and effectors in the metabolism of cLDs, has started to gain considerable importance only recently (Beller et al., 2008; Guo et al., 2008; Soni et al., 2009). cLDs consist of a neutral lipid core enclosed by phospholipid monolayer. They originate from the ER to eventually become separate organelles. cLDs respond to cell stimuli, growing, shrinking, fusing, fragmenting, clustering or dispersing (Klemm et al., 2013; D. Lohmann et al., 2013; Marcinkiewicz et al., 2006; Olofsson et al.,

2009; Orlicky et al., 2013). These processes mainly reflect responses to demands to modify lipid metabolism for energy needs or membrane rearrangement (Jambunathan et al., 2011). The different cLDs activities require efficient trafficking pathways to recruit and displace host factors to and from cLDs (Bartz, Zehmer, et al., 2007; Bouvet, Golinelli-Cohen, Contremoulins, & Jackson, 2013; Schulze et al., 2013). Arf1, its GEF GBF1, and COPI proteins were consistently identified in several genome-wide screenings for genes affecting the homeostasis of cLDs. Subsequent studies have demonstrated the role of individual factors in the metabolism of cLDs (**Figure 1.9**). Genetic depletion of Arf1, Arf1 GEFs, or components of COPI most often resulted in the accumulation of neutral lipids, likely by the inhibition of lipolysis (Beller et al., 2008; Guo et al., 2008). Arf1 and GBF1 may associate directly with cLDs in cell-based or cell-free assays (Bouvet et al., 2013; Ramaen et al., 2007). Arf1 status influences its affinity to bind or dissociate from cLDs. Similar to the role of Arf1 in the formation of transport vesicles, Arf1-GTP and COPI proteins associate with cLDs and in the presence of ArfGAP1 could mediate the budding of 60–100-nm diameter droplets from artificial droplets. Replacing Arf1-GTP with Arf1-GDP in the assay inhibited the association with cLDs and therefore, the budding of droplets (Thiam et al., 2013).

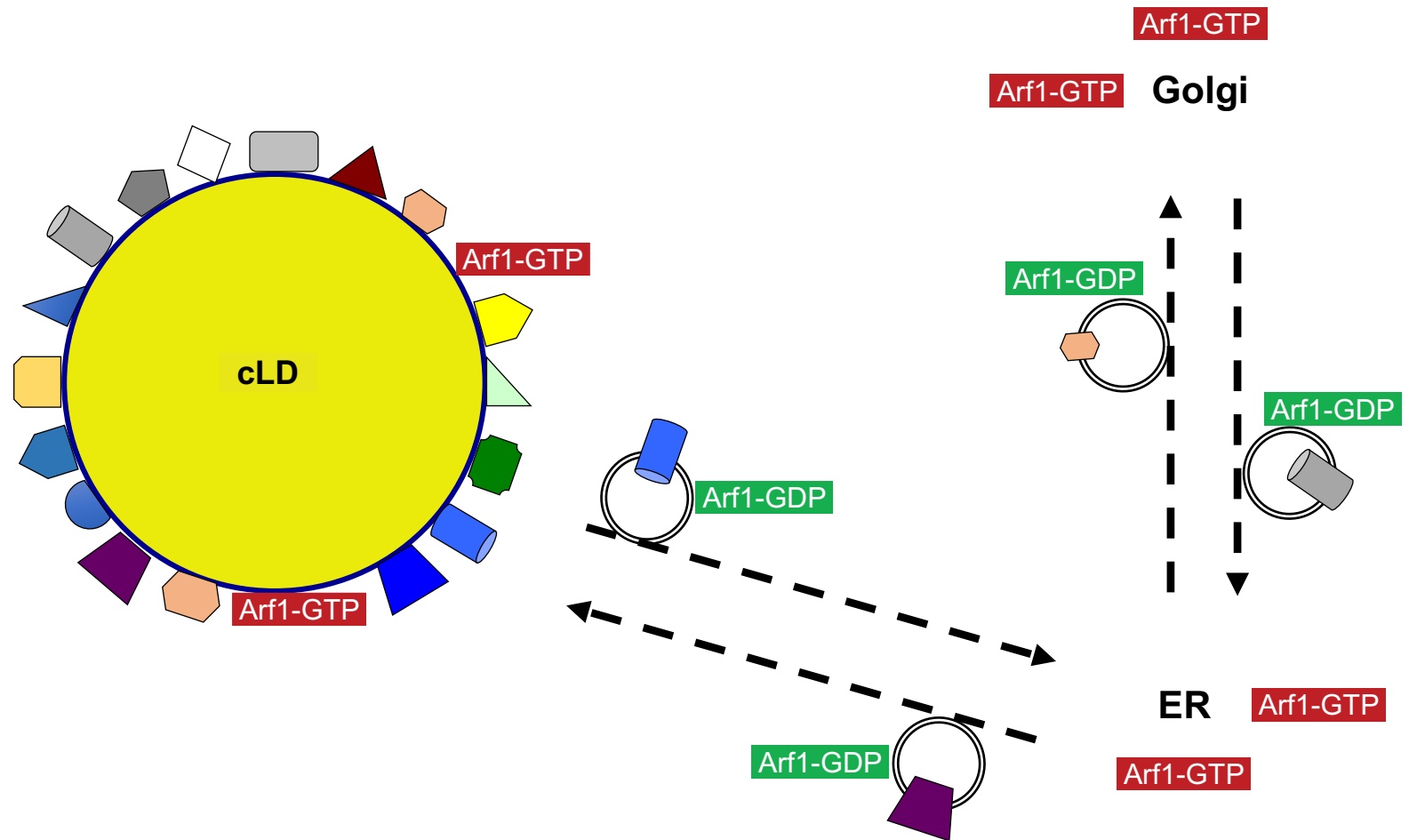


**Figure 1.9. A schematic presentation of the role of Arf1 on proteins trafficking to and from cLD.**

Cycling of Arf1 between ER and Golgi mediates the transport of the membrane vesicles through the secretory pathway. Arf1-GTP is bound to membranes while Arf1-GDP is dispersed in transit between the donor and target membranes. Arf1 is involved in binding and dissociation of host factors to and from cLD. Arf1-GTP binds to cLD and dissociates upon hydrolysis into Arf1-GDP by ArfGAP1 which also bind to the cLD. Cycling of Arf1 between GTP and GTP bound statuses regulates the set of 150-300 host proteins present on the surface of cLD at any given moment.

## **1.3 DIRECT CELL-TO-CELL HCV SPREAD**

### **1.3.1 Evidence**

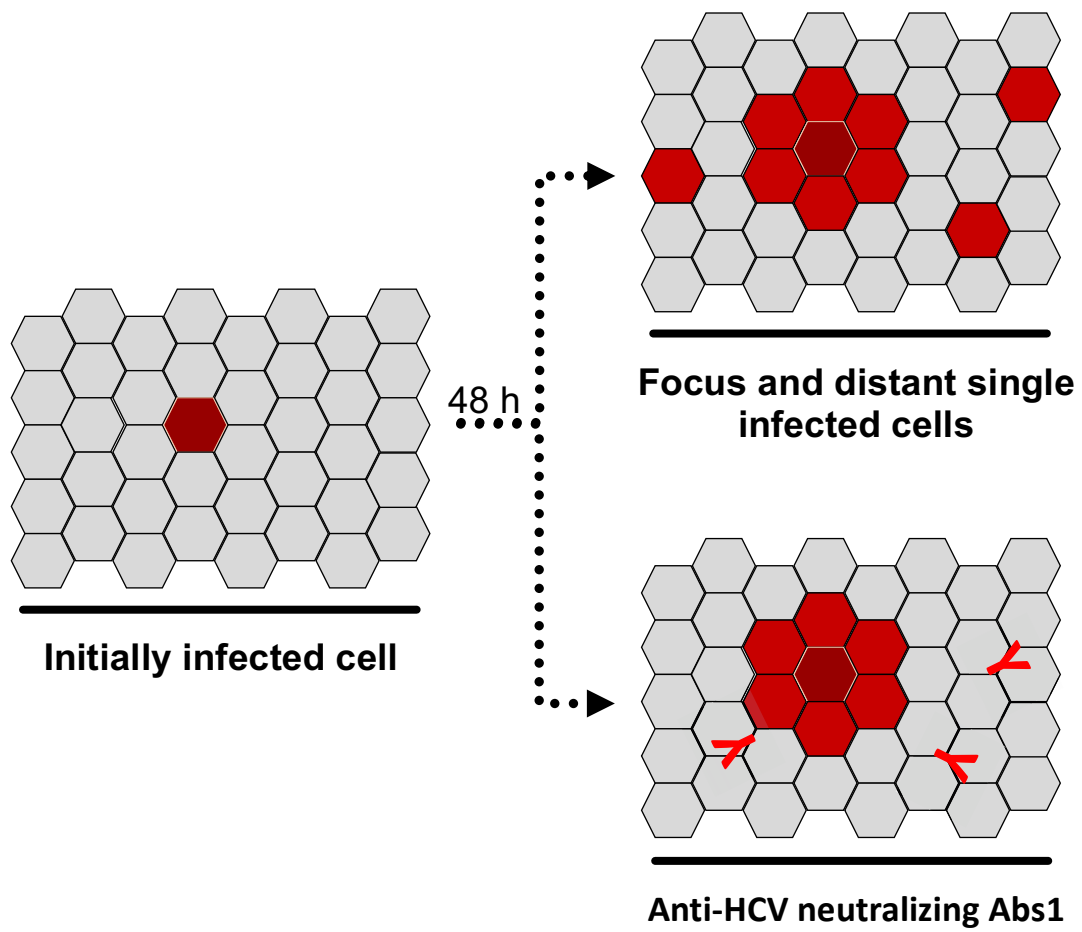
Direct cell-to-cell spread of HCV infection refers to the direct transmission of infection between adjacent cells without the release of the infectious virions into the extracellular space and reinfection of neighboring cells. The latter is known as an entry of cell-free virions. Entry of cell-free virions requires assembly and egress of infectious viral particles. For (+) ssRNA viruses, theoretically, a productive infection could be established by delivering just the genomic material into a permissive adjacent cell. Direct transmission of HCV RNA between cells may be more efficient than transmission by released cell-free virions (Longatti, Boyd, & Chisari, 2015; Mittelbrunn & Sanchez-Madrid, 2012; Y. Zhang et al., 2016).

Cell-to-cell direct transmission of HCV as a mode of infection between adjacent cells was proposed early on as a major route for HCV spread within the infected liver. The proposition was based on the morphological characteristics of HCV spread pattern in the histological analysis of biopsies from infected livers (Agnello, Abel, Knight, & Muchmore, 1998; Gosalvez et al., 1998). Like other members of the Flaviviridae family, HCV replication involves the formation of replication intermediate negative-sense RNA strands from the genomic (+) ssRNA RNA strands (M. Chang et al., 2000; Pal et al., 2006). Replication intermediates in a cell indicates active replication and synthesis of genomic RNA (King et al., 2002; Shulla & Randall, 2015). The positive- and negative-sense strands of HCV RNA were detected in infected hepatocytes by in situ hybridization (Ming Chang et al., 2003). The relative abundance and spatial distribution of the two strands were different, suggesting that pattern of HCV infection within the liver is compartmentalized

(Y. Liang et al., 2009). The (+) ssRNA cells ranged from 5-90%, whereas the negative-sense RNA cells ranged from 5 to only 25%. It appears that only a subset of all infected cells is actively replicating the virus at any given time. There was a gradient of HCV (+) ssRNA staining signal radiating from the most intense signals in the center of the image. The staining intensity over the distance from the most intense signal was inversely correlated ( $R^2=0.92$ ) (Agnello et al., 1998; Ming Chang et al., 2003; Gosalvez et al., 1998), which constitutes an indication of the focal spread of the infection. The focal spread is most consistent with replication starting in the cell at the center of the focus then spreading outward to cells in direct contact.

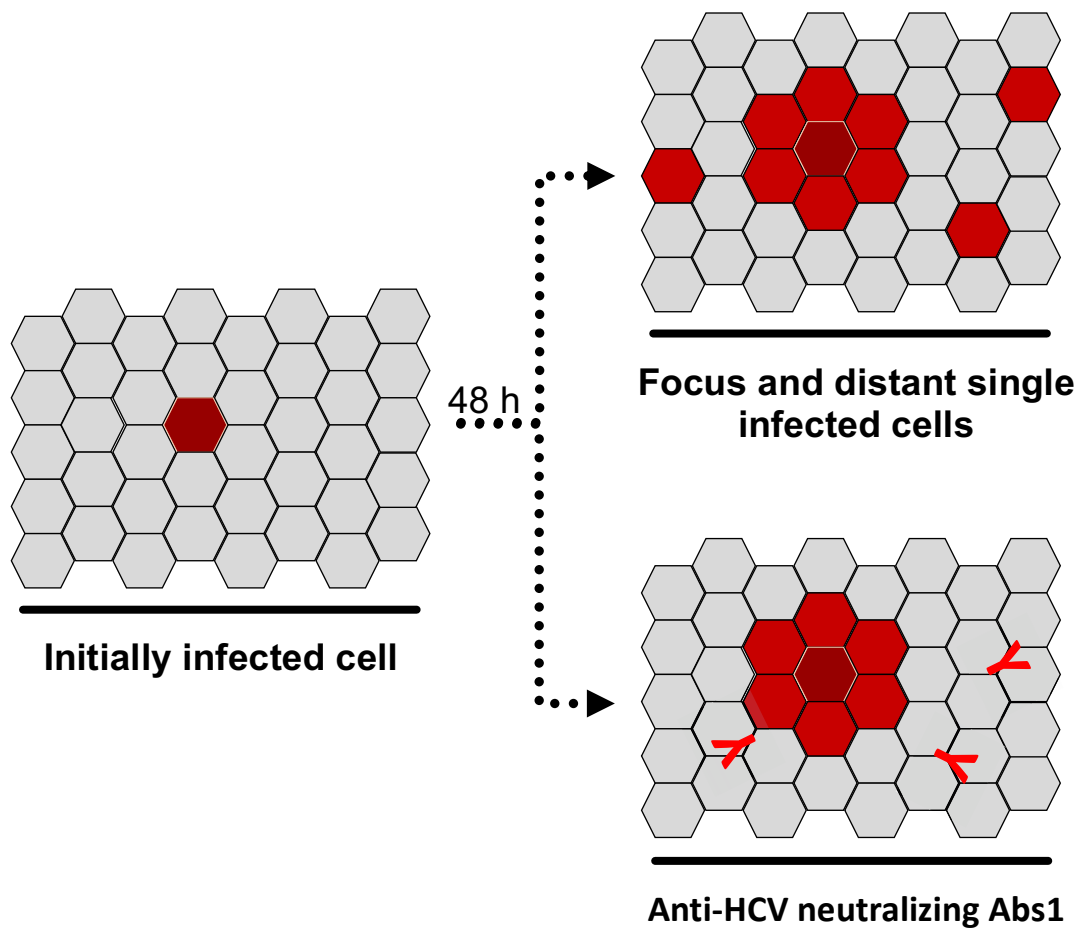
HCV (+) ssRNA was also detected in fibroblasts and macrophages in the surrounding connective tissue. However, intermediate negative-sense RNA showed focal distribution exclusively in hepatocytes. Consistently, the percent of hepatocytes with an HCV (+) ssRNA was higher (28-86%) than that with intermediate negative-sense RNA (4-25%) (M. Chang et al., 2000; Ming Chang et al., 2003). The frequency of intermediate negative-sense RNA is directly correlated with liver injury as evidenced by hepatic inflammation profile (G. Li et al., 2013; Mishiba et al., 2013). Samples from patients with HCV-related cirrhosis had higher percent of intermediate negative-sense HCV RNA positive cells than samples from patients with minor lesions (Mishra et al., 2006).

The proposal of cell-to-cell spread has been also demonstrated in vitro by infection at low moi. Infection spread appears as foci and single infected cells. Addition of anti-HCV neutralizing antibodies inhibits the infection of cells at distant from foci. (



Figure

1.10).



**Figure**

### 1.10. Spread of HCV infection.

Infection of Huh7.5 cells with HCV-JFH1 for 48 h results in foci composed of approximately 15-30 contacting infected cells and single infect cells at distance from foci. Addition of anti-HCV neutralizing antibodies inhibit infection of distant cells but not the foci formation. It was proposed that cells at distant from foci are infected by virions released into culture supernatant

### **1.3.2 Experimental approaches**

An experimental approach that test specifically for cell-to-cell spread of HCV has yet to be developed. Demonstration of HCV infection transmission directly between adjacent cells requires of several parameters. Infected and uninfected cells need to be in direct contact which means cells at complete confluence at the start of the assay. Cells seeded at low or high density differentiate variably, affecting the order of the cell structures and functions (Granneman, Moore, Krishnamoorthy, & Rathod, 2009). HCV infection, like that of any virus, at different densities affect the spread of the infection and therefore, produce different size foci (Brimacombe et al., 2011b; Timpe et al., 2008). The longer the cells stay in direct contact, the higher the expression of the cell contact factors, like tight junctions, that participate in HCV entry and cell-to-cell spread (Granneman et al., 2009). The type of cell line used in the assays to attempt to characterize HCV cell-to-cell spread has resulted in different results (Brimacombe et al., 2011a; Timpe et al., 2008; Witteveldt et al., 2009). Hepatocytes are highly specialized and polarized cells concerning metabolism and secretion of lipids, which is likely critical for the natural spread of HCV infection between cells (Brazzoli et al., 2008; Decaens, Durand, Grosse, & Cassio, 2008; Harris et al., 2008; Mee et al., 2009). Unfortunately, cultured primary hepatocytes are not permissive for HCV infection and lose their normal polarity and architecture. Cell lines of hepatic origin are essential to recapitulate as close as possible the mechanism of transmission of HCV between cells. Infection by entry of cell-free virions must be inhibited. Several approaches have been employed to this end. The most widely used one is the use of neutralizing antibodies. HCV cross neutralizing antibodies activity across multiple genotypes are rare. They are unavailable commercially, and only a few labs worldwide



have produced. Cell lines that are refractive to entry of cell-free virions but can be infected when co-cultured with infected cells can be used as well. These cell lines are of hepatic origin, like HepG2 (Valli et al., 2007) or variants of Huh7.5 expressing low levels of CD81 (Brimacombe et al., 2011a) or non-hepatic cells like B-lymphocytoid cells (Valli et al., 2006) and 293T (Timpe et al., 2008) or Hela (Timpe et al., 2008). Such cells cannot be used evaluate any role CD81 or its signaling pathways. Non-hepatic cell line does not provide the hepatocyte-specific cellular factors required for effective cell-to-cell HCV transmission. A single report used semi-solid media overlay to show that infection was confined to foci of adjacent cells, compared to foci and distant infected cells (secondary infections) in liquid media (Timpe et al., 2008). The extracellular infectivity was not evaluated, and this report has not been replicated. Semisolid media limits the diffusion of cell-free virions resulting in the confined spread of infection to neighbouring cells. Absence of secondary infection can result from slowed diffusion or from or from lack of cell-free virion infectivity.

The role of HCV entry factors in cell-to-cell spread was primarily tested by antibodies against entry receptors (Fofana et al., 2013; Ji et al., 2014) or by genetic methods, such as transient or stable knockdown (Barretto, Sainz, Hussain, & Uprichard, 2014; Fan et al., 2017a; Z. Liu & He, 2013; Meredith, Zitzmann, & McKeating, 2013; Zhao et al., 2017). Conversely, host factors to confer have also been tested by their ectopic expression in cells that do not express them (Brimacombe et al., 2011a; Gondar et al., 2015; Hueging et al., 2014). Small molecules that inhibit the function or the cellular localization of HCV entry factor have also been used to test cell-to-cell spread (Barretto et al., 2014; Xiao et al., 2014; Xiao et al., 2015).

To recapitulate the real infection transmission between cells, co-culture of HCV donor and target cells to study cell-to-cell spread should be done at low ratio using donor cells population with synchronized infected. Under a proper condition of the assay, single donor cell should transmit the infection to every adjacent target cells. Cell-to-cell spread of HCV has been characterized using co-cultures. HCV infected cells, which serve as the donors of the infection, are co-cultured with uninfected cells, which serve as the target for the infection. The host factor under study is manipulated either in the donor or target cells before co-culture (Hueging et al., 2014; Z. Liu & He, 2013; Meredith et al., 2013), or in both during the co-culture (Barretto et al., 2014; Xiao et al., 2014; Xiao et al., 2015). These models have resulted in some inconsistencies in the findings (Barretto et al., 2014; Catanese, Loureiro, et al., 2013; Gondar et al., 2015).

Either donor or target cells are labeled to differentiate between the two cell populations (Gondar et al., 2015; Xiao et al., 2014; Zhao et al., 2017). Detection of infection is by immunofluorescence labeling of an HCV viral protein in two sets, one at the beginning and another at the end of the co-culture. Subsequently, infected cells are visualized and imaged using immunofluorescence microscope (Barretto et al., 2014; Gondar et al., 2015; Mathiesen et al., 2015; Zhao et al., 2017) or by flow cytometry (Brimacombe et al., 2011a; Z. Liu & He, 2013; Witteveldt et al., 2009; Xiao et al., 2014). Immunofluorescence provides several advantages over FACS. First, it allows the evaluation of transmission by the foci that are composed of a HCV donor cell in the center surrounded by infected target cells (Fan et al., 2017b; Gondar et al., 2015). It enables the parallel assessment of inhibition of cell-free virion infection, which show as satellite infections lacking a donor cell and producing small foci (Timpe et al., 2008; Zhao et al.,

2017). It also facilitates a quantitative analysis of spread by analyzing the number of infected target cells per focus containing a donor cell (Barretto et al., 2014; Zhao et al., 2017). Detection of HCV infection transmission by flow cytometry potentially offers precise quantitative assessment, it requires losing the spatial information about the physical location of donor and recipient cells.

### **1.3.3 Mechanisms**

The molecular mechanism of HCV cell-to-cell spread remains largely uncharacterized. Nearly all the studies of HCV cell-to-cell spread targeted host factors involved in the entry of cell-free virions, based on the assumption that the host factors involved in entry of cell-free virions may also participate in cell-to-cell spread. Some pieces of evidence from the infected liver suggested that cell-to-cell spread may potentially a major route for transmission between hepatocytes prompted many studies in the potential mechanism. However, most results are inconclusive and not always consistent (Brimacombe et al., 2011a; Fofana et al., 2013; Timpe et al., 2008; Witteveldt et al., 2009). The inconsistencies may just highlight the complexity of the molecular mechanism, likely involving the coordination of multiple host factors.

The receptors, CD81 and SR-B1 (Fofana et al., 2013), the tight junctions OCLD-1 and CLDN (Brimacombe et al., 2011a), the apolipoproteins E and B (Gondar et al., 2015; Hueging et al., 2014), and the cholesterol transporter NPC1L1 (Barretto et al., 2014) have all been tested for their potential roles on direct cell-to-cell transmission. The results have been varied. CD81 was found to be required for HCV cell-to-cell spread in two studies and dispensable in two others. Knockdown of CD81 for 48 h in the target cells then co-culture for 24 h with donor cells, inhibited cell-to-cell spread by 72% (Z. Liu & He, 2013).

However, RNA of HCV-W529A, a mutant defective in E1E2-CD81 interaction which is non-infectious as cell-free virions, electroporated into donor cells and co-cultured with naïve cells spread to 12 or 20% Huh7.5 or Huh7.5-lunet cells, respectively (Witteveldt et al., 2009). Ectopic expression of CD81 in target Huh7.5-lunet cells increased cell-to-cell spread from 0.9 to 14% (15-fold) (Brimacombe et al., 2011a), but treatment of target cells with anti-CD81 reduced cell-to-cell spread to only 1-fold (Timpe et al., 2008). Cell-to-cell spread to HepG2 or HeLa, which are refractory to entry of cell-free virions due to absence of CD81 was 5.5 or 0.3%, compared to 35.7% in Huh7.5 (Timpe et al., 2008). Cell-to-cell spread is inhibited when CD81 is targeted cells in the target but not in the donor cells. CD81 may be involved in low pH dependent HCV fusion (Onlamoon et al., 2011). Such role would affect the establishment of infection in the target cell but would not affect the donor cell. This model requires that cell-to-cell spread involves enveloped virions, which is not yet known. Virion maturation through the lipoprotein secretion pathway was apparently not required for cell-to-cell spread (Gastaminza et al., 2008a; Nahmias et al., 2008). Two independent studies targeting SR-B1 in target cells, one by siRNA knockdown (Z. Liu & He, 2013) and the other by anti-SR-B1 (Brimacombe et al., 2011a) antibody, both inhibited cell-to-cell spread by 68% and 80%, respectively.

Until now, inhibition of cell-to-cell spread by small molecule that do not affect replication has not been reported. Ezetimibe, a small molecule that targets NCP1L1 (cholesterol transporter), has been reported to block HCV cell-to-cell spread by monitoring foci formation in non-dividing cells treated 16 h after infection (Barretto et al., 2014). However, ezetimibe had been previously identified and characterized as an HCV entry inhibitor (Sainz et al., 2012). Ezetimibe thus likely inhibited subsequent rounds of

infection by blocking virion entry into the target cells. Erlotinib, a small molecule inhibitor of EGFR, was reported to play a role in cell-to-cell spread of HCV (Lupberger et al., 2011; Xiao et al., 2015). However, siEGFR and erlotinib inhibited entry of cell-free virions by targeting post-binding steps that include CD81-CLDN1 interaction and viral fusion (Diao et al., 2012).

The current models for HCV assembly and egress state HCV core protein associates with cLDs nearby the HCV replication complexes (Shavinskaya, Boulant, Penin, McLauchlan, & Bartenschlager, 2007b), whereas the HCV envelopes glycoproteins E1 and E2 are tethered to the inner ER membrane leaflet. Core protein and HCV RNA are packaged into the E1E2 coated ER regions, which that are eventually enclosed and bud into the ER lumen (Blanchard et al., 2003). From there, the enveloped virions follow the VLDL maturation and secretory pathway, which uses the ER-Golgi anterograde transport pathway (H. Huang et al., 2007).

#### **1.3.4 Roles of cell-to-cell spread**

The acute HCV infection is characterized by a rapid increase in HCV RNA within the first three weeks, reaching a peak of approximately  $10^5$  to  $10^7$  IU/ml. The levels of alanine aminotransferase (ALT) in blood, an indicator of liver injury, rise between 4 to 12 weeks. Any clinical symptoms start to appear 2 to 12 weeks after infection, although acute HCV infection is generally asymptomatic. Up to 80% of acutely infected individuals present with only non-specific symptoms. Jaundice occurs in 50 to 84% symptomatic patients. Clearance of infection has been estimated to occurs from 1 to 2 weeks up to 1 to 3 years. Seroconversion occurs 4 to 6 weeks after the onset of viremia. Approximately 20 to 40% of infected individuals clear the infection spontaneously, whereas up to 80% develop

chronic infection. The transition of acute to chronic HCV infection is defined by sustained viremia for more than six months after detection.

The identification of the factors associated with spontaneous clearance or progression to chronicity has proven to be a challenge. Several models have been proposed to predict the outcomes of HCV infection. These models are based on demographic, immunological, or virological differences. Testing these models yields varied results. No factor firmly associated with HCV infection outcome has been identified. The hurdles to defining reliable predictors for the outcomes of HCV infection include the usually asymptomatic nature of the HCV infection. Most of the infections are first diagnosed only during the chronic phase. The rate of progression to chronic HCV infection maybe directly related to age. In Italy, the chronicity rate was 56% for ages 12 to 25 or 87% for patients older than more than 25 years. Chronicity rate in women was lower than in men in this retrospective study. However, a subsequent large-cohort study demonstrated no difference in gender in the progression to chronic infection. Also, Caucasians and Hispanic white may have a lower rate of chronicity that African-Americans.

Individuals who spontaneously clear acute HCV infection develop robust and broad CD4<sup>+</sup> and CD8<sup>+</sup> responses that are specific for multiple epitopes of structural and non-structural HCV proteins. The adaptive cell-mediated immune (CMI) responses is considered essential for the elimination of the acute infection. However, only 20% of resolvers developed HCV specific CD4<sup>+</sup> and CD8<sup>+</sup> responses. Depletion of CD4<sup>+</sup> cells in chimpanzee resulted in progression to chronic HCV infection, while that of CD8<sup>+</sup> did

not. However, both cell types appear to be required to clear acute HCV infections in human or mice.

Only limited studies have analyzed the virological factors involved in the progression into chronic infection have been published. The attempts to relate the viral load, dynamic of replication, mutation rate or breadth of quasispecies to the development of chronic HCV infection or the severity of liver damage did not produce solid results. Several relationships were made between genotypes or strains and persistence of HCV infection based on single case reports. The role of HCV infectious dose, the source of infection, or the mechanism of spread in the liver have rarely been discussed. Specific immune responses are essential for long-term protection against pathogenic microbes. Specific cell-mediated and humoral immune response are produced upon antigen presentation and stimulation by organ-resident phagocytes. The specific immune response protects against subsequent exposure to the same virus if the responses were mounted against conserved epitopes.

HCV infection results in the induction of HCV-specific cell-mediated immunity (CMI) in the absence of viremia and anti-HCV antibodies (Scognamiglio et al., 1999). Seronegative individual presenting HCV-specific CMI are often observed among spouses of infected individuals, (Bronowicki et al., 1997), healthcare workers with needle-stick injury (Koziel, Wong, Dudley, Houghton, & Walker, 1997), injection drug users who share needles (Freeman et al., 2004; Mizukoshi et al., 2008), household contacts of infected individuals (Al-Sherbiny et al., 2005), siblings of children with chronic HCV infection (Hashem et al., 2011), prisoners (Post et al., 2004), and children born to infected women (El-Kamary et al., 2013). These groups of people infected with HCV are aviremic and

seronegative, but they mount CD4<sup>+</sup> and CD8<sup>+</sup> responses similar in strength and breadth to the HCV epitopes to that mounted by acutely infected individuals who spontaneously clear the infection (Kamal et al., 2004). These protective responses could persist as long as two decades (Takaki et al., 2000). Chimpanzees who recover from transient low-level HCV viremia clear an ensuing infection rapidly. The elicited CMI responses were the most robust against the non-structural proteins NS3, NS4A, and NS4B. These proteins are critical for replication (such as the protease NS3/4A) or membrane modifications (NS4B) (Paredes & Blight, 2008). Thus, early robust CMI response could inhibit HCV replication, allowing the host to clear the infection. This phenomenon is not only pertinent to HCV as a group of commercial sex workers in Kenya, which are heavily exposed to HIV, appear to be immune to HIV infection (Alimonti et al., 2006; Fowke et al., 1996; Kaul et al., 2004). Thus, repeated exposure to low dose HCV may elicit protective and long-term CMI that rapidly clear the infection after each exposure.

Uninfected chimpanzee where they were successively challenged with 1, 10, or 100 chimpanzees infectious unit of HCV-1b every six months. Infection with 1 or 10 infectious unit elicited HCV-specific CD4<sup>+</sup> and CD8<sup>+</sup> response while the chimpanzees remained aviremic and seronegative. Infection with 100 infectious units elicited comparable CMI response, but the responses were associated with viremia, seroconversion, and the typical (in chimpanzees) 50% progression rate to chronicity (Shata et al., 2003). The challenge with 100 infectious unit increased the level of cell-mediated responses elicited upon exposure with 1 or 10 infectious units. Thus, a dose-threshold appears to exist to the establishment of HCV infection and elicitation of protective and long-term HCV-specific cell-mediated immunity. Exceeding the dose



threshold that produces protective immune response would result in viremia and seroconversion associated with acute HCV infection. Based on increase above the protective threshold, acute HCV infection could be cleared or progress into chronicity. Beside these dose thresholds, there are many potential effects of other factors related to the demographic or immunological status of the infected individuals. The protective immune response elicited due to exposure to low infectious dose varied among certain groups, such as healthy (e.g., couples, household contacts, healthcare worker) or likely not healthy (injection drug user). The efficiency of the immune response to HCV infection enables it to eliminate the infection up to a particular dose, above which HCV infection outpaces it, leading the viremia and seroconversion.

The vast majority of acute HCV infections are asymptomatic or present with only non-specific symptoms. However, there are a few severe cases of acute HCV infections, fulminant hepatitis (FH), have been reported. FH is characterized by rapid deterioration of liver function and hepatic encephalopathy. FH can be idiopathic or induced by drug toxicity, but viral infections are the most prevalent cause. HBV or HAV are the most frequent FH etiologic agents. NANB-associated FH were as frequent as that caused by HBV or HAV. HCV-associated FH has been reported mainly from individuals who received blood transfusions before the implementation of the HCV screening of a blood. The determining factors, and the mechanism, of HCV-associated FH are not entirely known. However, the onset of HCV-associated FH shortly after transfusion was a common clinical factor. In addition to post-transfusion, HCV-associated FH occurs upon infection of individuals who were already infected with HBV or HAV. The average risk of HCV-associated FH in 39 participants positive for HBV surface antigen and underlying

chronic HBV 23% and of 2.9% in individuals who did not. Development of FH did not correlate with HCV genotype, HCV RNA titre, age or gender. Clinical and virological status of those with underlying chronic HBV did not correlate with the development of FH, either (Chu, Yeh, & Liaw, 1999). 62% of 29 participants infected with HBV or HAV who presented with FH tested positive for HCV RNA or anti-HCV antibodies before plasma exchange. The FH mortality rate was as high as 89% in HCV viremic or seropositive individuals compared to 42% of patients who are neither (Yanagi et al., 1991). HCV infection produces neutralizing anti-HCV antibodies and high-level viremia. HCV virions in the blood products from infected donors would thus contain HCV-anti-HCV immune complexes. Injection of this exceptionally high level of immune complexes would exceed the clearance capacity of the phagocytic cells. The immune complexes would then be deposited in the liver and may be other organs, eliciting complement activation, severe local inflammation and the ensuing lesions. Histopathological assessment shows massive hepatic necrosis marked by collapsed reticulin with no viable hepatocytes in between. Viable hepatocytes are seen in other acini. (Farci, Alter, et al., 1996). The extent of the liver damage in such a short period post-transfusion with HCV contaminated blood appears to correlate with the exceptionally high-level HCV immune complexes.

The relationship between HCV infectious dose and the dynamics of infection spread within the infected liver may not have been studied. The variation in the virological characteristics may have hurdled the standardization of infection outcomes. The average estimate of HCV infected hepatocyte is 10 to 40%, although as low as 1.7% or as high as 100% have been reported. The HCV +ssRNA was estimated at ten copies per infected hepatocytes, with a range of 1 to 100 copies per infected hepatocytes. The daily output

of HCV virions in chronically infected individuals has been consistently reported to be approximately  $10^{12}$ , while that during the acute infection varies 1,000-fold. The number of virions produced per infected hepatocyte is between 1 to 50, and the specific infectivity of the HCV virions released from infected liver was reported between 1 to 0.01.

The minimum infectious dose of HCV that results in detectable viremia is hardly possible to determine in human. In chimpanzees, it is 100 HCV infectious units. The human liver consists of approximately  $1 \times 10^5$  acini. Infecting human liver with 100 HCV infectious units would infect a single cell in an equivalent number of acini by more than 99% probability. Considering a specific infectivity of 1 and a daily output of 1 virion per infected hepatocyte could theoretically infect every acinus in less than a month with increasing moi after each round of replication. Such scale of infection in such a short period may result in severe liver damage. However, only 20 to 40 % of the liver is infected during two decades of chronic infection. It appears that a dose-dependent HCV-host response interaction balance determines the outcome of the HCV infection. The infectious dose and the virions released into the blood-stream would infect hepatocytes in isolated acini. The phagocytic capacity may not be able to cope with the rate of initial HCV infection spread. The effector functions of CMI response may be counter measured by viral factor, or eventually exhausted after continuous stimulation. The neutralizing antibodies prevent the cell-free infections after the initial weeks. Because acini are individually vascularized and separated by connective tissue, the infection may persist in any acini during this period and before the appearance of the neutralizing antibodies. HCV cell-to-cell spread appear to allow for the persistence of HCV infection with minimal damage to the liver.

Thus, HCV cell-to-cell spread could be the predominant mechanism of infection transmission in chronic infection.

## 1.4 MODEL AND HYPOTHESIS

Several aspects of intrahepatic HCV infection dynamics remain elusive, including the primary route of infection spread. In most patients, HCV RNA can be detected in blood within the first two weeks after acquisition of infection followed by 8 to 12 days of exponential replication. The peak level of HCV RNA reaches plateau 3 to 4 weeks after infection. At this peak level of replication, the infected liver produces  $10^{10}$  to  $10^{12}$  virions per day. This level of viremia remains through the months of the acute, and the years of chronic, HCV infection. Considering the number of hepatocytes in the human liver, amount of HCV virions produced by each infected cell, the specific infectivity of the released virions, and the percent of infected hepatocytes during chronic infection, the establishment of acute infection with 100 infectious virions would produce an average of 5 infectious virions per day. The produced infectious virions would infect the entire hepatocytes within approximately 7 to 8 weeks. This magnitude and rate of infection spread would result in a massive inflammatory response. However, clinical manifestations of liver damage start to appear two years after infections then progress into advanced stages resulting in hepatic cirrhosis after 20-25 years, at which only ~20% of the liver hepatocytes are infected.

The ratio of the infectious dose to the number of hepatocytes within human liver would most likely results in the infection of individual acini. After a couple of rounds of replication and before complete neutralization of released virions by anti-HCV neutralizing antibodies, a certain number of acini are individually seeded with a single infectious virion. The neutralizing antibodies of virions in the bloodstream and the connective tissue barrier between acini would prevent the infection of more acini. The infection spreads within

hepatocytes in initially seeded acini, and by 20 to 25 years, approximately 20% of the liver hepatocytes are infected. This percentage of spread resulted from the balance between cell division, infected cell death, and infection of new hepatocytes.

Infected hepatocytes in liver biopsy samples of patients chronically infected with HCV are distributed in clusters. Characterization of the internal structure of these clusters showed that individual clusters range in size from 4 to 50 infected cells. Also, the content of HCV RNA decreases from the cell that presumably founded the cluster to the cells at the maximal cluster extension. These observations may indicate that HCV infection in the liver is seeded randomly from the blood and then spreads locally.

I hypothesize that HCV spread preferentially by direct cell-to-cell transmission between hepatocytes within the infected liver. Characterization of HCV infection spread in human and chimpanzee's livers by direct visualization of infected cells in biopsy samples or by mathematical modeling of infection dynamics suggested that HCV infection may spread by cell-to-cell transmission. Subsequent characterizations of HCV infection spread in vitro have corroborated the in vivo observations. HCV infected cells release approximately 5% of the infectious progeny virions into the bloodstream. Thus, intracellular infectivity may favor efficient spread between directly between cells and that the released 5% may egress the cell via an inefficient pathway. The molecular mechanisms of the proposed cell-to-cell spread and the release pathway remain inadequately characterized. I plan to test the hypothesis that HCV may spread preferentially by direct cell-to-cell transmission, evaluate the efficiency of infection spread in a situation where the infectivity of the released virions is inhibited such as in the

presence of anti-HCV neutralizing antibodies, and characterize the involved molecular mechanisms.

## CHAPTER TWO: Materials and methods

### 2.1 MATERIALS

#### 2.1.1 Compounds

1-benzyl derivatives of 5-(arylamino)uracils were synthesized by Dr. Mikhail Novikov (**Figure 2.1**). The compounds were synthesized based on lead scaffolds (Maruyama et al., 2004; Nair et al., 2007), within the aromatic fragment relocated from C-6 or N-3 to C-5 of the uracil and a nitrogen into the bridging group. Test compounds were supplied as powder and the stocks were prepared at 10 to 100  $\mu$ M in DMSO as solubility allowed. Stocks were aliquoted into 20  $\mu$ l and stored at -20°C. Frozen aliquots were thawed rapidly at 37°C in a water bath. Stocks were further diluted in DMSO or directly in culture media such that the final concentration of DMSO in the media in contact cells does not exceed 0.2%.

#### 2.1.2 Chemical and general reagents

Bovine serum albumin and normal goat and donkey sera were obtained from abcam (Cambridge, MA). Cell-culture grade oleic acid (OA)-albumin solution (2 mol OA/mol albumin, 100 mg/ml BSA) from bovine serum, OA powder, and methylthiazolyl-diphenyl tetrazolium bromide (MTT) were obtained from Sigma (St. Louis, MO). Pierce™ 16% methanol-free formaldehyde (w/v) was obtained from Thermofisher (Waltham, MA), cOmplete, EDTA-free was obtained from Roche Diagnostics GmbH (Mannheim, Germany), Tween-20, 4x Laemmli sample buffer polyacrylamide gel components, polyvinylidene fluoride (PVDF) membrane, and Clarity™ Western ECL Substrate reagent were obtained from Bio-Rad (Hercules, CA).



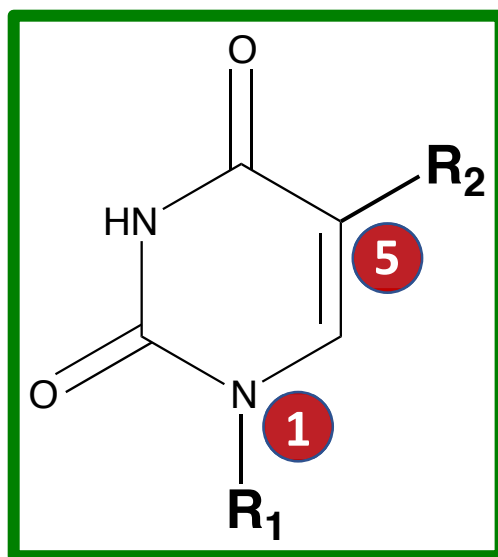


**Figure 2.1. Small molecule scaffold diaryl-substituted uracil to test for antiviral activity.**

The scaffold is a heterocyclic aromatic compound containing two nitrogen atoms at positions 1 and 3 of the six-membered rings. uracil core substituted at atom number 1 with arylamino functional group and in atom number 5 with aromatic group. The derivatives of this scaffold contain pyrimidine moieties which have biological and pharmacological interests. Compounds with pyrimidine cores have anticancer (5-fluorouracil), antiviral (idoxuridine and trifluridine), antibacterial (trimethoprim and sulfamethazine), antihypertensive (minoxidil and prazosin), and antihistaminic (thinozylamine) activities, among others.

### 2.1.3 Fluorescence microscopy reagents

The following reagents were obtained from Invitrogen (Waltham, MA, USA): *i*) lipid droplet staining BODIPY™ 493/503 and BODIPY™ 505/515. *ii*) Filamentous actin (F-actin) staining Alexa Flour™ 488 phalloidin and Alexa Flour™ 647 phalloidin. *iii*) Coverslip mounting media ProLong™ Gold, SlowFade™ Gold, and SlowFade™ Diamond Antifade Mountant, *iv*) cell labelling kit Vybrant™ CFDA SE Cell Tracer, *v*) DNA staining reagents 4',6-diamidino-2-phenylindole (DAPI) and 2'-(4-Ethoxyphenyl)-6-(4-methyl-1-piperazinyl)-1H,3'H-2,5'-bibenzimidazole (Hoechst).

### 2.1.4 Molecular biology reagents

GeneJET RNA purification kit for cellular RNA extraction and purification was obtained from ThermoFisher Scientific (Waltham, MA, USA). High pure viral RNA kit for RNA purification from medium was obtained from Roche Diagnostics GmbH (Mannheim, Germany). Superscript III reverse transcriptase kit cDNA for synthesis of cDNA was obtained from Invitrogen (Waltham, MA, USA). cDNA real-time PCR was performed using the TaqMan universal PCR master mix (Applied Biosystems). HCV forward primer 5'-TCT GCG GAA CCG GTG AGT A-3', reverse primer 5'GTG TTT CTT TTG GTT TTT CTT TGA GGT TTA GG-3', and 6-carboxyfluorescein (FAM)-labeled reporter probe 5'-/56-FAM/CAC GGT CTA CGA GAC CTC CCG GGG CAC /36-TAMSp/-3' were obtained from Integrated DNA Technologies.

*E. coli* Subcloning Efficiency™ DH5α™ Competent Cells and the restriction enzymes EcoRI and Xba1 (catalog number, 18265017 and FD0274 and FD0684, respectively) for plasmid growth and analysis, respectively, were obtained from ThermoScientific (Waltham, MA). Super optimal broth with catabolite repression (SOC)

and lysogeny broth (LB) media were obtained from Sigma as powder. QIAprep® Spin Miniprep kit and QIAGEN® Plasmid Mini kit (catalog number 27104 and 12123, respectively), for purification of plasmid DNA, were obtained from Qiagen (Germantwon, MD).

### **2.1.5 Antibodies**

The LDAP (lipid droplet associated protein) proteins ADRP (adipocyte differentiation-related protein) and TIP47 (tail-interacting protein 47) were detected using rabbit polyclonal antibodies ab52355 (1:1,000) and ab47638 (1:100) from Abcam, respectively. Arf1 (ADP-ribosylation factor 1) was detected using rabbit and mouse monoclonal antibodies ab108347 (1:200) and ab11038 (1:100) from Abcam, respectively. ArfGAP1 (Arf1 GTPase activating protein 1) was detected using rabbit monoclonal (EPR13650) antibody ab183746 (1:500) from Abcam. Tubulin was detected using rat monoclonal antibody ab6160 (1:1,000) from Abcam. Hsp90 alpha (D7a) was detected using mouse clonal antibody ab59459 (1:1,000) from Abcam. Golgi apparatus was detected using anti-GM130 goat polyclonal antibody sc-16268 (1:300) from Santa Cruz and anti-TGN46 rabbit polyclonal antibody ab50595 (1:500) from Abcam. ER (endoplasmic reticulum) was detected using anti-PDI (H-17) sc-30932 (1:200) and anti-calnexin (C-ter) AB 0037-200 (1:300) goat polyclonal antibodies from Santa Cruz and SICGEN, respectively. Flag and HA tags were detected using rabbit polyclonal antibodies ab1162 (1:500) and ab9110 (1:500) from Abcam, respectively. Myc tag was detected using goat polyclonal antibody ab9132 (1:500) from Abcam. HCV viral proteins were detected using the following antibodies. Mouse monoclonal antibody ALX-804-277-C100 (1:2000) from Enzo Life Sciences against an HCV core fusion protein (genotype 1b) epitope aa residues between

21-40. Mouse monoclonal antibody ab65407 (1:500) from Abcam against an NS3 protein epitope aa residues between 1340-1470. Mouse monoclonal antibody LS-C102960 (1:50) from LifeSpan BioSciences against HCV NS5A genotypes 1a and 2a. DV was detected with rabbit polyclonal antibody ab155042 (1:1,000) from Abcam against an epitope between aa residues 2-43 capsid protein C chain. HCV-1 (1a) (G757) and JC6 (2a) goat neutralizing antibodies (1:50) raised against recombinant envelope glycoproteins E1E2, were a generous gift from Dr. Houghton (University of Alberta, Edmonton) (**Table 2.1**) .

Secondary antibodies. Goat anti-mouse IgG conjugated to fluorescent probes Alexa Fluor 488, 555, 594, or 647, goat-anti rabbit IgG Alexa Fluor 488, 568, or 647, and goat anti-rat IgG Alexa Fluor 568 were obtained from Life Technologies, Inc. Donkey anti-mouse IgG conjugated to fluorescent probe Alexa Fluor 488 or 568 or to horse-radish peroxidase (HRB), donkey anti-rabbit Alexa Fluor 488, 568 or 647 or HRB, and donkey anti-goat IgG Alexa Fluor 568 or HRB were obtained from Abcam (Cambridge, MA, USA) (**Table 2.2**).

### **2.1.6 Plasmids**

Arf1-myc 546 bp cDNA (RefSeq BC009247) and 528 bp cDNA (RefSeq BC008918) Arf6-Flag cloned into pCMV3-C-Myc or pCMV3-C-Flag vector, respectively, were obtained from Sino Biological Inc. Both plasmids encode for kanamycin resistance. The plasmids were confirmed by full-length sequence using forward primer pCMV3 5' CAGGTGTCCACTCCCAGGTCCAAG 3' and reverse primer pcDNA3 5' GGCAACTAGAAGGCACAGTCGAGG 3'. Ten micrograms lyophilized plasmid were

**Table 2.1 List of primary antibodies**

<b>Primary antibodies</b>					
<b>Supplier</b>	<b>Catalogue number</b>	<b>Species</b>	<b>Clonality</b>	<b>Antigen</b>	<b>Dilution</b>
Abcam	ab52355	Rabbit	Polyclonal	ADRP	1:1,000
Abcam	ab57638	Rabbit	Polyclonal	TIP47	1:100
Abcam	ab108347	Rabbit	Monoclonal	Arf1	1:200
Abcam	ab11038	Mouse	Monoclonal	Arf1	1:100
Abcam	ab183746	Rabbit	Monoclonal	ArfGAP1	1:500
Abcam	ab6160	Rat	Monoclonal	Tubulin	1:1000
Abcam	ab59459	Mouse	Monoclonal	HSP90 $\alpha$	1:1000
Abcam	ab1162	Rabbit	Polyclonal	Flag	1:500
Abcam	ab9110	Rabbit	Polyclonal	HA	1:500
Santa Cruz	sc-16268	Goat	Polyclonal	GM130	1:300
Abcam	ab50595	Rabbit	Polyclonal	TGN46	1:500
Santa Cruz	sc-30932	Goat	Polyclonal	PDI	1:200
SICGEN	AB 0037-200	Goat	Polyclonal	Calnexin	1:300
Enzo Life Sciences	ALX-804-227-C100	Mouse	Monoclonal	HCV core	1:2000
Abcam	ab65407	Mouse	Monoclonal	HCV NS3	1:500
LifeSpan BioSciences	LS-C102960	Mouse	Monoclonal	HCV NS5A	1:50
Abcam	ab155042	Rabbit	Polyclonal	Dengue virus core	1:1000
BioFront Tech	BF-1225-06	Mouse	Monoclonal	Zika NS1	1:200
Dr. Houghton	G757	Goat	Polyclonal	HCV-1 rE1E2	1:50
Dr. Houghton	N/A	Goat	Polyclonal	HCV-JC6 rE1E2	1:50

**Table 2.2 List of secondary antibodies**

<b>Secondary antibodies</b>				
<b>Supplier</b>	<b>Catalogue number</b>	<b>Species</b>	<b>Clonality</b>	<b>Antigen</b>
Life Technology	ab52355	Goat	AlexaFluor-488	Mouse IgG
Life Technology	ab57638	Goat	AlexaFluor-555	Mouse IgG
Life Technology	ab108347	Goat	AlexaFluor-594	Mouse IgG
Life Technology	ab11038	Goat	AlexaFluor-647	Mouse IgG
Life Technology	ab183746	Goat	AlexaFluor-488	Rabbit IgG
Life Technology	ab6160	Goat	AlexaFluor-568	Rabbit IgG
Life Technology	ab59459	Goat	AlexaFluor-647	Rabbit IgG
Life Technology	ab1162	Goat	AlexaFluor-568	Rat IgG
Abcam	ab9110	Donkey	AlexaFluor-488	Mouse IgG
Santa Cruz	sc-16268	Donkey	AlexaFluor-568	Mouse IgG
Abcam	ab50595	Donkey	HRB	Mouse IgG
Santa Cruz	sc-30932	Donkey	AlexaFluor-488	Rabbit IgG
SICGEN	AB 0037-200	Donkey	AlexaFluor-568	Rabbit IgG
Enzo Life Sciences	ALX-804-227-C100	Donkey	AlexaFluor-647	Rabbit IgG
Abcam	ab65407	Donkey	HRB	Rabbit IgG
LifeSpan BioSciences	LS-C102960	Donkey	AlexaFluor-568	Goat
Abcam	ab155042	Donkey	HRB	Goat

collected by centrifugation at 5,000 g for 5 minutes before resuspension in 100  $\mu$ l sterile water. Dissolved plasmid DNA was incubated at room temperature for 10 minutes, briefly vortexed, and centrifuged for 30 seconds at 5,000 x to collect solution. Plasmid solution was aliquoted into 20  $\mu$ l and stored at -20°C.

Wild-type Arf1 and non-cycling mutants T31N (GDP-locked) and Q71L (GTP-locked) are described in (YUTAKA TAKEBE & KEN-ICHI ARAI, 1988). These constructs encode the respective proteins fused to a hemagglutinin (HA) tag at the C-terminus cloned into a pcD-cDNA expression vector with the SR $\alpha$  promoter. This promoter consists of the simian virus 40 (SV40) early promoter and the R segment and part of U5 sequence (R-U5') of the long terminal repeat of human T-cell leukemia virus type 1. These plasmids encode for ampicillin resistance. All plasmids were transformed into competent *E. coli* DH5 $\alpha$ . Briefly, 20 ng of plasmid was added to 50  $\mu$ l *E. coli* DH5 $\alpha$  and chilled on ice for 30 minutes, mixing by tapping the tubes every 5 minutes. Cells were then heat shocked at 42°C for 90 seconds and placed on ice again for 2 minutes. 800  $\mu$ l 37°C SOC media was added and the mix was incubated at 37°C for 1 h, shaking at 220 revolutions per minute (rpm). The culture was serially diluted 10-fold in SOC media and 150  $\mu$ l of the dilution was inoculated into LB plates supplemented with the appropriate antibiotic. Inoculated plates were incubated at 37°C overnight, individual colonies were picked and inoculated into 3 ml LB media supplemented with the appropriate antibiotic and incubated at 37°C for 16 h, shaking at 220 rpm. Plasmids were purified using commercial purification kits (QIAprep® Spin Miniprep kit or QIAGEN® Plasmid Mini kit, catalog number 27104 or 12123, respectively) and analyzed by digestion with diagnostic restriction enzymes EcoRI and XbaI.

### 2.1.7 siRNA

siRNA reagents were obtained from Dharmacon. ON-TARGETplus SMARTpool siRNA targeting the coding region of human Arf1 includes a mixture of four individual siRNA against all Arf1 splice forms. The targeted sequences are UGACAGAGAGCGUGUGAAC, CGGCCGAGAUCACAGACAA, ACGAUCCUCUACAAGCUUA, and GAACCAGAAGUGAACGCGA (NCBI reference sequence identifiers [NM\\_001024226.1](#), [NM\\_001024227.1](#), [NM\\_001024228.1](#), [NM\\_001658.3](#), and [XM\\_017001233.1](#)). Accell SMARTpool siRNA targeting non-coding regions within the 3'-untranslated region (3'UTR) of human Arf1 includes a mixture of four individual siRNA against the same splice variants targeted by On-TARGETplus SMARTpool siRNA. Non-targeting siRNA pools contain at least four mismatches to any human, mouse, and rat gene. The sequences of non-targeting siRNA are UGGUUUACAUGUCGACUAA, UGGUUUACAUGUUGUGUGA, UGGUUUACAUGUUUUCUGA, and UGGUUUACAUGUUUUCCUA. siRNA Stocks were prepared at 20  $\mu$ M in siRNA resuspension buffer (300 mM KCL, 30 mM HEPES pH 7.5, 1.0 mM  $MgCl_2$ ) and stored at -20°C. Reagent DharmaFECT formula 4 was used for siRNA transfection except for co-transfections with plasmid DNA, for which the TransIT-X2 (Mirus) reagent was used.

### 2.1.8 Cell culture reagents

Cell culture reagents were obtained from ThermoFisher Scientific (Waltham, MA). Gibco Dulbecco's Modified Eagle Medium (DMEM) containing 1 g/L D-glucose (dextrose), 584 mg/L l-glutamine, 110 mg/L sodium pyruvate, and 15 mg/L phenol red, supplemented with 5 or 10% FBS was used for cell culture. Gibco Opti-MEM™ Reduced Serum Medium



which is a Minimal Essential Medium (MEM) modified with propriety components, was used for transfection experiments. For cell detachment, Gibco 10x trypsin-EDTA diluted 10-fold.

#### **2.1.9 Cells**

African green monkey Vero fibroblasts, Madin-Darby canine kidney (MDCK), and HeLa cells from were obtained from American Type Culture Collection (catalog number CCL-81, CCL-34 and CCL-2, respectively). Human hepatoma Huh7.5 cells were provided from Dr. Charles Rice (Rockefeller University, NY, US) and obtained through Dr. Lorne Tyrrell (University of Alberta, Edmonton, Canada), under agreement with Apath, Inc.

Vero, MDCK, HeLa, and Huh7.5 cells were cultured in DMEM supplemented with 5 (Vero and MDCK) or 10% (Huh7.5 and HeLa) FBS at 37°C in 5% CO<sub>2</sub>. For passaging or seeding, cells in T150 flasks were washed once with PBS and detached by incubation at 37°C in 0.05% trypsin-EDTA for approximately 5 (Vero and Huh7.5) or 15 (MDCK) minutes. Detached cells were resuspended in DMEM-5 or 10% for Vero and MDCK or Huh7.5, respectively, and seeded into flasks or plates at the required densities.

#### **2.1.10 Viruses**

HCV strain JFH-1 (genotype 2a) was obtained from Dr. Takaji Wakita (Tokyo Metropolitan Institute for Neuroscience, Tokyo, Japan) (Wakita et al., 2005) through Lorne Tyrrell (University of Alberta, Edmonton, Canada), under agreement with Apath, Inc. HCV strains Jc1 (J6-JFH1 chimera, genotype 2a) and H77 (genotype 1a) were obtained from Dr. Michael Houghton (University of Alberta, Edmonton, Canada). Herpes simplex virus 1 strain KOS (HSV1-KOS) was obtained from the late Dr. Priscilla Schaffer (Harvard Medical School, Boston, MA). Dengue virus (DV) type 2 strain New Guinea-C and Zika

virus strain PCla, Vesicular stomatitis virus (VSV), vaccinia virus (VACV) strain Western Reserve (WR), poliovirus (PV) strain Mahoney and human respiratory syncytial virus (HRSV) type A strain Long were provided from Drs. Tom Hobman, Paul Melancon, David Evans, Michael N. James and David Marchant, respectively (University of Alberta, Edmonton, Alberta, Canada) (**Table 2.3**).

<b>Virus</b>	<b>Genome</b>	<b>Virion</b>	<b>Replication</b>
<b>Vaccinia</b>	dsDNA	Enveloped	Cytoplasmic
<b>HSV1</b>	dsDNA	Enveloped	Nuclear
<b>Influenza A</b>	-ssRNA	Enveloped	Nuclear
<b>VSV</b>	-ssRNA	Enveloped	Cytoplasmic
<b>HCV</b>	+ssRNA	Enveloped	Cytoplasmic
<b>Poliovirus</b>	+ssRNA	Non-enveloped	Cytoplasmic

**Table 2.3 List of viruses used in the testing for antiviral activity of the initial derivatives of the small molecule scaffold shown in Figure 2.1.**

A panel of 6 viruses that are unique in their genome, envelope, and replication strategy. They have dsDNA, -ssRNA, or +ssRNA genome, enveloped or non-enveloped virion, and replicate in the cytoplasm or the nucleus.

## **2.2 METHODS**

### **2.2.1 Preparation of viral stocks**

Stocks of HCVcc-JFH1 were prepared by inoculating  $3.5 \times 10^5$  Huh7.5 cells seeded 24 h earlier in each well of 6-well plates at an moi of 0.003 in 0.5 ml DMEM for 4 h. Inocula were removed and cells were washed twice with 2 ml per well of 6-well plates 4°C DMEM before being overlaid with 3 ml per well DMEM-10% FBS. Infected cells were incubated for 72 h at 37°C in 5% CO<sub>2</sub>. Supernatants were collected and the cells were trypsinized and resuspended in 1 ml DMEM-10% FBS, pooled, transferred to a T150 flask, and taken to 30 ml with 12 ml of the collected supernatants and 12 ml of fresh DMEM-10% FBS. Cells were split into two T150 flasks 48 h later and virus was harvested 48 h after splitting. Medium was collected, transferred into 50 mL centrifuge tubes, and spun at 1,000 g for 5 minutes at 4°C to pellet cellular debris. Cleared culture media were filtered through 0.22 µm filters and concentrated in 15 mL 100K Amicon Ultra centrifugation tubes at 3220 g for 25 minutes at 4°C. Filtrates were pooled and aliquoted into 100 µL per 1.8 ml borosilicate glass vials and stored at -80°C.

Stocks of DV type II strain New Guinea C and Zika virus PCla were prepared by inoculating  $5 \times 10^6$  Vero cells seeded in T150 flask with 3 ml inocula in DMEM at moi of 0.01 for 1 h at 37°C. Inoculated cells were washed twice with 10 ml of 4°C DMEM before being overlaid with 25 ml of warm DMEM-10 or 5% FBS for Zika virus or DV, respectively, and incubated 37°C in 5% CO<sub>2</sub>. Infected cells were checked daily for cytopathic effect (CPE) from two to three days after infection. Culture media was collected when 70% of cell showed CPE and concentrated as described earlier with HCV.

Stocks of HSV1 strain KOS was prepared by infecting  $1.0 \times 10^7$  Vero cells in T150 flask at moi of 0.05 with 3 ml inoculum in DMEM for 1 h at 37°C. Inoculum was removed and cells were washed twice with 10 ml 4°C DMEM before they were overlaid with DMEM-5% FBS and incubated at 33°C until appearance of >95% CPE which typically took 2 to 4 days. Cells were scraped into the culture media, transferred into 50 ml conical centrifuge tubes, and centrifuged at 4000 rpm for 30 minutes at 4°C. The supernatant was transfer into a new 50 ml conical tube and centrifuged at 10,000 x g at 4°C for 2 h. The pellet was resuspended in 1 mL DMEM, transferred into 15 mL conical centrifuge tubes, and subjected to three cycles of freeze-thawing in ethanol-dry ice bath. The cell lysate was sonicated medium level three times for 30 seconds each separated by 15 seconds pauses, and centrifuged at 4000 rpm for 30 minutes at 4°C. The supernatant was collected and used to resuspend the viral pellet from the high centrifuge. The pellet from the cell lysate was resuspended in 0.5 mL of DMEM, sonicated at medium level three times for 30 seconds each separated by 15 seconds pauses, and centrifuged at 4000 rpm for 30 minutes at 4°C. The resulting supernatant was pooled with the resuspended viral pellet, sonicated at medium level three times for 30 seconds each separated by 15 seconds pauses at, aliquoted into 75 µl per 1.8 ml glass vials, and stored at -80°C.

Stocks of VSV, VACV, PV, and RSV were prepared by inoculating  $1 \times 10^7$  Vero cells in in T-150 tissue culture flask in 3 ml inoculum in DMEM at moi of 0.01 to 0.05 for 1 h at 37°C. Inoculated flasks were then washed twice with 5 mL of 4°C DMEM. Infected cells were then overlaid with 22 mL of warm DMEM-5% FBS and incubated at 33°C until full CPE, which typically occurred after 2 to 4 days. Supernatants were collected into 50 mL conical centrifuge tubes and centrifuged at 4000 rpm for 30 minutes at 4°C. The

resulting supernatant was transferred into new conical centrifuge tubes and spun at 10,000 x g for 2 h at 4°C. The supernatant was pipetted, the pellet was resuspended in DMEM, and the virions suspension was then aliquoted into 150 µl aliquots in 1.8 ml glass vials and stored at -80°C.

Stocks of IAV were prepared by infecting 10<sup>7</sup> MDCK cells with 3 ml inoculum in influenza growth medium (DMEM/0.2% BSA/2 µg/mL TPCK trypsin) at moi of 0.01 for 1 h at 37°C. The inoculum was removed and the infected cells were washed twice with 10 mL of 4°C DMEM. The infected cells were overlaid with 22 mL of influenza growth medium and incubated at 33°C until at least 75% CPE detected. The supernatant was collected into 50 mL conical centrifuge tubes and spun at 4000 rpm and for 30 minutes at 4°C. The resulted supernatant was transferred into a new conical centrifuge tube and spun at 10,000 x g and for 2 h at 4°C. Supernatant was discarded and the pellet was resuspended with DMEM, aliquoted into 1.8 ml borosilicate glass vials, and stored at -80°C.

### **2.2.2 Virus titrations**

Cells (3.5 x 10<sup>5</sup> Vero (for HSV-1, VSV, PV, vaccinia), MDCK (for IAV), or Huh7.5 (for DV or Zika virus)) were seeded into each well of 6-well plates the day before infection and incubated at 37°C in 5% CO<sub>2</sub>. Aliquots of viral stocks or samples were thawed rapidly at 37°C in a water bath and immediately placed on ice. Ten-fold serial dilutions were then prepared in serum-free DMEM (SFM) mixing briefly by gentle vortexing. Cells were inoculated with 200 µl of the diluted stocks or samples and incubated at 37°C for 1 h rotating and rocking every 10 minutes. Inocula were removed and the cells were washed twice with 2 ml per well 4°C DMEM. IAV infected cells were overlaid with DMEM containing 0.8% agarose and 0.5 µg/ml TPCK trypsin. Cells infected with all other viruses

were overlaid with DMEM-5% FBS (10% for DV or Zika virus) containing 2% methylcellulose. Overlaid cells were incubated for 2 to 4 days at 37°C in 5% CO<sub>2</sub> until plaques developed. Cells were fixed and stained overnight with a solution of 0.5% crystal violet in 17% methanol.

For HCV,  $9.0 \times 10^4$  Huh7.5 cells were seeded into each well of 24-well plates one day prior to infection. Duplicates wells were inoculated with 150 µl of diluted stocks or samples for 4 h. Inocula were removed and the cells were washed twice with 0.5 ml per well of 4°C DMEM before they were overlaid with 1 ml per well DMEM-10% FBS. Cells were processed for immunofluorescence for HCV core protein 48 h later. To this end, infected cells were washed twice with 1 ml 4°C PBS and fixed in 1 ml ice cold-methanol:acetone (1:1) for 30 minutes at -20°C. Fixed cells were washed thrice with 1 ml room temperature PBS thrice for 5 minutes each wash. Cells were blocked with 200 µl 5% normal goat or donkey sera on a rotator for 1 h at room temperature. Blocking solution was removed and cells were then incubated for 3 h at room temperature or overnight at 4°C with primary mouse monoclonal anti-HCV core antibody diluted in 1% normal serum. Primary antibody was removed and cells were washed thrice for 10 minutes each with 0.5 ml PBS before adding secondary antibody goat or donkey anti-mouse IgG conjugated with Alexa-488 and incubating at room temperature for 1 h protected from light in a light-tight box. Cells were then washed three times and examined by fluorescent microscope, with a 500-550 nm transmission light filter.

### **2.2.3 Transfections**

Knockdown of Arf1 in Huh7.5 cells was performed using ON-TARGETplus SMARTpool siRNA and DharmaFECT formula 4 transfection reagent. Simultaneous knockdown of

endogenous Arf1 and ectopic expression of wild type or non-cycling mutant Arf1 was performed using an Accell SMARTpool siRNA, which targets sequences within the 3'UTR of human Arf1, using TransIT-X2 transfection reagent. For Arf1 knockdown,  $5.0 \times 10^4$  Huh7.5 cells were seeded into each well of 24-well plates. The next day, transfection media was prepared by diluting ON-TARGETplus Arf1 siRNA to 75 nM and separately the transfection reagent 1:167 in 50  $\mu$ l DMEM each. Diluted siRNA and transfection reagent were separately mixed gently by pipetting  $\frac{1}{4}$  volume up and down three times and then incubating at room temperature for 5 minutes. The two mixes then combined, gently mixed as described for the siRNA and transfection reagent, and incubated for 20 minutes at room temperature. Opti-MEM (400  $\mu$ l) was added and mixed gently as described above. Then, 0.5 ml of the mix was added dropwise to cells that had been washed with 1 ml per well Opti-MEM. Cells were incubated with transfection media for 24 h at 37°C in 5% CO<sub>2</sub> before any further processing.

For ectopic expression of Arf1 simultaneously with siRNA knockdown,  $8.0 \times 10^4$  Huh7.5 cells were seeded into each well of 24-well plates and incubated overnight at 37°C in 5% CO<sub>2</sub>. Transfection media was prepared by diluting the Arf1 plasmids, 125 ng DNA per well, with or without 50 nM of Accell siRNA and, separately the transfection reagent TransIT-X2 in 100  $\mu$ l Opti-MEM 1:333. The mixture was mixed gently by pipetting up and down 5 times, incubated at room temperature for 25 minutes, and added dropwise to cells in 0.5 ml seeding culture media. Cells were incubated with transfection media at 37°C in 5% CO<sub>2</sub>. The efficiency of transfection or knockdown was evaluated by indirect immunofluorescence for the HA tag or Western blot for Arf1, respectively.



#### **2.2.4 Plaque formation assay**

Cells ( $3.5 \times 10^5$  Vero (for HSV-1, VSV, PV, vaccinia), MDCK (for IAV), or Huh7.5 (for DV or Zika virus)) were seeded the day before infection into each well of 6-well plates and incubated at 37°C in 5% CO<sub>2</sub>. Cells were inoculated the following day with 200 plaque forming units (PFU) of the respective virus in 200 µl DMEM and incubated at 37°C for 1 h rocking and rotating every 10 minutes. Cells were washed twice with 2 ml per well of 4°C DMEM. IAV infected cells were overlaid with DMEM containing 0.8% agarose and 0.5 µg/ml TPCK trypsin. Cells infected with all other viruses were overlaid with 2.5 ml per well of 37°C DMEM-5% FBS (or 10% FBS for DV and Zika virus) containing 1% methylcellulose, supplemented with Z390 or not. Overlaid cells were incubated for 2 to 4 days at 37°C in 5% CO<sub>2</sub> until plaques developed. Cells were fixed and stained overnight with a solution of 0.5% crystal violet in 17% methanol and number of plaques normalized to DMSO control. Half maximum effective concentration (EC<sub>50</sub>) was calculated as the concentration of Z390 that reduced the number of plaques by 50%.

#### **2.2.5 Foci formation assay**

Huh7.5 cells ( $1 \times 10^5$ ) were seeded in 1 ml DMEM-10% FBS per well of 24-well plates and incubated at 37°C in 5% CO<sub>2</sub>. The cells were inoculated 24 h later with 100 FFU of HCV-JFH1 in 150 µl DMEM or 100 FFU of RSV in 100 µl DMEM, per well and adsorbed for 4 or 2 h, respectively, at 37°C, rocking and rotating the plates every 30 or 15 minutes, respectively. Inocula were removed and the infected cells were washed twice with 0.5 ml per well of 4°C DMEM. Cells were then overlaid with 1 ml per well DMEM-10% FBS supplemented with Z390 or not and incubated for 48 h at 37°C in 5% CO<sub>2</sub>. Cells were fixed and processed for direct or indirect immunofluorescence for HCV core protein or

RSV fusion protein. The number of foci normalized to DMSO treated control infections, and expressed as percentage of control. Half maximum effective concentration ( $EC_{50}$ ) was calculated as the concentration of Z390 that reduced the number of foci by 50%.

### **2.2.6 Antiviral activity**

Compounds were tested for antiviral activity against HCV, HSV-1, VSV, PV, IAV and vaccinia virus. These viruses differ in their virion structures, genetic material, sites of replication. Cells ( $3.5 \times 10^5$  Vero (HSV-1, VSV, PV, DV, or Zika virus) or MDCK (IAV)) were seeded into each well of 6-well plates. Huh7.5 cells were seeded into each well of 6 ( $(3.5 \times 10^5)$  for DV or Zika virus) or 24-well ( $(1.0 \times 10^5)$  for HCV or RSV) plates. Cells seeded in 6-well plates were inoculated 24 h later with 200 PFU of HSV-1, VSV, PV, IAV, DV, or Zika virus in 200  $\mu$ l DMEM for 1 h. Cells seeded in 24-well plates were inoculated with 100 FFU of HCV or RSV in 150  $\mu$ l DMEM for 4 h. Inocula were removed and the cells were washed twice with 2 or 0.5 ml per well of 4°C DMEM for infections in 6 or 24-well plates, respectively. Semi-logarithmic concentrations of test compounds diluted in DMEM supplemented with 5 (Vero and MDCK) or 10% FBS (Huh7.5 and HeLa cells) were added and the infected cells were incubated at 37°C in 5%  $CO_2$  for the appropriate time for each virus. Antiviral activity of compounds was evaluated by foci forming assay (HCV and RSV) or plaque forming assay (all other viruses) (**Figure 2.2**).

### **2.2.7 Single-step replication assays**

Huh7.5 cells ( $2.5 \times 10^4$ ) were seeded into each well of 96-well plates a day before they were inoculated with HCVcc-JFH1 at an moi of 5 for 4 h at 37°C. Cells were washed twice with 100  $\mu$ l per well 4°C DMEM, 150  $\mu$ l DMEM-10% FBS was then added, and the cells were incubated for up to 48 h at 37°C in 5%  $CO_2$ . Culture media and cells were harvested

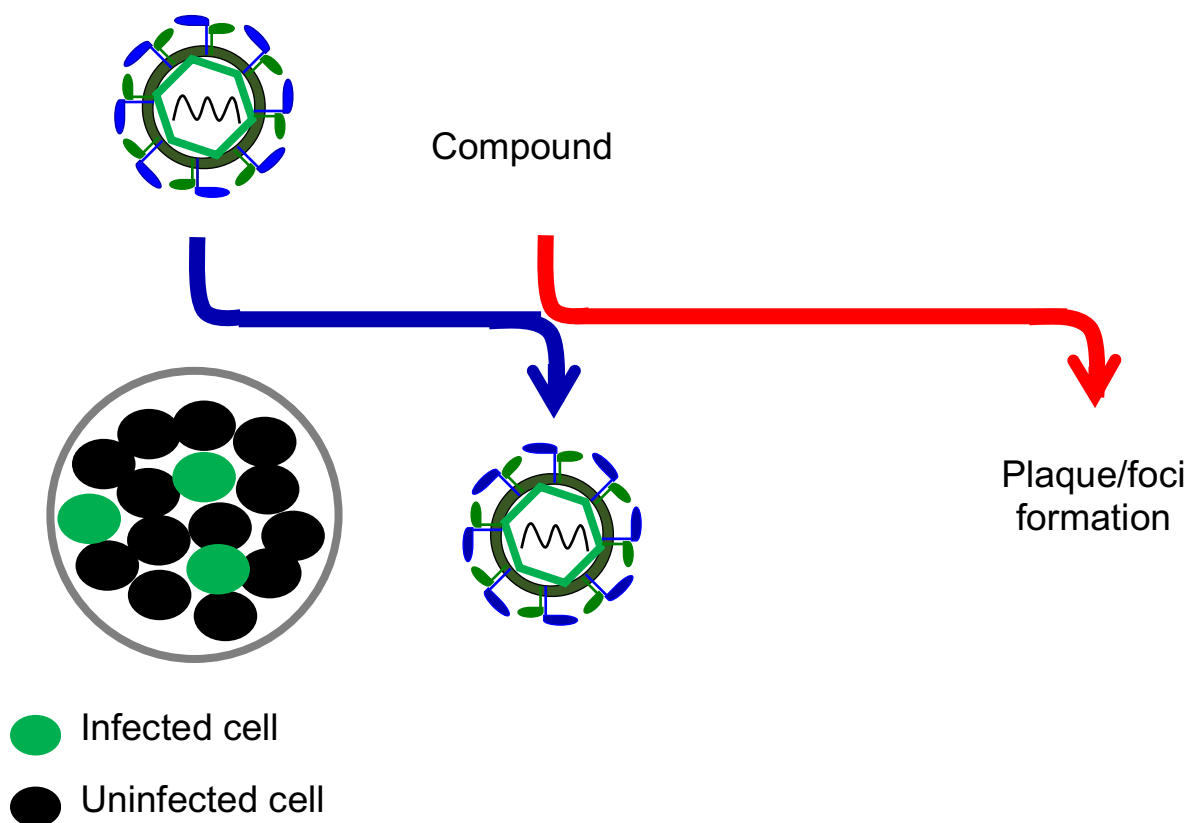


**Figure 2.2. Testing the candidate small molecules for antiviral activity.**

Cells are infected with viruses at  $\text{moi} = 0.001$  for 1 h (4 h for HCV), unbound virions are removed and infected monolayers are overlaid with complete media containing several dilutions of test compound. Infections are incubated for 2-3 days then monolayers are stained with vital stain to detect plaques or immunolabeled for immunofluorescence microscopy to detect foci.

at pre-selected times. Medium was collected into 0.6 ml Eppendorf tubes and centrifuged at 5,000 g for 10 minutes at 4°C to pellet cell debris. The supernatants were collected, flash-frozen in ethanol-dry ice, and stored at -80°C until titration or RNA extraction. Cells were washed thrice with 100 µl per well 4°C DMEM, trypsinized for 5 minutes at 37°C, resuspended in 200 µl DMEM-10% FBS, subjected to three freeze-thaw cycles in dry ice-ethanol bath and 37°C water bath. Cell lysates were cleared by spinning at 5,000 g for 10 minutes at 4°C. Supernatants were collected, flash-frozen in ethanol-dry ice, and stored at -80°C until titration (**Figure 2.3**).

Infectivity was evaluated by incubation of Huh7.5 cells with 10-fold dilutions of supernatants or cell lysates for two days before they were processed for indirect immunofluorescence for HCV core protein. Infectivity was expressed as number of FFU per infected cells.

### **2.2.8 Quantitation of HCV RNA**

HCV RNA from infected Huh7.5 cells or their supernatant was isolated using GeneJET RNA purification kit (Thermo Scientific) or high pure viral RNA kit (Roche), respectively. cDNA was synthesized using the Superscript III reverse transcriptase kit (Invitrogen) and HCV forward 5'-TCT GCG GAA CCG GTG AGT A-3' and reverse 5'GTG TTT CTT TTG GTT TTT CTT TGA GGT TTA GG-3' primers. The 50 µl reactions were incubated for 50 and 15 minutes at 37°C and 70°C in a thermal cycler, respectively, and then kept at 4°C. Real-time PCR was performed using the TaqMan universal PCR master mix (Applied Biosystems) and 6-carboxyfluorescein (FAM)-labeled reporter probe 5'-/56-FAM/CAC GGT CTA CGA GAC CTC CCG GGG CAC /36-TAMSp/-3' (Integrated DNA Technologies). Linearized plasmid of HCV-JFH1 genome was diluted in nuclease-free

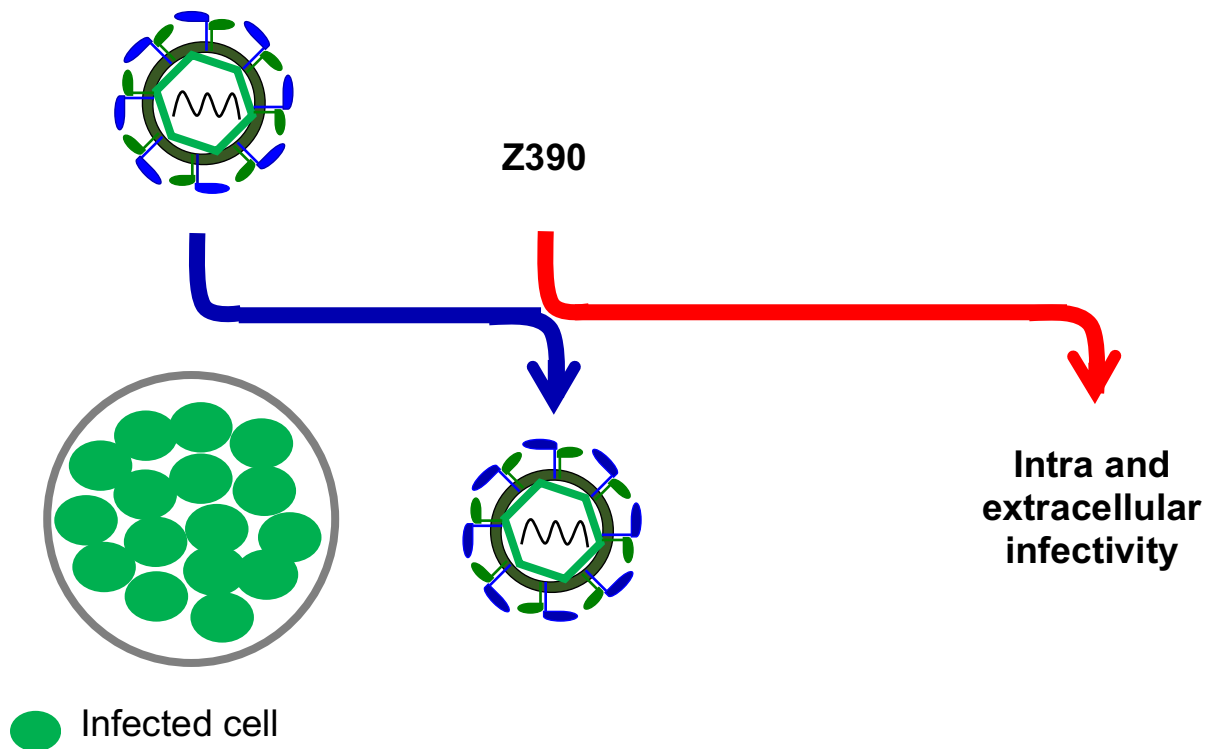


**Figure 2.3. Single-step replication assay for HCV.**

Huh7.5 cells are infected with 5 FFU/cell HCV-JFH1 for 4 h, unbound virions are removed and infected monolayers are overlaid with complete media containing 40  $\mu$ M Z390 or vehicle. Supernatants and cells are collected at time intervals up to 48 h. Intra and extracellular infectivities are determined by infecting naïve Huh7.5 cells with serial dilutions of harvested supernatants or cells for 4 h. Infected cells were then overlaid with complete medium for 2 days before they were immunostained for HCV core protein to quantitate foci.

water and used as standard. A 25 µl reaction mix containing 1/10 of the synthesized cDNA was incubated at 50 and 95°C for 2 and 10 minutes, respectively, followed by 45 cycles at 95 and 60°C for 15 and 60 seconds, respectively. Results were expressed as number of genome equivalents per infected cells.

### **2.2.9 Pre-treatment of HCV virions or Huh7.5 cells before infection**

For pre-treatment of virions, 100 FFU of HCVcc-JFH1 inoculum was incubated with Z390 or DMSO vehicle in 150 µl DMEM for 1 h at 37°C before infecting  $1.0 \times 10^5$  Huh7.5 cells seeded into each well of 24-well plates for 4 h at 37°C. Inocula were removed and cells were washed twice with 1 ml 4°C DMEM before overlaying them with 1 ml DMEM-10% FBS. Plaquing efficiency of pretreated virions was determined 48 h later by foci detection using indirect immunofluorescence for HCV core protein. Foci were normalized to DMSO control and are expressed as percent plaquing efficiency.

For pre-treatment of cells,  $7.5 \times 10^4$  Huh7.5 cells were seeded into each well of 24-well plates a day before they were incubated with Z390 or DMSO vehicle control at 37°C in 5% CO<sub>2</sub>. One, two, or three days after starting the treatment, the cells were inoculated with 100 FFU HCVcc-JFH1 in 150 µl DMEM for 4 h at 37°C. Inocula were removed and cells were then washed twice with 1 ml 4°C DMEM before overlaid with 1 ml DMEM-10% FBS. Foci formation in the pre-treated cells was determined 48 h later by foci detection using indirect immunofluorescence for HCV core protein. Foci were normalized to DMSO control and are expressed as percent foci formation.

### **2.2.10 Serum neutralization**

Pre- or post-immune goat sera against recombinant glycoproteins E1E2 derived from strains HCV-1 (genotype 1a) or HCV-J6 (genotype 2a) were kindly provided by Dr.

Michael Houghton. Sera were diluted serially 10-fold in DMEM before incubating with 50 FFU HCVcc-JFH1 or HCVcc-J6/JFH1 (Jc1) for in 60  $\mu$ l for 30 minutes at 37°C. Huh7.5 cells,  $5 \times 10^4$  in each well of 48-well plates, were inoculated with the preincubated HCV for 4 h at 37°C. Inocula were removed and the cells were washed twice with 0.5 ml 4°C DMEM. Infected cells were then overlaid with 0.5 ml warm DMEM-10% FBS and incubated for 48 h at 37°C in 5% CO<sub>2</sub>. Cells were fixed and processed for indirect immunofluorescence for HCV core. Number of foci in each dilution was normalized to no serum control.

#### **2.2.11 Co-culture assay**

Cell-to-cell HCV spread was tested by co-culturing infected and uninfected cells. Huh7.5 cells ( $2.5 \times 10^4$  per well of 96-well plates) were inoculated with HCVcc-JFH1 at moi of 5 in 30  $\mu$ l DMEM at 37°C for 4 h before overlaying with 120  $\mu$ l warm DMEM-10% FBS. Infected cells were washed with PBS 48 h later and trypsinized with 30  $\mu$ l 4°C trypsin-EDTA for 5 minutes at 37°C. Detached cells were resuspended in 200  $\mu$ l DMEM-10% FBS and labelled with Vybrant™ CFDA SE Cell Tracer labeling kit according to the manufacturer's instructions. Briefly, the detached infected cells were centrifuged at 750 g for 5 minutes at 4°C. Pelleted cells were resuspended in 500  $\mu$ l warm 5  $\mu$ M carboxyfluorescein diacetate succinimidyl ester (CFDA SE) in PBS and incubated at 37°C for 15 minutes for internalization. Cells were pelleted again, resuspended in 500  $\mu$ l DMEM-10% FBS and incubated at 37°C for 30 minutes for SE cleavage of CFDA-SE by cellular esterases. Cells were pelleted once again and resuspended in 500  $\mu$ l DMEM-10% FBS. Infected and labelled cells were then mixed with uninfected and unlabelled

Huh7.5 cells at a ratio of 1:200 and overlaid with 1:50 HCV neutralizing sera in DMEM-10% FBS supplemented or not with 30  $\mu$ M Z390 (**Figure 2.4**).

For OA treatment of donor infected cells, cells were infected at an moi of 5 for 48 h and then treated with 0.5 mM OA-BSA in DMEM-10% FBS or BSA carrier control for 24 h before co-culturing them with uninfected cells ().

To knockdown Arf1, in cells infected at an moi of 5 for 48 h were transfected with 75 nM ON-TARGETplus SMARTpool siRNA targeting sequences within the Arf1 coding region, or non-targeted control siRNA, in Opti-MEM 24 h before co-culturing them with uninfected cells (**Figure 2.6**).

Mixes of HCV infected and labelled donor with uninfected and non-labelled cells were plated on 12mm circular coverglasses in 24-well plates for 24 h then fixed and processed for indirect immunofluorescence.

#### **2.2.12 Lipid droplets synthesis stimulation with oleic acid**

Stimulation of lipid droplet synthesis was achieved by addition of oleic acid to  $5 \times 10^4$  starved Huh7.5 cells seeded onto 12mm circular coverglass into each well of 24-well plates. The following day, the cells were treated with 30  $\mu$ M Z390 or DMSO for 1 h at 37°C. Treatment medium was removed and fresh media containing 0.5 mM oleic acid and 30  $\mu$ M Z390 or DMSO were added. Cells were then incubated at 37°C for 3 h and processed for immunofluorescence for TIP47 and lipid droplet staining.

#### **2.2.13 Transwell infection**

Huh7.5 cells ( $2.5 \times 10^4$  per well in 96-well plates) were infected at an moi of 5 with HCVcc-JFH1, Zika virus, or RSV. The following day,  $4.0 \times 10^5$  uninfected cells in 2.5 ml DMEM-10% FBS were seeded into each well of a 6-well transwell plate and the inserts were



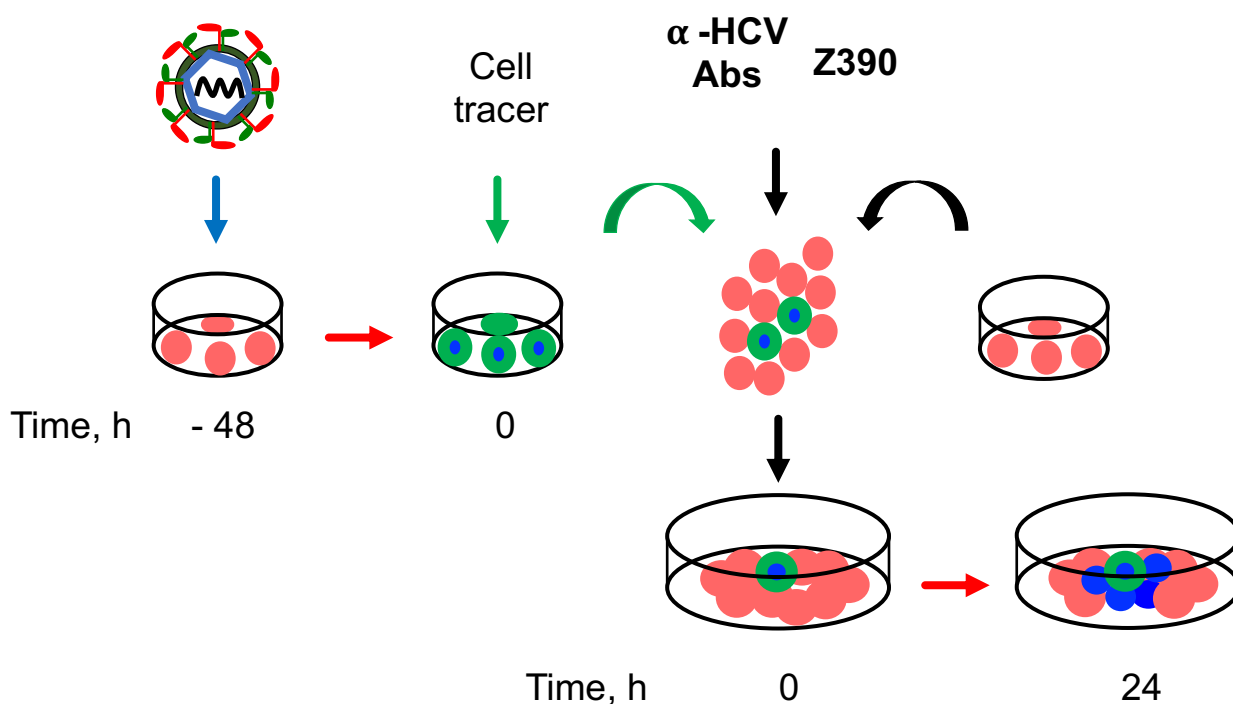


#### Figure 2.4. Co-culture assay.

Huh7.5 cells are infected with 5 FFU/cell HCV-JFH1 for 2 days then they are resuspended, labeled with cell tracer dye, and mixed 1:1000 with naïve Huh7.5 cells. Anti-HCV neutralizing antibodies at a dilution that inhibit virion infectivity by 80% and 40  $\mu$ M Z390 are added to the cell mix and seeded for 24 h before processing for immunofluorescence to detect the infection spread from the infected and labeled to uninfected and unlabeled cells.

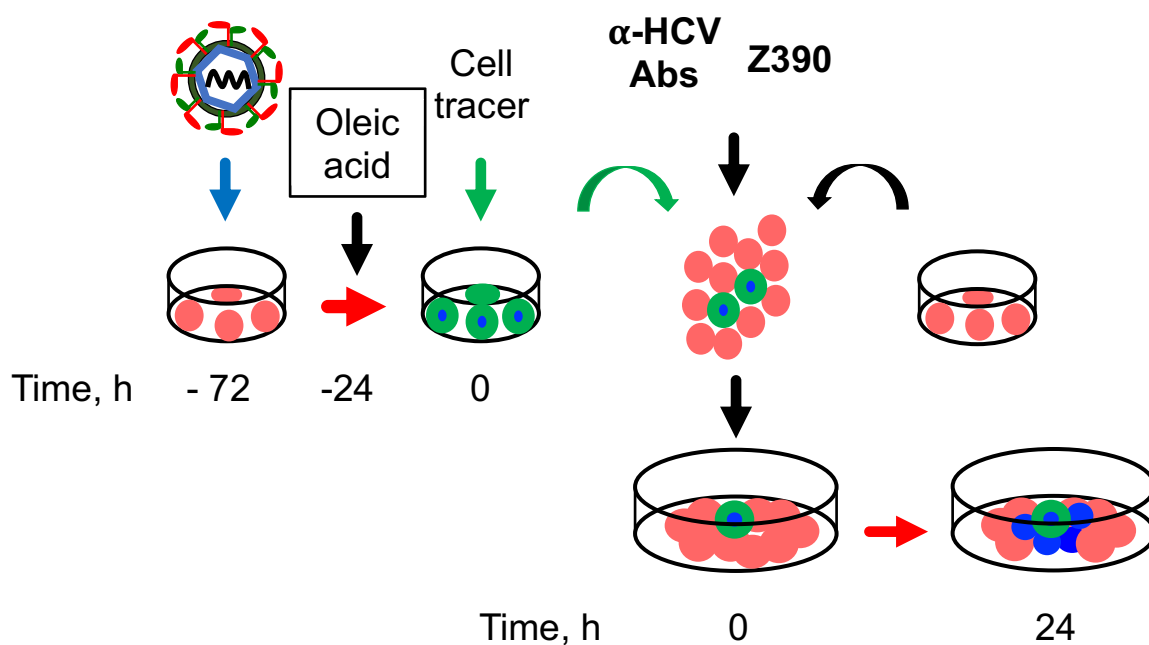


**Figure 2.5. Co-culture assay for oleic acid-treated donor cells.**

Huh7.5 cells are infected with 5 FFU/cell HCV-JFH1 for 2 days then they are treated with 0.5 mM oleic acid for 24 h before they are resuspended, labeled with cell tracer dye, and mixed 1:1000 with naïve Huh7.5 cells. Anti-HCV neutralizing antibodies at a dilution that inhibit virion infectivity by 80% are added to the cell mix and seeded for 24 h before processing for immunofluorescence to detect the infection spread from the infected and labeled to uninfected and unlabeled cells.

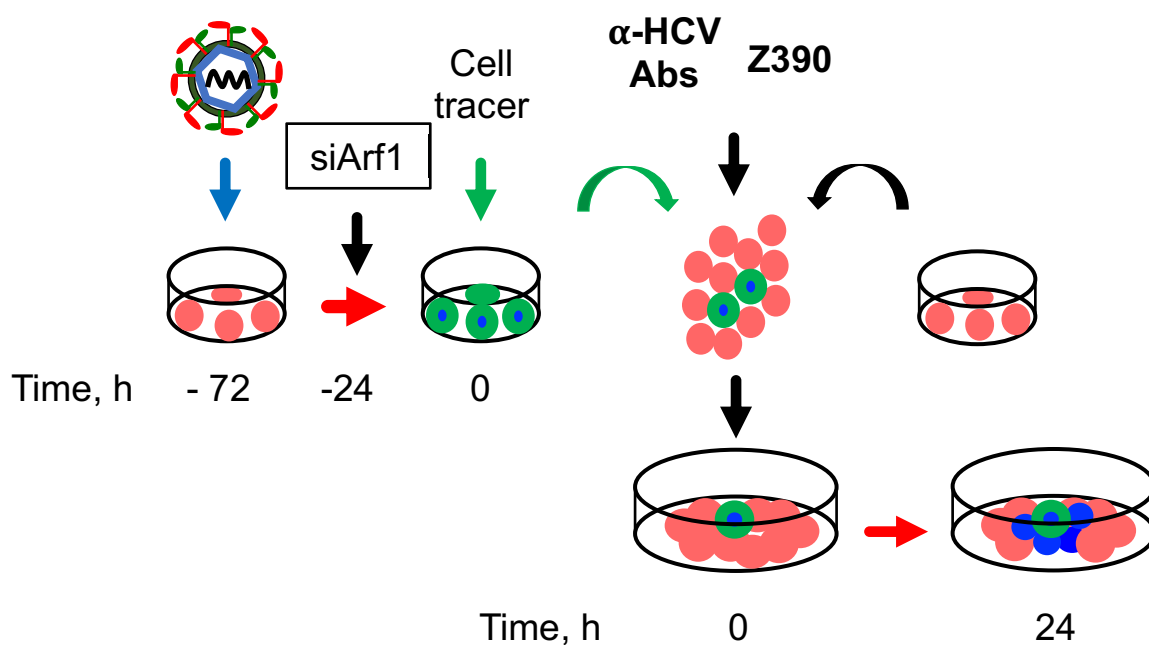


**Figure 2.6. Co-culture assay for Arf1-knocked down donor cells.**

Huh7.5 cells are infected with 5 FFU/cell HCV-JFH1 for 2 days then they are treated with 75 nM Arf1 siRNA for 24 h before they are resuspended, labeled with cell tracer dye, and mixed 1:1000 with naïve Huh7.5 cells. Anti-HCV neutralizing antibodies at a dilution that inhibit virion infectivity by 80% are added to the cell mix and seeded for 24 h before processing for immunofluorescence to detect the infection spread from the infected and labeled to uninfected and unlabeled cells.

equilibrated in DMEM-10% FBS. The previously infected donor infected cells were detached 24 h later, resuspended, and mixed 1:1,000 with  $7.5 \times 10^5$  uninfected Huh7.5 cells. The mixes of infected and uninfected cells were seeded onto the inserts, which were then placed onto the wells previously seeded with uninfected cells. Transwell plates were incubated at 37°C in 5% CO<sub>2</sub> for 48, 72, and 96 h before processing for immunofluorescence (**Figure 2.7**).

#### **2.2.14 Serial passaging of HCV infection**

For passaging of cell-associated infectivity,  $2.5 \times 10^4$  Huh7.5 cells seeded in each well of 96-well plates were inoculated with HCVcc-JFH1, RSV, or Zika virus in 30 µl DMEM at moi of 5 for 4 h. Inocula were removed and the cells were washed twice with 100 µl per well 4°C DMEM before overlaying with 150 µl DMEM-10% FBS. Four hours later, the infected cells were detached and co-cultured 1:1,000 with  $1.5 \times 10^5$  uninfected cells in each well of 24-well plates in the presence of 1:50 HCV neutralizing serum at 1:50. Co-cultures were then incubated at 37°C in 5% CO<sub>2</sub> for 48 h when media were removed and the co-cultured cells were detached and co-cultured 1:1,000 with  $1.5 \times 10^5$  uninfected cells, again in the presence of HCV neutralizing sera. Passaging was repeated for a total of four passages (**Figure 2.8**).

For passaging cell-free virion infectivity,  $1.5 \times 10^5$  Huh7.5 cells in each well of 24-well plates were infected with one infectious virus particle per 200 cells of HCVcc-JFH1, RSV or Zika virus in 150 µl for 4 h. Inocula were removed and cells were washed twice with 1 ml per well 4°C DMEM before overlaying with 1 ml per well DMEM-10% FBS. Infected cells were incubated at 37°C in 5% CO<sub>2</sub>. Media were collected 48 h later and diluted 1:200 before infecting another  $1.5 \times 10^5$  Huh7.5 cells. Passaging was repeated for

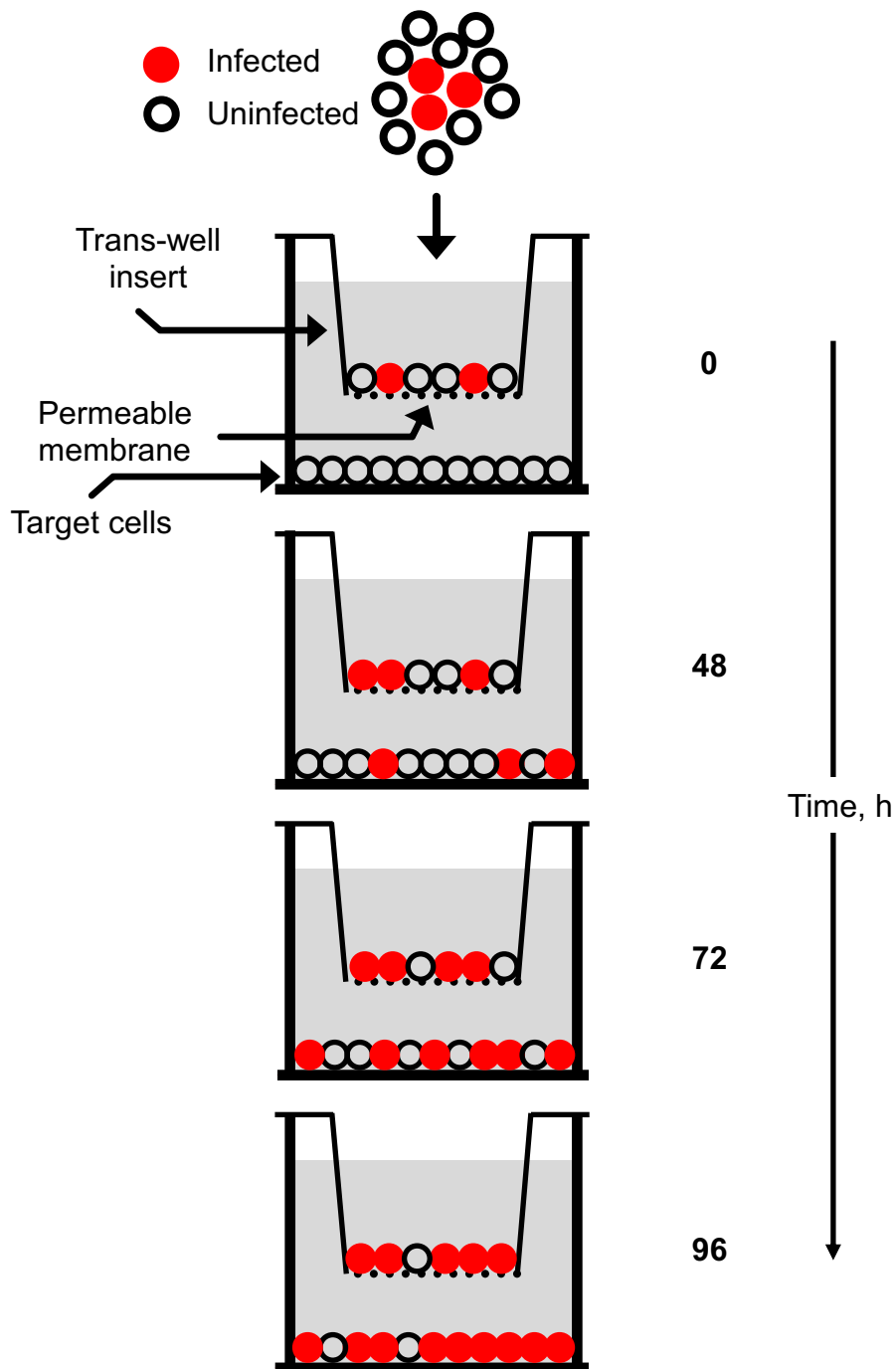


**Figure 2.7. Spread of HCV infection by cell-free or cell-associated virions.**

HCV-JFH1, Zika, or RSV infected and uninfected Huh7.5 cells are mixed 1:1000 then seeded on the inserts in transwell plates. Uninfected Huh7.5 cells are seeded at 95% confluence on the wells underneath. After 48, 72, and 96 h, monolayers on inserts and wells are immunolabeled to detect HCV core or Zika NS1, or RSV fluorescent fusion protein is visualized, using fluorescence microscopy. Results are expressed as the percent of infected cells in the monolayers on inserts and wells at each time point.

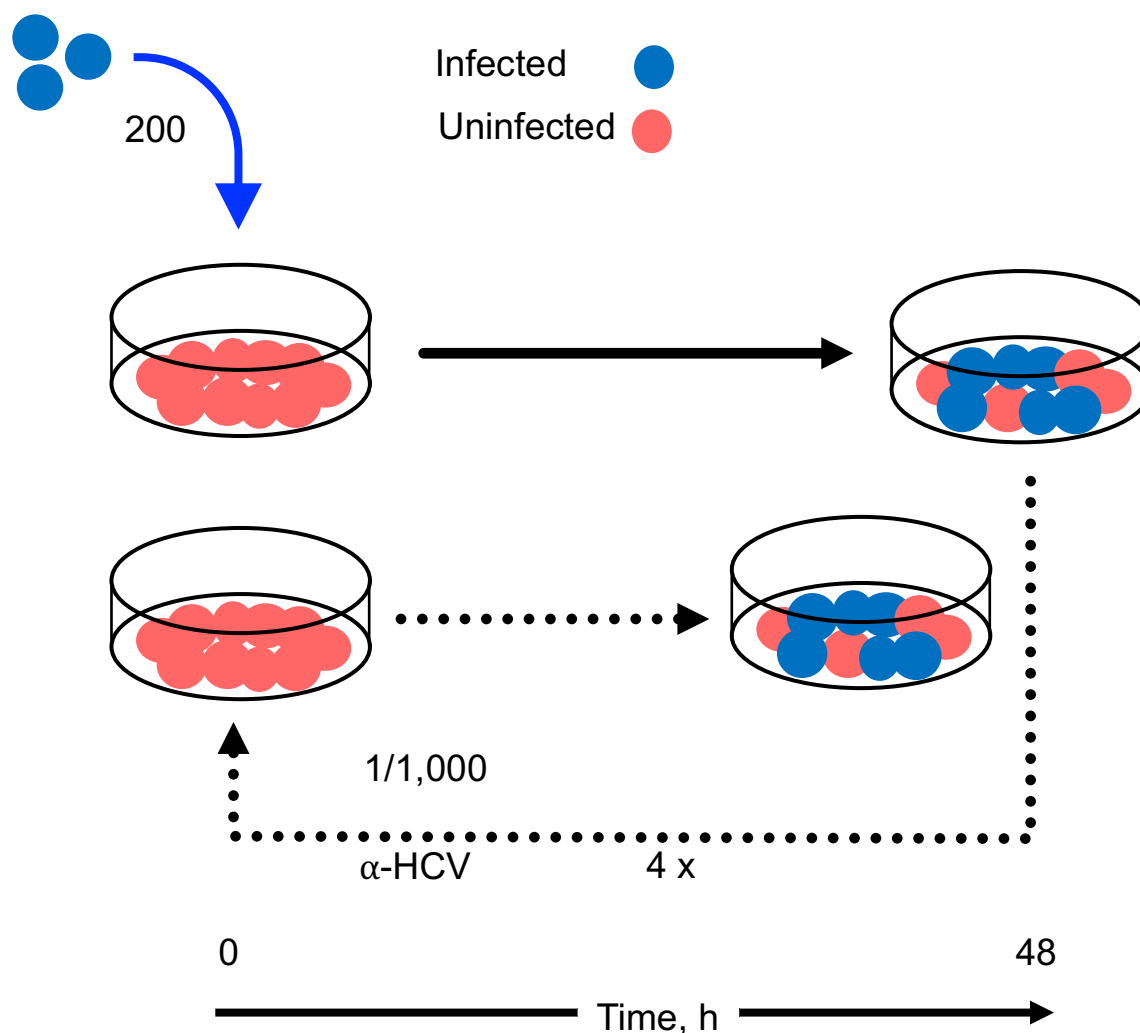


**Figure 2.8. Passaging of HCV cell-associated virions.**

200 HCV-JFH1 infected and  $1 \times 10^5$  uninfected Huh7.5 cells are co-cultured in the presence of anti-HCV neutralizing antibodies at dilution that inhibit 80% of the infectivity of cell-free virions. Two days later, co-cultured cells are resuspended and co-cultured 1:1000 with uninfected Huh7.5 cells in the presence of neutralizing antibodies for 2 days. Co-cultured cells are immunolabeled to detect HCV core or Zika NS1, or RSV fluorescent fusion protein is visualized, using fluorescence microscopy. The cycle is repeated 4 times.

a total of four times. All passages were evaluated for infection spread by direct (RSV) or indirect (HCV and Zika virus) immunofluorescence (**Figure 2.9**).

#### **2.2.15 Western blots**

Huh7.5 monolayers in 6-well plate were scraped into 100  $\mu$ l ice-cold lysis buffer (10 mM Tris HCl (pH 8), 140 mM NaCl, 1% Triton-X100, 0.1% SDS, 1% deoxycholic acid) supplemented with protease inhibitor cocktail cOmplete, EDTA-free. The samples were collected into 1.6 ml Eppendorf tubes, vortexed briefly, and incubated in ice for 15 minutes, vortexing briefly every 5 minutes. The samples were centrifuged at 20,000 g for 30 minutes at 4°C. Supernatants were collected, mixed 4:1 with 4X Laemmli buffer and incubated for 10 minutes at 95°C.

Proteins were separated by electrophoresis in 14% polyacrylamide gels and transferred to a PVDF membrane. Membranes were blocked with PBS containing 0.1% Tween-20 (PBST) supplemented with 5% skim milk. Primary antibodies diluted in PBST were added to the membranes and incubated overnight at 4°C. The membranes were washed with PBST three times for 10 minutes each and then incubated for 1 h at room temperature with the corresponding horseradish peroxidase-conjugated secondary antibody. The membranes were washed as after the primary antibodies. Secondary antibodies were detected using the Clarity™ Western ECL Substrate reagent according to the instructions of the manufacturer. Signal was detected using the ImageQuant LAS4000 (GE Healthcare, Chicago, IL).

#### **2.2.16 Cytotoxicity**

Cytotoxicity and cytostaticity of Z390 to Huh 7.5 cells were tested using MTT assays. Huh7.5 cells ( $4.0$  or  $1.0 \times 10^4$ ) per well were seeded into 96-well plate (at 100 or 25%

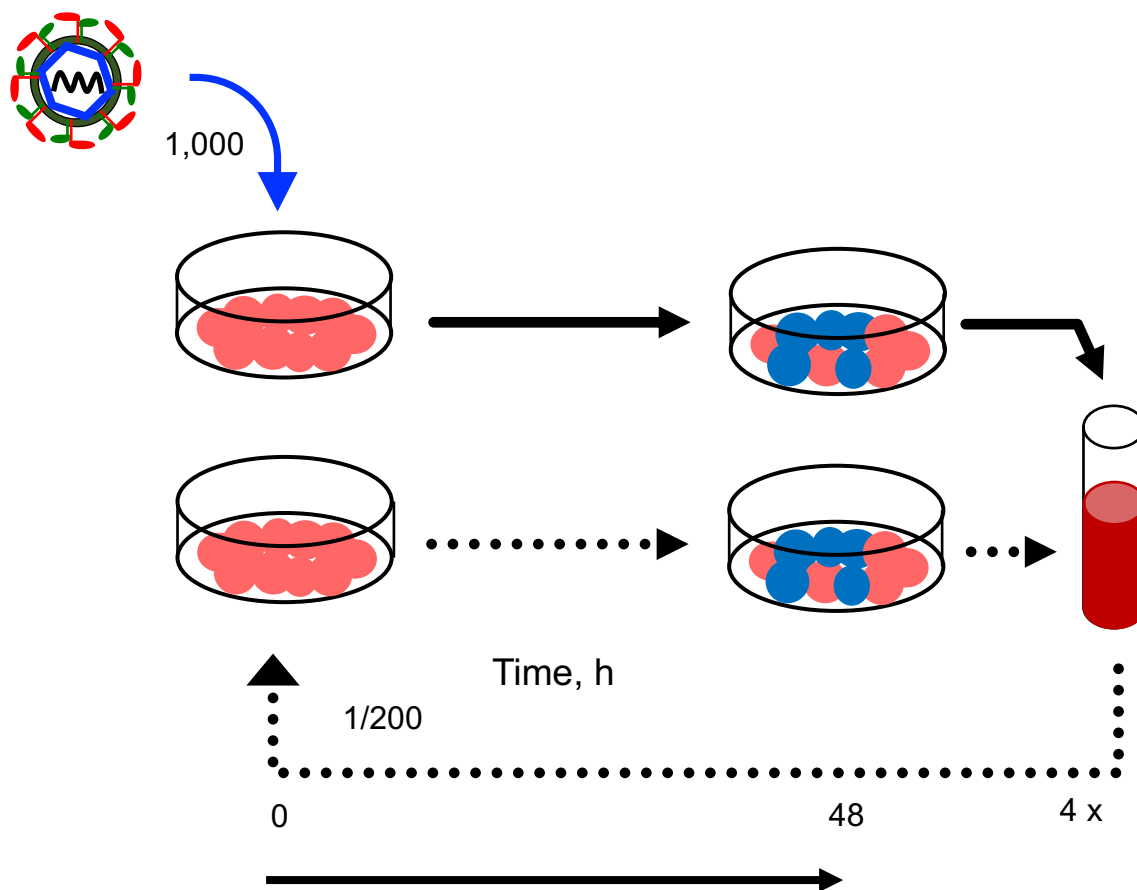


**Figure 2.9. Passaging of HCV cell-free virions.**

$1 \times 10^5$  Huh7.5 cells are infected with 1,000 FFU HCV-JFH1 for 2 days then culture supernatants are harvested, diluted 1:200, and used to infect  $1 \times 10^5$  Huh7.5 cells for 2 days. Infected monolayers are immunolabeled to detect HCV core or Zika NS1, or RSV fluorescent fusion protein is visualized, using fluorescence microscopy. The cycle is repeated 4 times.



confluence, respectively). Test compounds diluted in 150 µl DMEM-10% FBS were then added and incubated for 4 days at 37°C in % CO<sub>2</sub>. Media were removed and the cells were washed twice with 100 µl per well of phenol-red free DMEM before adding 200 µl per well MTT reagent diluted in phenol-red free DMEM and incubating for 3 h at 37°C. MTT was removed and the cells were washed twice with 100 µl per well DMEM before dissolving of formazan by adding 200 µl per well DMSO:isopropanol (1:1) and rotating for 15 minutes at room temperature. Absorbance was read at 570 nm with background at 680 nm. The relative cell number was determined daily and the results are expressed as fold difference to the day before treatment.

#### **2.2.17 Immunofluorescence and fluorescence labelling**

Cells seeded on poly-L-lysine-coated No 1.5 circular 12 mm diameter coverglass in each well of 24-well plates were washed twice with 1.0 ml room temperature PBS. Cells were then fixed with 0.5 ml per well 10% formalin, prepared from 16% formaldehyde methanol-free, for 15 minutes at room temperature. Formalin was removed and the cells were washed thrice 5 minutes with 1.0 ml PBS per well per wash. Cells were blocked with 200 µl 5% normal goat or donkey sera-0.05% saponin in PBS per well for 45 minutes at room temperature. Primary antibodies diluted in 1% normal goat or donkey sera-0.05% saponin in PBS were incubated with the cells for 3 h at room temperature or overnight at 4°C. Primary antibodies were removed, and cells were washed thrice for 10 minutes with 0.5 ml per wash per well of 0.1% BSA and 0.05% saponin in PBS. Fluorescently-conjugated secondary antibodies were diluted to the required concentration in 1% normal goat or donkey sera-0.05% saponin in PBS, incubated with the cells at room temperature for 1 h (protected from light in a light-tight box), and then washed as described for the primary

antibodies. To stain lipid droplets, Bodipy493 was diluted to the required concentration in PBS (2-5  $\mu\text{g/ml}$  depending on each experiment condition), incubated with the cells for 30 minutes at room temperature, and washed twice for 5 minutes with 1 ml PBS per wash. Cells were counterstained with 2  $\mu\text{g/ml}$  DAPI in PBS for 10 minutes at room temperature followed by two 5-minute washes with PBS. Coverglasses were removed from the wells, rinsed briefly in  $\text{dH}_2\text{O}$ , and overlaid on a 6  $\mu\text{l}$  SlowFade Diamond mounting media spotted on 25x75 mm glass microscope slide. The edges of the mounted coverglasses were sealed with CoverGrip coverslip sealant. The slides were protected from light until imaging.

## **CHAPTER THREE: Identification of A small molecule inhibitor of HCV cell-to-cell spread**

### **3.1 INTRODUCTION**

HCV RNA has been detected by in situ hybridization in liver biopsies from HCV-infected individuals. Hepatocytes with detectable HCV RNA are distributed in clusters resembling foci, mostly in the portal and periportal areas (Agnello et al., 1998; Haruna et al., 1993; Lau & Davis, 1994; G. Li et al., 2013; Nouri Aria et al., 1993; Tanaka et al., 1993; S. Yamada, Koji, Nozawa, Kiyosawa, & Nakane, 1992). Homogeneously disseminated infections in liver lobules have also been reported (Gosalvez et al., 1998; Hiramatsu et al., 1992; Lamas, Baccarini, Housset, Kremsdorf, & Brechot, 1992; G. Yamada, Takahashi, Tsuji, Yoshizawa, & Okamoto, 1992). The clustered or disseminated patterns of HCV infection in liver biopsies correlates with the severity of liver damage. Clusters of HCV infected hepatocytes RNA were associated with mononuclear infiltration in early stages, and liver pathology was minimal. The infection pattern becomes diffuse in biopsies from patients at advanced stages of HCV-associated liver damage (Agnello et al., 1998; M. Chang et al., 2000; Tanaka et al., 1993). HCV genomic RNA was detected in hepatocytes distributed throughout the entire tissue, while the anti-genomic HCV RNA replication intermediate was confined to foci of the hepatocytes (M. Chang et al., 2000). In another study, HCV RNA and antigens such as the envelope, core, NS3, or NS5A, were analyzed in seven formalin-fixed paraffin-embedded liver biopsies from patients with chronic HCV infections. HCV infection was again detected in clusters of hepatocytes (Hiramatsu et al., 1992; Negro et al., 1998; M. Tsutsumi, Urashima, Takada, Date, &

Tanaka, 1994). These early studies provided the very first evidence of localized spread of HCV infection within the human liver. HCV direct cell-to-cell spread of infection was first proposed only in the last fourteen years (Ming Chang et al., 2003), based on the analysis of digital fluorescent microscopy imaging. Among hepatocytes in biopsies of infected individuals, HCV RNA was not randomly disseminated, but rather appeared as scattered clusters of infected cells. The HCV RNA signal intensity showed a gradient radiating outward from the most intense signal in the center. This pattern suggests that the infection had probably started with a single cell in the centre and was then transmitted outwards to the neighboring cells, forming a focus. The intensity of the HCV RNA signal had an inverse linear relationship to the distance from the center of the focus. The gradient probably results from the differences in the infection time. Cells infected first would have accumulated more RNA than the cells infected later by the virions produced from the first rounds of infection. As the detection and imaging techniques have improved, foci of infected hepatocytes in biopsies of HCV-infected patients has been more clearly shown as a cluster of infected and adjacent cells (G. Li et al., 2013).

Nearly all studies of HCV cell-to-cell spread in vitro have used co-culture assays, in which infected donor cells were incubated with uninfected target cells (Valli et al., 2006). Either the donor or the target cells were usually labeled with a membrane dye, and the infection was detected by in situ hybridization (Z. Liu & He, 2013), immunofluorescence (Brimacombe et al., 2011a; Catanese, Loureiro, et al., 2013; Timpe et al., 2008; Witteveldt et al., 2009; Xiao et al., 2014), direct immunofluorescence microscopy using nuclear translocation of a fluorescent protein in the target cells in response to the expression of HCV proteins (Zhao et al., 2017), or indirect immunofluorescence microscopy (Gondar et

al., 2015). Inhibition of infection by cell-free virions is essential to evaluate HCV cell-to-cell spread in these co-culture assays. Cell-free infections were commonly inhibited by addition of HCV neutralizing sera (Brimacombe et al., 2011a) or using target cells refractory entry of cell-free virions such as Huh7.5-lunet, which express 1,000-fold less of the essential HCV entry receptor CD81 (Witteveldt et al., 2009). Donor or target cells received treatments to target factors under investigation.

The role of CD81 in HCV cell-to-cell spread was tested by siRNA knockdown of CD81 in the target cells, anti-CD81 antibodies added to the co-cultured donor and target cells, or HCV E1E2 mutants with impaired interactions between E1E2 and CD81. Anti-CD81 antibodies added to the co-culture together with HCV neutralizing antibodies HCV reduced HCV cell-to-cell spread by 92%, 93%, or 43% in donor to target cells ratio of 1:1 (Brimacombe et al., 2011a), 1:2 (Fofana et al., 2013), or 1:4 (Timpe et al., 2008), respectively, as evaluated by immunofluorescence flowcytometry. The ratio of donor to target cells in the co-culture affected the efficiency of cell-to-cell transmission. The transmission from donor to target cells was lowest at 1:4 donor to target ratio by 18%, while the highest was at 1:2 by 83%, and at 1:1 the transmission rate was 50% (Witteveldt et al., 2009), as evaluated by immunofluorescence flowcytometry. Using cells that express low to no CD81, such as Huh7.5-lunet or HepG2, reduced HCV cell-to-cell spread by >85% (Brimacombe et al., 2011a; Timpe et al., 2008), whereas using HeLa cells as the target in co-culture by 99%, despite the expression of 50% CD81 in HeLa as in Huh7.5 cells (Timpe et al., 2008), as also evaluated by immunofluorescence flowcytometry. The ineffective cell-to-cell spread to CD81 expressing HeLa cells could suggests the requirement for additional factors for efficient cell-to-cell spread. CD81

alone, might thus not be sufficient to allow for HCV cell-to-cell spread. Electroporation of HCV mutant replicons that impair E1E2 and CD81 interaction allowed as much 10% HCV cell-to-cell transmission, suggesting that several host or viral factors could facilitate HCV cell-to-cell spread in a coordinative manner (Witteveldt et al., 2009). Anti-SR-BI antibodies inhibited HCV spread by 40% or 95%, respectively in a co-culture with target cells knocked down for CD81 or not (Catanese, Loureiro, et al., 2013). HCV mutant JFH1-G451R displays lower level of dependence to SR-B1 for cell-to-cell transmission (Grove et al., 2008; J. Zhong et al., 2006). Percent of cell-to-cell transmission of HCV-JFH1 donor was 41.7%, while that of JFH1-G451R was 14.3%. Overexpression of SR-B1 in Huh7.5 cells infected with HCV-JFH1 increased the median of number of cells per focus by 2-fold, while that of HCV-G451R did not change (Brimacombe et al., 2011a), indicating that SR-B1 promote HCV cell-to-cell spread.

Targeting tight junctions CLDN-1 and OCLN, which also participate in entry of cell-free virions of HCV, inhibited direct transmission between cells in co-cultures. Knockdown of CLDN-1 or OCLN in target cells in co-cultures inhibited cell-to-cell spread by 47% or 60 to 60%, respectively (Brimacombe et al., 2011a; Z. Liu & He, 2013). Ectopic expression of CLDN-1 in 293T target cells increased the cell-to-cell transmission by 4-fold (Timpe et al., 2008). Addition of anti-CLDN-1 antibodies to the co-culture inhibited cell-to-cell spread by 88 to 90% (Barretto et al., 2014; Xiao et al., 2014).

ApoE and ApoB, which are involved in the assembly and release of HCV cell-free virions, also participate in the HCV cell-to-cell spread. Knockdown of ApoE in the donor or target cells inhibited cell-to-cell spread by 35 to 40% or had no effect (Gondar et al., 2015; Zhao et al., 2017), respectively, whereas knockdown of ApoE in both target and

donor cells inhibited cell-to-cell spread by 35% (Barretto et al., 2014). Thus, knockdown of ApoE in donor but not target cells, inhibit HCV cell-to-cell spread. Silencing of ApoB in the donor, target (Gondar et al., 2015), or both cells (Barretto et al., 2014), had no effect or minimally reduced of HCV cell-to-cell spread, respectively. Targeting other host factors involved in entry of cell-free virions of HCV using small molecule inhibitors of EGFR (Xiao et al., 2014) or NPC1L1 (Barretto et al., 2014) such as erlotinib or ezetimibe, respectively, inhibited HCV cell-to-cell spread by 80 to 90%, as assessed by reduction of number of cells per focus not in co-culture assays.

Heterocyclic rings are a common pharmacophore in medicinal chemistry that served as starting templates for the development of several therapeutic agents. They are heterocyclic aromatic compounds containing two nitrogen atoms at positions 1 and 3 of the six-membered rings. Heterocycles containing pyrimidine moieties are of great biological and pharmacological interest because many natural and synthetic compounds based on this moiety have useful biological activities and pharmacological applications (Lagoja, 2005; Sharma, Chitranshi, & Agarwal, 2014). Compounds with pyrimidine cores have anticancer (5-fluorouracil), antiviral (idoxuridine and trifluridine), antibacterial (trimethoprim and sulfamethazine), antihypertensive (minoxidil and prazosin), and antihistaminic (thinozylamine) activities, among others. Several pyrimidine derivatives could inhibit replication of viruses such as HIV, HSV-1, and CMV (Longley, Harkin, & Johnston, 2003; Sharma et al., 2014).

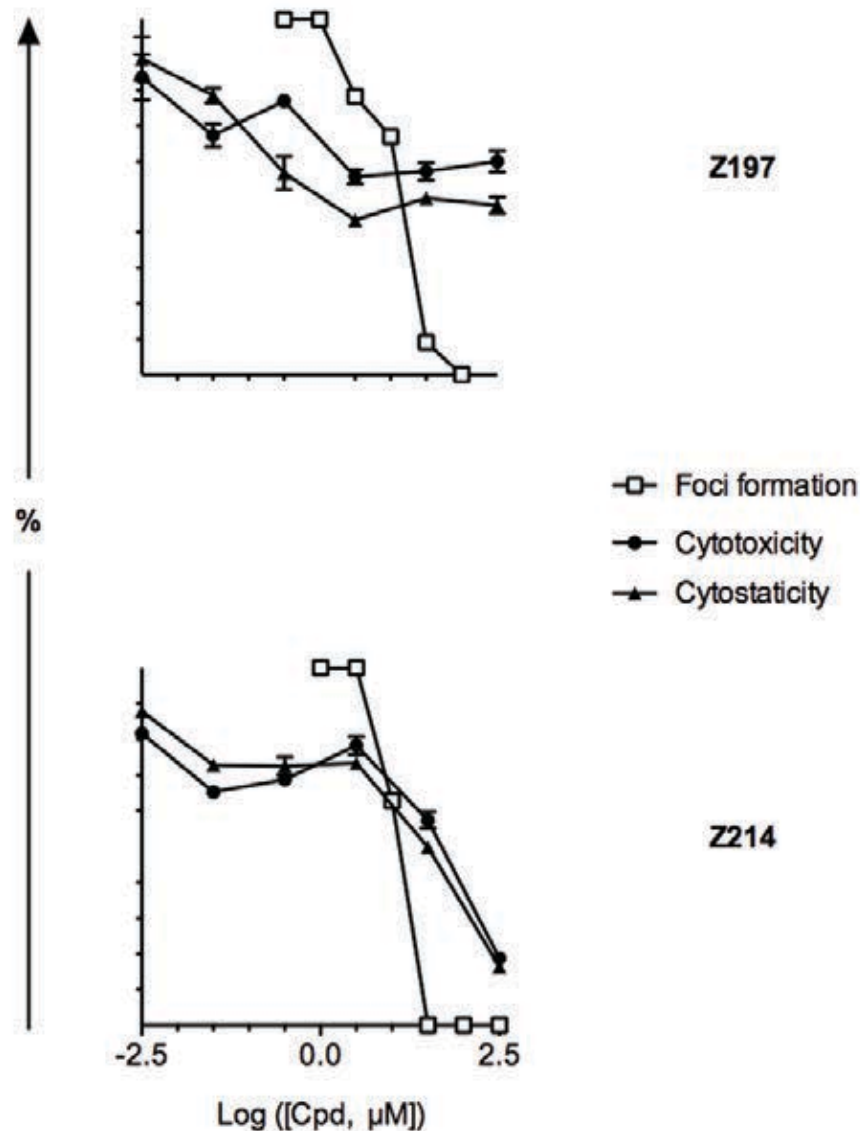
## 3.2 QRESULTS

### 3.2.1 1,5-substituted pyrimidines inhibit HCV foci formation

Nine pyrimidine derivatives were tested for activity against (HSV1-KOS), VSV, IAV, PV, VACV, and HCVcc-JFH1. The selected viruses selected are enveloped or not, contain DNA or RNA genomes, enter by pH-dependent or independent fusion at the plasma membrane or after internalization, and replicate in the cytoplasm or in the nucleus. To test the effects of the compound on virion infectivity, virions were treated with semi-logarithmic concentrations of test compounds for 15 minutes at 37°C before inoculating susceptible cells in multi-well plates for 1 h at 37°C. To test the effect of test compounds on viral replication, cells were infected for 1 h (or 4 h for HCV) at 37°C before they were overlaid with appropriate media containing semi-logarithmic concentrations of test compound. The effects on infectivity or replication were assessed by plaquing efficiency or plaque reduction assay (foci for HCV), respectively.

The nine derivatives had no effects on the infectivity or replication on any tested virus in up to 200  $\mu\text{M}$ , except for HCVcc-JFH1. Z197 and Z214 inhibited HCVcc-JFH1 foci formation in Huh7.5 cells ( $\text{EC}_{50}$ , 13.8 or 12.9  $\mu\text{M}$ , respectively) (**Figure 3.1**). Based on their activity, 55 new derivatives were designed, synthesized and tested for inhibition of HCVcc-JFH1 foci formation. Twenty-one inhibited HCV foci formation with different degrees of potency and selectivity ( $\text{EC}_{50}$ , 1.1-40.7  $\mu\text{M}$ , selectivity indices, 1.5-45); they also had different solubilities.



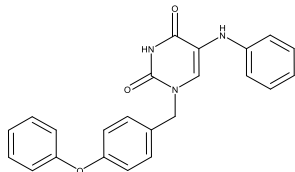
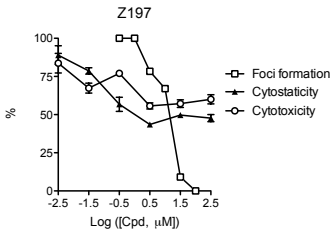
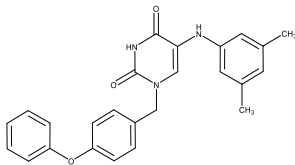
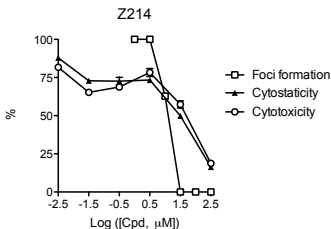


**Figure 3.1. Z197 and Z214 inhibit HCV foci formation.**

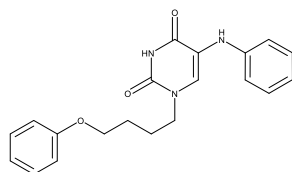
Dose-response line graph presenting foci formation and cytotoxicity. Huh7.5 cell monolayers were infected with HCVcc-JFH1 at an moi of 0.001. Inocula were removed 4 h later and fresh medium containing Z197 or Z214 was added. Replication was assessed by focus forming assays 48 h later, as evaluated by immunofluorescence against HCV capsid proteins. Cytotoxicity and cytostaticity were assessed by MTT assay (results from two independent experiments).

**Table 3.1 Chemical structures and anti-HCV activity and cytotoxicity profile of the 1,5-diarylpyrimidines.**

Activity against HCV was evaluated by foci formation assay using HCVcc-JFH1. Cytotoxicity was assessed by MTT assay in Huh7.5 cells

Name	Structure	IC <sub>50</sub> , μM	Cytostaticity		Cytotoxicity		Graph
			CC <sub>50</sub> , μM	Selectivity Index	CC <sub>50</sub> , μM	Selectivity Index	
Z197		13.8	1.0	0.1	> 316.2	> 22.9	
Z214		12.9	30.2	2.3	52.5	4.1	

Z246



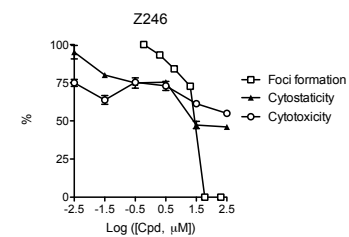
28.8

24.6

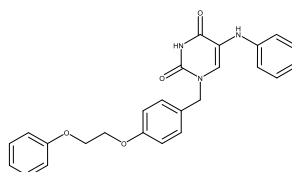
0.9

>  
316.2

&gt; 10.96



Z264



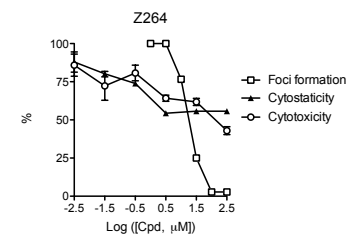
19.5

>  
316.2

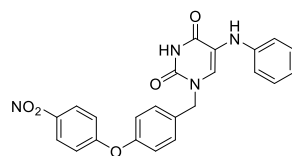
16.2

131.8

6.8



Z304



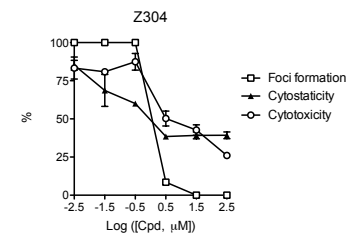
1.1

1.0

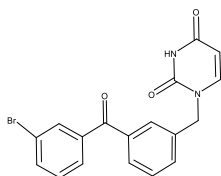
1.0

3.2

3.0



Z362



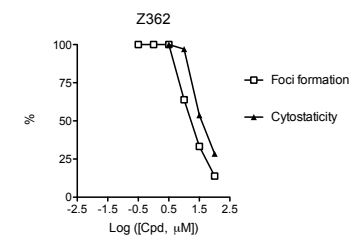
17.8

38.0

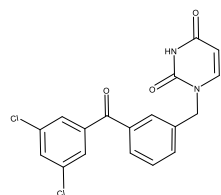
2.1

-

-



Z363



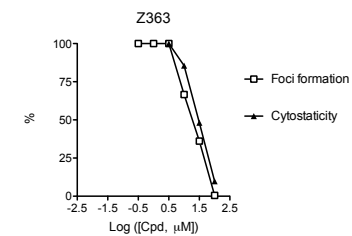
18.2

30.2

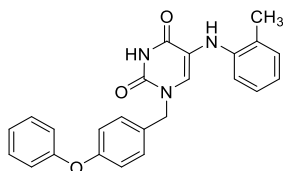
1.7

-

-



Z367



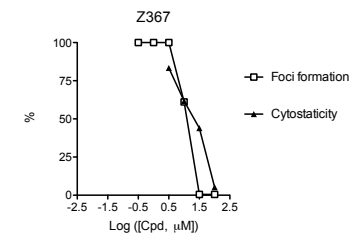
12.6

21.4

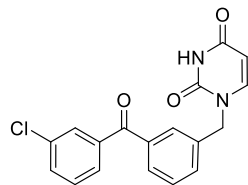
1.7

-

-



Z370



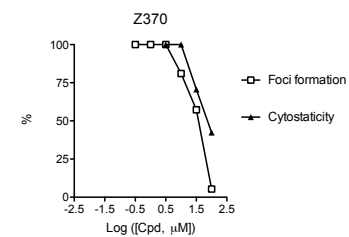
38.0

72.4

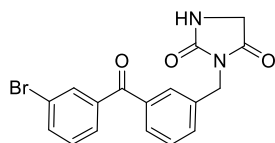
1.9

-

-



Z371



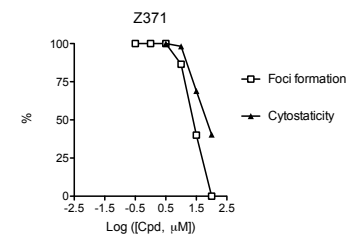
25.1

67.6

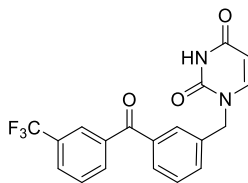
2.7

-

-



Z373



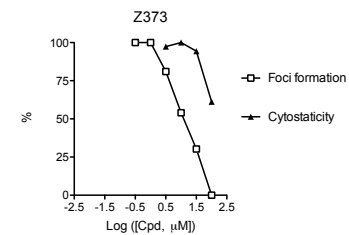
12.0

81.3

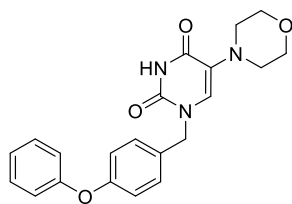
6.8

-

-



Z380



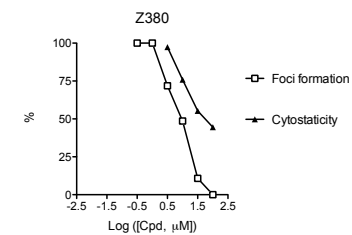
9.1

53.7

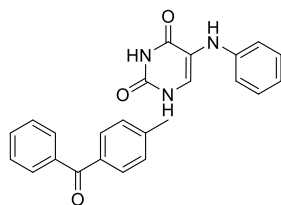
5.9

-

-



Z381



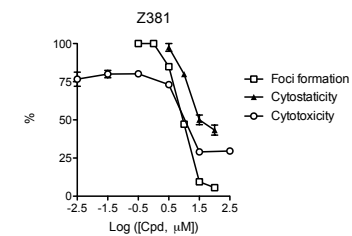
9.8

30.2

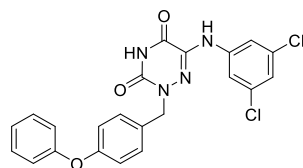
3.1

11.2

1.5



Z384



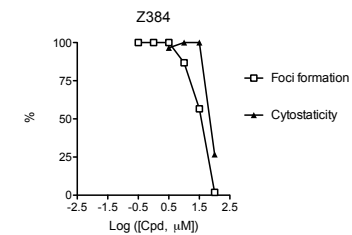
37.2

75.9

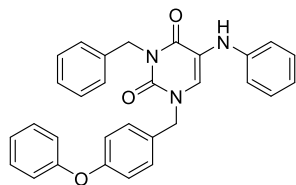
2.0

-

-



Z390



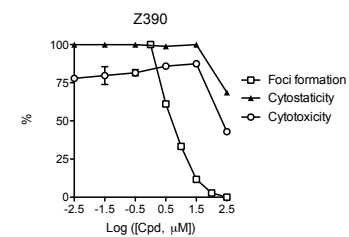
4.8

&gt; 100

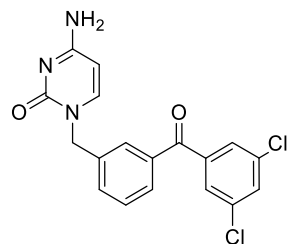
&gt; 20.88

218.8

45.7



Z391



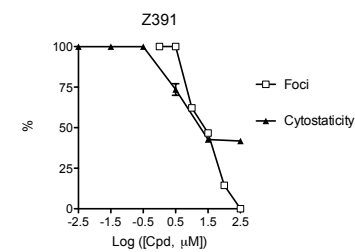
26.3

18.6

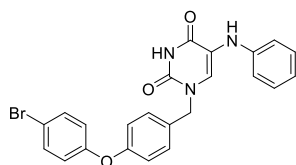
0.7

-

-



Z392



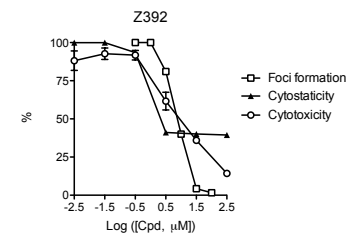
8.1

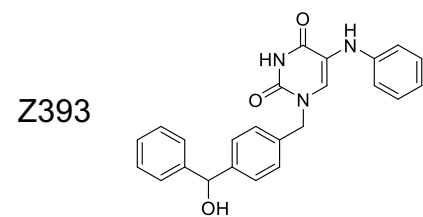
2.9

0.4

9.1

1.1





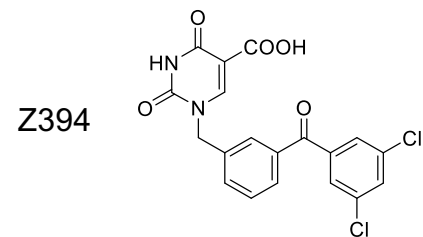
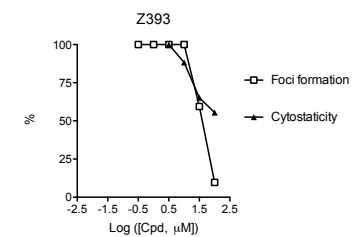
40.7

> 100

> 2.45

-

-



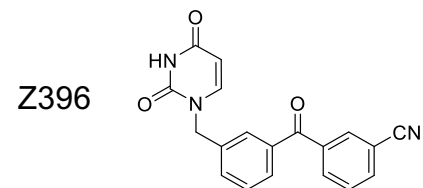
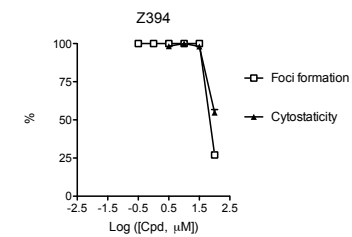
64.6

> 100

> 1.55

-

-



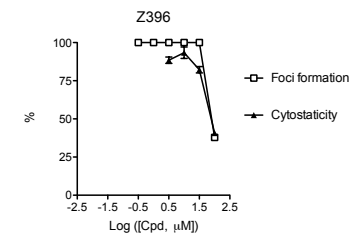
83.2

83.2

1.0

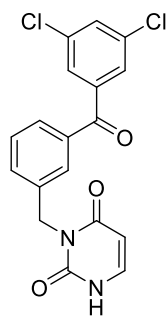
-

-





Z403



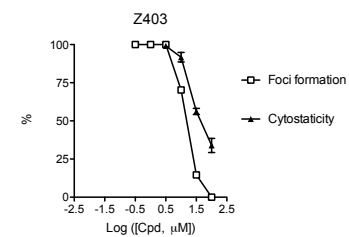
15.1

43.7

2.9

-

-



### 3.2.2 Optimization of Z390

Structure-activity relationship (SAR)-driven optimization led to compound Z390, a derivative that inhibited HCVcc-JFH-1 foci formation ( $EC_{50}$ , 4.8  $\mu$ M) at non-cytotoxic concentration ( $EC_{50}$ , 216; SI, 45) (**Figure 3.2**). HCVcc-JFH1 infection of Huh7.5 cells produce foci comprising of 20 to 40 infected adjacent cells after 48 h. Approximately 90 % of foci were composed of more than 5 cells in untreated infections, as expected. Only 10 % of foci had more than 5 cells in infections treated with 30  $\mu$ M Z390 (**Figure 3.3**). Z390 also inhibited foci formation of HCVcc-Jc1 (genotype 2a, JFH/JC6 chimera) (Pietschmann et al., 2006). Z390 had better solubility than Z197 or Z214. Therefore, Z390 was used in all subsequent characterization experiments.

The number of infected cells per focus decreased as the concentration of Z390 increased, but the number of foci forming unit per well did not, and infections of non-adjacent cells was not affected. The number of infected cells per focus increased from an average of approximately 12 to approximately 30 cells from 48 to 72 h after infection, respectively, in infections treated with DMSO vehicle. In contrast, the average number of infected cells per focus increased only approximately 4 to 5, 2 to 3, or 1 to 2 from 48 to 72 h in infections treated with 10, 20, or 40  $\mu$ M Z390. Z390 thus inhibits the spread of infection between adjacent cells (**Figure 3.4**).

### 3.2.3 Specificity of Z390 against flaviviruses

Z390 and derivatives were active against only HCV among many unrelated viruses. Z390 and derivatives could perhaps affect only viruses related to HCV. I therefore tested the effect of Z390 against two other flaviviruses, DV and Zika virus. Both viruses were tested in Huh7.5, as HCV, and in Vero cells. Huh7.5 or Vero cells infected with DV or Zika virus

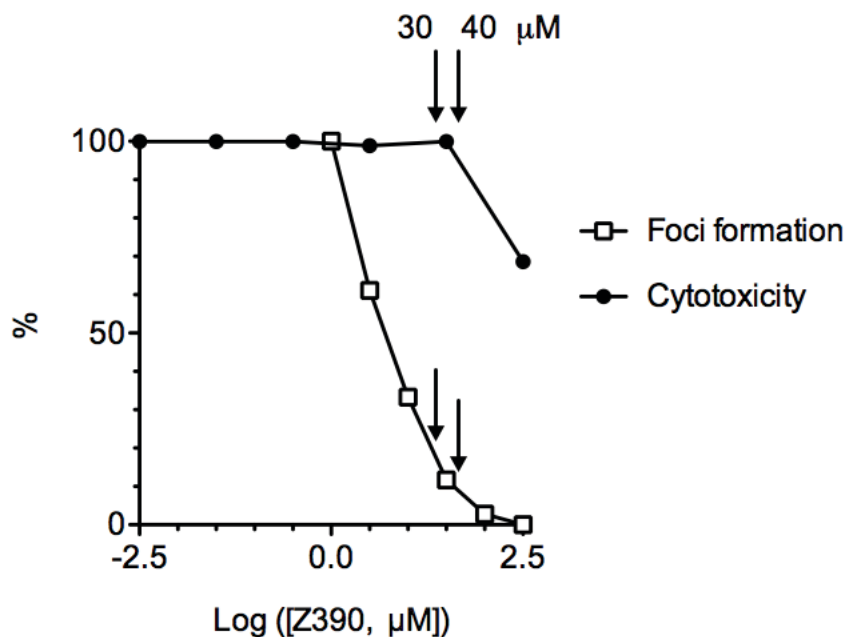


**Figure 3.2. Z390 inhibits HCV foci formation at non-cytotoxic concentrations.**

Dose-response line graph presenting foci formation and cytotoxicity. Huh7.5 cell monolayers were infected with HCVcc-JFH1 at an moi of 0.001. Inocula were removed 4 h later and fresh medium containing Z390 was added. Replication was assessed by focus forming assays 48 h later, using immunofluorescence against HCV core protein. Cytotoxicity was assessed by MTT assay.

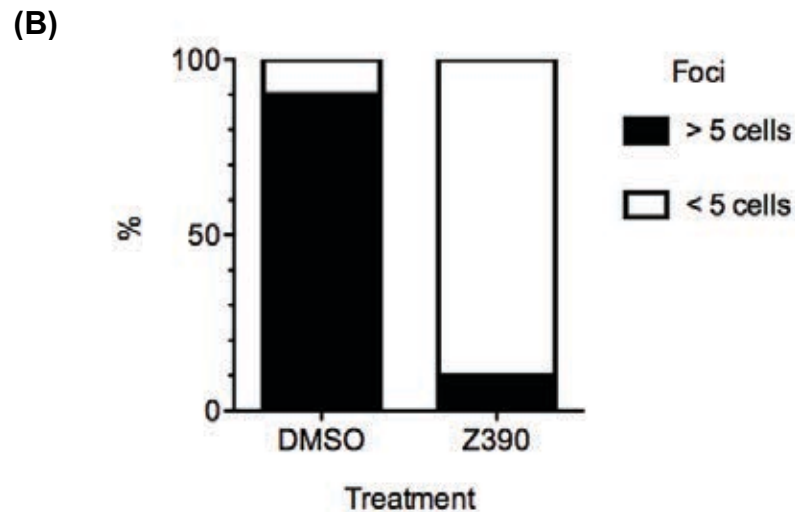
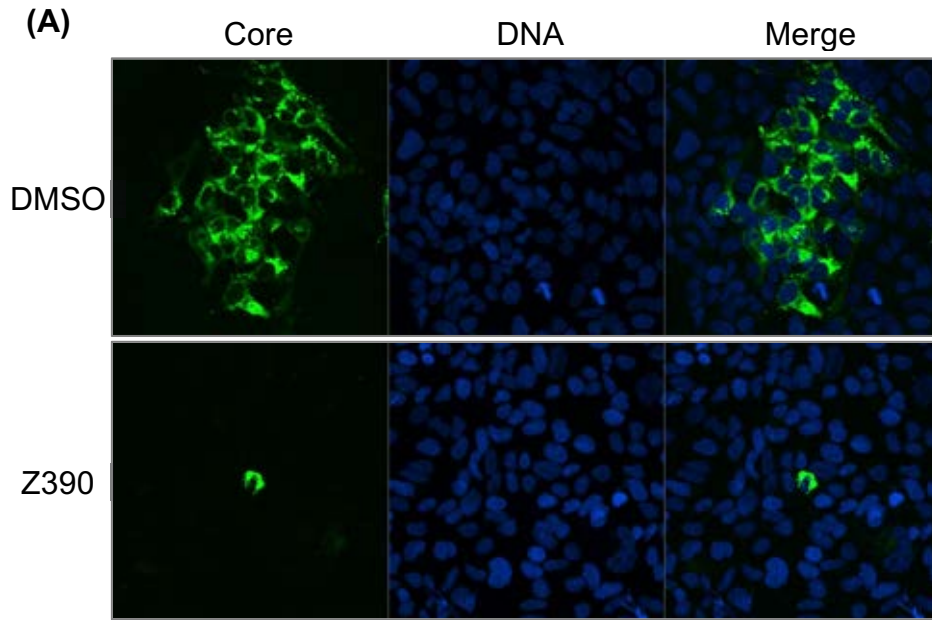


**Figure 3.3. Z390 inhibits HCV foci formation.**

**(A)** Immunofluorescence micrographs of HCV-infected cells treated with DMSO or 30  $\mu$ M Z390. Huh7.5 monolayers were infected with HCVcc-JFH1, moi=0.001. Inocula were removed 4 h later and fresh medium containing Z390 was added. Replication was assessed by focus forming assays 48 later, using immunofluorescence against HCV core protein. **(B)** Bar graph presenting percent of number of cells per focus.

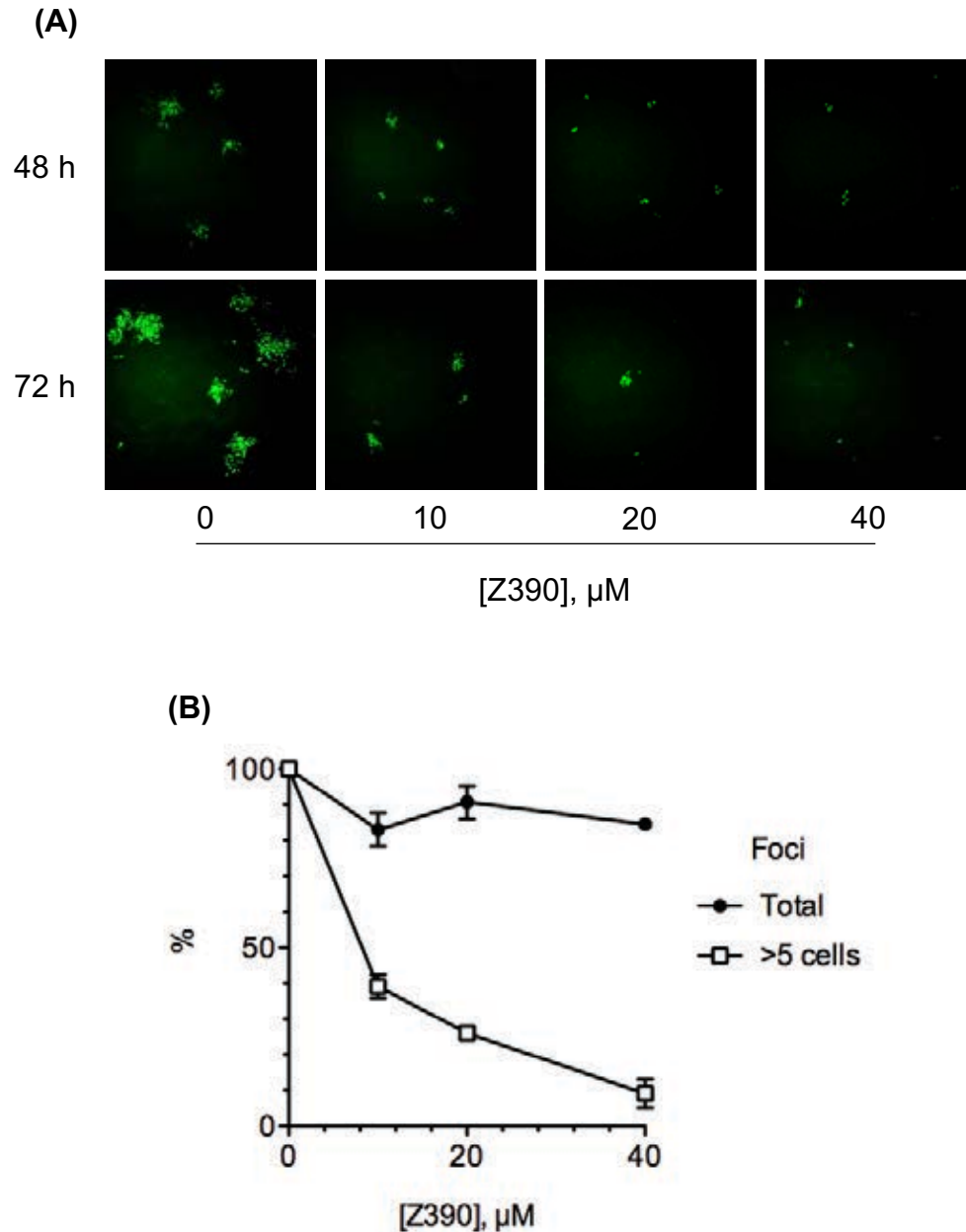


**Figure 3.4. Z390 reduces the number of cells per focus but not that of foci per well.**

(A) Immunofluorescence micrographs of HCV-infected cells treated with 0, 10, 20, or 40  $\mu\text{M}$  Z390. Huh7.5 monolayers were infected with HCVcc-JFH1,  $\text{moi}=0.001$ . Inocula were removed 4 h later and fresh medium containing Z390 was added. HCV was assessed by immunofluorescence against HCV core protein. (B) Dose-response line graph presenting number of foci per well and cells per focus (results from two independent experiments).

for 1 h were treated with Z390 for 2 to 4 days before visualizing plaques. Treatment with up to 40  $\mu$ M Z390 did not affect plaque formation by Zika (**Figure 3.5**) or DV (**Figure 3.6**). virus in Huh7.5 or Vero cells.

DV and Zika viruses spread mainly by the release of infectious virions that infect other cells by cell-free virion transmission (L. I. Tang, Ling, Koh, Chye, & Voon, 2012, Kurane, 1984). Therefore, I next tested the activity of Z390 against a virus which like HCV, spreads mainly between adjacent cells to form foci, respiratory syncytial virus (RSV). RSV is a negative-sense single-stranded RNA human orthopneumovirus (Huong, Iyer Ravi, Tan, & Sugrue, 2016; Mehedi, Collins, & Buchholz, 2017). RSV foci formation in Huh7.5 or HeLa cells was not affected by up to 40  $\mu$ M Z390 (**Figure 3.7**).

#### **3.2.4 Z390 does not inhibit HCV replication**

Z390 inhibited HCV foci formation as assessed by immunofluorescence detection of HCV core protein. Instead of formation of foci of infected cells, single or double infected cells were dominantly observed. Foci formation requires multiple cycles of replication which mainly involve entry, transcription, genome replication, assembly, and egress. It is not possible to identify which steps of the HCV replication cycle are inhibited by Z390 to inhibit the formation of HCV foci using plaque reduction assays. Therefore, I next tested the effect of Z390 on single-step HCV replication assays.

Huh7.5 cells were infected for 4 h at multiplicity of infection of 5, such that all cells are infected before treatment with 40  $\mu$ M Z390 or vehicle control. Infectivity and HCV RNA were assessed in the media and cell lysates at 0, 6, 12, 24, and 48 h after infection. The infectivity at time 0 is the virus in the inoculum. As the infection progresses (6 and 12),

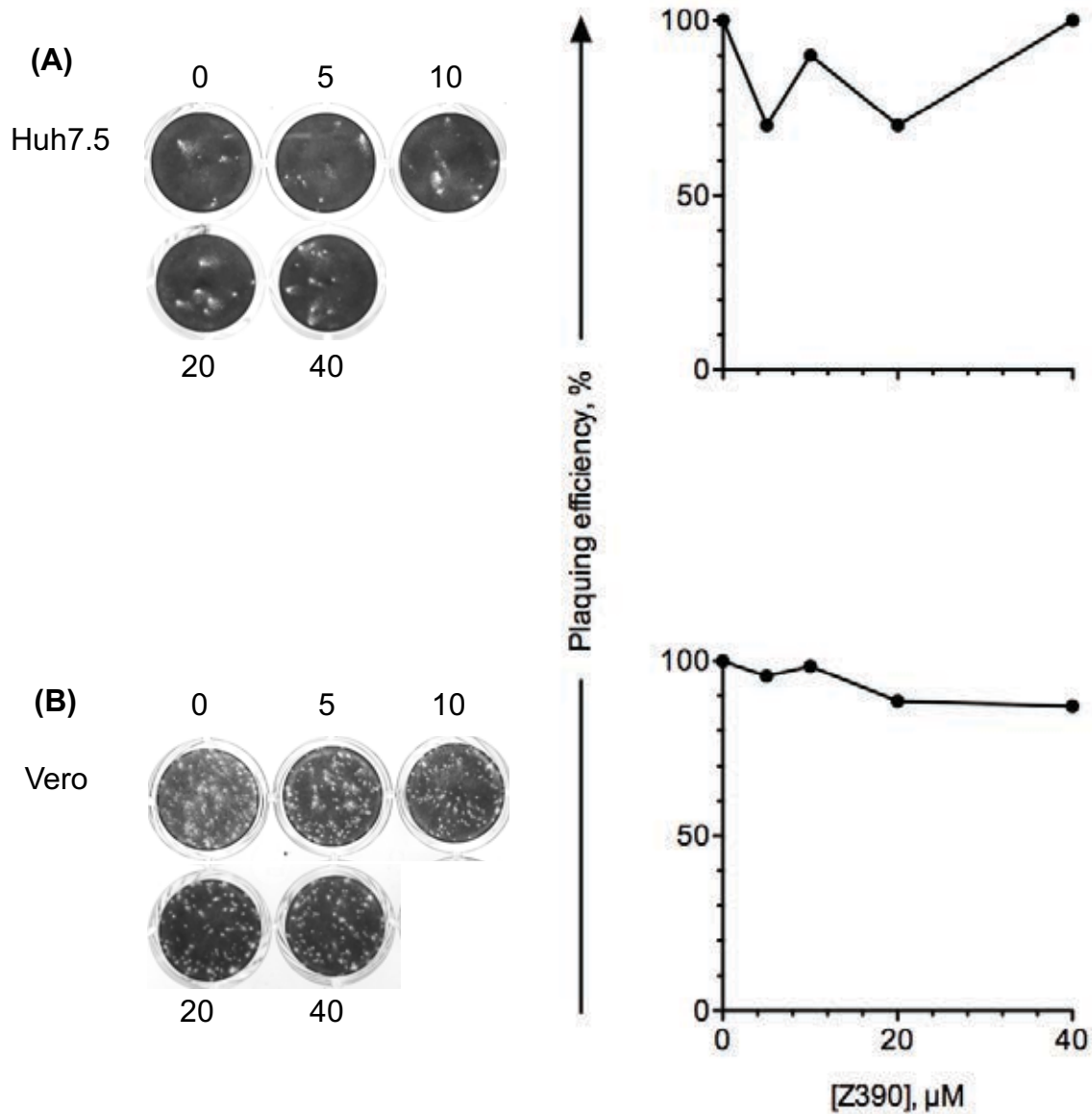


**Figure 3.5. Z390 does not inhibit replication of Zika virus.**

(A) Huh7.5 or (B) Vero cell monolayers were infected with Zika virus, at an moi of 0.001. Inocula were removed 1 h later and fresh medium containing Z390 was added. Replication was assessed by plaque formation at 48 to 72 h later (left). Dose-response line graph presenting number of plaques per well, normalized to vehicle control (left).

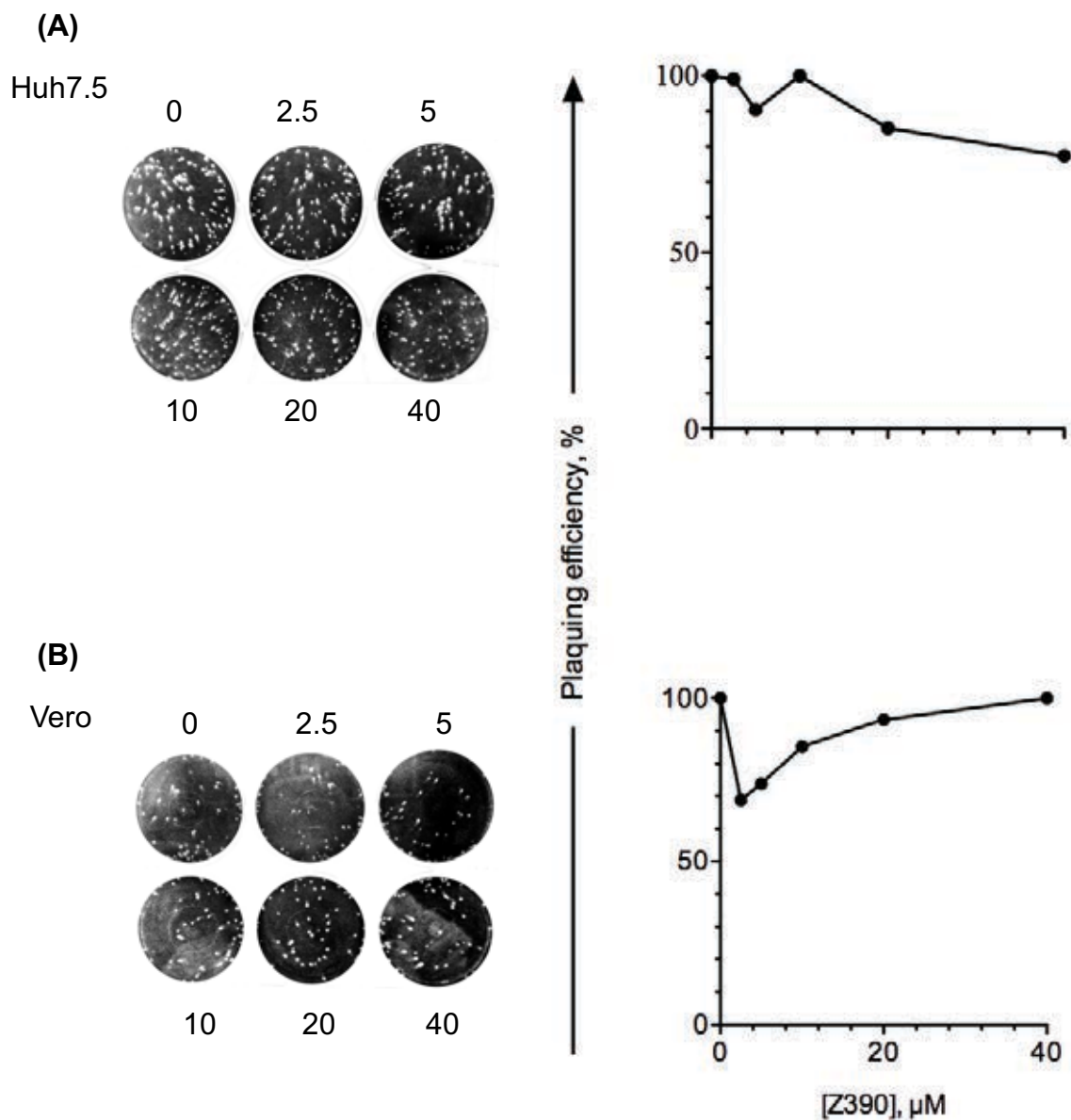


**Figure 3.6. Z390 does not inhibit replication of DV.**

**(A)** Huh7.5 or **(B)** Vero cell monolayers were infected with DV at an moi of 0.001. Inocula were removed 1 h later and fresh medium containing Z390 was added. Replication was assessed by plaque formation at 48 to 72 h later (left). Dose-response line graph presenting number of plaques per well, normalized to vehicle control (right).



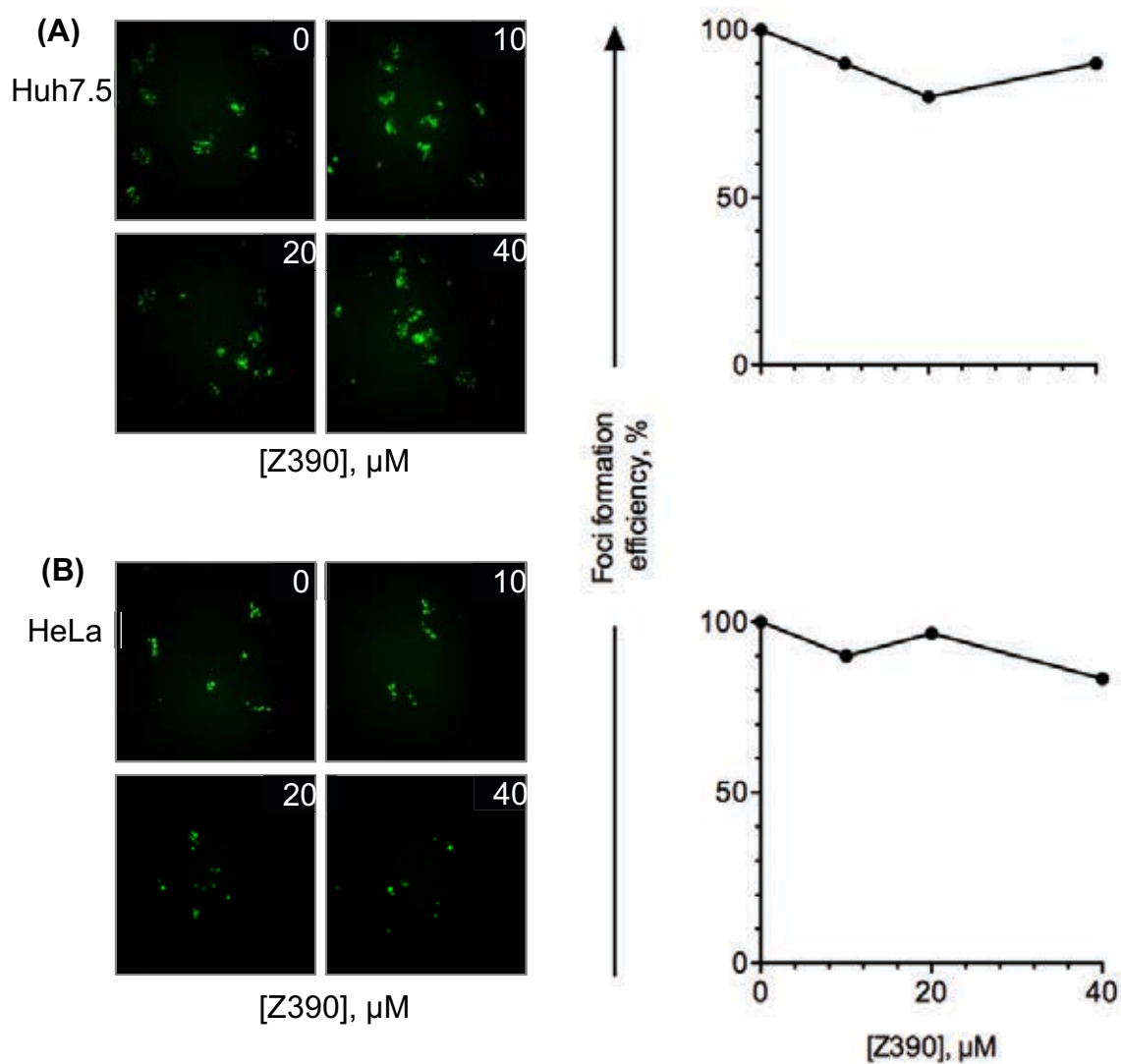


**Figure 3.7. Z390 does not inhibit RSV foci formation.**

Fluorescence micrographs of RSV-infected cells. (A) Huh7.5 or (B) HeLa cell monolayers were infected with RSV, at an moi of 0.001. Inocula were removed 2 h later and fresh medium containing Z390 was added. Replication was assessed by foci formation 48 h later using direct fluorescence for RSV fusion protein (left). Dose-response line graph presenting normalized number of foci per well (right).

infectivity is gradually lost due to fusion and uncoating of the infecting virions. Infectivity then starts to increase again as progeny virions are produced, reaching a plateau at 24 or 72 h for cell-associated or cell-free infectivity, respectively. HCV replication and release were not affected by Z390 (at its EC<sub>99</sub> for the inhibition of foci formation). Similar number of HCV genomes were produced and released, too, indicating that Z390 does not affect HCVcc-JFH1 replication (

**Figure 3.8-**

**Figure 3.9).** Therefore, Z390 inhibits HCV foci formation by inhibiting spread of the infection consistently with the effects observed on foci formation.

**3.2.5 Z390 does not inhibit HCV virion infectivity, or cell susceptibility or permissiveness to infection**

Z390 inhibits HCV foci formation in multiple-step infections without inhibiting HCV replication in single-step infections, indicating that it inhibits the spread of the infection between cells. For HCV foci to form, the virus first must replicate in the infected cell, infectious progeny must be produced, and then progeny virions must infect adjacent cells. The cells adjacent to the infected cells must thus be susceptible and permissive to HCV entry and replication. Z390 could interfere with the infectivity of the progeny infectious virions released to the extracellular space or render adjacent cells non-susceptible or non-permissive to HCV entry or replication, respectively (**Figure 3.10s**).

To test whether Z390 inhibits HCVcc-JFH1 virion infectivity, HCVcc-JFH1 virions were treated with Z390 for 1 h at 37°C before infecting susceptible Huh7.5 cells. To test if Z390 inhibit susceptibility or permissiveness of the cells to be infected, Huh7.5 cells

were treated with Z390 for 1, 2, or 3 days before infection with HCVcc-JFH1. Z390 pre-treatment of HCV virions or Huh7.5 cells before infection did not affect foci formation as

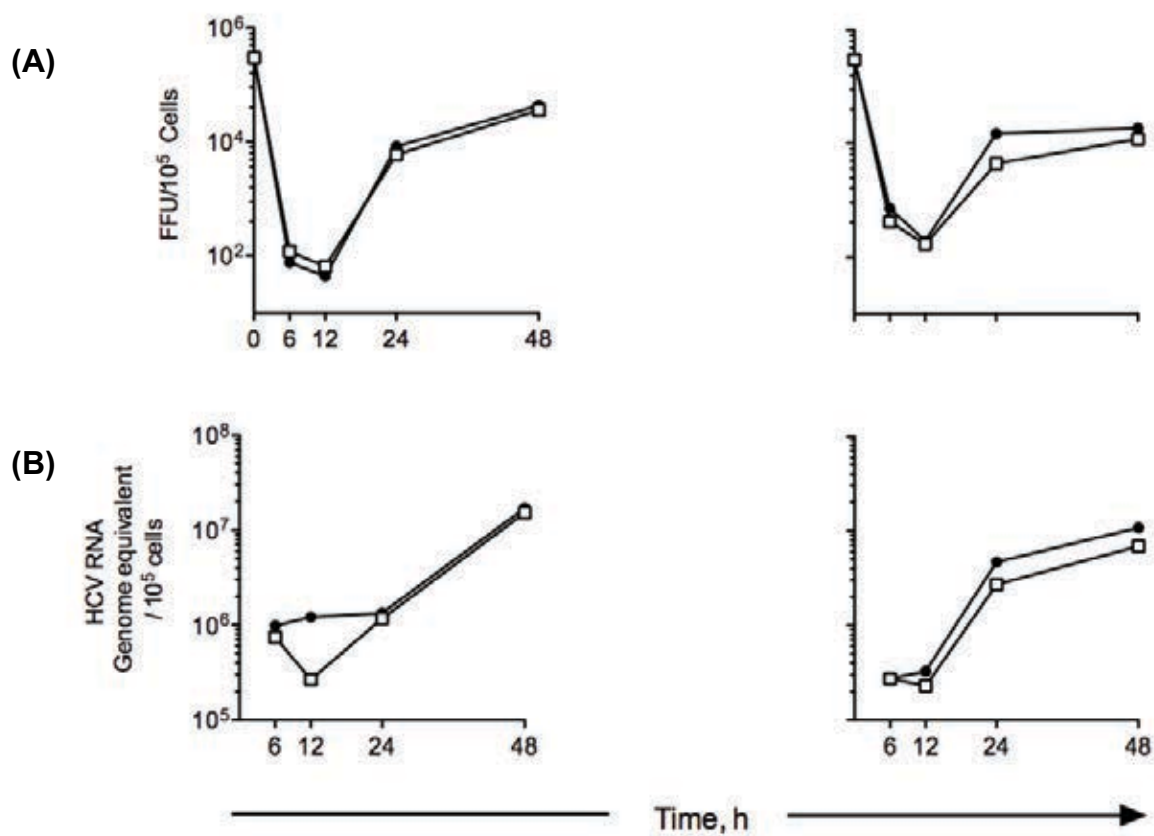


**Figure 3.8. Z390 does not inhibit HCV replication.**

Dose-response line graphs presenting cell-free and cell-associated HCV infectivity **(A)** or HCV RNA **(B)**. Huh7.5 monolayers were infected with 5 infectious HCVcc-JFH1 virions per cell. Inocula were removed 4 h later and fresh medium containing 40  $\mu$ M Z390 was added. Supernatant and cells were collected at 6, 12, 24, and 48 h after infection. Infectivity was determined by infecting Huh7.5 cell monolayers with 10-fold serial dilutions of supernatant or cell lysate. Inocula were removed 4 h later and fresh medium was added 48 later. Infectious foci were detected by immunofluorescence against HCV capsid proteins. HCV RNA was evaluated by quantitative RT-PCR. (results from one experiment).

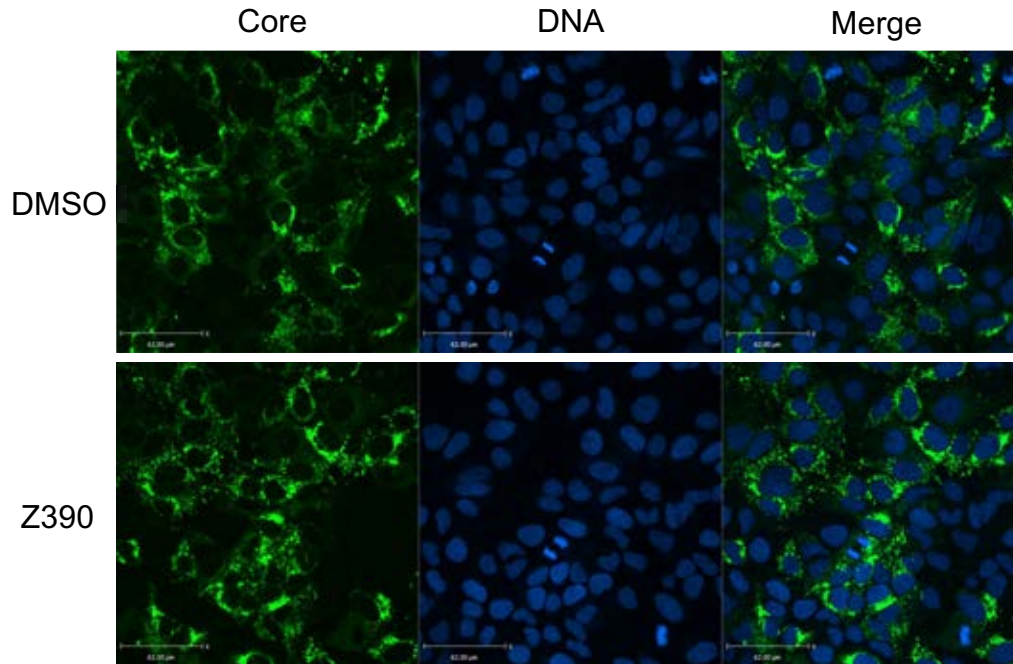


**Figure 3.9. Z390 does not inhibit HCV replication.**

Immunofluorescence micrographs of HCV-infected cells treated with DMSO or 40  $\mu$ M Z390. Huh7.5 monolayers were infected with HCVcc-JFH1, moi=5. Inocula were removed 4 h later and fresh medium containing Z390 was added. Replication was assessed by immunofluorescence against HCV core protein 48 h later.

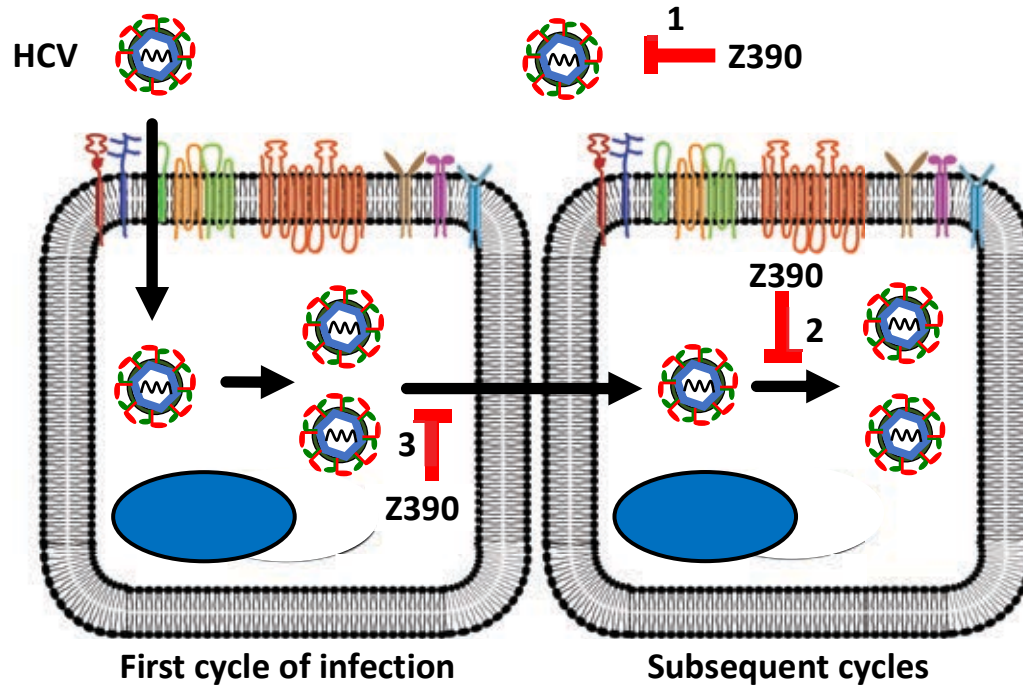


**Figure 3.10. Proposed mechanisms of action of Z390.**

Z390 inhibits HCV focus formation without inhibiting replication. Focus forms by transmission of progeny virions from infected cell to adjacent uninfected cells. Z390 could inhibit focus formation by inhibiting the transmission of the released virions into adjacent cells by blocking their infectivity (1). Z390 could inhibit focus formation by interfering with susceptibility or permissiveness of adjacent cells (2). Z390 could inhibit focus formation of the proposed direct cell-to-cell transmission (3).

evaluated by immunofluorescence for HCV core protein at 48 h. Thus, Z390 did not inhibit spread of HCV infection between cells by either impairing the infectivity of HCV virions or the susceptibility or permissiveness of the cells to HCV entry or replication, respectively (**Figure 3.11**).

### **3.2.6 Z390 inhibits cell-to-cell spread of HCV in co-culture assays**

Z390 inhibited the spread of HCV infection in Huh7.5 cell culture without affecting replication, virion infectivity, or cell susceptibility or permissiveness. Z390 could thus inhibit spread of HCV infection by inhibiting direct cell-to-cell HCV transmission. I tested this possibility. To perform these assays, I first needed to be able to neutralize the cell-free infectivity. HCVcc-JFH1 or Jc1 virions were incubated with 2-fold serial dilutions of anti-HCV or control sera for 30 minutes before infection, and plaquing efficiency was evaluated 48 h later by immunofluorescence detection of the core protein. Infections with virions treated with pre-immune sera resulted in primary infections, evidenced as foci composed of approximately 20 cells per focus and secondary infections of 1 to 4 cells, suggesting HCV infection spread by cell-to-cell or cell-free transmission, respectively. Infections treated with anti-HCV sera resulted only in primary foci without secondary infections, suggesting that HCV infection spread only by cell-to-cell transmission in the presence of neutralizing antibodies (**Figure 3.12**).

To test if Z390 inhibits HCV cell-to-cell spread, HCVcc-JFH1 infected cells (donors) were co-cultured 1:1,000 with uninfected cells for 24 h in the presence of neutralizing serum, to limit infection by cell-free virions, and 40  $\mu$ M Z390 [EC<sub>99</sub>] or the equivalent

volume of DMSO vehicle. Detection of HCV core protein in unlabeled target cells adjacent to labeled donor cells indicates direct transmission of HCV infection from donor to target



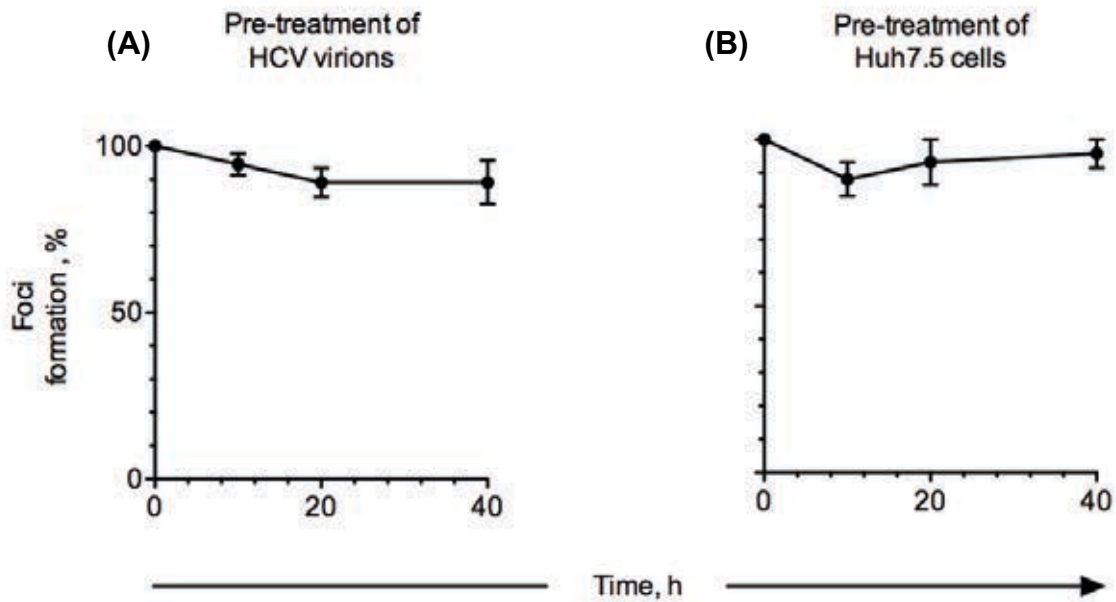
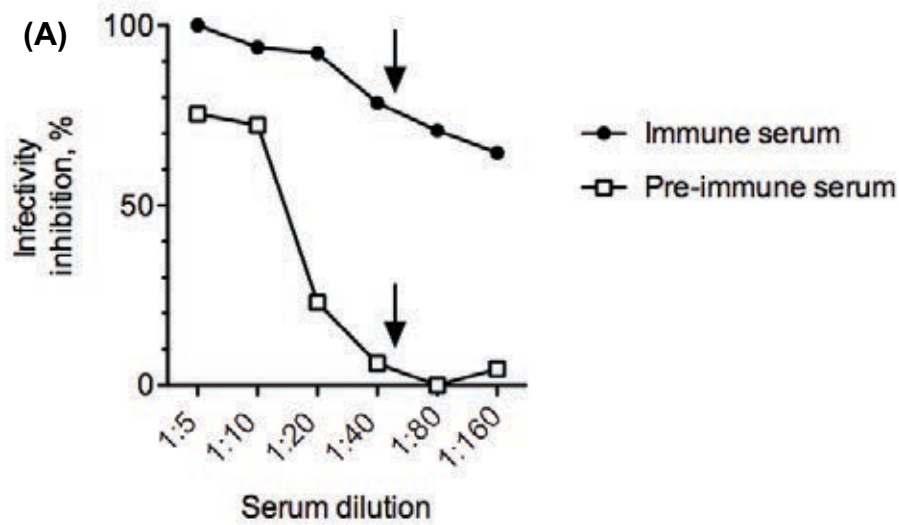


**Figure 3.11. Z390 does not affect virion infectivity or cell permissiveness to infection.**

Dose-response line graphs presenting HCV plaquing efficiency or foci formation in pre-treated Huh7.5 cells or HCV virions, respectively. **(A)** HCVcc-JFH1 virions were treated with Z390 for 1 h at 37°C before infection with HCVcc-JFH1. HCV inocula were removed after 4 h and fresh medium was added. **(B)** Huh7.5 monolayers were treated with Z390 for 48 h before infection with HCVcc-JFH1. HCV inocula were removed after 4 h and fresh medium containing Z390 was added. Foci formation was evaluated 48 h after infection. (results from two independent experiments).



(B)

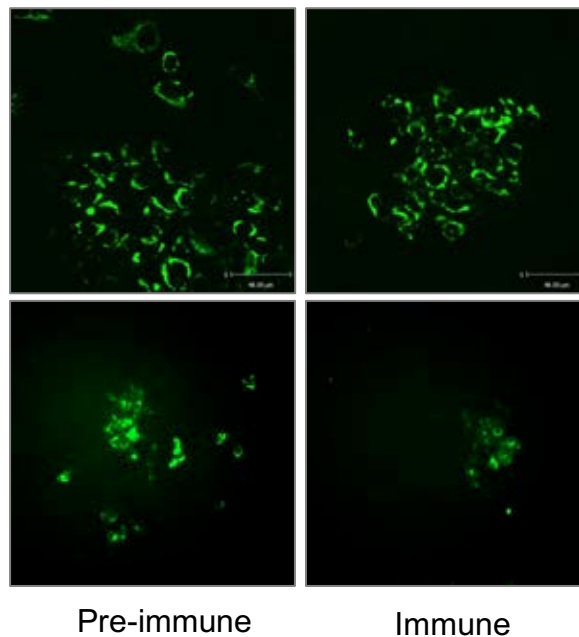


**Figure 3.12. Anti-HCV neutralizing antibodies inhibit secondary infections but not foci formation.**

(A) Dose-response line graphs of plaquing efficiency of HCV. Huh7.5 cell monolayers were infected with HCVcc-JFH1 virions treated for 1 h at 37°C with 2-fold serial dilutions of pre-immune or immune sera before infection of Huh7.5 cells. HCV inocula were removed after 4 h and fresh medium was added. Replication was assessed by focus forming assays 48 later, using immunofluorescence against HCV core protein. (B) Immunofluorescence micrographs of plaquing efficiency of HCVcc-JFH1 treated and processed as in (A) at 1:50 dilution of sera.

cells in the presence of neutralizing serum. HCV infection spread to every cell in direct contact with donor cells, and spread even further to other cells in direct contact with those infected in the first round. More than resulting in 90% of foci were composed of 5-30 target infected cells per donor cell. In contrast, the infection had spread to none or at most one adjacent target cell in co-cultures treated with Z390 (**Figure 3.13**). Therefore, Z390 inhibits HCV foci formation in the presence of neutralizing antibodies.

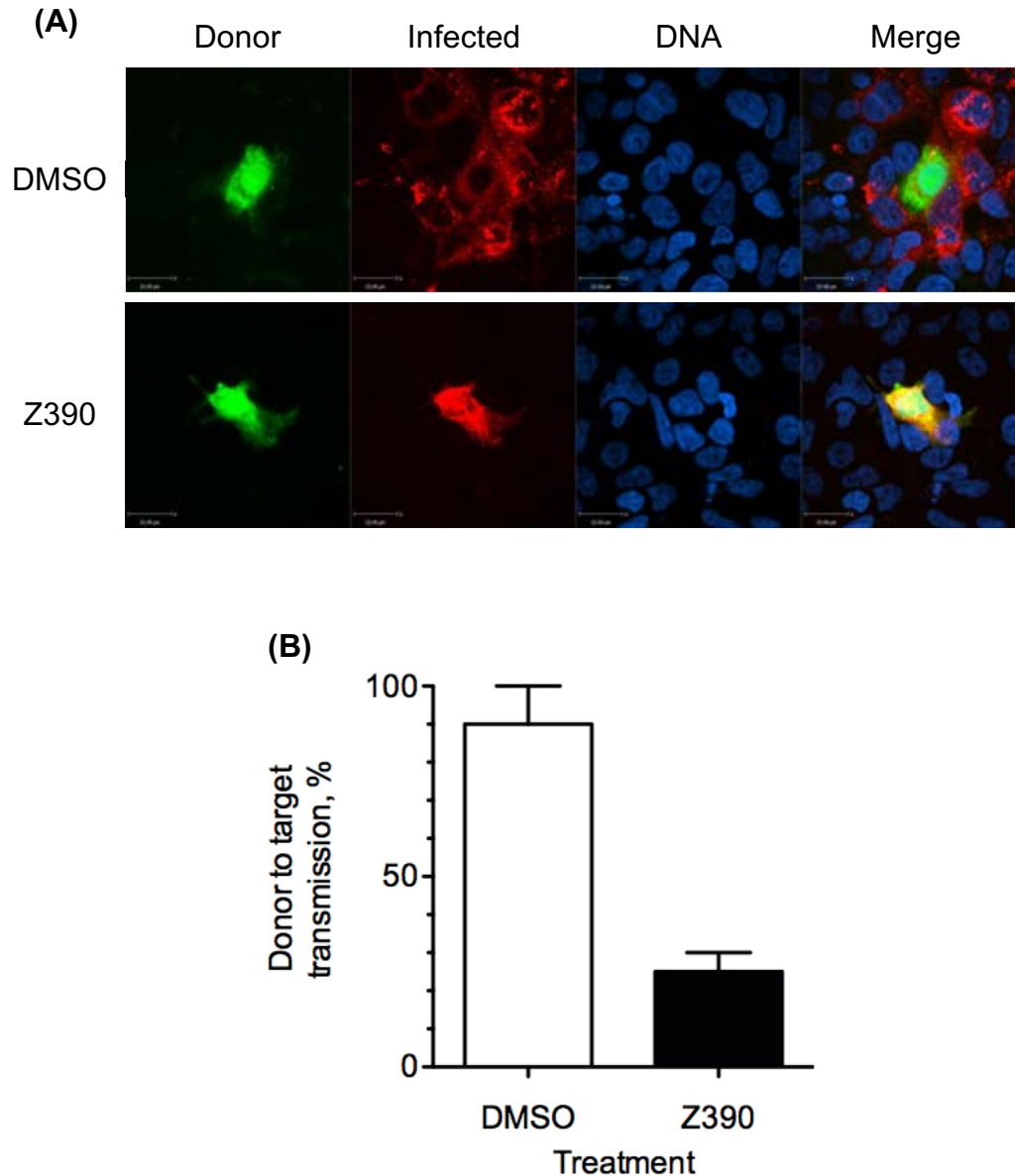


**Figure 3.13. Z390 inhibits HCV cell-to-cell spread.**

**(A)** Immunofluorescence micrographs showing CFDA SE-labeled cells (green) and HCV-infected cells (red) in co-cultures treated with DMSO or 40 $\mu$ M Z390. Huh7.5 monolayers were infected with 5 infectious HCVcc-JFH1 virions per cell. Donor infected cells were trypsinized, labeled with carboxy-fluorescein diacetate succinimidyl ester (CFDA SE), mixed with uninfected target cells at a ratio of 1 infected per 200 uninfected cells, and co-cultured with 40  $\mu$ M Z390 and 10% anti-HCV serum. Foci formation in the co-cultures was evaluated by immunofluorescence 24 h after co-seeding. **(B)** Bar graph presenting the percent of transmission from donor to target cells in DMSO or Z390 treated co-cultures (results from three independent experiments).

### 3.3 DISCUSSION

Pyrimidines are biologically active scaffold present in many essential metabolites and also in pharmacophore used to treat a diverse range of diseases (Kuppast & Fahmy, 2016). In collaboration with Dr. Novikov, we tested an initial group of nine 1,5-disubstituted uracil derivatives for their antiviral activities against a panel of different viruses. The compounds were tested against virion infectivity or viral replication. Two derivatives, Z197 and Z214, showed activity at low micromolar concentrations only against HCV. Z197 and Z214 were not sufficiently selective to use at more than  $EC_{50}$ . Therefore, an optimization of the lead active derivatives through structure-activity relationship studies was conducted and led to compound Z390, which did not differ much in absolute potency from Z214, but is less toxic and has better solubility. The selectivity of Z390 allowed to use it at  $EC_{90}$  (30  $\mu$ M) with cell viability near 100% (**Figure 3.2**). The concentration used in most of the subsequent characterization experiments were 30 to 40  $\mu$ M, concentrations at which viability was basically unaffected (**Figure 3.2**). In vehicle treated infections, 90% of the foci were comprised of >5 cells per focus, whereas in infections with 30  $\mu$ M Z390, only 10% of the foci had >5 cells (**Figure 3.3**). The number of HCV foci in Z390 or vehicle treated infections was equivalent to the number of the infectious particles inoculated. The doubling time of the Huh7.5 cells is approximately 24 h, cells would have doubled twice during the 48-h infection. Each focus comprised of less than five infected cells indicates that the infection did not transmit into adjacent cells.

Inhibition of HCV foci formation without inhibition of replication indicates that the two processes follow different mechanisms, which was not previously known. As Z390 inhibited foci formation but not the replication of HCV, it can be used to characterize HCV

foci formation separately from any other steps in the HCV replication cycle. The spread of the HCV infection to cells that are not adjacent to an infected cell in multiple-cycle replication assay occurs by diffusion of the infectious virions to infect distant cells by cell-free virion entry (Timpe et al., 2008). Similarly, infection of the cells adjacent to an infected cell could also result from cell-free virion entry. However, HCV neutralizing antibodies inhibited infections of distant but not adjacent cells, indicating that HCV spreads between adjacent cells predominantly by a mechanism which does not require the release of infectious virions (Brimacombe et al., 2011a; Xiao et al., 2014; Zhao et al., 2017). The effect of Z390 on the spread of HCV is the converse to that of the neutralizing antibodies. Z390 allows infection of distant but not adjacent cells.

The recent realization that cell-to-cell HCV transmission could be the primary mode of infection spread within the infected liver prompted the identification and characterization of host factors with a role in cell-to-cell spread. These factors are primarily the cell surface receptors that also facilitates the cell-free entry of HCV virions, including CD81, SR-BI, EGFR, NPC1L1 (Lupberger et al., 2011; Pileri et al., 1998; Sainz et al., 2012; Scarselli et al., 2002; K. Zhang & Kaufman, 2004), and the tight junctions occludin and claudin-1 (Evans et al., 2007; Ploss et al., 2009). The role of these host factors in HCV cell-to-cell spread has been characterized primarily using antibodies against the host factor under investigation at concentrations that inhibit cell-free entry of HCV virions. Genetic methods have also been used, either knockdown or ectopic expression in cells that express or lack the host factor under investigation, respectively. Targeting these host factors by antibodies or genetic methods inhibited HCV cell-to-cell spread with varying efficiency. However, no small molecule that inhibit cell-to-cell HCV

spread with no reported effects on any other replication steps has been described. Ezetimibe, an FDA approved cholesterol lowering agent that targets the cholesterol transporter NCP1L1, has been reported to inhibit HCV cell-to-cell spread by evaluating foci formation in non-dividing cells treated with ezetimibe 16 h after infection (Barretto et al., 2014). However, the effect of ezetimibe on HCV replication and entry was not assessed. Several other studies have identified and characterized ezetimibe as HCV entry inhibitor (Sainz et al., 2012). It is likely that ezetimibe inhibited the subsequent rounds of infection by blocking virion entry rather than inhibiting cell-to-cell spread. Erlotinib is a small molecule inhibitor of epidermal growth factor receptor (EGFR), a receptor that participates in the entry of HCV. It was reported to play a role in cell-to-cell spread of HCV. However, siRNA knockdown of EGFR or erlotinib treatment inhibited cell-free HCV virion entry by targeting post-binding steps, including mediation of CD81-CLDN1 interaction and viral fusion. Thus, Z390 represents the first small molecule that selectively inhibits HCV cell-to-cell spread. Using Z390 to study the mechanisms of inhibition would help identifying the specific mechanisms of HCV cell-to-cell spread.

Z390 inhibited HCV cell-to-cell spread with no effect on the release of infectious virions. Another important implication of this finding is the mechanism of HCV cell-to-cell spread with respect assembly and egress. Trafficking and secretion of HCV virions are the least understood step of HCV replication cycle. Whether the release of HCV virions to the extracellular space and the direct transmission to adjacent cells follow the same or different pathways is not known. For example, the current model of assembly and egress states that HCV core protein associates with cLDs near HCV replication complexes. The HCV envelope glycoproteins E1 and E2 are tethered toward the inner leaflet of the ER

membrane. Core protein and HCV RNA are packaged into the E1E2 coated ER region which is eventually enclosed and buds into the ER lumen (David Paul, Madan, & Bartenschlager, 2014; Syed, Khan, Yang, & Siddiqui, 2017; Zayas, Long, Madan, & Bartenschlager, 2016). Virions then follow the maturation and ER-to-Golgi secretory pathway to acquire ApoB100 (Nahmias et al., 2008) and ApoE (Benga et al., 2010) which are lipidated by MTP (Gastaminza, Kapadia, & Chisari, 2006b). Inhibition of ApoE or ApoB secretion or MTP activity inhibits the release of infectious HCV virions but not cell-to-cell spread (Barretto et al., 2014). Naringenin, a grapefruit flavonoid inhibitor of VLDL secretion, inhibits the release of ApoB (Nahmias et al., 2008) and infectious HCV virions (Barretto et al., 2014; Nahmias et al., 2008) by 70% or 75 to 90%, respectively. Treatment of HCVcc-JFH1 infected Huh7.5 cells with naringenin had no effect on cell-to-cell spread (Barretto et al., 2014). It is therefore possible that release of virions or transmission to adjacent cells follow different pathways. No cell-to-cell transmission was obtained when Huh7 cells electroporated with HCV RNA lacking E1E2-encoding sequences, were co cultured with uninfected Huh7 cells. Also, the density of intracellular infectious virions of HCV is higher than the released ones, suggesting that intracellular virions are enveloped but did not acquire the lipidated apolipoproteins (Gastaminza et al., 2006b). HCV glycoproteins or envelopment of HCV virions, is thus required for cell-to-cell spread. Enveloped, but not yet lipidated HCV virions could be transmitted between cells in co-culture assays (Catanese, Loureiro, et al., 2013; Witteveldt et al., 2009). Thus, it could be speculated that enveloped virions could either be driven to transmit to adjacent cells or to the secretory pathway where apolipoprotein components are acquired, and lipidation takes place.



The HCV replication cycle was characterized by studying the functions of the viral proteins and their interactions with host factors (Han, Niu, Wang, & Li, 2016; Moradpour & Penin, 2013). This characterization made it possible to design inhibitors to target specific viral proteins to inhibit their functions, thus blocking replication (Smith & Wu, 2003). A similar characterization of HCV cell-to-cell spread is still lacking. The assumption is that the receptors involved in the entry of cell-free virions are also the host factors involved in HCV cell-to-cell spread. This assumption may have limited the discovery of equally important host factors with exclusive roles in direct HCV cell-to-cell spread.

### 3.4 SUMMARY

Several selected derivatives of 1,5-uracil substituted with aromatic functional groups were tested against a panel of unrelated viruses representing a variety of virion structures, genomes, and entry and replication strategies. My hypothesis was that derivatives of 1,5-substituted uracils have antiviral activities. My objectives were to test selected 1,5-substituted uracils for activity against HSV-1, VSV, PV, IAV, vaccinia, and HCV, to subsequently characterize their mechanisms of action. I tested all compounds against the selected viruses for potential effects on virion infectivity or viral replication. Out of nine initial derivatives tested, two were active but exclusively against HCV replication. Serial optimizations led to a more potent and less toxic derivative that inhibited HCV foci formation in multiple-step replication assay at low micromolar concentrations. Surprisingly, none of these compounds inhibited HCV replication in single-step replication assays, suggesting that they inhibited spread of the infection instead. Further characterization showed that the derivatives of this novel scaffold inhibit direct cell-to-cell HCV spread.

## **CHAPTER FOUR: HCV spreads preferentially by cell-to-cell transmission**

### **4.1 INTRODUCTION**

#### **4.1.1 Spread of viral infections**

Viruses spread within cells primarily by two routes, release of cell-free virions which diffuse through the extracellular space to infect other cells or directly from infected to uninfected cells, without releasing infectious virions. These routes are known as entry of cell-free virions or cell-to-cell transmission, respectively (D. C. Johnson & Huber, 2002; Mothes, Sherer, Jin, & Zhong, 2010; P. Zhong, Agosto, Munro, & Mothes, 2013). Both spread mechanisms of spread of viral infection achieve efficient virus spreading, and different viruses tend to spread predominantly by one mechanism or the other. Transmission of infection by cell-free virions is essential to establish the primary infection in a susceptible host. It is also required to spread to distant organs within individual infected hosts, such as the transition of West Nile virus from the lymphoid drainage to the blood circulation, from which it penetrates the brain (Hasebe et al., 2010; Petersen, Brault, & Nasci, 2013). Transmission of viral infections between hosts, such as the oral contact in HSV-1 (Mertz, 2008), or across species, such as the influenza virus transmission from water birds to human (Parrish et al., 2008). Cell-free transmission of viruses is also required for the maintenance of viruses with life cycles including natural reservoirs such as for bats coronavirus (Calisher, Childs, Field, Holmes, & Schountz, 2006) or vectors, such as mosquitos for DV (Carrington & Simmons, 2014); all require cell-free infectious virions (Kuno & Chang, 2005).

For efficient spread by cell-free virions transmission, however, the infected cells must produce relatively large numbers of infectious virions to diffuse through the extracellular spaces and reach distant cells (Anekal, Zhu, Graham, & Yin, 2009; Bocharov, Meyerhans, Bessonov, Trofimchuk, & Volpert, 2016). Transmission by cell-free virions requires that infectious virions traffic through the egress pathway, then proceed through the entire replication cycle from entry to egress in the newly infected cells. Several bacteriophages and *Alphaviruses* are highly efficient for infection by cell-free virions. A single viral particle can infect a cell leading to a productive infection (Allue-Guardia, Jofre, & Muniesa, 2012; Helenius, Kartenbeck, Simons, & Fries, 1980). Direct cell-to-cell transmission of infection, on the other hand, could offer several advantages for efficient spread and persistence within the infected host. Evasion of the immune response and effectors in the extracellular space could account for the most critical role for the efficiency of infection spread via the cell-to-cell mode of transmission.

The mechanism of cell-to-cell spread of HIV is perhaps the best characterized. The role of HIV cell-to-cell spread has been investigated in several aspects including the dissemination of infection, resistance to anti-HIV drugs, and pathogenesis. HIV infects cells either by cell-free virions transmission or directly between cells (Durham & Chen, 2015; Iwami et al., 2015; Sourisseau, Sol-Foulon, Porrot, Blanchet, & Schwartz, 2007). Evidence from in vitro experiments show that HIV spreads more efficiently through the cell-to-cell transmission. The cell-to-cell transmission was estimated to account for 60% of the HIV-1 spread, which shortens the generation times of viruses or increases the viral fitness by 0.9 or 3.9 times, respectively (Iwami et al., 2015). HIV induces virological synapses at cell-cell contact sites, which facilitate firm interaction between the HIV-1

envelope glycoproteins in infected, and surface receptors on uninfected CD4<sup>+</sup> cells. (L. Wang et al., 2017). Synapses between HIV-infected and uninfected cells facilitate the transmission of a larger number of viral particles compared to cell free transmission. T cell uptake of HIV by cell-associated transmission is as much as 100-fold more efficient higher than uptake of cell-free virions (Debiaggi et al., 1999). Most of the nucleoside-analogue reverse transcriptase inhibitors (NRTIs) are less effective in inhibiting the cell-to-cell, than cell-free transmission of HIV-1. The potency of NRTIs tenofovir, azidothymidine, or lamivudine inhibition of HIV-1 infections transmitted by cell-free virions was 200 to 1,000-fold higher than in infections by cell-to-cell transmission (Agosto, Zhong, Munro, & Mothes, 2014). Infection of PBMCs with cell-free HIV-1 virions in the presence of 10  $\mu$ M tenofovir inhibited the transmission of HIV-1 infection by 25-fold whereas co-culture of PBMC target with HIV-1-infected PBMC donor cells in the presence tenofovir, the transmission was inhibited by only 1.4-fold (Sigal et al., 2011).

#### **4.1.2 Spread of HCV infection**

HCV infects hepatocytes by cell-free virions or direct cell-to-cell transmission. Infection by cell-free virions establishes the initial infection in the host by contaminated blood products and the spread from the infected liver to other organs. Cells free virions are susceptible to neutralizing anti-HCV antibodies. Direct cell-to-cell spread transmits the infection directly to the adjacent cells without release into the extracellular environment. Direct cell-to-cell transmission is resistance to neutralizing anti-HCV antibodies. Thus, HCV cell-to-cell spread is proposed to be responsible for the infection persistence. In a relatively similar mechanism, persistence of HIV-1 infection in the presence of neutralizing

antibodies is mediated by direct transmission between CD4+ cells (P. Chen, Hubner, Spinelli, & Chen, 2007).

HCV entry of cell-free virions is a complicated process. It is not entirely known how HCV particles transfer from the bloodstream to the liver, crossing the endothelial lining, and enter hepatocytes. It is proposed that HCV particles traverse the sinusoidal capillaries through the fenestrated endothelium into the, which mediates the exchange of molecules and fluid between the liver and blood. HCV particles cross the fenestrated endothelium into the space of Disse where they reach to the hepatocytes. After liver uptake of HCV particles, infection of hepatocytes starts by the attachment of the glycosylated envelope glycoproteins and the LDL protein components of the HCV LVP to the glycosaminoglycans and LDLR, respectively. After the initial attachment, HCV virions engage in a specific binding to a set of cell surface receptors and tight junctions leading to the internalization. The minimal receptors required for entry of HCV cell-free virions are the CD81, SR-BI, CLDN, and OCLN.

Assembled nucleocapsids of HCV are enveloped toward the ER lumen of the ER then traffic through the ER-to-Golgi secretory pathway, where virions acquire the lipoproteins and further enriched with neutral lipids before exiting Golgi into the cell plasma membrane (Gastaminza et al., 2008b). Envelopment is necessary for the infectivity of intracellular virions. Infectivity of the released virions requires the acquisition of lipoproteins and glycosylation with complex glycan at Golgi (Coller et al., 2012). LVPs should exit Golgi in transport vesicles that should fuse with the cell plasma membrane, although this event has not been visualized. Release of HCV virions requires interaction of host factors in the ER lumen, maturation, and regulated trafficking to the cell surface.

For example, the defective assembly and secretion of the VLDL in Huh7.5 cells are responsible for the lowered infectivity compared to the isolates recovered from infected individuals. Thus, release of HCV appears to be a complicated process.

The HCV-JFH1 based (genotype 2a) cell culture systems allowed characterization of several aspects of HCV life cycle including interaction with host factors and the functions of individual HCV proteins. HCV-JFH1 was then used to generate intra and inter-genotypic chimeras. Despite the importance of HCV-JFH1 cell culture system, the amount of virus produced was not sufficient for application such as studies in vaccines development. Thus, adaptive mutations were necessary to introduce to enhance the replication and release of infectious virions. A characteristic feature of the adaptive mutants obtained was more efficient cell-to-cell spread. Passaging of HCV-JFH1 core-NS2 recombinant genotype 5a, known as SA13/JFH1, in Huh7.5 cells resulted in the selection of a variant containing 13 amino acid changes. This variant had increased kinetics of replication, produced higher titer, and efficiently spread by direct cell-to-cell transmission. Infection with SA13/JFH1-derived adaptive mutant increased the number of cells per focus by 7-fold (Mathiesen et al., 2015).

HCV cell-to-cell transmission allows rapid transfer of virions between adjacent. The efficiency of HCV cell-to-cell spread is demonstrated in the infection persistence of variants resistance to HCV DAA. For example, HCVcc-Jc1-Luc mutant NS3-A156S is resistance to the HCV protease inhibitor telaprevir. In the presence of anti-HCV neutralizing antibodies, the NS3-A156S and wild-type HCV replicons had a similar increase in intracellular viral load as measured by the luciferase activity. Treatment with telaprevir inhibited the increase of the viral load of the wild-type, but not the resistance

mutant. Treatment of Huh7.5 containing wild-type or NS3-A156S replicon with anti-CLDN1 or erlotinib, a small molecule inhibitor of EGFR, inhibited the increase in viral load both replicons. Anti-CLDN1 or erlotinib inhibited transmission of infection from donor Huh7.5 cells transfected with wild-type or NS3-A156S to the target cells in co-culture assay by approximately 8.4 or 13.7-fold, respectively. Similar results were obtained with NS3-L36M/R155K or NS5A-Y93H variants resistance to boceprevir or daclatasvir.

Live imaging of HCV core motility showed many mobile puncta moving toward the periphery of the donor cells near the contact sites with the target cells. These puncta transmitted across the contact sites. Whether the motile core-labeled puncta represent a single virion, or more is not known. However, considering the size of the puncta and the average size of HCV virions, each punctum could contain approximately up to 1,000 particles (Counihan, Rawlinson, & Lindenbach, 2011). The average time for each punctum to transmit from the donor to the target cells was 18 minutes, while it took 2.85 h for a single donor cell to transmit at least one punctum to every adjacent target cell (Z. Liu & He, 2013). Thus, in 18 minutes a single punctum could deliver 100-1,000 virions, and in almost three hours, multiple adjacent cells acquired up to one or several thousand HCV virions. Only a fraction of the transferred virions may replicate, depending on the specific infectivity. However, the large number of the transferred virions ensures that each target cell in direct contact with the donor would be infected. Entry of cell-free virions, in contrast, is slower and multiphasic; biphasic followed by a plateau. 45% of the infectious virions in an inoculum achieve accelerated and productive entry in the first phase, 0 to 6 h. The remaining 65% of the infectious inoculum is achieved at a slower rate up to 22 h after inoculation, after which, a plateau is reached (Sabahi et al., 2010). Regardless



whether a single cell could be infected with more than single cell-free virion, the low titer of HCV may not allow infection at high moi. On the other hand, every cell in Huh7.5 confluent monolayer is in direct contact with roughly five cells. Therefore, co-culture of infected donor cells at least 1:5 with uninfected cells should results in the infection of every target cells. However, the high density intracellular HCV virions appear to lose their infectivity at faster rate than the low-density extracellular virions. Thus, intracellular virions could rapidly transfer to the adjacent cells or high density intracellular virions could have different biophysical features that allow them to maintain their infectivity. (Sabahi et al., 2010). Thus, comparing the transmission efficiency of cell-free or cell-associated might not be straightforward. Differences between the clinical isolates and the cell-culture grown HCV may not allow for accurate analysis that reflect the in vivo kinetic of the infection spread.

## 4.2 RESULTS

### 4.2.1 Spread of HCV infection by cell-free or cell-associated infectivity in transwell plates

Z390 inhibited foci formation even in the absence of neutralizing antibodies. The simplest explanation for such an effect would be if HCV primarily spreads by direct cell-to-cell spread. Thus, I next aimed at testing whether HCV preferentially spreads by cell-to-cell transmission. HCV infected cells were co-cultured 1:1,000 with uninfected cells on the insert of a transwell plate fitted with a membrane of 0.4  $\mu\text{m}$  diameter pores. Cells seeded in the well underneath the insert can only be infected by cell-free virions passing across the pores in this membrane and diffusing through the medium.

Infection spread across cells on the insert and well was evaluated over three days. At 48 h, the three viruses had infected 5 to 10% of the cells on the inserts, resulting in isolated foci and approximately 8 to 12 or 20 to 25 secondary infections per field for HCV or Zika virus, respectively. No secondary infections were observed for RSV. Very few infected cells were detectable in the cells on the wells in Zika virus or HCV infections and none in RSV infections (

**Figure 4.1-Figure 4.2).** At 72 h, HCV and Zika virus had infected >90% of the cells on the insert, whereas RSV had infected approximately 15% of them, in isolated foci. Zika virus had also infected 80% of the cells on the well at this time, whereas HCV infections did not exceed 1%, of the cells in the well, in small foci comprising of an average of 10 to 15 cells and the occasional secondarily infected cells. RSV infection was still undetectable in the cells on the well (

**Figure 4.1-Figure 4.2)** at this time. The frequency of infection events was nearly equivalent on the cells on the insert or well for Zika virus, with widespread infection in both compartments. HCV infection was

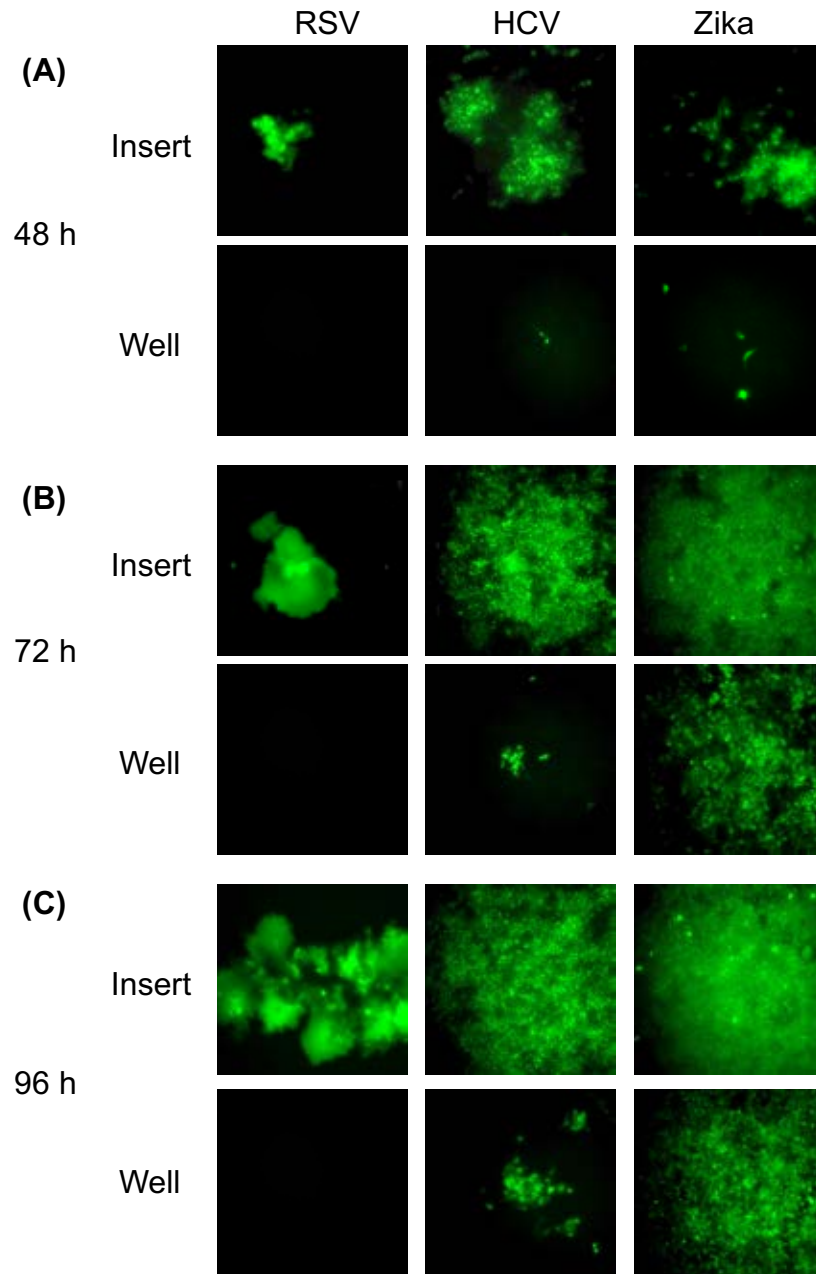


**Figure 4.1 HCV spreads primarily by cell-to-cell transmission.**

Immunofluorescence micrographs showing HCV, Zika virus, or RSV infected cells on insert (top) or well (bottom) of transwell plates at **(A)** 48, **(B)** 72, and **(C)** 96 h. Huh7.5 cells were infected at an moi of 5 with HCVcc-JFH1, Zika virus, or RSV. The following day,  $4.0 \times 10^5$  cells were seeded in each well of a transwell plate. 24 h later, donor cells were detached, resuspended, and added to uninfected Huh7.5 cells at 1:1.000. Cell mixes were seeded onto the inserts, and placed onto wells seeded the day earlier with Huh7.5 cells. Infections were incubated at 37°C and 5% CO<sub>2</sub> for 48, 72, or 96 h before processing for immunofluorescence for core. (results from two independent experiments).

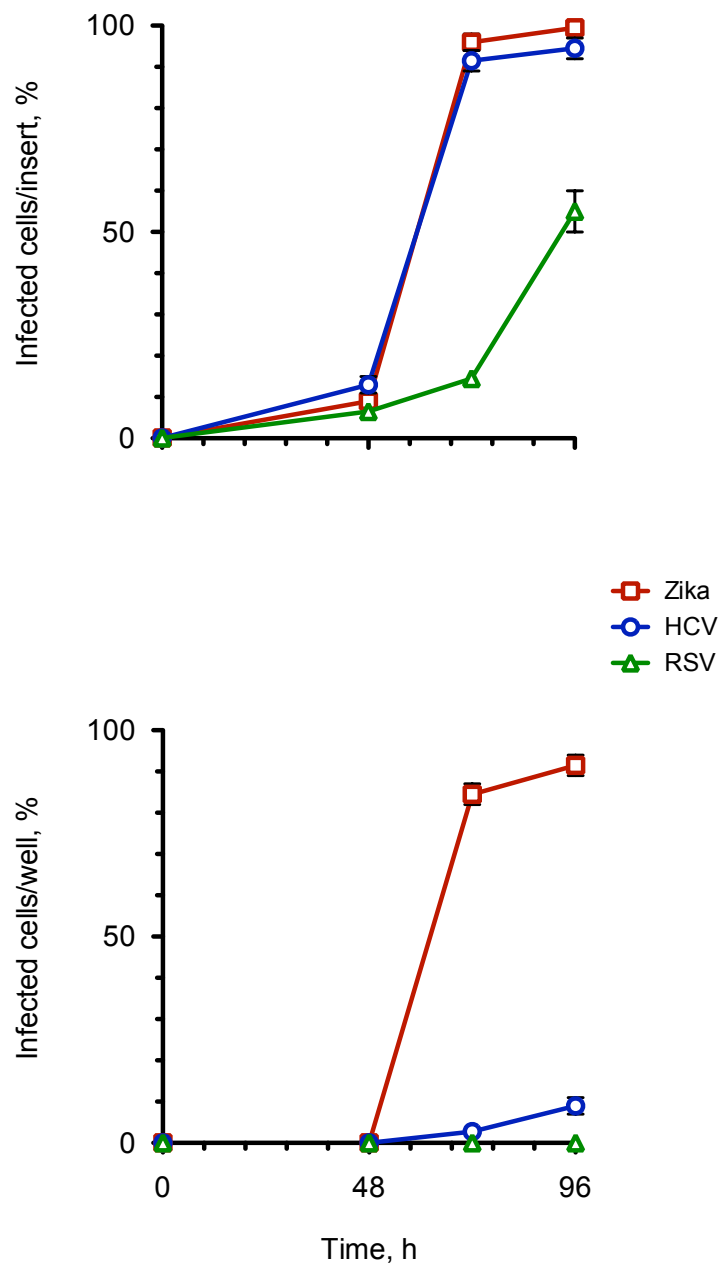


**Figure 4.2 Quantitation of HCV, Zika, or RSV spreads on inserts or in wells**

Bar graph presenting the percent of RSV, HCV, or Zika virus-infected cells on (A) inserts or on (B) wells of transwell plates. Five fields of fluorescent images at 20x magnification were used for the quantitation. Percent of infected cells per fields was calculated by dividing the image into grid squares, counting the squares containing fluorescent signal, and divide by the total number of grids. (results from two independent experiments).

also widespread among the cells on the insert, but there were only a few foci and a few secondary infected cells, on the well. RSV had failed to infect any cell in the well. At 96 h after co-culture, HCV and Zika viruses had infected almost all the cells on the insert, and RSV foci were even enlarged, involving 50% of the cells. Zika virus had also infected all cells in the well whereas HCV had only infected less than 5% of the cells in the well and the infected cells tended to be in discrete foci. No infected cells were detected in RSV infection (

**Figure 4.1-Figure 4.2)** throughout the time course. Zika virus spread was nearly synchronous on the cells on the insert and well, whereas HCV preferentially spread on the cells on the insert first and only later, spreading infection to the cells on the well. RSV spread on the cells on the insert by enlargement of the foci, which remained isolated and it did not infect the cells in the well, as expected. Therefore, HCV spread by cell-free virions across the membrane and by direct cell-to-cell transmission and cell-free virions among cells on the insert, but the latter was more efficient.

#### **4.2.2 Cell-free or cell-associated passaging of HCV infection**

Huh7.5 cells were infected either by inoculation with HCVcc-JFH1 or by co-culture with HCV infected cells. Media of the cells infected by with cell-free virions were diluted 1:200 48 h later and used to inoculate other cells. Infected cells can immediately transmit the infection to approximately five contacting adjacent cells whereas cell-free infectious virions can infect only a single cell. Cells infected by co-culture were then passaged 48 h later and co-cultured 1:1,000 with uninfected cells. Infection cycles were repeated three times every 2 days.

Two days after the initial infection with cell-associated virions (passage 0), there were 4 to 5 of HCV or RSV foci or Zika virus plaques per field. Subsequent passages of RSV cell-associated virions decreased the number of foci per well and the number of cells per focus, whereas that of HCV, in contrast, produced similar or more foci, infecting >75% of the monolayer in the last passage. Passages of Zika virus cell-associated virions spread over the entire monolayer in the first to the last passage. In the initial infection with cell-free virions, HCV or RSV infected over 50% of the monolayer, whereas Zika virus infected all cells with the appearance of multiple plaques. In the subsequent passages of HCV or RSV cell-free virions, the number of foci per field decreased between the initial and the first passage to approximately 2 to 3 to 1 to 2 foci, respectively. No infected cells were detected in the second to the last passage of RSV or HCV. Zika virus infections by cell-free virions spread to >90% of the monolayers in all passages (**Figure 4.3-Figure 4.4**).

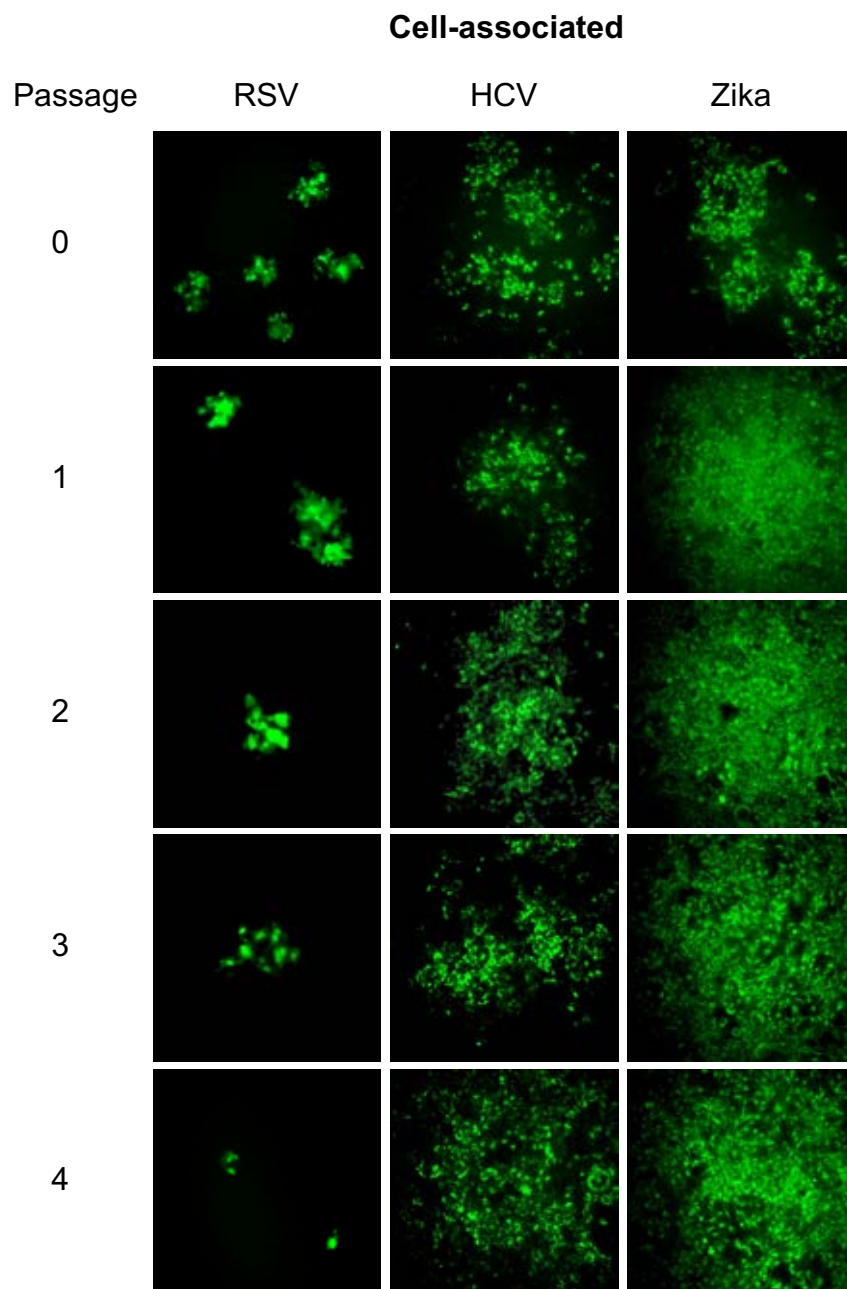


**Figure 4.3 HCV spreads primarily by cell-to-cell transmission.**

Immunofluorescence micrographs showing HCV, Zika virus, or RSV infected cells. Huh7.5 cells were infected at an moi of 5 with HCVcc-JFH1, Zika virus, or RSV. The following day (HCV) or 6 h later (Zika virus or RSV), infected cells (donor) were detached and co-cultured 1:1,000 with uninfected cells (target). 48 h later, the co-cultured cells were detached and co-cultured 1:1,000 with uninfected cells. HCV co-cultures were in the presence of neutralizing antibodies. The cycle was repeated four times. Co-cultures were incubated at 37°C and 5% CO<sub>2</sub> for 48 h before processing for immunofluorescence for core. (results from two independent experiments).



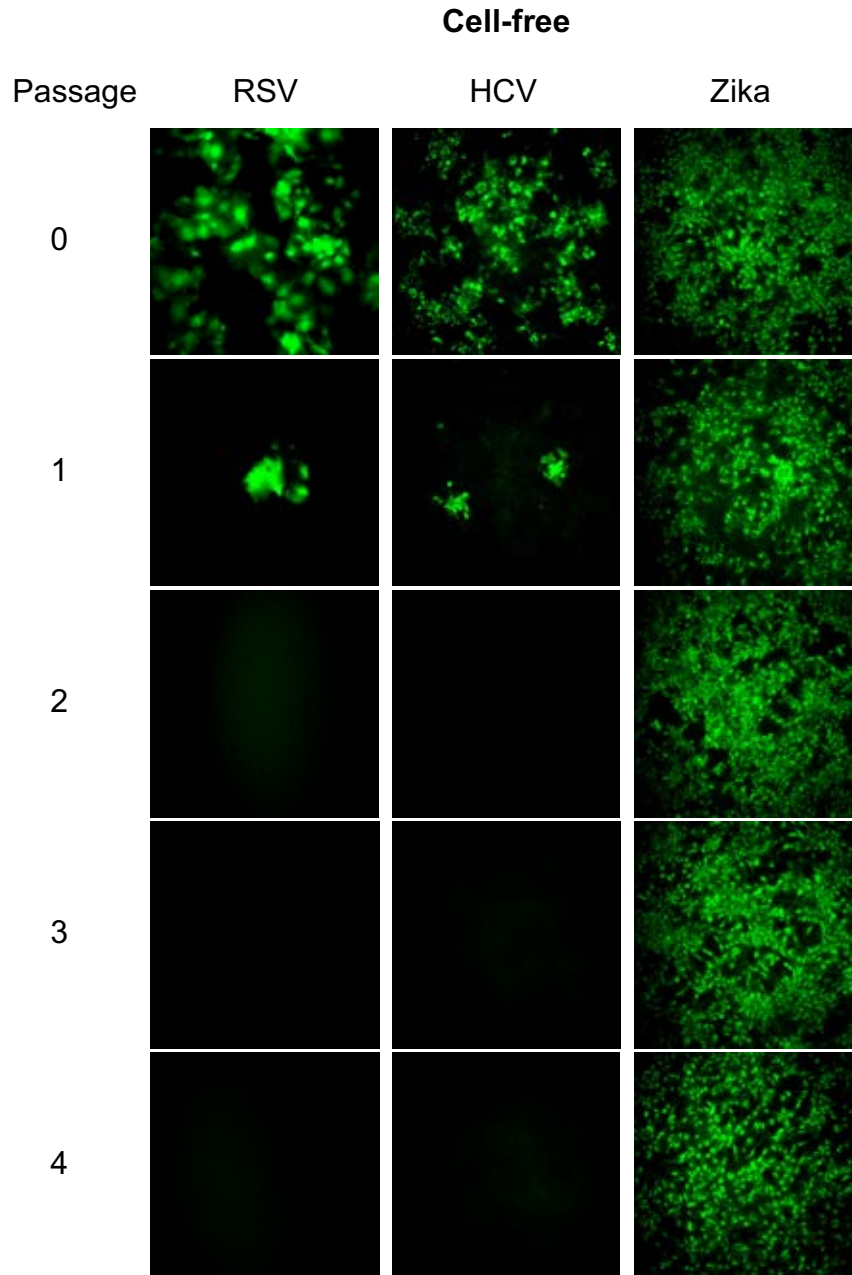


**Figure 4.4 HCV spreads primarily by cell-to-cell transmission**

Immunofluorescence micrographs showing HCV, Zika virus, or RSV infected cells. Huh7.5 cells were inoculated with HCVcc-JFH1, Zika virus, or RSV stock at a ratio of 1 infectious virion to 200 cells. 48 h later, the media were recovered, diluted 1:200, and used to infect Huh7.5 cells. The cycle was repeated four times. Infection were incubated at 37°C and 5% CO<sub>2</sub> for 48 h before processing for immunofluorescence for core. (results from two independent experiments).

### 4.3 DISCUSSION

HCV is transmitted directly between adjacent cells in liver of infected individuals (Agnello et al., 1998; Ming Chang et al., 2003; Lau & Davis, 1994) and in culture (Brimacombe et al., 2011a; Timpe et al., 2008; Valli et al., 2007; Witteveldt et al., 2009). However, the relative importance of HCV spread by direct cell-to-cell compared to infections with cell-free virions had not been evaluated. A single study attempted to compare the kinetic of HCV infection spread by cell-free or cell-associated virions (Z. Liu & He, 2013). The two routes of infection were assessed separately. HCV spread by infections with cell-free virions was evaluated in transwell plates that allow virions produced from HCVcc-JFH1 infected cells on inserts to diffuse across a permeable membrane to infect cells seeded on a well underneath. The spread of infections with cell-associated virions was evaluated in a co-culture assay of infected donor and uninfected target Huh7.5 cells at 1:1 ratio. Infected cells in the wells of the transwell plates or infected cells in the co-cultures were analyzed by flow cytometry. After 20 h, 11.7% of the target cells in the co-culture became infected, while 1% of the cells on the well became infected, it is increased to 30% or 55% at 48 or 72 h. The two systems of evaluation of infection spread, the co-culture or transwell, are different in terms of the duration of the infection and the time points of assessment of infection spread. In co-culture, because the spread is assessed after only 20 h, it evaluates one round of infection, which is the transmission from the donor to target cells. However, assessment of the infection of cells on the well of the transwell plate at 48 or 72 h involves multiple rounds of infection. Also, enumeration of infected cells by immunofluorescence flowcytometry does not allow differentiation between primary and secondary infections. Multiple rounds of infection produce foci and secondary infections.

Each focus comprises of infected cells that are more than the secondary infections produced by the same focus. Thus, the enumeration of infected cells on the well does not reflect the infection spread by cell-free virions, as it did for cell-associated spread in the co-culture. The infection spread by cell-associated virions in co-culture was linear on four points from 0 to 20 h. Assuming linearity up to 72 h, extrapolation of the infection spread at 48 or 72 h the infection would have spread to include 28.1% or 42.1%. Thus, the infection with cell-free virions would appear to spread more efficient than that with cell-free virions. Detection of the infected target cells by fluorescent microscope was at least twice as sensitive as by flow cytometry. The efficiency of infection transmission was therefore underestimated. Thus, the relative efficiency of cell-free versus cell-to-cell transmission of HCV infection in this orphan study could not be accurately demonstrated.

In the transwell experiment setting, the infection can spread in cells on the inserts by both cell-free virions and direct cell-to-cell transmission, while cells on the well underneath can only be infected by cell-free virions. The cells on the inserts were a 1:1,000 (0.1%) co-culture of HCVcc-JFH1- infected with uninfected Huh7.5 cells at. From 48 to 72 h, HCV infections in cells on the inserts increased exponentially from 10% to 90% and there was no further significant increase afterward till 96 h. The percent of infected cells on the well increased from 0 to 0.01, 2, and then 7% at 0, 48, 72, or 96 h, respectively. The fold difference of the infected cells on the inserts to that on wells was 1,250, 45, or 13 at 48, 72, or 96 h, respectively. The spread of HIV infection by cell-free or cell-associated virions has been evaluated using a relatively similar approach. Cell-to-cell spread of HIV is facilitated by the formation of virological synapses between CD4<sup>+</sup> cells. Co-culture of HIV-infected and labeled uninfected CD4<sup>+</sup> cells transmitted the

infection from donor to 21% of target cells within 3 h, compared to 1% transmission by cell-free virions within 3 h (P. Chen et al., 2007).

RSV infections in cells on the insert formed a certain number of foci that although they increased in size, did not change, and were isolated. RSV did not infect more than 70% of the monolayer and infections were not detected in any cell on the well. Spread of RSV infection was thus exclusively by cell-to-cell transmission. RSV infection spreads by cell-free or cell-associated virions in Hep2 cells that have been evaluated over five days (Huong et al., 2016). Infection by cell-associated virions was visible on the first day in the form of isolated foci which increased in size in a time-dependent manner comprising of approximately 25 cells per focus to >100 cells per focus at the second or third day after infection, respectively. Infection by cell-free virions not detected until the third day after infection. Cell-associated infection spread throughout the cell monolayer, compared to only 1% in the monolayers infected by cell-free virions. In contrast, no infection was detected in the transwell plates we used. RSV virions are released preferentially from the apical side of polarized epithelial cells such as the human epithelial cell line HEp2, which can be recovered from the media in single-compartment plates (Brock, Goldenring, & Crowe, 2003; Roberts, Compans, & Wertz, 1995; H. Tsutsumi et al., 2011).

Viruses that spread primarily by cell-free virions – at least in vitro – such as Zika virus disseminate rapidly throughout cell monolayers (Boehme, Lai, & Dermody, 2013; Onlamoon et al., 2011; S. L. Richards, Anderson, Lord, Smartt, & Tabachnick, 2012). HCV and RSV spread more efficiently in cells on the inserts than in cells on the wells, as expected. On the other hand, infection spread in cells on the wells was used to assess the infection efficiency by cell-free virions. Zika virus infection spread efficiently in cells

on the wells, as expected. However, the spread of Zika virus infection in cells on the inserts almost equally efficient. The efficiency of Zika virus spread in both compartments could be due to the burst size. The single-step replication cycle of Zika virus infection is 24 h, during which it produces approximately 60 infectious particles per cell, at least in hNPCs (human neural progenitor cells). At 48 h, Zika virus had infected 10% of the cells on the insert or  $7.5 \times 10^4$  cells. Therefore, Zika virus infection could have produced approximately  $4.5 \times 10^6$  infectious virions, which could infect cells in both compartments combined at an  $\text{moi}=3$ , which should result in infection of  $> 95\%$  of the cells.

We further tested the efficiency of the spread of HCV infection by cell-to-cell transmission or cell-free virions by passaging infections. The cell-associated passage was initiated by co-culturing infected cells with uninfected cells at 1:100 ratio in the presence of anti-HCV neutralizing antibodies to minimize infections by cell-free virions. After 48 h, the infection had spread to approximately 40% of the monolayer, which means that each infected donor cell had directly or indirectly transmitted the infection to a total of 40 target cells. A number within the range of the number of infected cells per focus that consistently detected at 48 h in co-cultures of infected and uninfected cells. Only 0.2% (1:500) of the cells in the initial co-culture infection was used to co-culture again with uninfected cells. As only 40% of the cells were infected at this time, the actual ratio in the passage was 1:1,250 infected to uninfected cells. Thus, it was expected that this ratio would result in infection of approximately 3 to 4% of the cells. However, the infection spread to approximately 15% to 20% of the cells. The subsequent three passages were also done at a ratio of 1:500 (cells from last passage to uninfected cells). Therefore, the percent of infection spread should have remained the same. However, the infection

spread more efficiently after each passage to infect >90% of the monolayer. The increase in HCV infection spread was gradual from the first to the last passage, which indicate that the actual ratio of infected and uninfected cells is increasing after each passage. It could also indicate the selection of variants more efficient in cell-to-cell spread.

HCV quasispecies include that prefer that could infect cells by both, cell-free or cell-associated<sup>1</sup> virions. Compensatory mechanisms between the two routes of transmission could exist. For example, serial passage of HCV-SA13/JFH1 (JFH1-based core to NS2 recombinant of genotype 5a) increased the yield of infectious virions by 1.4 orders of magnitude. A variant with 13 amino acid changes spanning HCV proteins core to NS5B, displayed increased assembly, specific infectivity, cell-to-cell spread and, sensitivity to neutralizing anti-HCV antibodies. The number of infected target per donor cells increased by 6.4-fold in co-culture. The sensitivity to neutralizing serum increased by 5.6-fold (Mathiesen et al., 2015). Thus, the passaging of HCV virus could favor the selection of variants efficient in cell-to-cell transmission. A similar phenomenon has been demonstrated in passaging of J6/JFH1 (intragenotypic recombinant genotype 2a virus containing J6 sequence core to NS2) in Huh7.5 cells. A variant with 12 culture-adapted nucleic acid mutations across the entire genome displayed 3-fold increase in the number of cells per focus in a co-culture assay. Again, the mutations in the selected variant did not affect the genome replication. The selected clone was also more sensitive than parent strain to the neutralizing antibodies by 1.6 to 42-fold to four different anti-HCV antibodies. Interestingly, the selected clone displayed less dependence on SR-BI in the cell-to-cell spread in co-culture assay. Using anti-SR-BI antibodies at [EC<sub>99</sub>] that inhibit entry of cell-free virions, inhibited cell-to-cell spread by 50% in the parental strain but did not affect the

selected clone. (Catanese, Loureiro, et al., 2013). Thus, the production of effective neutralizing antibodies in individuals chronically infected with HCV could select for variants that are more efficient in cell-to-cell spread and but also are less dependent on the host factors involved in cell-to-cell spread.

HCV appears to adapt to host factors involved in infectivity and cell-to-cell spread. HCV infects only human and chimpanzees. Infection of mouse cells requires the expression of at least the human CD81, SR-BI, CLDN-1, and OCLN. Adaptation of HCV-Jc1 to mouse CD81 in a subclone of Huh7-Lunet cells (Huh7L-N), expressing barely detectable level of human CD81, transfected to express mouse CD81 (Friebe, Boudet, Simorre, & Bartenschlager, 2005; Koutsoudakis, Herrmann, Kallis, Bartenschlager, & Pietschmann, 2007), selected a variant with three amino acid changes within the HVR1 of the envelope glycoproteins which allowed HCV entry into Huh7L-N expressing mouse CD81. This adapted variant was also able to infect NIH3T3 cells expressing mouse CD81, SR-BI, CLDN-1 and OCLN. These mutations in the envelope glycoproteins also conferred an increase in sensitivity to neutralization by anti-HCV antibodies (Bitzegeio et al., 2010), suggesting an inverse relationship between the efficiency of entry of cell-free virions and sensitivity to neutralization of infectivity by anti-HCV antibodies. Thus, it could be speculated that HCV species efficient in entry of cell-free virions, but sensitive to antibody neutralization, are dominated by species efficient in the cell-to-cell spread with greater sensitivity to neutralization antibodies resulting from the sustained selective pressure as in the case of chronic HCV infections.

#### 4.4 SUMMARY

Previously, I tested small molecules containing a 1,5-diarylpyrimidine core scaffold (Maruyama et al., 2007; Nair et al., 2007). The compounds were tested against a panel of viruses that differ in the structural properties and replication strategies. Two derivatives Z197, and Z214, inhibited HCV foci formation ( $EC_{50}$ , 13.8 and 12.9  $\mu$ M, respectively) but had no effects on any other virus. Optimization by structure-activity-relationship analysis led to compound Z390, which also inhibited HCV foci formation and has improved selectivity ( $EC_{50}$ , 4.8, SI, >21) and better solubility. Z390 inhibits HCV cell-to-cell spread but not replication, egress, or infection by cell-free virions.

In this chapter, my objectives were to evaluate the relative importance of HCV spread by cell-free virions or cell-to-cell transmission. I used two different experimental approaches. The first was a cell-culture system that allows simultaneous analysis of the two routes using transwell cell culture plates. The second was serial passaging of cell-free or cell-associated HCV virions. The efficiency of HCV spread was analyzed in comparison to that of two viruses that spread primarily by cell-free virions or direct cell-to-cell transmission, Zika virus or RSV, respectively. In both experimental approaches, HCV spread by direct cell-to-cell transmission was more efficient than by infection with cell-free virions.



## **CHAPTER FIVE: Z390 affects the localization of HCV core and NS5A proteins and cLD metabolism**

### **5.1 INTRODUCTION**

#### **5.1.1 Cellular distribution of HCV proteins**

Translation of HCV (+) ssRNA occurs at the rough ER producing a polyprotein precursor of ~3,000 amino acids long. The polyprotein precursor undergoes co- and post-translational processing by cellular and viral proteases (Houghton, Selby, Weiner, & Choo, 1994; Shimotohno et al., 1995). After translation, the minimum non-structural proteins NS3/4A, NS4B, NS5A, and NS5B are associated with ER membranes, where they replicate the HCV RNA genome to generate negative-sense RNA (replicative intermediate) by the RNA-dependent RNA polymerase NS5B (El-Hage & Luo, 2003; Moradpour, Brass, et al., 2004; Schmidt-Mende et al., 2001). (+) ssRNA is synthesized to generate more proteins, serve as template for RNA replication, or be packaged into progeny virions. After processing by cellular peptidases, mature HCV core protein associate with cLDs, a step that is essential for the assembly of progeny virions (Boulant, Targett-Adams, & McLauchlan, 2007; Shavinskaya, Boulant, Penin, McLauchlan, & Bartenschlager, 2007a). The envelope glycoproteins remain associated with the ER, until they are transferred via an interaction with NS2 and p7 to the assembly site nearby the cLDs (Shanmugam, Saravanabalaji, & Yi, 2015). Transition between RNA replication and assembly is essential for efficient production of progeny virions. It is facilitated by HCV proteins NS3 and NS5A through interaction with LD-bound core (Jirasko et al., 2010; Ma, Yates, Liang, Lemon, & Yi, 2008). Assembly of HCV involve cLD-bound core, RC (NS4B,

NS5A, and NS5B, and genomic RNA), and NS2 complex (E1, E2, p7, and NS3) (Jirasko et al., 2010; Popescu et al., 2011) to localize near cLDs. Beside these essential components, the remaining proteins NS4A (Phan, Kohlway, Dimberu, Pyle, & Lindenbach, 2011), NS4B (Jones, Patel, Targett-Adams, & McLauchlan, 2009), NS5A (Appel et al., 2008; Masaki et al., 2008), and NS5B were recently found to also participate in assembly (Dimitrova, Imbert, Kieny, & Schuster, 2003).

### **5.1.2 Association of HCV core with cLD**

Association of HCV core protein with cLDs requires distinct motifs of HCV core and host factors. Core protein is cleaved from the polyprotein and matured by proteolytic processing via cellular signal peptidases. The signal peptidase cleaves the polyprotein at the C-terminus located between core and E1 envelope glycoprotein (McLauchlan, Lemberg, Hope, & Martoglio, 2002). The resulted signal peptide, which contains the immature form of core and the N-terminus of E1 (P23) is then cleaved by intra-membraneous protease signal peptide peptidase (SPP) at the C-terminus of the core to produce the mature form (P21) which is the only form of core that can attach to cLDs (Vauloup-Fellous et al., 2006). Core association with cLDs is inhibited when the SPP is knocked down by siRNA or the amino acid residues at E1-core cleavage site is mutated (Targett-Adams, Hope, Boulant, & McLauchlan, 2008). The immature core is 191 amino acids in length and consist of three domains. The 120 amino acids hydrophilic domain 1 (D1) at the N-terminus, is highly basic, RNA-binding protein. The 50 amino acids hydrophobic domain 2 (D2) at the C-terminus is responsible for association with the ER and cLDs. The 20 amino acids signal peptide of the signal peptide peptidase downstream E1. D2 is composed of two  $\alpha$ -helices, helix I (HI) and II (HII) separated by helix loop (HL).

The  $\alpha$ -helices are amphipathic while the HL composed of hydrophobic residues. The minimal motif for core targeting to cLDs is the HI, HII, and HL through in-plane interaction with the cLDs monolayer membrane (Boulant et al., 2006; Boulant et al., 2005). The HL and the hydrophobic amino acid residues in HI and HII forms the in-plane interaction with membrane. Interaction with membrane is critical for the structural integrity and folding of D2.  $\alpha$ -helical conformation of core was obtained only in the presence of D2 and detergent (Boulant et al., 2005). Substitution of hydrophobic amino acids with hydrophilic residues (2 prolines to 2 alanine) within H1, HII, and HL abolishes attachment of core with cLDs (Boulant et al., 2006).

There are two host cell factors that promote targeting of HCV core to cLDs. DGAT1 is a diglyceride acyltransferase that, along with DGAT2, perform the last step in the synthesis of TG. A direct interaction of DGAT1 with core appears to facilitate the recruitment of core to cLDs (Herker et al., 2010). Inhibition of DGAT1 activity by small molecule inhibitor decreased extracellular HCV RNA while intracellular RNA remained unchanged. The intra- or the extracellular infectivity was decreased by 50% or 80%, respectively. Infection of shRNA expressing Huh7.5 with HCV-Jc1 had similarly affected the production of infectious HCV particles (Herker et al., 2010). Rab18, a regulator of the vesicular trafficking, is a cLD-binding protein that facilitates the contact sites between cLDs and ER membrane. The cLD-ER contact sites could serve as channels for lipid exchange (Ozeki et al., 2005). These cLD-ER channels were proposed to promote close opposition of core-loaded cLDs and RC to initiate virion assembly (Salloum, Wang, Ferguson, Parton, & Tai, 2013).

The mechanism of trafficking of HCV core to the cLDs has not been elucidated. It is proposed that core diffuse on the ER until cLDs is in contact with, or close to the ER. Transfer of core from ER to the cLDs could occur by the difference in the hydrophobicity between the cLDs and ER, in which cLDs has higher hydrophobicity. In general, cytosolic proteins, such as ADRP or Rab18, bind to cLDs through amphipathic and hydrophobic sequences, while ER-anchored proteins, such as DGAT1 or GPAT4, bind cLDs via hydrophobic hairpin/helix (Kory, Farese, & Walther, 2016). Binding of proteins to cLDs also requires positively charged sequence that mediate sorting into cLDs (Ingelmo-Torres et al., 2009). ER-anchored proteins, such as the plants oleosins and caleosins are proposed to target cLDs by lateral diffusion on ER (J. C. Chen, Tsai, & Tzen, 1999; Qu & Huang, 1990). The cLD-targeting domain of HCV or GB virus-B shared common characteristics with oleosin. Deletion mutations showed that oleosin and core proteins require the same region to bind to cLDs. Distinct motifs that critical for cLDs binding are rich in proline residues in core and oleosin. Mutagenesis of these residues blocks the binding to cLDs. Substitution of the oleosin cLD-binding domain with that of HCV core maintained the cLD binding of oleosin (Hope, Murphy, & McLauchlan, 2002).

Association of core to cLDs starts as single punctate at once side of cLDs that is opposed to the ER where core maturation occurs. As more of core synthesized, it progressively covers the entire surface of cLDs (Boulant et al., 2007; Rouille et al., 2006). The mechanism of progressive association of protein with cLDs has been also described for ADRP (Robenek et al., 2006; Robenek, Lorkowski, Schnoor, & Troyer, 2005) and Rab18 (S. Martin et al., 2005; Ozeki et al., 2005).

Association of core with cLDs is crucial for the assembly of progeny virions. Mutations in core D2 inhibits the production of HCV virions. Substitution of phenylalanine for glutamic acid in core D2 abolished association with cLDs (Boulant et al., 2007). The need for only core D2 to associate with cLDs has been exploited to replace D1 with GFP to investigate the live trafficking of core D2 and its correlation with assembly. It was found that association and displacement of core from cLDs depend on the strength of the interaction such that slow or fast rate of exchange indicates tight or weak binding, respectively. For example, replacement of alanine 147 of the core to valine, decrease core mobility which reflect an increase in the association of core to cLDs. Live tracking of core in HCV-infected cells demonstrated three distinct patterns of core. Slow motile core puncta traffic from the ER to cLDs is the newly synthesized core, enriched and static core on cLDs at the juxtanuclear region is core at assembly sites, and fast motile core puncta originate from the static core the juxtanuclear region represent the assembled virions. Fast motile puncta are blocked in mutant defective in assembly such HCV-Jc1/D88 which is characterized by large in-frame deletion of the E1, E2, and p7 genes (Counihan et al., 2011). HCV p7 mutants are usually defective in assembly. A point mutation of the diphasic motif in the loop region (p7-KR33/35QQ), which has no enzyme activity, or deletion of the N-terminal transmembrane helix of the HCV p7 protein inhibits the production of infectious virions and leads to retention of core on the surface cLDs. p7 mutants had decreased intra- and extracellular infectivity. The retention on cLDs was demonstrated by a shift of core to the cLDs fractions obtained by rate zonal centrifugation and by immunofluorescence imaging (Gentzsch et al., 2013). The latest report demonstrated retention of HCV core on cLDs due to defect in assembly involves the small GTPase

Rab32, a small GTPase regulator of mitochondrial-associated membrane (MAM), which link ER with mitochondria. siRNA knockdown of Rab32 decreased the extracellular infectivity and induced a juxtanuclear aggregation of HCV core and cLDs (Pham, Tran, Lim, & Hwang, 2016). Thus, Retention of core on the cLDs as associated with defect in assembly of HCV virions.

Virion release is the least understood step of HCV replication cycle. HCV exist as LVP which is composed of the HCV virion and several apolipoprotein components of the VLDL particles including ApoB-100, ApoE, and ApoCII/III (Andre et al., 2002; Catanese, Uryu, et al., 2013; Gastaminza et al., 2010; Nielsen et al., 2006). The association of HCV virion with VLDL suggested that release of HCV occurs via trafficking from the assembly sites to the ER-to-Golgi secretory pathway. HCV particle is heavily glycosylated, which indicate the transition through Golgi (Goffard et al., 2005; Meunier et al., 1999; Slater-Handshy, Droll, Fan, Di Bisceglie, & Chambers, 2004). Treatment of HCV-infected cells with BFA, which block ER-to-Golgi transport, decrease the extracellular infectivity substantially (Gastaminza et al., 2008a). siRNA interrogation of 122 host factors involved in the membrane trafficking pathways identified essential components of the secretory pathways including ER-to-Golgi, vesicle budding from TGN to the recycling endosomes to the plasma membrane (Coller et al., 2012).

However, HCV release has also been demonstrated to occurs through the endosomal VLDL-independent pathway. HCV-Jc1 with double fluorescent tags at E1 (E1-mCherry) and NS5A (NS5A-GFP), which allowed simultaneous live tracking of components of the virion and the RC, showed temporospatial pattern of expression of the NS5A and E1 where the NS5A puncta were decreasing while that of E1 was increasing.

The E1-mCherry puncta did not colocalize with Golgi, and the glycoproteins of the released virions were not glycosylated. Instead, E1-mCherry puncta colocalized with the endosomal marker Rab9 and inhibition of endosomal pathway with U18666A, small molecule inhibitor of endosomal trafficking pathway, reduced extracellular infectivity by 90% with no effect on intracellular infectivity (K. Bayer, Banning, Bruss, Wiltzer-Bach, & Schindler, 2016). Release of HCV infectious particles via exosomes has also been reported (Devhare et al., 2017; Ramakrishnaiah et al., 2013)

### **5.1.3 Association of NS5A with cLD**

NS5A, a 447-amino acid phosphoprotein (Kaneko et al., 1994; Tanji, Kaneko, Satoh, & Shimotohno, 1995), is essential for HCV replication and assembly. NS5A binds to HCV RNA (L. Huang et al., 2005), interacts with core (Masaki et al., 2008), and associates with cLDs (S. T. Shi et al., 2002). Thus, NS5A appears to be a link between RC and assembly. NS5A is composed of three domains and N-terminal amphipathic  $\alpha$ -helix that anchors NS5A to the cytosolic leaflet of bilayer membranes. D1, amino acid 28-213, is a dimer tethered to the ER membrane, is essential for RNA replication (Brass et al., 2002). D2, amino acids 250-342 promote dimerization, bind to HCV RNA, and is involved in genome replication but not assembly (Ross-Thriepfand, Amako, & Harris, 2013). The C-terminus D3, amino acids 356-447, is a major determinant of HCV assembly with no known role in replication (Tellinghuisen, Marcotrigiano, Gorbalenya, & Rice, 2004). Deletion of the NS5A D3 inhibits the production of HCV-Jc1 infectious virus leading to the aggregation of NS5A around, and accumulation of core on the surface of, cLDs (Appel et al., 2008).

Characterization of the cellular distribution of HCV proteins, core and NS5A were found to associate with cLDs. However, higher resolution imaging has helped to

demonstrate the fine details of this association. While core was surrounding the entire surface of cLDs, NS5A was occasionally or partially on the surface of cLDs. NS5A was mainly on the ER in close proximity to the core-covered cLDs on one side, and to the RC on the other. NS5A is a target of several cellular kinases, including casein kinase 1 (CK1), and CK2. Thus, it is detectable in infected cells as a basal or a hyperphosphorylated form with apparent molecular weights of 56 and 58 kDa, respectively (Masaki et al., 2014). NS5A binds to the viral RNA and colocalize close to cLD-bound core. It is assumed that newly synthesized viral RNA is transported to cLDs by NS5A whose phosphorylation state possibly regulating the balance between viral RNA replication and particle assembly (Fridell et al., 2011).

NS5A interacts with several host factors during assembly. NS5A interacts with Rab18 to facilitate interaction between RC and cLDs (Salloum et al., 2013). Rab1 is a small GTPase involved in biogenesis of Golgi, ER-to-Golgi transport. TBC1D is a Rab1 GTPase activating protein (Haas et al., 2007) required for HCV replication (Sklan et al., 2007). NS5A recruits Rab1 and Rab1-GAP TBC1D20, which have roles in homeostasis of cLDs and promotion of HCV infectious cycle. Expression of the dominant negative Rab1 mutant abolished steady-state cLDs and induced removal of NS5A from the RC (Nevo-Yassaf et al., 2012). Interaction of NS5A with ApoE result in recruitment of ApoE to site of virus assembly (Benga et al., 2010; Cun, Jiang, & Luo, 2010).

NS5A facilitates the recruitment of RC to cLDs. Expression of HCV subgenomic replicon renders NS5A localizes as puncta on ER but not close to cLDs (Miyazaki et al., 2007), whereas expression of full-length HCV replicon localizes NS5A close to cLDs via an interaction between the hyperphosphorylated NS5A and core (Masaki et al., 2014;



Masaki et al., 2008). Hyperphosphorylation of NS5A prompts the switch from RNA replication to assembly (Evans, Rice, & Goff, 2004). Last step for completion of the components of the assembly platform is the recruitment of the NS2 complex including NS2, p7, NS3, E1, and E2. NS2 interacts with E2 through the host factor signal peptidase subunit 1 (SPCS1) (Suzuki et al., 2013). NS2 complex accumulates around NS5A at assembly site (Jirasko et al., 2010; Popescu et al., 2011).

The association of NS5A with cLDs is less apparent than core as the majority of NS5A is localized at the ER membrane. Compared to core, the mechanism of NS5A binding to cLDs has not been well-characterized. The amphipathic helix of NS5A enables it to bind to cLDs. The cLDs targeting motif within NS5A is similar to at least three host proteins, Ancient ubiquitous protein 1, interferon-stimulated gene viperin, and patatin-like phospholipase domain-containing 5 (PNPLA5).

Host factors involved in targeting of core to cLDs could also facilitate targeting of NS5A. NS5 interaction with DGAT1 is necessary for recruitment of NS5A to cLDs. DGAT1 facilitates the interaction of core with NS5A at assembly sites by directly interacting with both proteins. Huh-1 cells expressing shRNA against DGAT1 or treatment with small molecule inhibitors, inhibits localization of NS5A by 5-fold around cLDs, whereas expression of catalytically inactive DGAT1 inhibits secretion of infectious HCV virions by 60% (Camus et al., 2014). TIP47 is a cLD-binding protein belonging to the perilipin family with primary function in the synthesis and maturation of nascent cLDs by regulating the incorporation of neutral lipid into growing nascent cLDs (Bulankina et al., 2009). TIP47 interacts with the N-terminus of NS5A leading to the association of the two proteins to cLDs (Vogt et al., 2013a). Rab9, a small GTPase with primary functions in endosomal

transport and lysosome biogenesis, binds to TIP47 in HCV-infected cells to promote the release of assembled virions. While lentiviral transduction silencing of Rab9 inhibits HCV replication, preventing the interaction of TIP47 and Rab9 by deletion or mutation inhibits the release of HCV virions without affecting the replication (Ploen, Hafirassou, Himmelsbach, Schille, et al., 2013). It is worth mentioning that inhibition of assembly or release by interference of TIP47-Rab9 or DGAT1 had no effect on the homeostasis of cLDs. Other host factor with an effect on NS5A is ADP-ribosylation factor 1 (Arf1). Arf1 is a small GTPase of the ARF gene family within the Ras superfamily of small GTPases. Arf1 is a major factor involved in ER-to-Golgi and intra-Golgi vesicular trafficking. Treatment of Huh7 cells harboring full-length HCV replicon genotype 1b (FLRP1) with Arf1 guanine exchange factor (GEF) inhibitors, BFA or GCA, redistribute HCV NS5A from dispersed pickle-like structures onto the surface of cLDs, which were fewer and larger in size. siRNA knockdown of Arf1 recapitulated the effect of BFA or GCA on NS5A redistribution and cLDs homeostasis. Knockdown of Arf1 decreased HCV RNA by 40% and infectivity by approximately 3-fold (Matto et al., 2011).

#### **5.1.4 Role of cLD in HCV**

cLDs vary in number, size distribution, and associated protein, which are regulated by the attachment and displacement of different sets of proteins. These proteins mainly regulate enzymatic reactions involved in lipogenesis and lipolysis, and are primarily proteins in the LDAP family (Kaushik & Cuervo, 2015; Paar et al., 2012). Intracellular trafficking factors regulate these protein associations with cLDs according to the cell energy status. The number of cLDs increases often with a shift toward smaller size indicates the synthesis of new cLDs immediately after excess lipid intake. Fewer cLDs

usually of larger size results from TG and CE accumulation later after lipid intake. Promotion of lipogenesis or inhibition of lipolysis induces the accumulation of enlarged cLDs.

In hepatocytes, cLDs are usually dispersed throughout the cytoplasm where they can be static or undergo microtubule-dependent short distance movements. HCV infection or expression of core progressively redistributes cLDs toward the periphery of the nucleus, which usually tend to be on one side around the MTOC. The redistribution of cLDs by core via microtubule-dependent motility, which mostly depends on the proteins associated with cLDs, is necessary for the assembly of virions. Nocodazole, antineoplastic agent disrupting polymerization of microtubules, interferes with the core-induced redistribution of cLDs and consequently decrease the production of HCV virions (Nan, Potma, & Xie, 2006). Percent of cytoplasm occupied by cLDs is approximately 67%, 48%, or 33% at 24, 48, or 72 h after infection with HCVcc-JFH1, compared to 71% in mock infected Huh7.5 cells. Core was at the edge, partially, or fully covering cLDs at those time points (Boulant et al., 2008). cLDs is considered to be the site of assembly of HCV particles as HCV proteins involved in the assembly of HCV localize near cLD during the time post infection that coincide with the assembly and release of infectious virus (Miyanari et al., 2007). Inhibiting the formation of cLDs abrogates assembly of HCV (Liefhebber, Hague, Zhang, Wakelam, & McLauchlan, 2014). The redistribution of cLDs bring them close to the replication vesicles where most NS proteins are located and nascent RNA is generated. This close proximity of cLDs to the sites of RNA synthesis is necessary for production of virions. HCV RNA co-fractionate the cLDs and mutations that disable core association with cLDs sites prevent the close proximity of cLDs with sites of

RNA synthesis. At the sites of the opposition of cLDs to the RNA replication vesicles, core (on the surface of cLDs) interacts with NS5A (on ER near the RV) to facilitate the transfer of the RNA for packaging into assembling virions.

#### **5.1.5 Role of LDAPs in cLD and HCV**

Large cLDs forms by the growth of small cLDs, through the increase of lipogenesis or inhibition of lipolysis, or by fusion of several cLDs. The regulation of the cLDs size is controlled by the association and dissociation of proteins to and from the cLD surface. The PAT proteins, also known collectively as perilipins or lipid droplet associated proteins (LDAP), constitute the largest protein family involved in cLD biogenesis regulation. Perilipins have no putative transmembrane domains. The PAT and 11-mer repeat motif of some of the family members are essential for association with cLDs. For example, TIP47 associates with cLDs through exposition of its C-terminal amphipathic helices, which bind to the monolayer cLDs membrane. While ADRP localize exclusively to cLDs, TIP47 is both on cLDs and cytosolic. Perilipins also differ in their preferential association of various sizes of cLDs. While TIP47 and PLIN5 primarily localize to small cLDs, PLIN1 and ADRP predominantly localized to large cLDs. Several modes for the binding preferences have been proposed, including the suitability of the membrane curvature, which is related to the size of cLDs, or the presence of different interacting proteins at cLDs of different sizes. ADRP and TIP47 are ubiquitously expressed and have principal functions in the formation and stabilization of cLDs. ADRP also participates in adipocyte differentiation and TIP47 plays a role in intracellular protein trafficking, including that of lipid modifying enzymes.

### **5.1.6 Role of ADRP in cLD**

ADRP is a 50 kDa protein. It is the major protein associated with hepatic cLDs, where it mediates accumulation of lipids, by promoting the formation of cLDs and protecting them from lipolysis. Evidences supporting the role of ADRP in the maintenance of cLDs have been demonstrated in mice and cell lines. ADRP-deficient mice displayed 25% reduction in hepatic TG associated with decrease in the size of cLDs and relieve of fatty liver and improve insulin sensitivity (B. H. Chang, Li, Saha, & Chan, 2010). ADRP knockout prevented TG increase in high fat-fed mice and decreased liver TG by 16-fold in chow-fed mice (McManaman et al., 2013). Antisense oligonucleotide against ADRP suppressed expression of lipogenic genes, drastically reduced cLDs, and reduced liver TG in diet induced obese mice by 50% (Imai et al., 2007) (Varela et al., 2008). ADRP regulates production of cLDs in mammary epithelial cells during differentiation of mammary gland into a secretory organ. The increase in size of cLDs in differentiating mammary glands was inhibited by 50% in ADRP-deficient mice. This inhibition of formation of large cLDs resulted in localization of ATGL to the surface of cLDs, suggesting that ADRP promote the growth of cLDs by inhibition of lipolysis (Russell et al., 2011). ADRP knockdown increases lipolysis rate, decreases the number of cLDs per cell by 5.5-fold, and decreases the cellular contents of TG by 30% in macrophages (Larigauderie et al., 2006). siRNA knockdown of ADRP reduced TG or CE by 2.4 or 3-fold, respectively (Larigauderie et al., 2004). Overexpression of ADRP in THP-1 macrophages in the presence of acetylated LDL increased TG and CE by 40% and 67%, respectively, and cholesterol efflux was reduced by 47% (Larigauderie et al., 2004). Overexpression of ADRP increased TG content in Swiss-3T3 cells by 2.3-fold and increased the size and

number of cLDs in time- dependent manner with the localization of ADRP to “ring-like” on the surface of the cLDs. (Imamura et al., 2002). Expression of ADRP in HEK293 cells which express low level of endogenous ADRP, increases TG in basal and in oleic acid-supplemented conditions while decreased TG hydrolysis by 50%. ADRP expression was associated with striking decrease in ATGL association with cLDs (Listenberger et al., 2007). ADRP is a constitutive cLD-binding protein, which if displaced from cLDs during lipolysis, degraded rapidly through the ubiquitin/proteasomal pathway

### **5.1.7 Role of ADRP in HCV**

Percentage of cells with co-localization between core and ADRP increased in time-dependent manner reaching a maximum of 90% by 72 hpi. Production of infectious of virus correlated with increasing association of ADRP with core (Boulant et al., 2007). Live imaging of core showed three forms. ER-associated, cLDs-associated, and motile puncta cLDs-independent. Core displaces ADRP forming a polarized cap at close opposition of ER-localized core represent site of transfer from ER to cLDs (Counihan et al., 2011), which also has been seen before (Boulant et al., 2008; Boulant et al., 2007). Juxtanuclear large cLDs covered by core are immotile and their appearance coincides with the peak of virus assembly (Boulant et al., 2008; Lyn, Kennedy, Stolow, Ridsdale, & Pezacki, 2010). The association of HCV core or ADRP with cLD is reciprocal. At 24 hpi when cLDs are dispersed, 71% or 6% are covered with ADRP or core, respectively, whereas at 48 h, cLDs are partially redistributed, and are covered 31% or 18% with ADRP or core, respectively. At 72 h, cLDs are fully redistributed, and ADRP or core covers 14% or 38% of cLDs surface, respectively (Boulant et al., 2008). Rab18 induces close opposition of cLDs to ER, a process that result in reduction of ADRP on cLDs. Knockdown of ADRP

decreases virus production in RSc and Huh7.5 cells, whereas overexpression of Rab18 recovered the loss of virus production. (Targett-Adams et al., 2008)

#### **5.1.8 Role of TIP47 in cLD**

TIP47 is 47 kDa protein with 47% sequence similarity to ADRP. Initially, the role of TIP47 was identified in the intracellular trafficking of lysosomal enzymes from the trans-Golgi network to the lysosome, which is regulated by oligosaccharide chains modifications then binding to M6PR. TIP47 binds to the cytosolic domain of M6RP which leads to its inclusion in transport vesicles (Diaz & Pfeffer, 1998). Unlike ADRP, TIP47 is stable in the cytosol (X. Lu et al., 2001) and translocate into the sites of cLDs synthesis in response to lipid loading. Knockdown of TIP47 led to decreased TG levels, while overexpression resulted in the accumulation of TG in macrophages. TIP47 binds to the sites of cLDs formation where diacylglycerol accumulate between the leaflets of ER membrane. The C-terminal of TIP47 shares four biphasic helices bundle structure such that of ApoE (Hickenbottom, Kimmel, Londos, & Hurley, 2004), which allows it to interact with lipid and proteins. TIP47 forms deep cleft by the four-helix structure, by which it binds to fatty acid and cLDs (Ohsaki, Maeda, Maeda, Tauchi-Sato, & Fujimoto, 2006). siRNA knockdown of TIP47 in THP-1 macrophages decreased TG content, whereas overexpression increased accumulation of TG (Buers et al., 2009). Binding of TIP47 to sites of nascent cLDs synthesis occurs subsequent to accumulation of DAG in ER (Skinner et al., 2009). Recruitment of TIP47 to cLDs occurs upon generation of all-trans-retinoic acid after photo bleaching in the retinal pigment epithelium (Tsuiki et al., 2007). TIP47 was induced by LPS and localized to cLDs in immortalized HL-60 originated from human promyeloleukemia differentiated into neutrophil or macrophages (Nose et al., 2013).

Proteomic analysis of cLDs fraction of SZ95 sebocytes showed high level of ADRP and TIP47 (Dahlhoff et al., 2015). Treatment of sebocytes with linolenic acid stimulates the formation of cLDs, while silencing of TIP47 inhibited it (Straub, Stoeffel, Heid, Zimbelmann, & Schirmacher, 2008).

TG is stored in cLDs in intestinal enterocytes after absorption of dietary fats. ADRP and TIP47 are the only LDAP found in mouse intestinal mucosa. Expression of ADRP and TIP47 is upregulated after high fat challenge, 6 or 12-fold, respectively. Acute fat feeding was by fasting for 4 h then feeding with olive oil by oral gavage for 3 h before sample collection. Chronic fat feeding was by feeding high-fat diet for 3 weeks. While TIP47 is upregulated, and associated with cLDs after acute fat intake, ADRP is upregulated and associated with cLDs after chronic fat intake (B. Lee, Zhu, Wolins, Cheng, & Buhman, 2009). Similar results have been reported (M. Zhu, Ji, Jin, & Yuan, 2009). The 11-mer repeat of TIP47 is sufficient for targeting to cLDs (Bulankina et al., 2009). Detection of TIP47 in cells depends on the presence of cLDs in steady state. While cLD present in HepG2, Huh-7, CHO, or Cos-7, HeLa cells lack cLDs without addition of fatty acid. TIP47 is undetectable in starved cells. TIP47-stained punctate start to appear 5 or 10 minutes after addition of oleic acid with no staining for neutral lipids. Within 3 to 16 h, the number of TIP47-stained structures increase in number and size with increase in the brightness of neutral lipid dye (Bulankina et al., 2009). Compensatory mechanism exists between ADRP and TIP47. Knockdown of TIP47 result in increase in the level of ADRP (Sztalryd et al., 2006).



### 5.1.9 Roles of TIP47 in HCV replication

The N-terminal amphipathic  $\alpha$ -helix of NS5A interact with TIP47. HCV infection decreases TIP47 protein level while TIP47 mRNA is increased. shRNA knockdown of TIP47 decreased HCV RNA replication by approximately 10-fold. NS5A binds to the TIP47 N-terminus. The inhibitory effect of TIP47 silencing on HCV replication was only observed in complete infection cycles, but not for subgenomic replicons. Decreased HCV replication was rescued by transfection of TIP-47-deficient cells with TIP47 expression vector. The rescue did not happen with TIP47 lacking the N-terminal domain (Ploen, Hafirassou, Himmelsbach, Sauter, et al., 2013). TIP47, via its PAT domain which has affinity to cLDs, could target NS5A-bound to HCV RNA, from the replication complex to the cLDs to interact to core. TIP47 is required for the interaction of HIV Gag and Env (Bauby et al., 2010; Lopez-Verges et al., 2006).

ApoE is structurally similar to TIP47, and also binds to NS5A and this binding is also required for the production of virus (Benga et al., 2010; Jiang & Luo, 2009). Like ApoE (Catanese, Uryu, et al., 2013; Owen et al., 2009), TIP47 was found to be a component of the HCV particle. TIP47 co-purified of by HCV virions, immunoprecipitation or supernatant from HCV-infected cells, and HCV particles were detected by immuogold electron microscopy (Ploen, Hafirassou, Himmelsbach, Schille, et al., 2013).

The intracellular sorting function of TIP47 (Diaz & Pfeffer, 1998) depends on its interaction with Rab9 (Aivazian, Serrano, & Pfeffer, 2006; Carroll et al., 2001; Hanna, Carroll, & Pfeffer, 2002), which is a member of Rab family of proteins that mediate vesicular transport (Zerial & McBride, 2001). TIP47 partially localized to Rab9 in HCV

infected cells. Transfection of Rab9-deficient stable cell line with HCV-Jc1 result in inhibition of HCV RNA replication and production of infectious virus by >90%, whereas overexpression increased them by 25% or 50%, respectively. TIP47 deletion mutant in the binding site of the Rab9, inhibit production of infectious HCV virions and traffic HCV virions to autophagosomes (Ploen, Hafirassou, Himmelsbach, Schille, et al., 2013).

## 5.2 RESULTS

### 5.2.1 Treatment with Z390 results in HCV core protein more efficient localization to the surface of enlarged cLD

The mechanism of HCV cell-to-cell spread is still poorly understood, beyond the involvement of a subset of the known HCV entry receptors. To evaluate the mechanism of inhibition of HCV cell-to-cell spread by Z390, we visualized the cellular distribution of HCV proteins by high-resolution fluorescence imaging. Huh7.5 cells were infected with HCVcc-JFH1 at an moi=1 and then processed for immunofluorescence and confocal microscopy for HCV core 48 h after infection. Core localized mostly as small clusters of different sizes dispersed throughout the cytoplasm. Core accumulations at the juxtanuclear region are slightly aggregated, larger in size, and forming occasional ring-like structure. Core also localized to cLDs. The limited core spheres that did not localize to cLDs are thought to be associated with lipid rafts. In Z390 treated infections, in contrast, 90% of infected cells had core predominantly enriched as ring-like structures around enlarged cLDs that were of homogenous size, compared to only 10% in vehicle treated infections (**Figure 5.1-Figure 5.2**). Z390 treatment had the same effects on core of HCV-H77 (G-1a) (**Figure 5.3**) or HCV-Jc1 (G-2a) (**Figure 5.4**). HCV-Jc1 core does not normally associate with cLDs to the same extent as core of JFH1 or H77 strains, and it is mostly dispersed throughout the cytoplasm. Therefore, the relocalization of HCV-Jc1 core to cLDs in infections treated with Z390 was even more obvious than that of JFH1 or H77. Ring-like structures of core around cLDs start to appear at 36 h after infection and then increase in untreated infections. At 72 h, most core is in these ring-like structures. The appearance of these ring-like core structure coincides temporarily with the beginning of

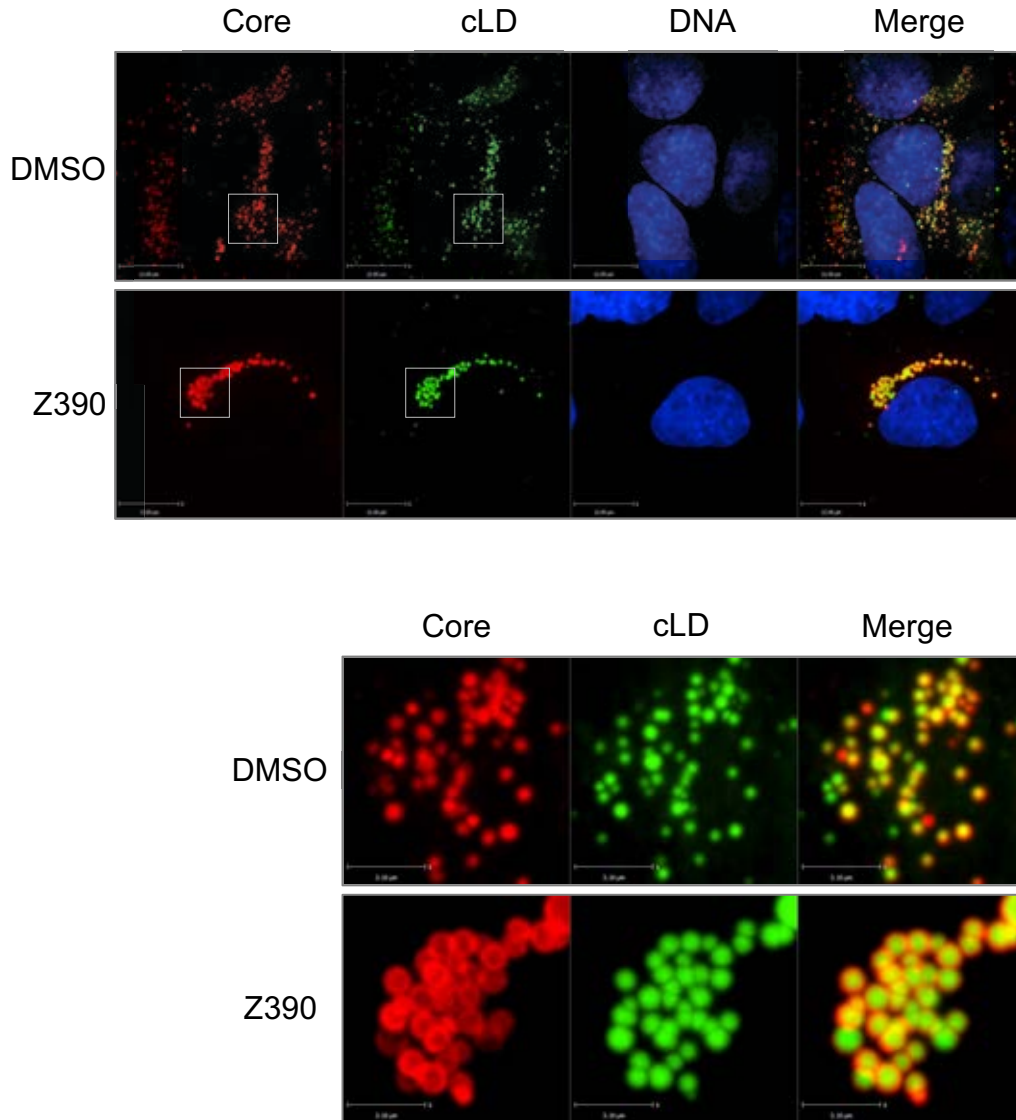


**Figure 5.1 HCVcc-JFH1 core localizes in ring-like structures around enlarged cLD in the presence of Z390.**

Top, immunofluorescence micrographs showing HCV core (red) or cLDs (green) in HCV-infected cells treated with DMSO or Z390 at 60x magnification. Bottom, the areas indicated by the squares at the top showing magnified region. Huh7.5 monolayers were infected with 0.01 infectious HCVcc-JFH1 virions per cell. Inocula were removed 4 h later and fresh medium containing 40  $\mu$ M Z390 or DMSO was added. Two days later, infected cells were processed for immunofluorescence for core protein and evaluated by confocal microscopy (results from five independent experiments).

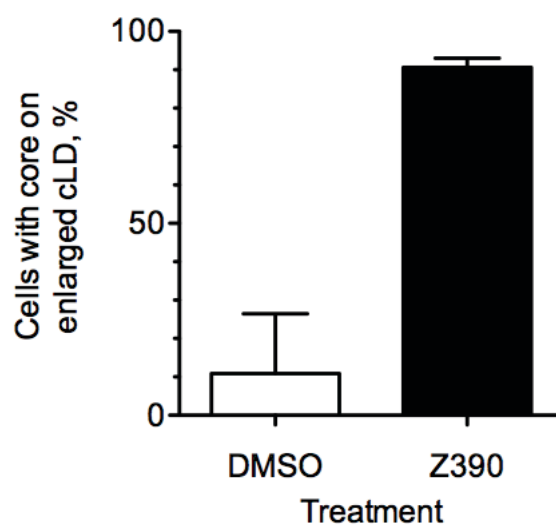


**Figure 5.2 Quantitation of Z390 effect on HCV core and cLD in HCV-infected cells.** Bar graph showing the percent of cells with normal or enriched localization of HCV core on the surface of enlarged cLDs. 148 infected cells treated with DMSO or Z390 were counted. The percent was calculated by dividing the cells showing the enrichment of core on enlarged cLDs by the total number of cells counted (results from five independent experiments).

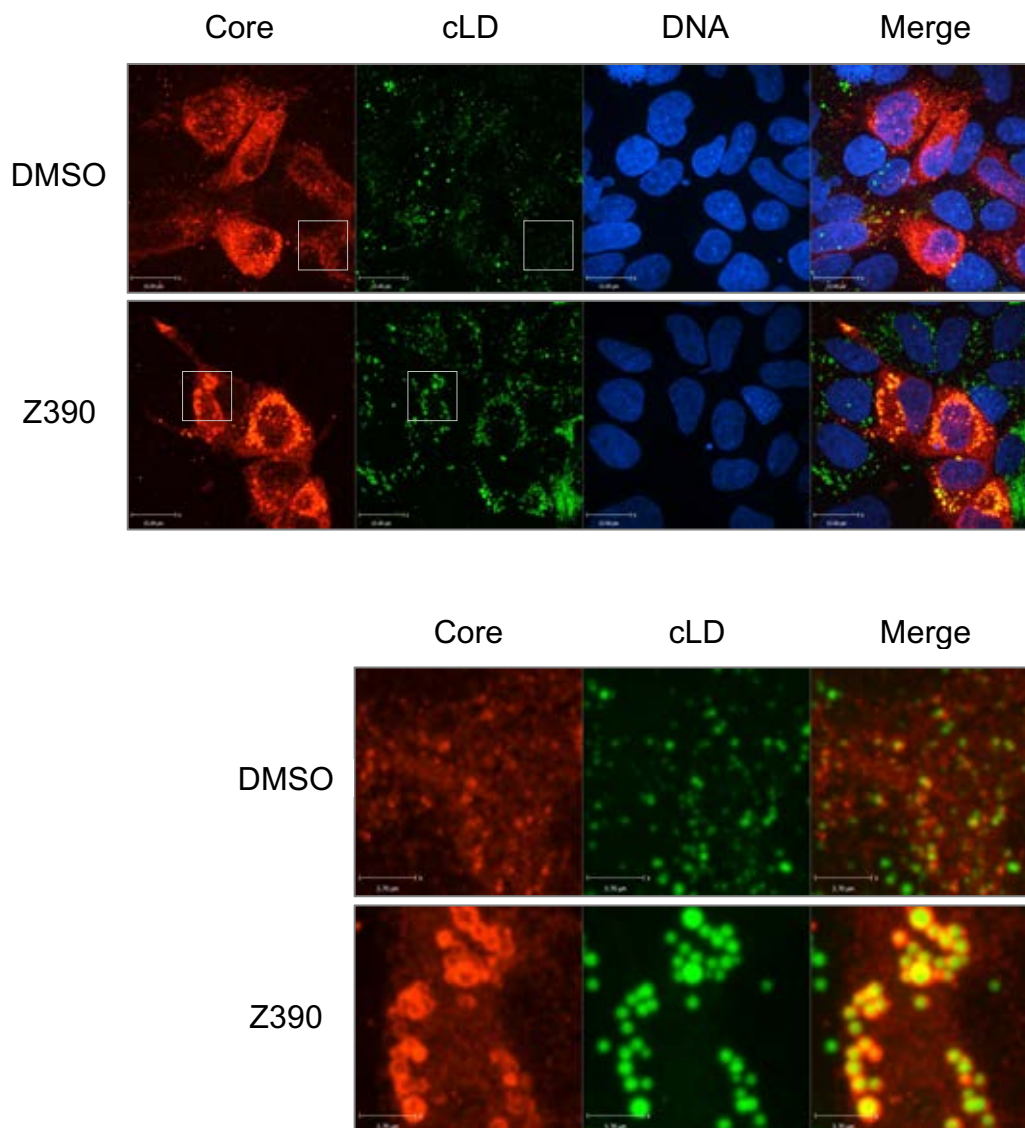


**Figure 5.3 HCV-Jc1 core localizes in ring-like structures around enlarged cLD in the presence of Z390.**

Top, immunofluorescence micrographs showing HCV core (red) or cLDs (green) in HCV-infected cells treated with DMSO or Z390 at 60x magnification. Bottom, the areas indicated by the squares at the top showing magnified region. Huh7.5 monolayers were infected with 0.01 infectious HCV cc (Jc1) virions per cell. Inocula were removed 4 h later and fresh medium containing 40  $\mu$ M Z390 or DMSO was added. Two days later, infected cells were processed for immunofluorescence for core protein and evaluated by confocal microscopy

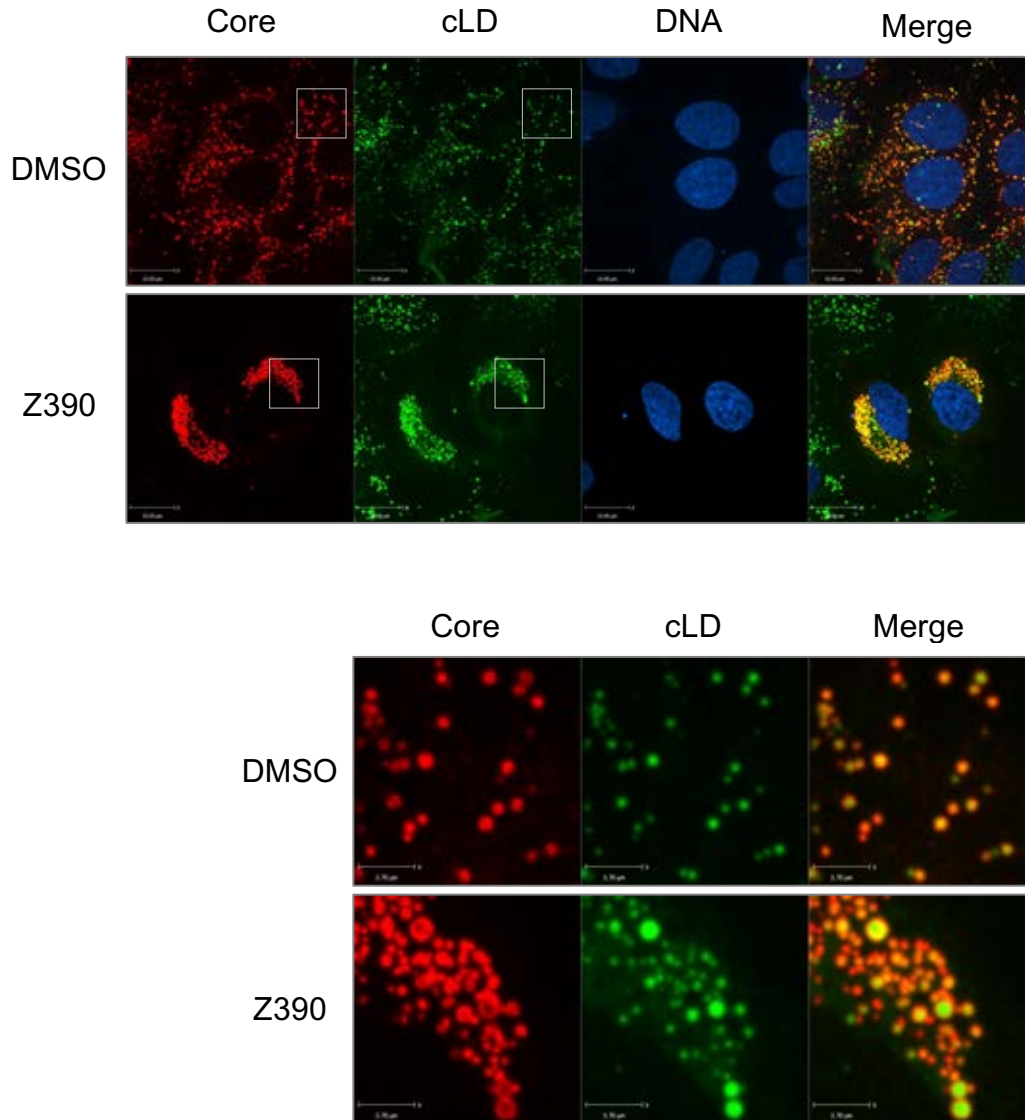


**Figure 5.4 HCVcc-H77 core localizes in ring-like structures around enlarged cLD in the presence of Z390.**

Top, immunofluorescence micrographs showing HCV core (red) or cLDs (green) in HCV-infected cells treated with DMSO or Z390 at 60x magnification. Bottom, the areas indicated by the squares at the top showing magnified region. Huh7.5 monolayers were infected with 0.01 infectious HCV cc (H77) virions per cell. Inocula were removed 4 h later and fresh medium containing 40  $\mu$ M Z390 or DMSO was added. Two days later, infected cells were processed for immunofluorescence for core protein and evaluated by confocal microscopy.

release of infectious HCV virions, suggesting that these ring-like structures are required for assembly. However, the effect of Z390 on the core ring-like structures did not correlate with changes in the assembly or release of HCV virions, as shown in single-step replication assays. Z390 did not affect HCV specific infectivity, defined as the infectivity of HCV virions (infectious particles per genome), either. Localization of core to cLDs had no effect on HCV genome replication or infectivity.

Enrichment of HCV core on ring-like structures on the surface of cLDs was decreased for HCV mutants defective in assembly. It was proposed that core was retained on the cLDs in the absence of assembly. However, Z390 did not inhibit production or release of infectious virions indicating that the accumulation of core onto cLDs in Z390 treated infections is not a consequence of assembly defects.

### **5.2.2 Z390 redistributes HCV NS5A protein from ER to the surface of enlarged cLD**

Enrichment of HCV core on the surface of enlarged cLDs without an inhibition of production or release of infectious virions prompted us to evaluate the cellular distribution of other HCV proteins involved in assembly. NS5A is essential for assembly, coordinating assembly by facilitating the transfer of HCV genomic RNA from the replication complexes to the assembling virions. This process involves the direct interaction between core on the surface of the cLDs and NS5A in the replication complexes. NS5A is primarily localized scattered throughout the ER, with increased concentration near cLDs.

Huh7.5 cells were infected with HCVcc-JFH1 for 4 h before treating them with 40  $\mu$ M Z390 or DMSO vehicle control. The distribution of NS5A was evaluated 48 h after infection by immunofluorescence. NS5A was predominantly dispersed in the cytoplasm, with accumulations adjacent to cLDs, and partially around cLDs, in control infections. The



dispersed localization is proposed to be associated with ER at early post translation stages. NS5A adjacent to cLDs is proposed to be associated with sites of active assembly. NS5A was confined to juxtannuclear region in infections treated with Z390, almost exclusively associated with cLDs as ring-like structures in 50% of infected cells (**Figure 5.5**), compared to vehicle (**Figure 5.6**).

### **5.2.3 Effect of Z390 on other HCV proteins**

The effect of Z390 on HCV core and NS5A proteins raised the question of whether Z390 affected the localization of all HCV proteins. We next evaluated the cellular distribution of HCV NS3, a serine-protease/helicase/NTPase that participates in virion assembly via unknown mechanisms through its linker region and helicase domain. The direct of interaction of NS3 with oligomerized core is required for the production of infectious progeny virus.

We tested the cellular distribution of NS3 in HCVcc-JFH1 infected Huh7.5 cells 48 h after infection by immunofluorescence. NS3 signal was mostly dispersed throughout the cytoplasm with areas of more intense signal near by the nucleus. No cLDs localization of NS3 was observed, as expected. The distribution of NS3 was not affected in infections treated with Z390 (**Figure 5.7**).

### **5.2.4 Z390 treatment induces the formation of mature cLDs**

ADRP colocalizes with cLDs regardless of synthesis and maturation stages. Nonetheless, the level of association of ADRP with cLDs correlates with the metabolic status of cLDs. ADRP association with cLDs increases during lipogenesis, whereas ADRP is displaced from cLDs during lipolysis. Expression of HCV core alone in Huh7.5 is sufficient to induce lipogenesis, which results in progressive increase in the number

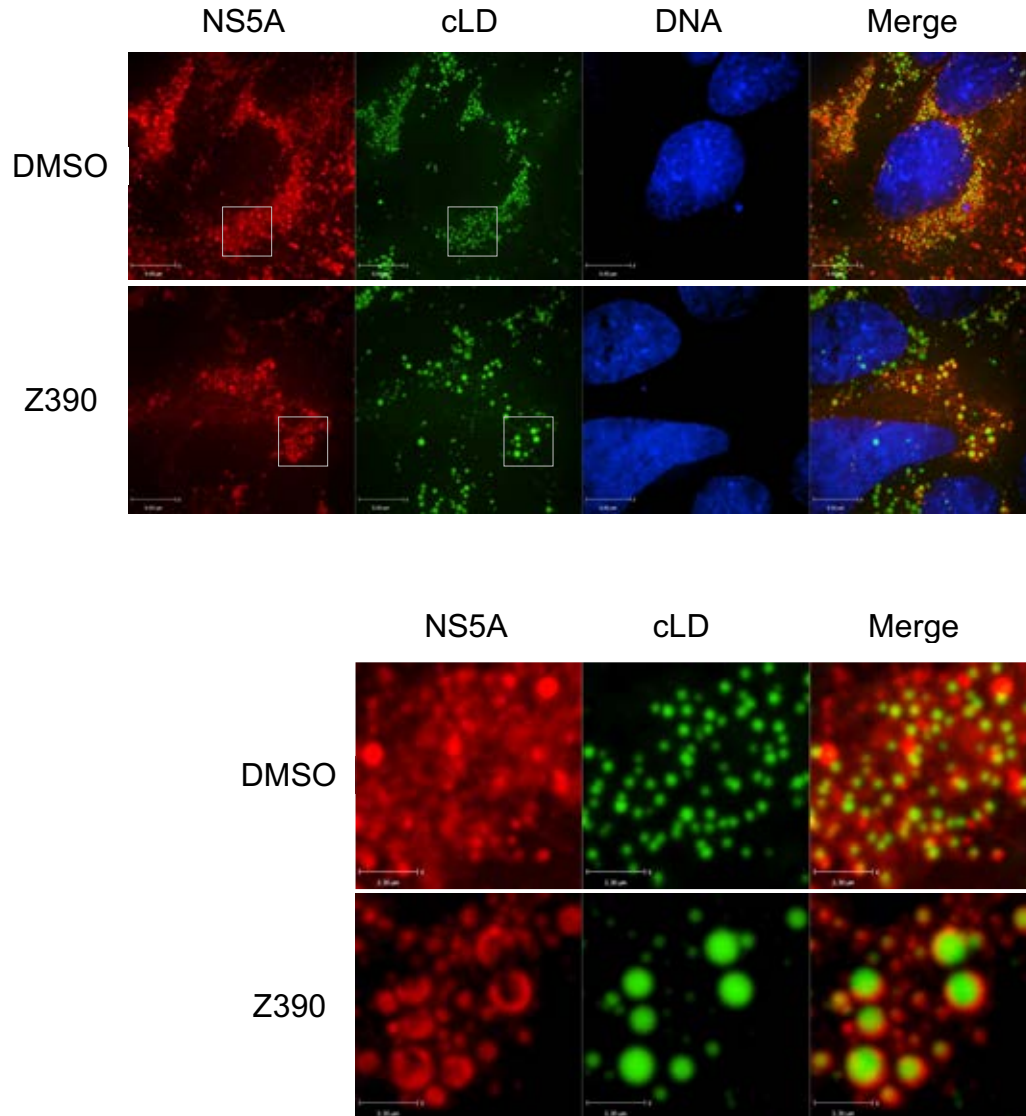


**Figure 5.5 HCV NS5A redistributes from the ER to enlarged cLD in the presence of Z390.**

Top, immunofluorescence micrographs showing HCV NS5A (red) or cLDs (green) in HCV-infected cells treated with DMSO or Z390 at 60x magnification. Bottom, the areas indicated by the squares at the top showing magnified region. Huh7.5 monolayers were infected with 0.01 infectious HCV cc (JFH1) virions per cell. Inocula were removed 4 h later and fresh medium containing 40  $\mu$ M Z390 or DMSO was added. Two days later, infected cells were processed for immunofluorescence for NS5A and evaluated by confocal microscopy (results from four independent experiments).

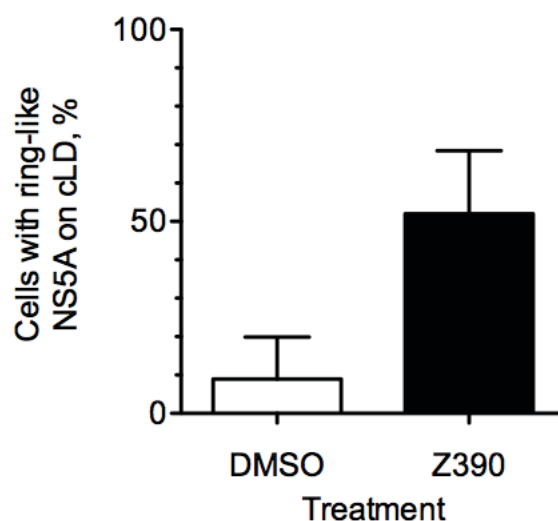


**Figure 5.6 Quantitation of Z390 effect on HCV NS5A localization in HCV-infected cells.**

Bar graph showing the percent of cells with normal or redistributed NS5A onto enlarged cLDs. 134 infected cells treated with DMSO or Z390 were counted. The percent was co calculated by dividing the cells showing the NS5A on the surface of enlarged cLDs by the total number of cells counted (results from four independent experiments).

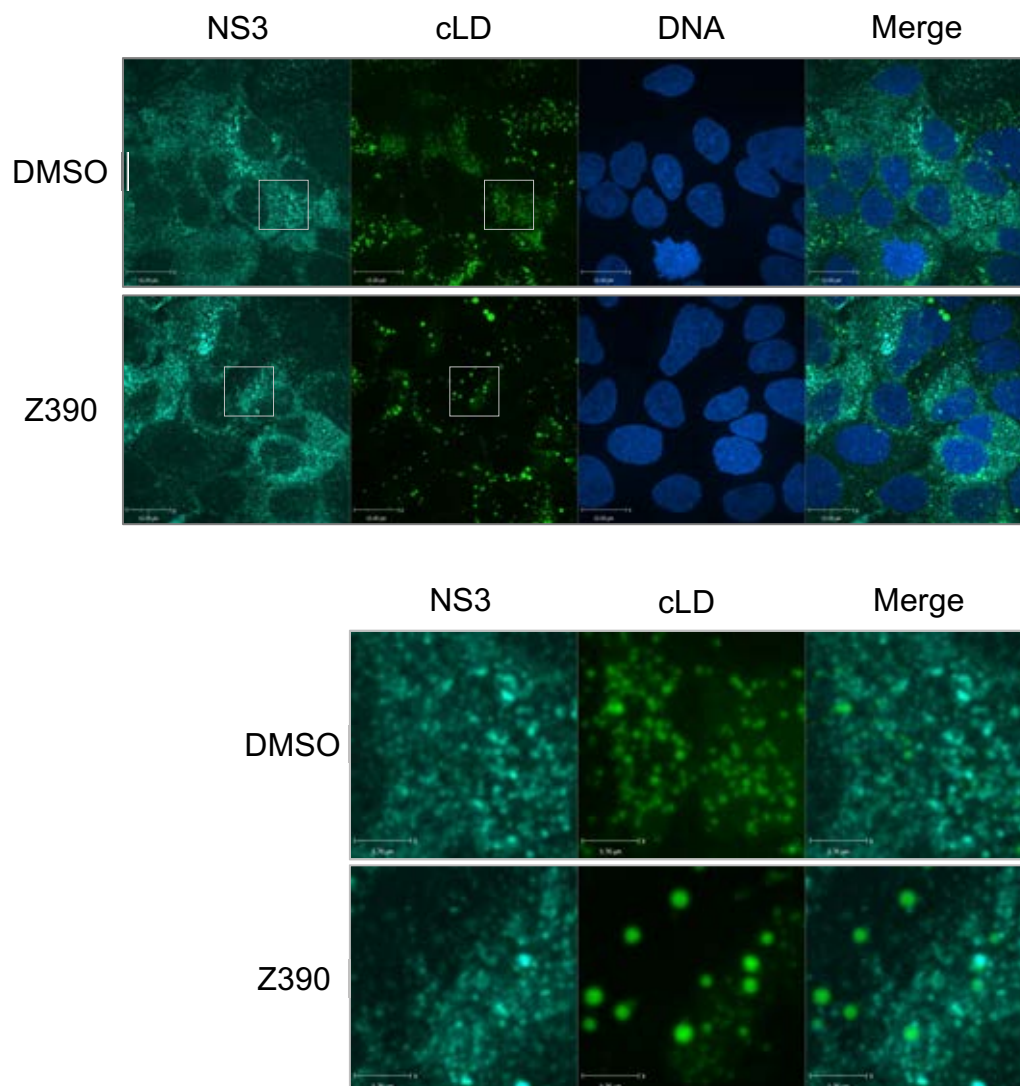


**Figure 5.7 Effect of Z390 on NS3 distribution.**

Top, immunofluorescence micrographs showing HCV NS3 (cyan) or cLDs (green) in HCV-infected cells treated with DMSO or Z390 at 60x magnification. Bottom, the areas indicated by the squares at the top showing magnified region. Huh7.5 monolayers were infected with 0.01 infectious HCV cc (JFH1) virions per cell. Inocula were removed 4 h later and fresh medium containing 40  $\mu$ M Z390 or DMSO was added. Two days later, infected cells were processed for immunofluorescence for NS3 and evaluated by confocal microscopy.

and size of cLDs. Z390 induced an enrichment of HCV core on the surface of enlarged cLDs. Z390 could thus induce enlargement of cLDs either by direct effect on cLDs or indirectly through its effect on core. Therefore, we next evaluated the association of ADRP with cLDs in the absence of HCV infection.

Uninfected Huh7.5 cells were treated with 40  $\mu$ M Z390 for 48 h before processing for immunofluorescence for ADRP and staining of cLDs. ADRP and cLDs colocalized scattered throughout the cytoplasm, occasionally with areas of intense signal with no particular pattern. ADRP and cLDs in untreated cells also colocalized in Z390 treated infections. However, the size distribution of cLDs population was different (**Figure 5.8**). A subset of cLDs were much enlarged and predominantly juxtanuclear in approximately 85% of the cells, whereas the other 12% of cells had few cLDs similar in size to those in control treated cells (**Figure 5.9**). Thus, Z390 induces enlargement of cLDs independently of HCV core enrichment.

#### **5.2.5 The number of small cLD decreases in cells treated with Z390**

Z390 could inhibit the formation of nascent cLDs. TIP47 is essential for the formation of cLDs and it translocates from cytoplasm to the sites of nascent cLDs upon brief oleic acid stimulation. We next tested the effect of Z390 on the formation of cLDs by immunofluorescence imaging for TIP47 and cLDs staining.

Huh7.5 cells were treated with 40  $\mu$ M Z390 for 1 h and then stimulated with 0.5 mM oleic acid in the presence of Z390 for 3 h before immunofluorescence. Stimulation of Huh7.5 cells with oleic acid resulted in the expected enrichment of TIP47 to small size cLDs. Pre-treatment with 40  $\mu$ M Z390 for 1 h before and during the stimulation with oleic acid resulted in TIP47 staying dispersed in the cytoplasm, and only a few and small nascent

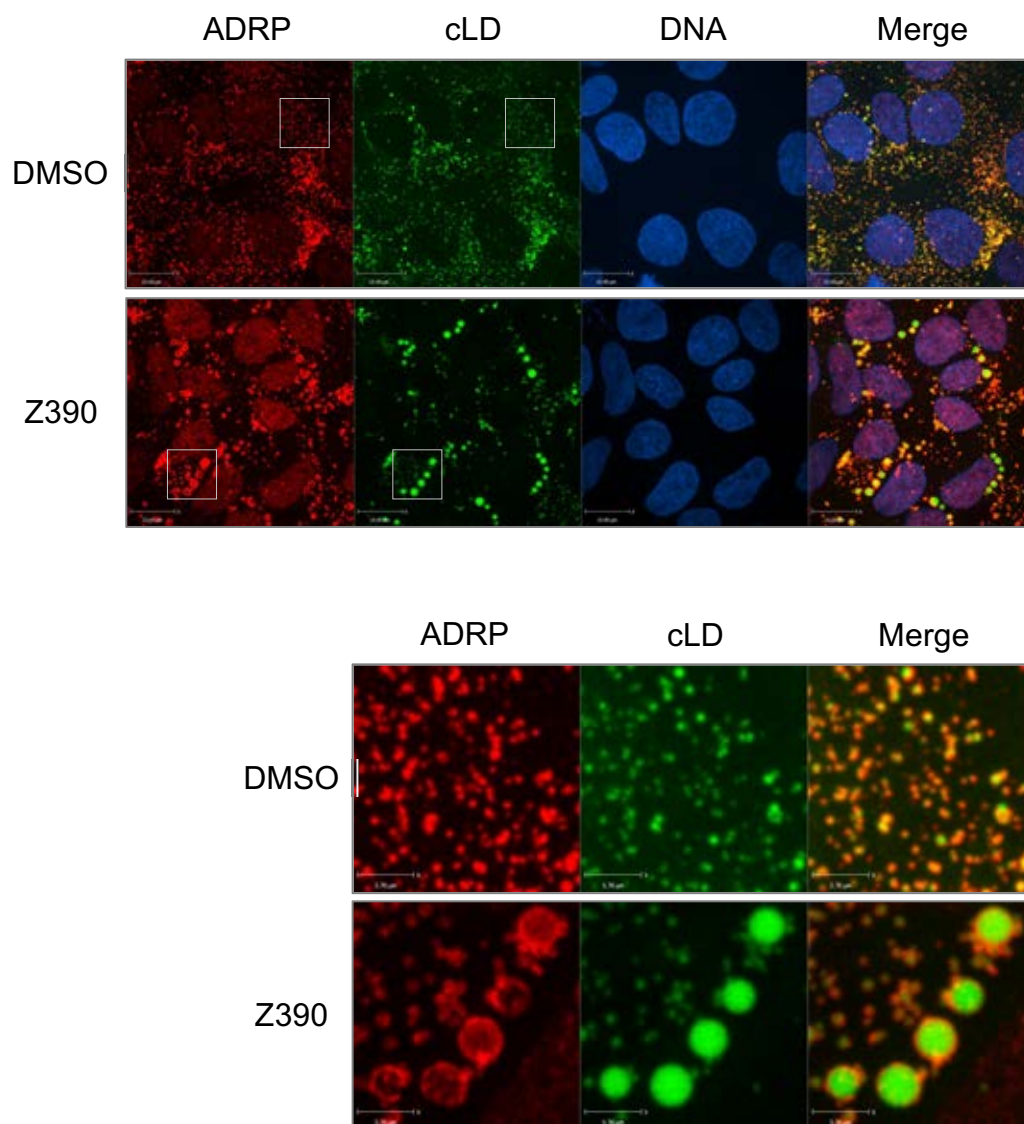


**Figure 5.8 Z390 results in more ADRP localized around mature cLD.**

Top, immunofluorescence micrographs showing ADRP (red) or cLDs (green) in Huh7.5 cells treated with DMSO (top) or Z390 (bottom) at 60x magnification. Bottom, the areas indicated by the squares at the top showing magnified region. Huh7.5 monolayers were treated with 40  $\mu$ M Z390 or DMSO for two days before they were processed for immunofluorescence for ADRP and evaluated by confocal microscopy (results from five independent experiments).

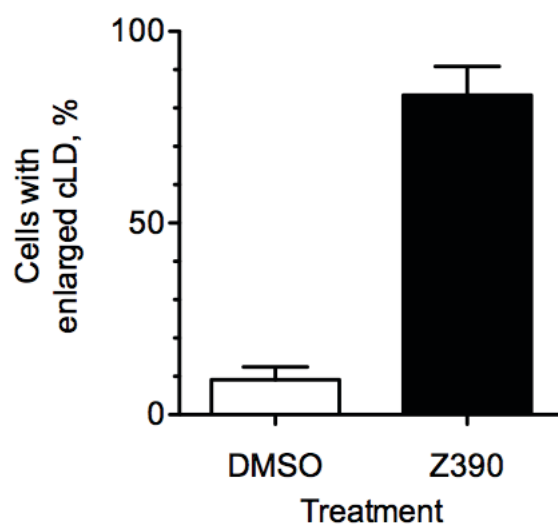


**Figure 5.9 Quantitation of Z390 effect on the size of cLD).**

Bar graph showing the percent of cells with normal size distribution or predominantly enlarged cLDs. 414 Huh7.5 cells treated with DMSO or Z390 were counted. The percent was calculated by dividing the cells showing the enlarged cLDs by the total number of cells counted (results from five independent experiments).

cLDs (**Figure 5.10**). In 85% of the treated cells, cLDs were fewer, smaller, and less fluorescent, compared to 25% of the cells in the control treatment (**Figure 5.11**). Z390 thus interferes with TIP47 translocation to the sites of nascent cLDs and the formation of nascent cLDs.

#### **5.2.6 Oleic acid also enriches core on enlarged cLD**

Z390 induced enlarged cLDs clustered at juxtanuclear region and reduced the number of small cLDs dispersed throughout the cytoplasm. To further test if the cLDs phenotype induced by Z390 was secondary to the enrichment of HCV core on the surface of cLDs, we treated the cells with oleic acid. Enlarged cLDs at the juxtanuclear region prevailed 12-24 h after addition of 0.5 mM oleic acid, while the number of small dispersed cLDs decreased. We thus tested whether oleic acid treatment of Huh7.5 cells infected with HCVcc-JFH1 affected HCV core distribution.

Huh7.5 cells were infected with HCVcc-JFH1 and treated with 0.5 mM oleic acid for 1 or 24 h before immunofluorescence for core and ADRP (as cLD maker) 48 h after infection. Core and ADRP were colocalized and dispersed through the cytoplasm in control infections treated with vehicle control. Oleic acid increased the size of cLDs in time-dependent manner. Oleic acid stimulation for 1 h resulted in two populations of core and ADRP fully clustered around the nucleus and one scattered away from the nucleus. In contrast, core and ADRP in fully cluster around the nucleus in ring-like structures when infected cells were stimulated for 24 h (**Figure 5.12**). Core was enriched on enlarged and clustered cLDs in more than 80% of the infected cells treated with OA for 24 h, compared to less than 30% of the cells treated for 1 h (**Figure 5.13**).



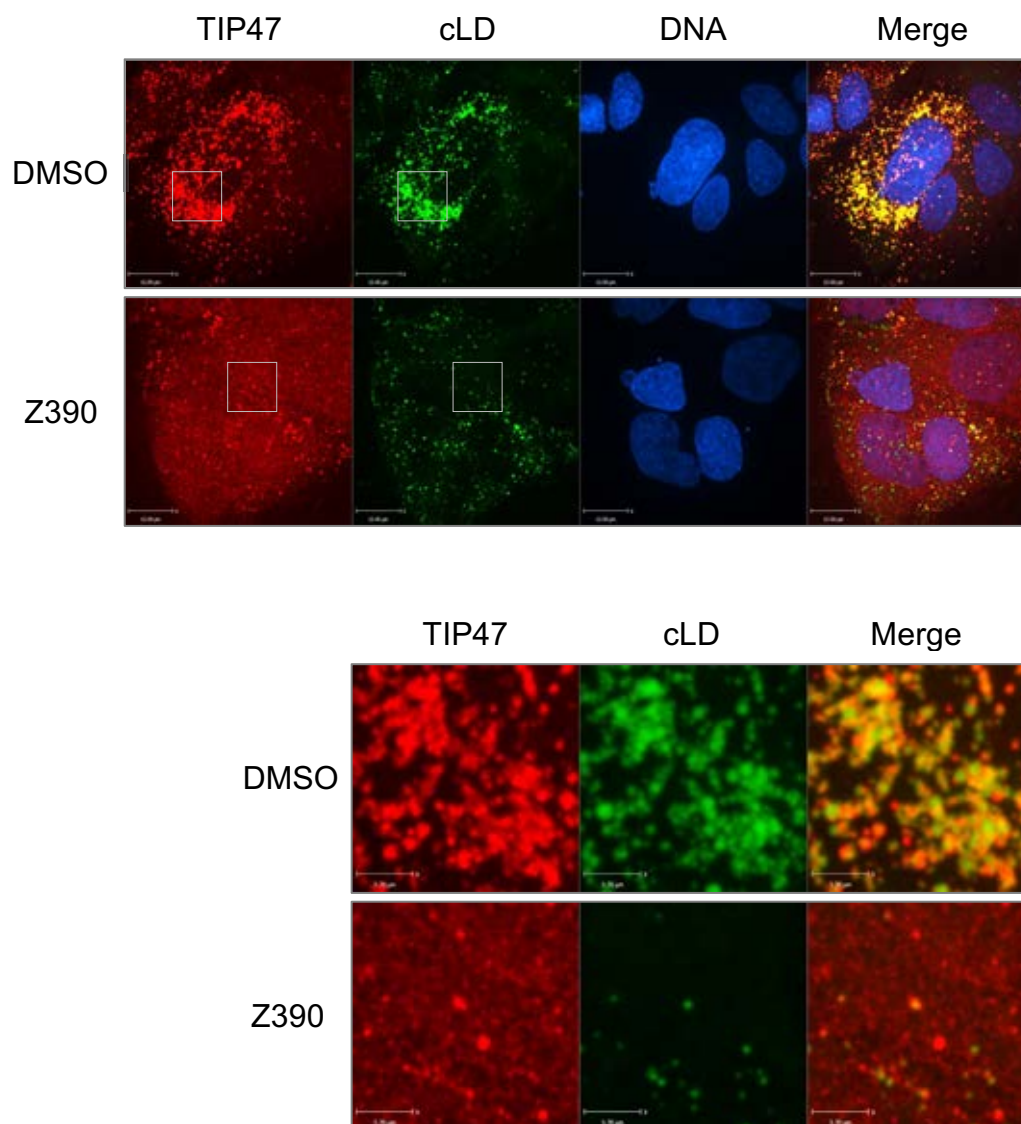


**Figure 5.10 Z390 decreases small nascent cLD.**

Top, immunofluorescence micrographs showing TIP47 (red) or cLDs (green) in Huh7.5 cells treated with DMSO (top) or Z390 (bottom) at 60x magnification. Bottom, the areas indicated by the squares at the top showing magnified region. Huh7.5 monolayers were treated with 40  $\mu$ M Z390 or DMSO for two days before they were processed for immunofluorescence for TIP47 and evaluated by confocal microscopy (results from three independent experiments).

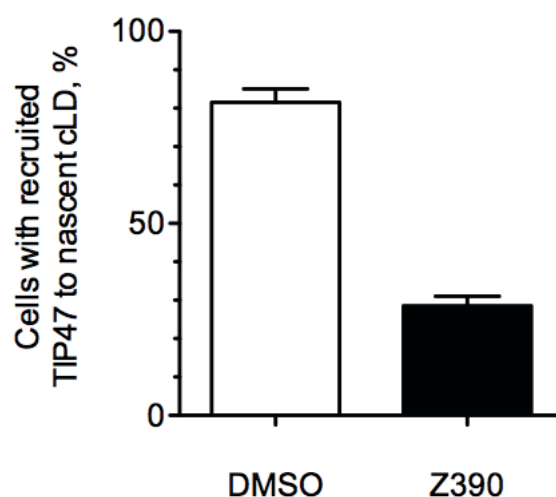


**Figure 5.11 Quantitation of Z390 effect on enrichment of TIP47 at sites of nascent cLD.**

Bar graph showing the percent of cells with TIP47 enriched at nascent cLDs or dispersed in the cytoplasm. 86 infected cells treated with DMSO or Z390 were counted. The percent was calculated by dividing the cells showing the enrichment of core on enlarged s by the total number of cells counted (results from three independent experiments).

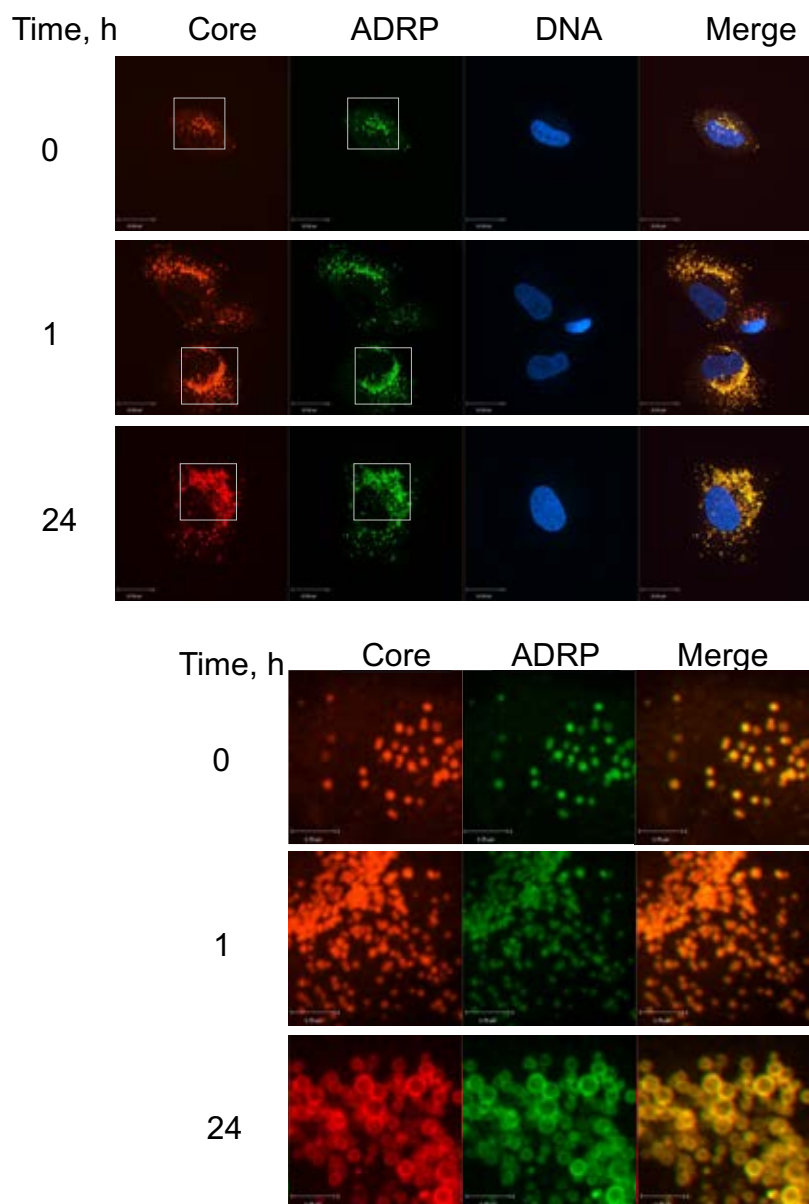


**Figure 5.12 HCV core associates with enlarged cLD in cell treated with OA. HCV core associates with enlarged cLD in cell treated with OA.**

Top, immunofluorescence micrographs showing HCV core (red) or cLD marker ADRP (green) in HCV-infected cells treated with oleic acid or vehicle. Bottom, the areas indicated by the squares at the top showing magnification. Huh7.5 monolayers were infected with 0.01 infectious HCVcc-JFH1 virions per cell. Inocula were removed 4 h later and fresh medium containing 0.5 mM oleic acid for 1 or 24 h or vehicle. Two days later, infected cells were processed for immunofluorescence for core and evaluated by confocal microscopy (results from three independent experiments).

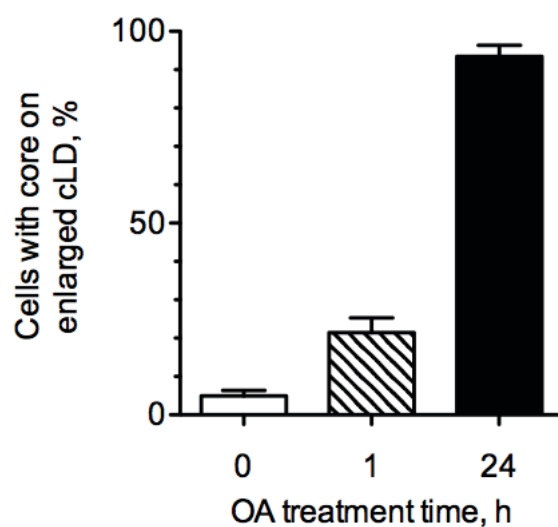


**Figure 5.13 Quantitation of OA effect on HCV core and cLD in HCV-infected cells.**

Bar graph showing the percent of cells with enriched localization of HCV core on the surface of enlarged cLDs. 79 infected cells treated with OA for 1 or 24 h, or not were counted. The percent was calculated by dividing the cells showing the enrichment of core on enlarged cLDs by the total number of cells counted (results from three independent experiments).

### **5.2.7 Oleic acid induces redistribution of HCV NS5A from the ER to the surface of enlarged cLD**

Like Z390, oleic acid induced enrichment of HCV core on cLDs in ring-like structures. Z390 also induced a similar redistribution for NS5A. We thus tested if oleic acid induced a similar redistribution of NS5A from ER into cLDs.

Huh7.5 cells were infected with HCVcc-JFH1 and treated with 0.5 mM oleic acid for 1 or 24 h before immunofluorescence for NS5A and ADRP at 48 h after infection. Like core, NS5A and ADRP colocalized and clustered. Oleic acid increased the size of cLDs in time-dependent manner. Oleic stimulation for 1 h resulted in two populations of NS5A and ADRP, clustered around the nucleus or scattered away from it. NS5A and ADRP were entirely clustered around the nucleus in ring-like structures when the infected cells were stimulated for 24 h (**Figure 5.14**). NS5A was redistributed to enlarged and clustered cLDs in more than 90% of the infected cells treated with OA for 24 h, compared to less than 25% of the cells treated for 1 h (**Figure 5.15**).

### **5.2.8 Oleic acid inhibits cell-to-cell HCV spread**

Oleic acid induced enrichment of core on cLDs and redistribution of NS5A from ER to enlarged cLDs, mimicking the effects of Z390. Huh7.5 cells were infected with HCVcc-JFH1 for 48 h, when they were treated with 0.5 mM oleic acid for 1 or 24 h before labelling and co-culturing with uninfected cells. Co-cultures were incubated and incubated for 24 h in the presence of HCV neutralizing anti-serum. Transmission of HCV from donor labeled to target unlabeled cells was evaluated by immunofluorescence for HCV core. Extracellular infectivity was not affected by the treatment of the donors with oleic acid for 24 h before co-culture. HCV infection spread from donor to every cell in direct contact

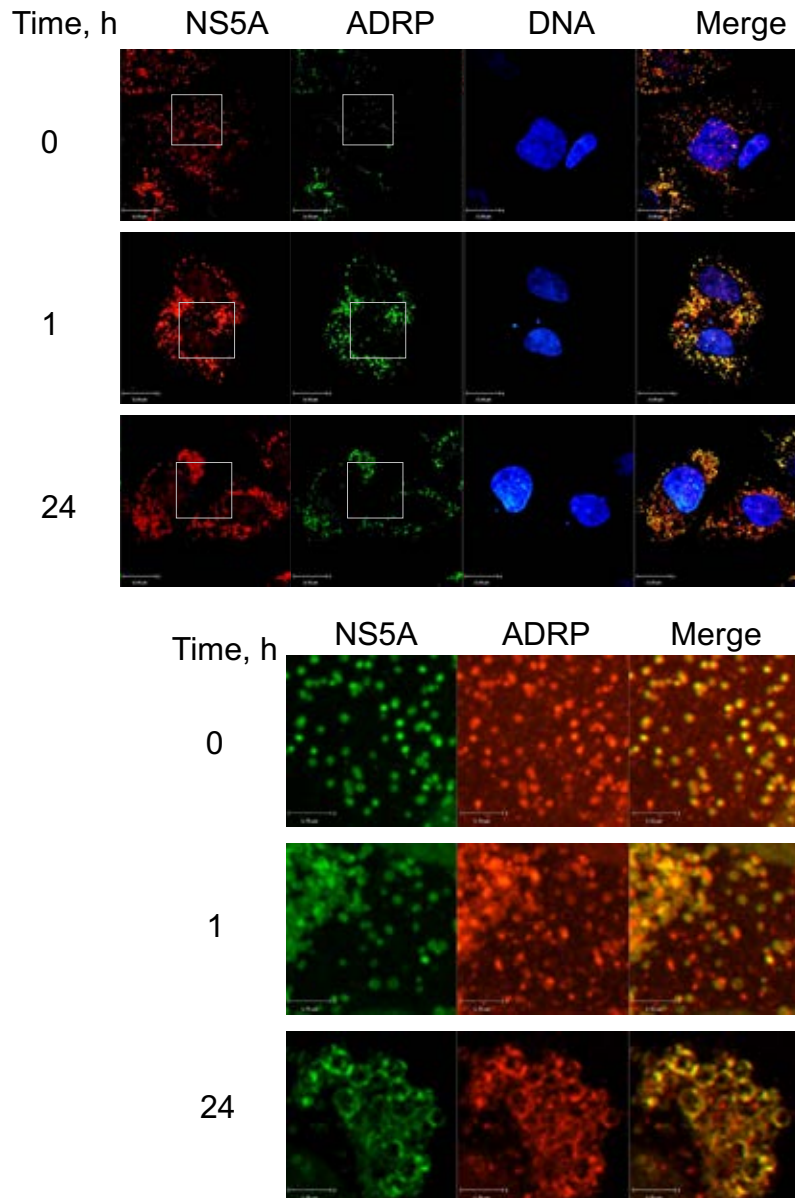


**Figure 5.14 HCV NS5A associates with enlarged cLD in cell treated with OA. HCV core associates with enlarged cLD in cell treated with OA.**

Top, immunofluorescence micrographs showing HCV NS5A (red) or cLD marker ADRP (green) in HCV-infected cells treated with oleic acid or vehicle. Bottom, the areas indicated by the squares at the top showing magnification. Huh7.5 monolayers were infected with 0.01 infectious HCV cc (JFH1) virions per cell. Inocula were removed 4 h later and fresh medium containing 0.5 mM oleic acid for 1 or 24 h or vehicle. Two days later, infected cells were processed for immunofluorescence for core and evaluated by confocal microscopy (results from three independent experiments).

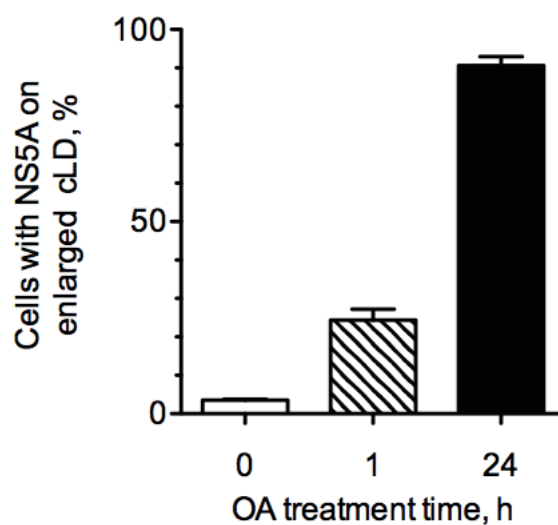


**Figure 5.15 Quantitation of OA effect on HCV NS5A and cLD in HCV-infected cells.** Bar graph showing the percent of cells with HCV NS5A ring-like structures on enlarged cLDs. 86 infected cells treated with OA for 1 or 24 h, or not were counted. The percent was calculated by dividing the cells showing redistribution of NS5A onto the surface of cLDs by the total number of cells counted (results from three independent experiments).

with the donor and further outward to form foci comprised of an average of 20 target per donor cell in vehicle treated co-cultures. Similar result was obtained in approximately 85% of events when the donor cells were treated with oleic acid for 1 h before co-culture. In contrast, donor cells treated with oleic acid for 24 h before co-culture failed to transmit HCV infection to any adjacent cells (**Figure 5.16-Figure 5.17**).

Thus, treatment of HCV donor cells with oleic acid before co-culture inhibited HCV cell-to-cell spread. The status of lipid droplet metabolism is thus involved in the of HCV cell-to-cell spread.



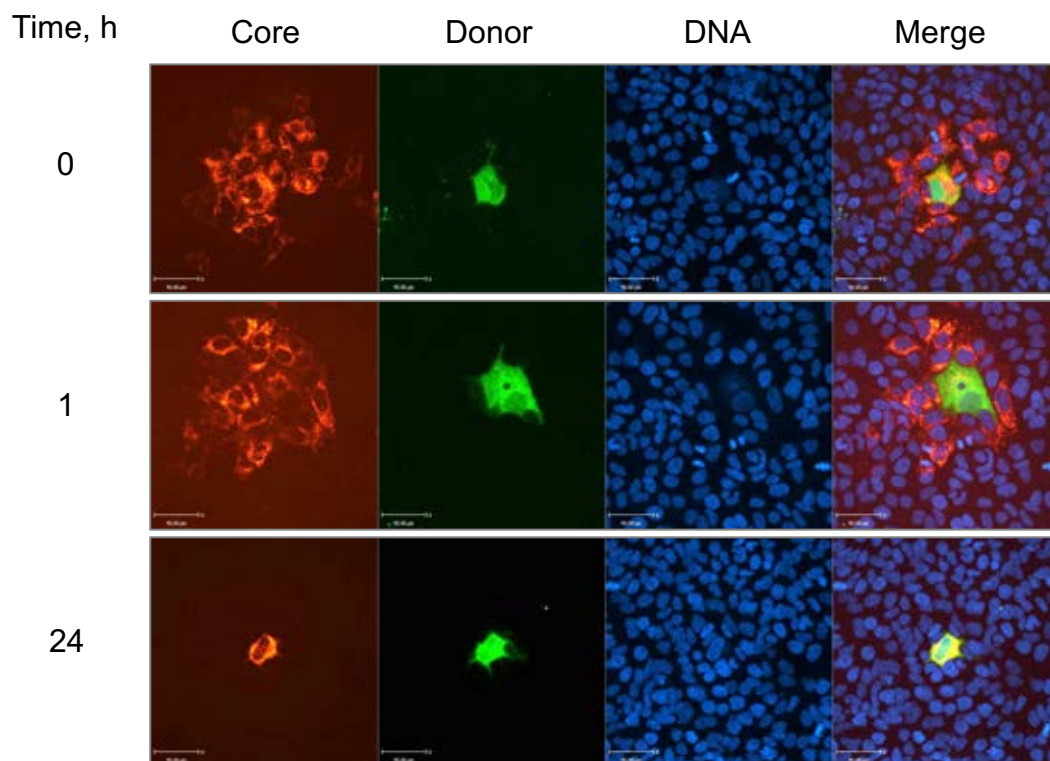


**Figure 5.16 Oleic acid inhibits HCV cell-to-cell spread.**

Immunofluorescence micrographs showing HCV core (red) and CFDA SE-labeled cells (green) in co-cultures treated with vehicle or oleic acid for 1 or 24 h. Huh7.5 monolayers were infected with 5 infectious HCV cc (JFH1) virions per cell. 48 h later, donor infected cells were treated with vehicle or 0.5 mM oleic acid for 1 or 24 h before they were labeled with carboxy-fluorescein diacetate succinimidyl ester (CFDA SE), trypsinized, and co-cultured with uninfected cells at a ratio of 1 infected per 200 uninfected cells in the presence of 10% anti-HCV serum. Foci formation in the co-cultures was evaluated by immunofluorescence for core 24 h after co-seeding (results from three independent experiments).

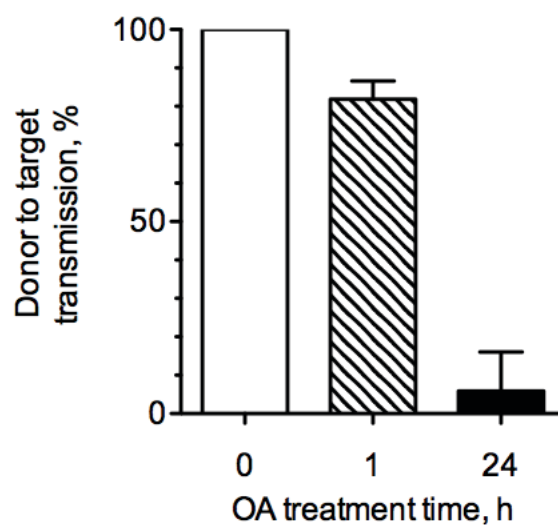


**Figure 5.17 Quantitation of OA effect HCV cell-to-cell spread.**

Bar graph showing the percent of HCV-infected and OA-treated Huh7.5 cells for the indicated times transmitted the infection to adjacent uninfected cells. 49 donor cells were counted. The percent was calculated by dividing the cells transmitted the infection by the total number of cells counted (results from three independent experiments).

## **5.3 DISCUSSION**

### **5.3.1 Z390 effect on HCV core**

HCV infection of Huh7.5 cells results in an increase in size and movement of core-covered cLDs in ring-like structures from the periphery of the cells toward the MTOC at the juxtanuclear region in a time-dependent manner. A few core ring-like structures heterogeneous in size start to appear 48 h after infection. They increase in number and become homogenous in size at 72-96 h post-infection. Treatment of HCV infections with Z390 further increased the size and the juxtanuclear clustering of cLDs enriched with ring-like core structures. The same effects occurred in cells infected HCV strains JFH-1 and Jc1 (genotype 2a) and H77 (genotype 1a), indicating that the effects are not genotype or strain specific. The enrichment of core on cLDs was more obvious in HCV-Jc1 infections than in JFH1 or H77, as Jc1 core association with mature cLDs is minimal in untreated infections. The faster rate of liberation off cLDs in Jc1 infections results in accelerated and efficient assembly and release of cell-free virions (Andre & Lotteau, 2008; Eggert, Rosch, Reimer, & Herker, 2014; Pietschmann et al., 2006). 91% of Japanese fulminant hepatitis 1 core is associated with cLDs compared to 2% of Jc1 core (Shavinskaya et al., 2007a). Jc1 core is homogeneously dispersed throughout the cytoplasm in untreated infections but localized to cLDs in Z390 treated ones, indicating that liberation of Jc1 core from cLDs was delayed.

The enrichment of core on enlarged cLDs in HCV infections treated with Z390 resembles that in infections with HCV mutants defective in assembly such as HCV-Jc1/D88 or HCV-Jc1/p7-QQ. The accumulation of core on cLDs results from the immobilization into assembling virions. As a result, cLDs are enlarged and clustered at

the juxtanuclear region. The cLDs size, number, and cellular distribution in mutant infections were mostly heterogeneous, unlike that in infections treated with Z390. Also, the core mutants were associated with either the ER (core before association with cLDs) or the cLDs (core at assembly site), while the cLD-independent puncta (core in assembled virions) were absent. Core in infections treated with Z390 were almost exclusively associated with cLDs (Counihan et al., 2011; Noppornpanth et al., 2007).

Trafficking of HCV core protein from the ER to cLDs is necessary for the assembly of progeny virions. Accumulation of HCV core on enlarged cLDs is characteristic of defects in virion assembly. HCV-Jc1 with p7 point mutation in the diphasic motif in the loop region p7-KR33/35QQ (or p7-QQ) (Steinmann et al., 2007), which abolishes its ion channel activity, decreased extracellular infectivity and core level by 100 or 10-fold, respectively, while intracellular core levels remained unchanged. In WT infection, 15% of the cells showed clustered cLDs, while it was >95% in p7-QQ. Core on cLDs was less than 5% in WT infection, in contrast, it was >90% in p7-QQ. The level of core on cLDs was 30-fold higher in p7-QQ than WT (Gentzsch et al., 2013). A deletion mutation in the p7 N-terminal transmembrane helix (p7 amino acid residues 1-32), known as p7<sub>half</sub> (Steinmann et al., 2007), inhibited infectivity and decreased the extracellular level of core by 2.5-log while the intracellular level of core remained unchanged (Gentzsch et al., 2013). The accumulation of core on cLDs in infections treated with Z390 indicates that core had matured and trafficked from the ER to the surface of cLDs and had not inhibited assembly or release of infectious HCV particles.

### **5.3.2 Z390 effect on HCV NS5A**

NS5A coordinates progeny virion assembly by facilitating the transfer of HCV RNA to the assembling capsids. NS5A associates with ER in a speckle-like pattern that is mostly adjacent, but does not localize to, the surface of cLDs. Z390 redistributed NS5A from ER to the surface of cLDs, resulting in ring-like structures resembling those formed by core. Z390 treatment resulted in more core localizing to cLDs, and in a changed localization of NS5A to the surface of cLDs. The effect of Z390 on core or NS5A localization is not generalized effect on all HCV proteins, however the localization of NS3, another protein that participates in the assembly of HCV virions, was not affected by Z390. Redistribution of NS5A from ER to the surface of cLDs has been reported previously as a result of a direct NS5A inhibitor identified by library screening (Targett-Adams et al., 2011). This inhibitor inhibited the formation of replication complexes, and consequently, of HCV replication. Z390 does not inhibit HCV replication and it is thus not a direct NS5A inhibitor. NS5A was also redistributed from ER to cLD by Arf1 knockdown. Arf1 is a small GTPase of the Ras superfamily with a primary function in vesicular trafficking. Knockdown of Arf1 resulted in a limited 3-fold increase in NS5A localization in ring-like structures to enlarged cLDs. No other HCV proteins were examined but a decrease in HCV RNA replication was observed. The similarity of the effects of Z390 and Arf1 knockdown on NS5A and cLDs size suggested to us that Z390 could target Arf1.

### **5.3.3 Z390 effect on cLD and ADRP**

Z390 could affect either core or cLDs. A direct effect on core is unlikely, as small molecule targeting of core would likely inhibit infectivity. Z390 could accelerate the rate of core trafficking to cLDs, producing homogeneous ring-like structures earlier than in

untreated infections. Z390 would then be expected to also accelerate production of infectious virions. Z390 did not, as reflected in single-step replication. We thus focused on the potential Z390 effects on cLDs. Core translation at ER-cLD contact sites was postulated by co-fractionation of ribosome and cLDs, but subsequent studies have suggested this co-fractionation was artefactual. Core is normally barely detected by immunofluorescence at 12 h because it is dispersed throughout cytoplasm. Z390 treatment resulted in large core puncta associated with cLDs at 12 h, indicating that translation of core likely occurs on ER near the cLD-ER contact sites as previously proposed. The progressive increase in core levels stimulates *de novo* synthesis of nascent cLDs, to increase the surface area for incorporation of the increasing core amounts. Z390 induced accumulation of core on cLDs while inhibiting nascent cLDs synthesis, thereby increasing the ratio of core to cLD.

The major LDAP ADRP promotes cLDs formation and limits cLD-targeted lipolysis. ADRP prevents lipolysis of cLD by competing for the binding site of lipases such as adipocyte triglyceride lipase (ATGL) and co-factor CGI-58. Overexpression of ADRP thus prevents lipolysis and promotes enlargement of cLDs, whereas ADRP<sup>-/-</sup> cells have high lipolysis rate. ADRP is degraded rapidly upon dissociation from cLDs, via lysosomal or proteasomal pathway depending on the energy status of the cell. There is normally no pool of ADRP not bound to cLDs. ADRP appears as a ring around mature cLDs. ADRP also localizes to nascent cLDs, but because the size of nascent cLDs is too small, it is not detected at this localization even by the highest-resolution confocal microscopy. ADRP appears as patches on ER. ADRP localization to visible spherical structures cLDs stained with bodipy493 indicates mature cLDs. Patchy ADRP localization to sites of no

Bodipy493-staining indicates sites of nascent cLDs formation on ER. Z390 resulted in decreased number of larger cLDs and exclusive localization of ADRP to the surface of mature cLDs. Z390 induces a cell status that would normally prevent the lipolysis of neutral lipids in cLDs. Z390 could induce such status by either induction of lipogenesis and inhibition of lipolysis or by regulating trafficking to and from cLDs. The absence of ADRP patches in the ER could indicate the inhibition nascent cLDs formation.

Z390 resulted in enlarged clustered cLDs at juxtanuclear region, suggesting an increased lipogenesis or decreased lipolysis. Increased lipogenesis results in fewer but enlarged and clustered cLDs, which occurs at later time after lipid intake. Earlier after lipid intake, cLDs are abundant but vary in size and are dispersed throughout cytoplasm. Z390 decreased the number and increased the size of cLDs early after treatment, and this likely not through increased lipogenesis. Z390 could inhibit lipolysis. ADRP maintain mature cLDs. Increased localization of ADRP on ER or on mature cLDs indicates increased synthesis of nascent cLDs, or inhibition of lipolysis of mature cLDs respectively. Z390 resulted in increased and exclusive localization of ADRP to mature cLDs. Thus, Z390 increased the size of mature cLDs by inhibition of lipolysis and inhibition of nascent cLDs formation. We thus tested the effect of Z390 on the recruitment of TIP47 to site of nascent cLDs synthesis.

#### **5.3.4 Z390 effect on TIP47**

TIP47, which is a member of LDAP family, is essential for the formation of nascent cLDs. TIP47 is translocated from ER to the site of cLDs formation upon brief stimulation with OA. Stimulation of Huh7.5 cells with 0.5 mM OA for 3 h showed enriched localization of TIP47 and numerous small cLDs, as expected. Pre-treatment with 40  $\mu$ M Z390 for 1 h

before stimulation with OA inhibited the enrichment of TIP47 and resulted in fewer small cLDs. Z390 results in the inhibition of the formation of nascent cLDs than in cells treated with DMSO vehicle and of TIP47 translocation to sites of nascent cLDs. Thus, Z390 inhibits the formation of nascent cLDs, and protects the mature ones. These processes involve different sets of enzymes and cofactors but both require trafficking of proteins into and out of cLDs. Z390 thus may likely act on trafficking processes.

#### **5.3.5 Effect of oleic acid on HCV core, NS5A, and cLD**

Treatment of several cell lines including Huh7.5 with oleic acid stimulates synthesis of nascent cLDs, which increase in size, decrease in number, and cluster at the juxtanuclear region, in a time-dependent manner. Oleic acid stimulates the synthesis of nascent cLDs early after treatment, which continue to grow under steady incorporation of TG of oleic acid into mature and aggregated cLDs at the juxtanuclear region. To a lesser extent, similar effects on cLDs homeostasis is observed in Huh7.5 cells infected with HCV. HCV stimulates accumulation of enlarged mature cLDs mostly by decreasing the turnover of TG via core inhibition of LD-associated ATGL. HCV infection also stimulates synthesis of cLDs by activation of transcription factors that upregulate genes involved in regulation of lipid metabolism. The result of this activation by HCV infection is increased synthesis and decreased turnover of TG (Camus et al., 2014). Thus, treatment of HCV-infected cells with oleic acid results in an increase in the number of enlarged mature and aggregated cLDs. In untreated HCV-infected cells, core is enriched on enlarged cLDs and distributed throughout the cytoplasm, while the treatment with oleic acid result in exclusive association of core to cLDs in ring-like structures at the juxtanuclear region. Thus, exclusive localization of HCV core and NS5A to cLDs occurs when cLDs were



homogenously enlarged and aggregated or the absence of heterogeneously dispersed cLDs, a phenotype that is similar to that obtained with HCV infection treated with Z390. While Z390 inhibits the synthesis of nascent cLDs, preventing the appearance of heterogeneous in size and dispersed cLDs, oleic acid is known to affect synthesis of nascent cLDs. Although treatment with oleic acid stimulates synthesis of nascent cLDs, however the accelerated incorporation of TG into cLDs results in a homogenous population of aggregated mature cLDs within the first 6 to 12 h after addition of oleic acid.

### **5.3.6 Effect of oleic acid on HCV cell-to-cell spread**

The effect of oleic acid on the cellular distribution of HCV core and NS5A and on homeostasis of cLDs resembled that obtained with treatment of HCV infections with Z390 where core was enriched and NS5A was redistributed to enlarged and aggregated cLDs inhibited HCV cell-to-cell spread. The similar effects induced by Z390 or oleic acid on cLDs and HCV inhibition of HCV cell-to-cell spread implicate a major role of cLDs homeostasis in HCV cell-to-cell spread. Inhibition of cell-to-cell spread may result from the promotion of juxtanuclear clustering of mature cLDs or the absence of nascent cLDs.

## 5.4 SUMMARY

In the previous chapter, I also showed that HCV spread preferentially by cell-to-cell transmission, which was more efficient and maintained for longer than infection by inoculation. We compared the total (cell-free or cell-associated) infection spread on cells in the insert and infections by cell-free virions on cells in the well of a transwell plate. HCV spread throughout the cells on the inserts, but to only a few cells were on the well underneath the membrane. Passaging of HCV infections by inoculation of cell-free virions or by co-culture of infected cells also showed the preference for cell-to-cell transmission. We next applied high-resolution imaging to examine the effects of Z390 on the localization of certain HCV proteins with well-established interacting organelles. Cell-to-cell spread of viruses including HCV would involve.

In this chapter, microscopic examination of Z390 treatment of HCV infections showed an altered cellular distribution of HCV proteins core and NS5A and affected the homeostasis of cLDs. The phenotype resulting from Z390 treatment was characterized by the accumulation of mature cLDs and the absence of nascent cLDs, due to both inhibition of nascent cLDs synthesis and steady growth of existing mature cLDs. The enlarged cLDs induced enrichment of core and redistribution of NS5A from the ER to the cLDs. The (almost) exclusive localization of HCV core and ADRP onto mature cLDs in HCV infections treated with Z390 synergistically promoted growth of mature cLDs. Because Z390 treatment promoted enlargement of mature cLDs in uninfected cells, the enrichment for core and the NS5A redistribution around cLDs were a consequence of the effect on cLDs. Treatment of HCV infections with oleic acid reproduced the effects of Z390 on HCV proteins and cLDs homeostasis and inhibited cell-to-cell spread, thus,

supporting the conclusion that Z390 effect on cLDs alters cellular distribution of core and NS5A leading to inhibition of HCV cell-to-cell spread.

## **CHAPTER SIX: Arf1 is required for cLD metabolism and cell-to-cell HCV spread**

### **6.1 INTRODUCTION**

#### **6.1.1 Role of Arf1 in vesicular trafficking**

Proteins synthesized newly at the ER are transported by COPI system to their destination through the secretory pathway between ER and Golgi. In parallel, proteins endocytosed from the plasma membrane are transported to the endosomes for sorting (Rothman & Wieland, 1996). This bidirectional trafficking is required for the maintenance of the membranous organelles (Nickel & Wieland, 1997). The transport between ER and Golgi is a regulated stepwise process which includes sorting of the secretory proteins, recruitment of cargo carrier components, transport of the cargo vesicle to the target membrane, and recycling of the cargo components (Stephens & Pepperkok, 2001).

The Arf family of proteins is classified in the Ras superfamily of small GTPases. Arf proteins cycle between GDP or GTP-bound conformations. Arf proteins are categorized in three classes, based on their amino acid sequence homology. Class I includes Arf1 and Arf3, class II includes Arf4 and Arf5, and class III includes Arf6 (Kahn et al., 2006). Although the functions of the different Arf proteins overlap, Arf1 and Arf3 regulate the formation and budding of cargo vesicles on the secretory pathway and activate lipid-modifying enzymes (Bonifacino & Glick, 2004). Arf4 and Arf5 participate in early Golgi transport and recruitment of the coat components (Claude et al., 1999). Arf6 is involved in the trafficking of endosomal membrane and formation of cell surface

structures that require remodeling of cytoskeleton such as micropinocytosis (W. Tang et al., 2015) or endocytosis (D'Souza-Schorey, Li, Colombo, & Stahl, 1995).

Transport through the early secretory pathway from Golgi to ER and across Golgi cisternae depends on the formation of cargo vesicle by Arf1-dependent recruitment of coat components (Popoff et al., 2011). Also, Arf1 recruits heterotetrameric adaptor proteins AP-1, AP-3, and AP-4 complexes to regulate the recruitment of the clathrin to late Golgi and endosomes (Boehm, Aguilar, & Bonifacino, 2001; Y. Zhu, Drake, & Kornfeld, 1999). Arf1 is activated by the exchange of GDP for GTP, which is mediated by a family of proteins called nucleotide exchange factors (GEFs). GEFs contain a conserved 200 amino acid catalytic domain Sec7 (H. W. Shin & Nakayama, 2004). Arf1 GEF GBF1 is involved in the trafficking between ER and Golgi, whereas BIG1 and BIG2 are involved in the transport from TGN. GBF1 or BIG1 and BIG2 localize to cis or trans-Golgi, respectively. GBF1 is involved in the recruitment of COPI to the cis-Golgi membrane, while BIG2 is involved in the association of AP-1 to the trans-Golgi (Ishizaki, Shin, Mitsuhashi, & Nakayama, 2008; Kawamoto et al., 2002; Szul et al., 2007). The C-terminal region of Arf1-GDP interacts with the p23 cytoplasmic tail, which is a member of the p24 type I transmembrane Golgi-cargo receptors. Upon exchange of GDP for GTP, Arf1-GTP dissociates from p23, thus, providing a binding site for the coatomer coat to assemble (Gommel et al., 2001). Dissociation of the COPI from the cargo vesicles requires hydrolysis of Arf1-bound GTP, which is catalyzed by Arf GTPase activating proteins (GAPs) (Malsam, Gommel, Wieland, & Nickel, 1999). GAPs are essential for the functions of Arf proteins because Arf intrinsic hydrolysis is negligible.

### **6.1.2 Role of Arf1 in HCV life cycle**

Genetic interference to Arf1, Arf isoforms, GEF GBF1, or the GAP ArfGAP1, or treatment with GBF1 inhibitors brefeldin (BFA) or Golgicide A (GCA), suggested that Arf family participate in the life cycle of HCV (Goueslain et al., 2010). siRNA knockdown of Arf1 in Huh7 cells three days before infection with HCVcc-JFH1 inhibited HCV relative infection by 25-35% (Matto et al., 2011). Treatment of BFA-sensitive cells infected with HCV in the presence of BFA inhibited HCV replication by approximately 1-log, while that in BFA-resistant cells was not (Farhat et al., 2013). Knockdown of Arf1, 3, 4, or 5, or every pair combinations, except Arf3 and 5 and Arf4 and 5, inhibited the relative infection by approximately 30%. Knockdown of Arf3 and 5 or Arf4 and 5, inhibited the infection by 10% or 80%, respectively (Farhat et al., 2016). Thus, it appears that Arf proteins are involved in the susceptibility to HCV infection, although knockdown of Arf1 in Huh7 harboring HCV-1b replicon (FLRP1), inhibited HCV RNA replication by 40% (Farhat et al., 2013; Matto et al., 2011). The inhibition of HCV replication could not be produced (Farhat et al., 2016).

GBF1 binding to Arf1 leads to the displacement of GDP and binding of GTP which allows Arf1 to traps on membrane to facilitate the formation of cargo vesicles. Inhibition of GBF1 prevents the exchange, hinders the binding of Arf1 to the membrane, and Arf1 becomes mostly cytosolic. Knockdown of GBF1, but not BIG1 or BIG2 before infection, reduced HCV infection by 45-60% (Goueslain et al., 2010), which was identical to the inhibition due to knockdown of CD81, an essential cell surface receptor for HCV entry (Goueslain et al., 2010). Overexpression of GBF1 rescued the inhibition of HCV infection due to treatment with 0.1 µg/ml BFA by 50%, while the catalytically inactive mutant GBF1-

E794K did not (Goueslain et al., 2010). Thus, knockdown of GBF1, or overexpression of GBF1 in cells treated with 0.1  $\mu$ g/ml BFA, should, at least theoretically, increase or normalize the ratio of Arf1-GTP:GDP, respectively. Therefore, increasing Arf1-GDP:GTP by knockdown of GBF1 or expression of Arf1-T31N inhibits HCV infection. On the other hand, overexpression of GBF1 or the expression of Arf1-Q71L should normalize or decrease Arf1-GDP:GTP, respectively. Consistently, expression of Arf-Q71L, but not GBF1, inhibited the HCV infection.

Arf1 has a negligible activity of intrinsic GTPase. Therefore, ArfGAP1 is required to facilitate the hydrolysis of Arf1-bound GTP into GDP which releases the cargo vesicle. Knockdown of ArfGAP1 for three days before HCVcc-JFH1 infection reduced HCV RNA by 60-75%. Infection of Huh7.5.1 with HCVcc-JFH1 for 2 h before treatment with QS11, a small molecule inhibitor of ArfGAP1, reduced HCV RNA by approximately 8-fold (L. Zhang et al., 2012). ArfGAP1 interacts directly with NS5A, deletion of the ArfGAP1 binding domain within NS5A reduced HCV RNA by 2.3-fold (H. Li et al., 2014). Thus, interference of ArfGAP1 by chemical or genetic means also inhibits the susceptibilities of Huh7 cells from HCV infection.

Treatment of HCVcc-JFH1 infected Huh7 cells with 0.1  $\mu$ g/ml BFA for the first 8 h of infection including inoculum adsorption reduced the relative infection by approximately 10-fold. Treatment with BFA for 30 min before inoculation or up to 2 h after did not affect replication, while treatment up to 10 h reduced HCV RNA by approximately 11-fold. BFA appears to inhibit post-entry steps. BFA or GCA treatment of Huh7.5 cells containing HCV-Jc1 replicon for 12, decreased the extracellular and increased the intracellular infectivity by 3.5 and 3-log, respectively. Therefore, BFA or GCA treatment appears to

inhibit secretion. However, knockdown of Arf1 reduced both by 3 and 0.5-log, respectively, indicating that knockdown of Arf1 inhibits replication. Thus, Treatment with BFA or GCA or Arf1 siRNA suggests different mechanisms of action.

Interestingly, treatment of FLRP1 cells with BFA or GCA induced redistribution of NS5A, but not NS3, by 55% or 35%, respectively, while BFA resulted in 40% redistribution of NS3 and had no effect on the core association with cLDs. The cLDs were also enlarged in size. Knockdown of Arf1 redistribution of NS5A onto enlarged cLDs in 60% of the cells compared to 20% in control (Matto et al., 2011).

### **6.1.3 Role of Arf1 in cLD homeostasis**

Several genomic and proteomic studies of the hepatic purified cLD in basal (Bartz, Zehmer, et al., 2007; Cermelli et al., 2006), stimulated (Brasaemle et al., 2004), dietary restricted (Baumeier et al., 2015; Crunk et al., 2013; D'Aquila et al., 2015; Hartler, Kofeler, Trotschmuller, Thallinger, & Spener, 2014), or special conditions such HCV infection (Rosch et al., 2016) or stressed mouse model (Hartler et al., 2014) have identified several categories of host factors involved in the biogenesis of cLD. These include the family of perilipin proteins such as ADRP and TIP47, lipid metabolizing enzymes such ACAT1, 3, and 4, ATGL, HSL, cytoskeleton factors such as vimentin, or small GTPases such as Rab18, Arf1, Arf4, and their effectors GBF1, ArfGAP1, and COPI coatomer components (Brasaemle et al., 2004; Cermelli et al., 2006; Crunk et al., 2013; D'Aquila et al., 2015; Hartler et al., 2014; Rosch et al., 2016).

ADRP and TIP47 are members of the perilipin family of cLD-binding proteins with an essential role in the synthesis and growth of cLD. TIP47 is primarily involved in the synthesis of the nascent, and growth of the mature cLD, likely by transporting TG



synthesizing enzyme to the sites of nascent cLD synthesis or the surface of mature cLD. ADRP maintains mature cLDs mainly by the protection of cLDs from the lipase ATGL. Knockdown of ADRP and TIP47 decreases the amount of TG and cLD while it increases the release of free fatty acids (Nakamura et al., 2004). Fatty acids undergo  $\beta$ -oxidation at mitochondria to generate ATP. Excess fatty acids are recycled into TG by esterification and utilized to synthesize new cLDs, generating numerous small cLDs. Evidence has demonstrated the involvement of Arf1/COPI in the trafficking of ADRP, but not TIP47, to and from the cLDs. Treatment of HepG2 cells with BFA or expression of Arf1-T31N mutant, both should increase the ratio of Arf1-GDP:GTP, dissociates ADRP from cLDs, and reduces the number cLDs (Nakamura et al., 2004). Addition of BFA to oleic acid-treated NIH3T3 cells, which is supposed to stimulate synthesis of nascent cLDs, inhibits the formation of cLDs and ADRP association (Nakamura, Banno, & Tamiya-Koizumi, 2005).

Adipose triglyceride lipase (ATGL) is a lipase that initiates the hydrolysis of TG in the core of cLD by catalyzing the removal of the first fatty acid generating diacylglycerol. Hormone sensitive lipase (HSL) and monoacylglycerol lipase (MGL) catalyze the removal of the second and the third fatty acid generating monoacylglycerol and glycerol, respectively. Delivery of ATGL to cLDs depends on GBF1 and the components of COPI coat. The C-terminal domain of ATGL interacts with the N-terminal of GBF1 including the Sec7 domain, while the N-terminal domain of ATGL including the lipase domain interacts with the homology downstream of Sec7 (HDS) 1 and HDS2 within the C-terminal domain of GBF1. HDS1 or HDS2 could bind to the cLD (Bouvet et al., 2013) (Elong et al., 2011). Thus, HDS1 and HSD1 may facilitate the delivery of ATGL to cLD, implicating Arf1-GBF1-

COPI system in the targeting of ATGL to the cLDs. Silencing of ATGL increases the formation of TG and decreased the release of fatty acids, as expected (Beller et al., 2008). Transfection of HeLa cells with inactive GBF1 (E794L) or the Arf1-T31N inhibited the translocation of ATGL into the cLDs during stimulation of lipolysis (Soni et al., 2009). Similarly, knockdown of GBF1,  $\beta$ -COP, or treatment of HeLa cells with BFA before stimulation with oleic acid inhibits the association of ATGL, but not TIP47 with cLD.

The Arf1/COPI involvement in the trafficking of host factors required for homeostasis of cLD requires COPI coat for the formation of the vesicle. Silencing of COPI components  $\gamma$ -Cop or  $\zeta$ -Cop, or treatment with 5  $\mu$ M BFA or Exo1, a small molecule that affects the assembly or the stability of the COPI coat, increases the formation of TG and decreases the release of fatty acids (Beller et al., 2008). The Arf/COPI machinery is conserved among species at different ranks in the hierarchy of biological classification including human, plants, and arthropod. Knockdown of Arf1/COPI regulates cLD homeostasis by targeting lipid modifying host factors to or from cLDs. For example, cLD in *Drosophila* S2 cells are bimodal in size and clustered at the periphery. Knockdown of Arf79F, its GEF garz, or the COPI components, except  $\epsilon$ -Cop, inhibits the recruitment of GPAT4 to the surface of cLDs and produces dispersed cLDs with a uniform size between the large and the small. Arf79F, Arf1 orthologue in *Drosophila*, or expression of Arf79F mutant T31N (GDP-locked) decreases the release of fatty acid, while expression of Arf79F mutant Q71L (GTP-locked) increases the release of fatty acid (Guo et al., 2008). Knock down of the Arf79F or either of the COPI coat components except  $\epsilon$ -COP, in mouse AML12 cells (Beller et al., 2008) or *Drosophila* S2 cells (Beller et al., 2008; Guo et al., 2008), increased the cellular content of TG (Beller et al., 2008; Guo et al., 2008). Similarly,

knockdown of Arf79F GEFs, garz, GBF1 orthologue in *Drosophila* S2 cells, but not sec71 or CG31158, or the Arf GAPs, ArfGAP1 or Gap69C, increased the cellular TG (Guo et al., 2008).

(Nakamura et al., 2005) reported that ArfGAP1 and TIP47 localize on cLDs during the synthesis of cLDs. Association peaks at 4 h after addition of oleic acid and they dissociate when lipolysis is stimulated by cAMP treatment of McA-RH7777 cells (Gannon et al., 2014). Association of ArfGAP1 with cLDs after addition of oleic acid is transient, peaks at 4 h, partially dissociates at 10 h, and by 24 h, cLD are devoid of ArfGAP1. Knockdown of ArfGAP1 in cells treated with 500  $\mu$ M oleic acid distorts the cLDs in HepG2 or McA-RH7777, while it increases TG content in HeLa. Therefore, it is not unexpected that Arf1/COPI trafficking machinery is not required. Localization of the Arf1/COPI components on cLDs occurs at the beginning of the stimulation of lipogenesis or lipolysis where certain sets of enzymes and cofactors are recruited to the cLDs and displace integral cLD-associated proteins.

In addition to the role of Arf1/COPI in the trafficking of host factors involved in the homeostasis of cLD, Arf1/COPI could also act directly on the surface of cLDs, releasing Nano-droplets. In an artificial system, Arf1 binds to liposome or TG droplet in a GTP-dependent manner. Binding of Arf1-GTP to the lipid membrane recruits COPI coatomer. Using fluorescence labeled coat and Arf1 allowed visualization of budding of approximately 60 nm vesicles from the artificial LDs in ArfGAP1-dependent manner. Budding of these vesicles increases the surface tension of the LDs. Budding of five 60 nm droplets from 500 nm synthetic LDs decreases the density of the phospholipid in the LDs membrane by 10%, which results in increasing the surface tension by 3-fold. The

increase in the surface tension promotes binding of  $\alpha$ -synuclein, a cytosolic protein known to bind cLDs (Thiam et al., 2013). This process has been also replicated in cell-based settings. (Wilfling et al., 2014).

## 6.2 RESULTS

### 6.2.1 Arf1 knockdown affect core and NS5A association with cLD

Treatment of HCVcc-JFH1 infected cells with Z390 resulted in obvious changes to the cellular distribution of HCV proteins core and NS5A. Z390 also noticeably affected the population of cLDs in both infected or uninfected Huh7.5 and primary hepatocytes. In the previous chapter I used oleic acid to evaluate the effect of mimicking the phenotype of Z390 on cLDs, cellular distribution of core and NS5A, and cell-to-cell spread. Redistribution of NS5A from ER to cLDs in ring-like like structures is not common in HCVcc-JFH1 infections but could appear occasionally after 72 h of the infection. A single report showed that knockdown of Arf1 had resulted in redistribution of HCV NS5A from ER to cLDs in over 60% of the cells and that the cLDs were markedly enlarged (Matto et al., 2011). Thus, I proposed that interference of Arf1 would also inhibit HCV cell-to-cell spread. The effect of Arf1 knockdown on core had not been tested. Therefore, I first aimed to test if core localization was affected by knockdown of Arf1.

Huh7.5 cells were infected with HCVcc-JFH1 for 48 h, and were then knocked down for Arf1 for 24 h before evaluation by immunofluorescence imaging for HCV core and cLDs. Infections treated with control siRNA showed a dispersed pattern of colocalized core and ADRP, as expected. Treatment with Arf1 siRNA resulted in enlargement of cLDs without affecting the core association, indicating that knockdown of Arf1 mimics the effect of Z390 on the cellular distribution of core and size of cLDs (**Figure 6.1-Figure 6.2**). Knockdown of Arf1 in FLRP1 cells (a Huh 7 clonal cell line harboring full-genome HCV 1b replicon) resulted in ring-like structures of NS5A around enlarged cLDs. To account for possible

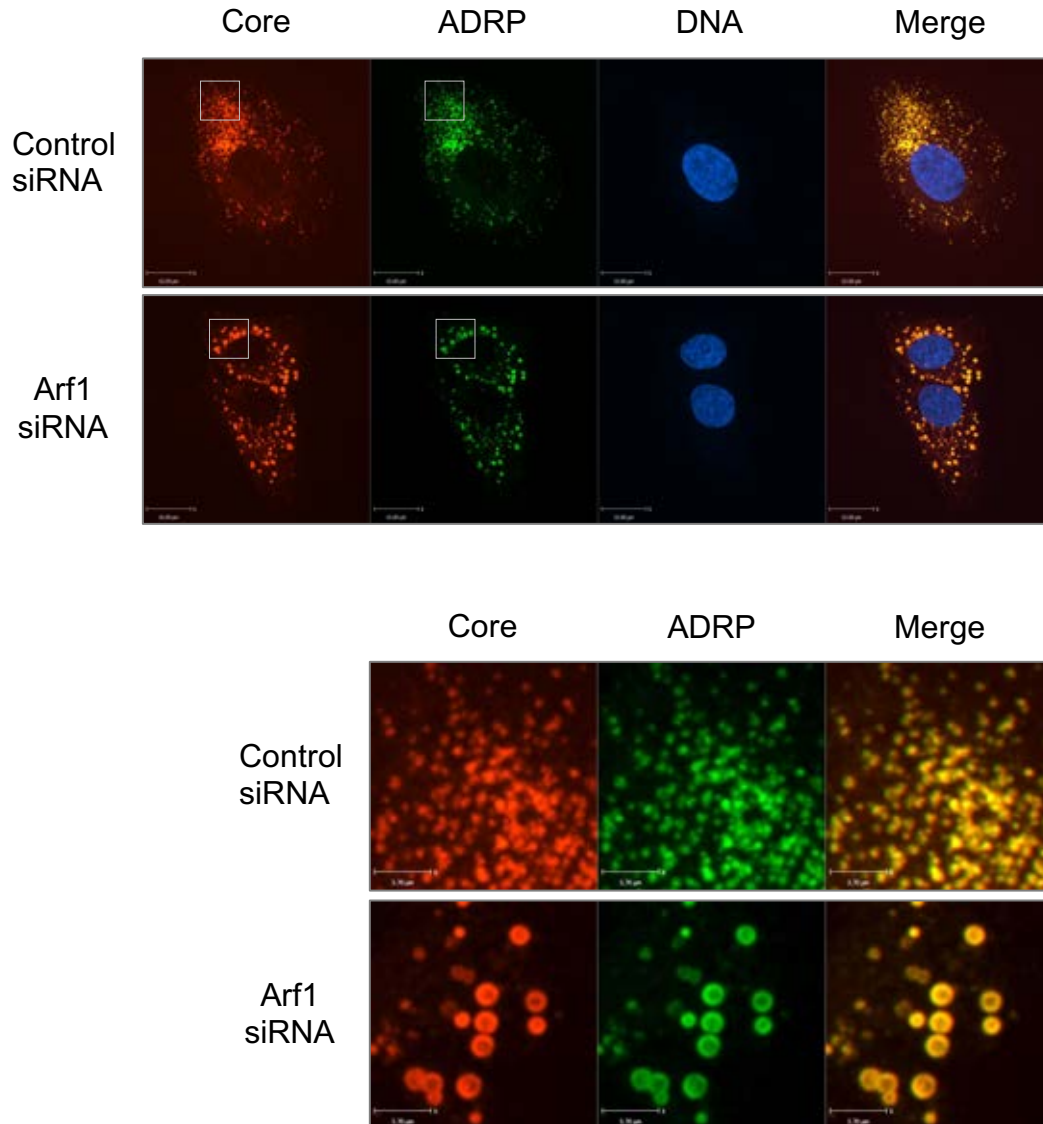


**Figure 6.1 Knockdown of Arf1 affects the distribution of HCV core and cLD.**

Top, immunofluorescence micrographs showing HCV core (red) or cLDs (green) in HCV-infected cells treated with control or Arf1 siRNA at 60x magnification. Bottom, the areas indicated by the squares at the top showing magnification. Huh7.5 monolayers were infected with 0.01 infectious HCV cc (JFH1) virions per cell. Inocula were removed 4 h later and after 48 h, infected cells were treated with control or Arf1 siRNA for 24 h before processing for immunofluorescence for core and evaluation by confocal microscopy (results from two independent experiments).

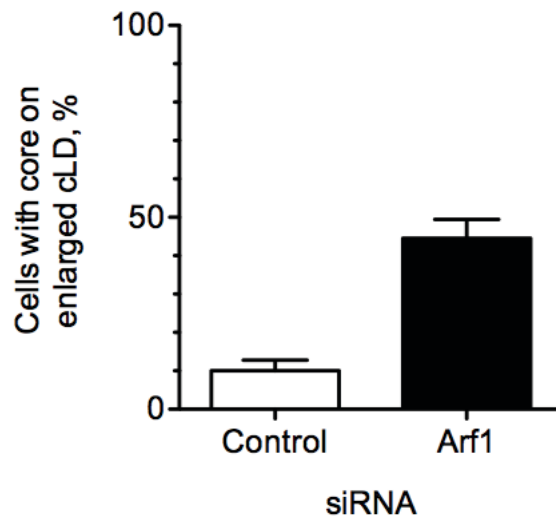


**Figure 6.2 Quantitation of Arf1 knockdown effect on HCV core and cLD in HCV-infected cells.**

Bar graph showing the percent of cells with normal or enriched localization of HCV core on the surface of enlarged cLDs. 72 infected cells treated with control or Arf1 siRNA were counted. The percent was calculated by dividing the cells showing the enrichment of core on enlarged cLDs by the total number of cells counted (results from two independent experiments).

differences between cell lines and HCV genotypes or strains, we next aimed to test if knockdown of Arf1 would reproduce the phenotype reported in FLRP1 cells.

Huh7.5 cells were infected with HCVcc-JFH1 for 48 h and then they were knocked down for Arf1 for 24 h before being evaluated by immunofluorescence imaging for HCV NS5A and cLDs. Infections treated with control siRNA showed dispersed pattern of NS5A and ADRP, as expected. Treatment with Arf1 siRNA resulted in ring-like structures of NS5A around enlarged cLDs, indicating that knockdown of Arf1 mimics the effect of Z390 on the cellular distribution of core and size of cLDs (**Figure 6.3-Figure 6.4**).

### **6.2.2 Knockdown of Arf1 inhibits cell-to-cell spread**

Knockdown of Arf1 reproduced the effect of Z390 or oleic acid on cellular distribution of HCV core and NS5A and on cLDs. Therefore, I next tested the effect of Arf1 knockdown on HCV cell-to-cell spread in co-culture assay.

Huh7.5 cells in 96-well plate were infected with HCVcc-JFH1 for 48 h, detached and reseeded in 24-well plate. 24 h later, cells were knocked down for Arf1 for 24 h before they were labeled and co-cultured with uninfected cells in the presence of HCV neutralizing serum. Transmission of HCV infection from Arf1-knocked down donor to naïve Huh7.5 cells was evaluated 24 h after co-culture by immunofluorescence imaging. In cells treated with non-targeting siRNA, the infection had spread from the HCV-infected and labeled (donor) cells to at least 20 adjacent unlabeled cells. In contrast, infection was limited to the donor or single adjacent cell when the donor cells were knocked down for Arf1 (**Figure 6.5**). Knockdown of Arf1 inhibited HCV cell-to-cell spread by 70% in three independent replicates (**Figure 6.6**).



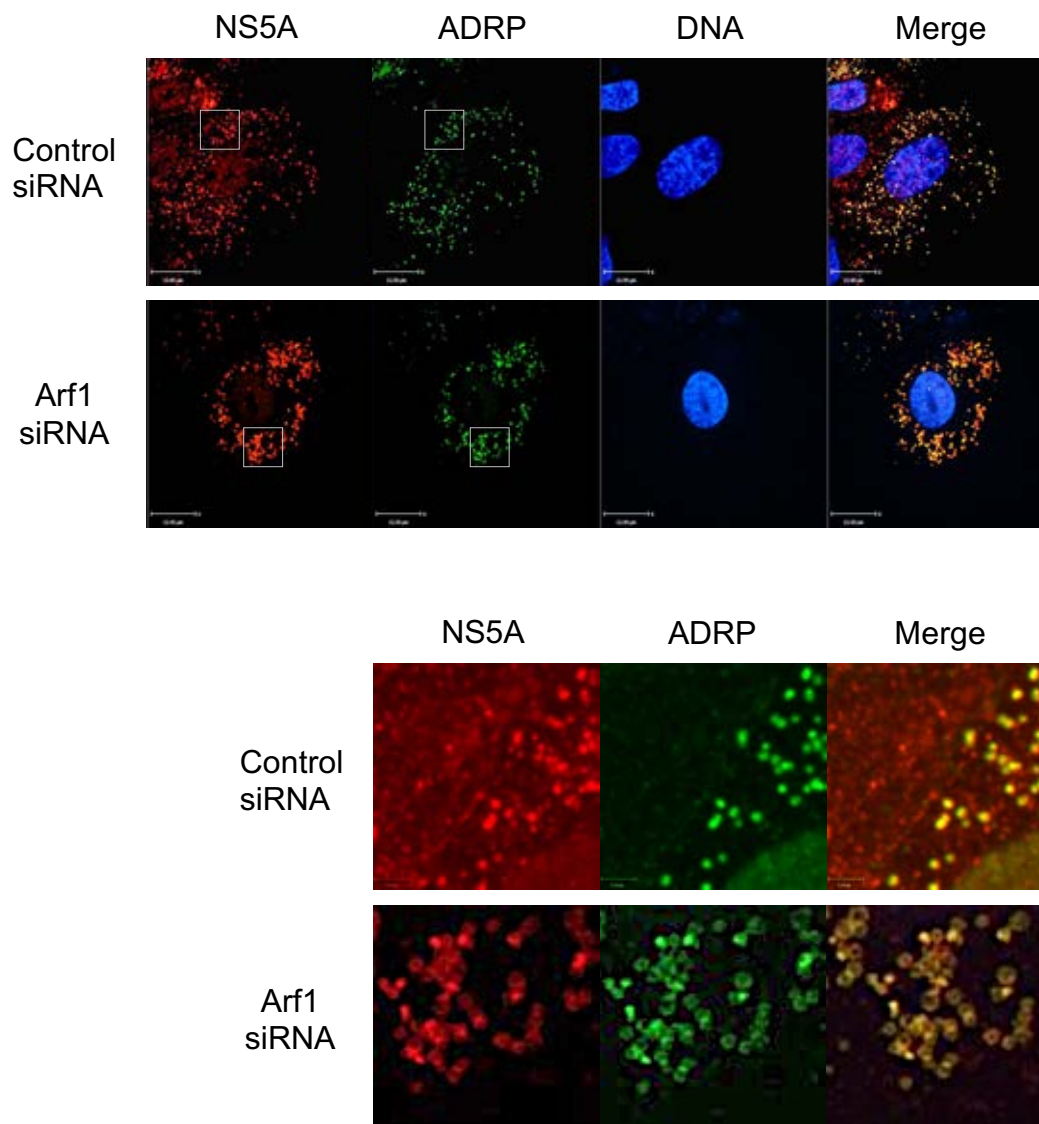


**Figure 6.3 Knockdown of Arf1 affects the distribution of HCV NS5A and cLD.**

Top, immunofluorescence micrographs showing HCV NS5A (red) or cLD (green) in HCV-infected cells treated with control or Arf1 siRNA at 60x magnification. Bottom, the areas indicated by the squares at the top showing magnification. Huh7.5 monolayers were infected with 0.01 infectious HCV cc (JFH1) virions per cell. Inocula were removed 4 h later and after 48 h, infected cells were treated with control or Arf1 siRNA for 24 h before processing for immunofluorescence for NS5A and evaluation by confocal microscopy (results from two independent experiments).

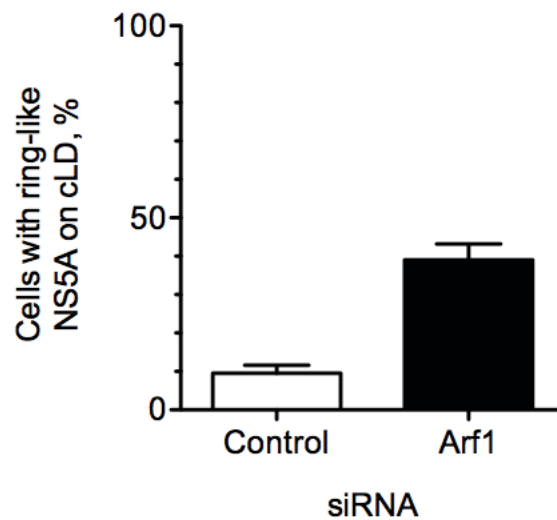


**Figure 6.4 Quantitation of Arf1 knockdown effect on HCV NS5A and cLD in HCV-infected cells.**

Bar graph showing the percent of cells with normal or enriched localization of HCV NS5A on the surface of enlarged cLDs 61 infected cells treated with control or Arf1 siRNA were counted. The percent was calculated by dividing the cells showing the ring-like structure of NS5A on enlarged cLDs by the total number of cells counted (results from two independent experiments).

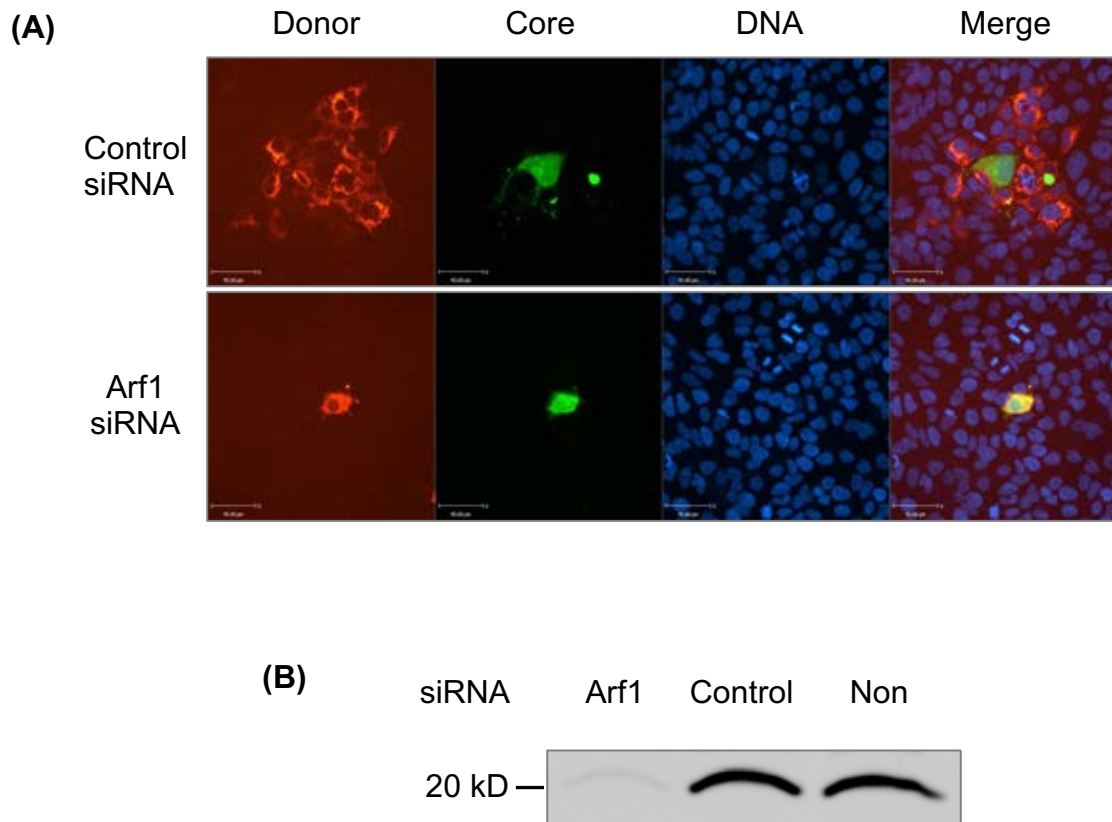


**Figure 6.5 Knockdown of Arf1 inhibits HCV cell-to-cell spread.**

**(A)** Immunofluorescence micrographs showing HCV-infected cells (red) and CFDA SE-labeled cells (green). Co-cultures treated with control or Arf1 siRNA. Huh7.5 monolayers were infected with 5 infectious HCV cc (JFH1) virions per cell. 48 h later, infected donor cells were treated with 50 nM control or Arf1 siRNA for 48 h before they were trypsinized, labeled with (CFDA SE), and co-cultured with uninfected cells at a ratio of 1 infected per 200 uninfected cells in the presence of 10% anti-HCV serum. Foci formation in the co-cultures was evaluated by immunofluorescence for core 24 h after co-seeding. **(B)** Western blot of Arf1 in cells treated with control or Arf1 siRNA or not (results from three independent experiments).

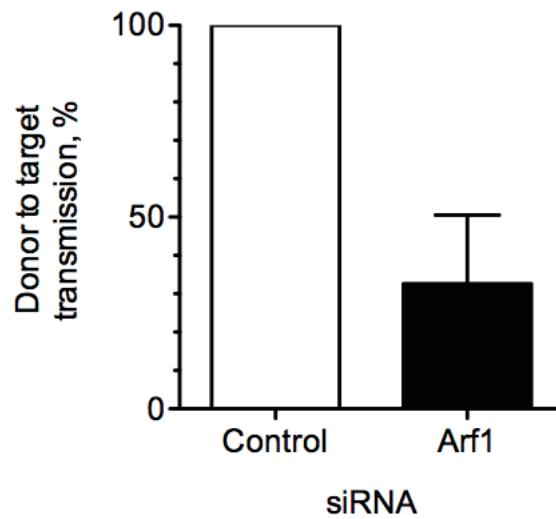


**Figure 6.6 Quantitation of Arf1 knockdown effect on HCV cell-to-cell spread.**

Bar graph showing the percent of HCV-infected and Arf1-knockdowned Huh7.5 cells transmitted the infection to adjacent uninfected cells. 42 donor cells were counted. The percent was calculated by dividing the donor cells that had transmitted the infection by the total number of cells counted (results from three independent experiments).

In addition to the reported effects of Arf1 knockdown on NS5A and cLDs, HCV RNA and infectivity were reduced by approximately 40% and 3-fold, respectively. Unfortunately, the report lacks critical details on the duration of knockdown before analysis or correction for cytotoxicity. Knockdown of Arf1 for 24 h after 48 h infection with HCVcc-JFH1 had no effect on the replication of HCV (**Figure 6.7**). Thus, the inhibition of cell-to-cell spread is not due to inhibition of HCV replication.

### **6.2.3 Arf1 non-cycling mutants enrich core and NS5A around enlarged cLD**

Knockdown of Arf1 reproduced the effect of Z390 on the cellular distribution of HCV proteins and cLDs and on the inhibition of cell-to-cell spread. Thus, Z390 could inhibit HCV cell-to-cell spread by targeting Arf1. Arf1 cycles between GDP or GTP-bound states. The binding of Arf1 to GTP and subsequent hydrolysis to GDP is required for the function of Arf1 in vesicular transport. Expression of Arf1 non-cycling mutants locked in the GDP or GTP states inhibit Arf1 cycling and consequently interfere with its localization and function. Z390 could inhibit Arf1 cycling. To test this model, I aimed at evaluating the cellular distribution of HCV core or NS5A and cLDs in infected cells expressing the Arf1 non-cycling mutants.

Huh7.5 cells were simultaneously knocked down for endogenous Arf1 and transfected with wild-type or non-cycling Arf1 mutants before co-culturing them with HCV infected cells that were not manipulated for Arf1 expression. The co-cultures were evaluated for expression and localization of HCV core, NS5A, or cLDs after two or three days. Huh7.5 cells were transfected with Arf1 wild-type or GDP (T31N) or GTP-locked (Q71L) mutants for 48 h and then they were co-cultured with HCVcc-JFH1 infected cells

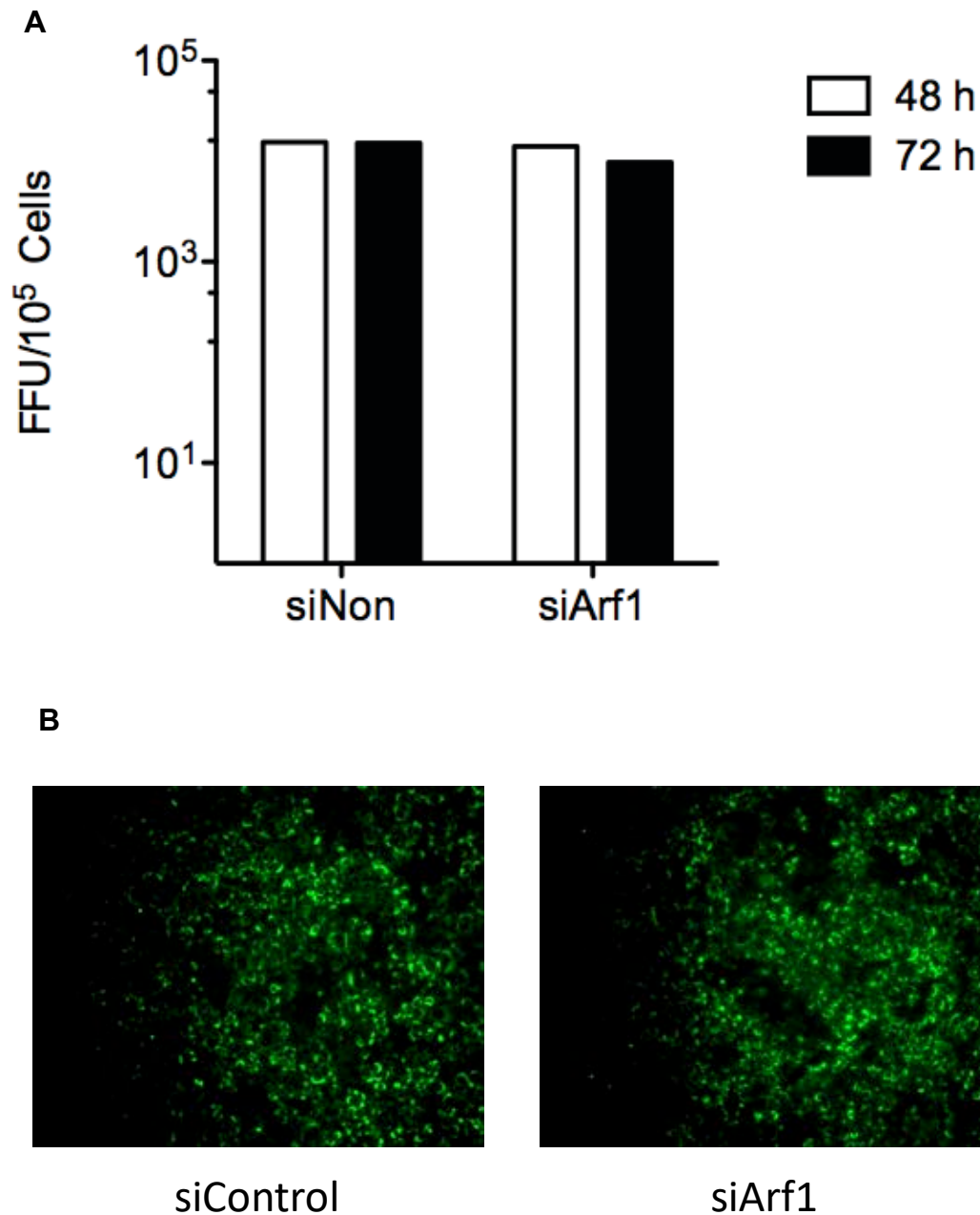


**Figure 6.7 Knockdown of Arf1 does not inhibit HCV replication in donor cells.**

**(A)** Bar graph showing the extracellular infectivity of HCV-infected and Arf1-knockdown cells. Huh7.5 cells were infected with HCVcc-JFH1 at an moi of 5 for 24 h before knocked down for Arf1. Twenty-four hours later, prior to the co-culture (48 h), or after (72 h), culture media were collected for infectivity titration. **(B)** Immunofluorescence micrograph showing HCV infected donor cells treated with siControl (left) or siArf1 (right) of the same infection in **(A)**. (results from one (A) or three (B) independent experiments)

for 48 or 72 h before processing for immunofluorescence (**Figure 6.8**). In wild-type Arf1 transfected cells, HCV core and cLDs were colocalized and dispersed. In cells expressing the GDP-locked, and to a lesser extent GTP-locked Arf1, core (**Figure 6.9-Figure 6.10**) or NS5A (**Figure 6.11-Figure 6.12**) was confined in ring-like structures around cLDs that were fewer and larger than in cells expressing wild-type Arf1.

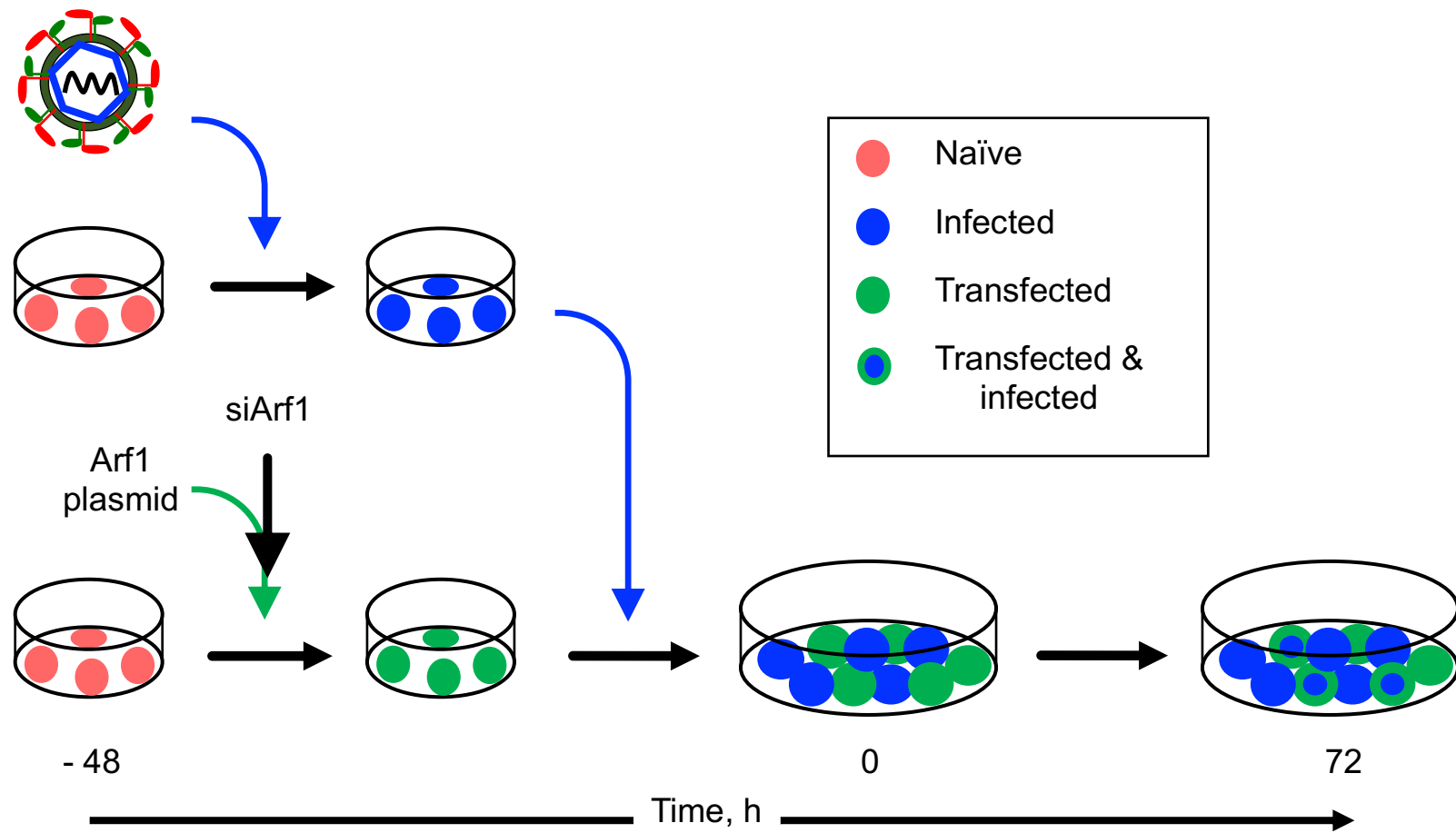


**Figure 6.8 Experiment design of the effect of Arf1 mutants on the localization of HCV core and NS5A and cLD.**

Huh7.5 cells were infected with 5 FFU/cell HCV-JFH1 or transfected with Arf1 plasmid. After 48 h, infected and transfected cells were resuspended and mixed 1:1 then they were seeded into new plates. Seventy-two hours later, monolayers were fixed and processed for immunofluorescence. Transfected cells were detected using anti-HA to label HA-tagged Arf1, while infected cells were detected using anti-core or anti-NS5A antibodies.



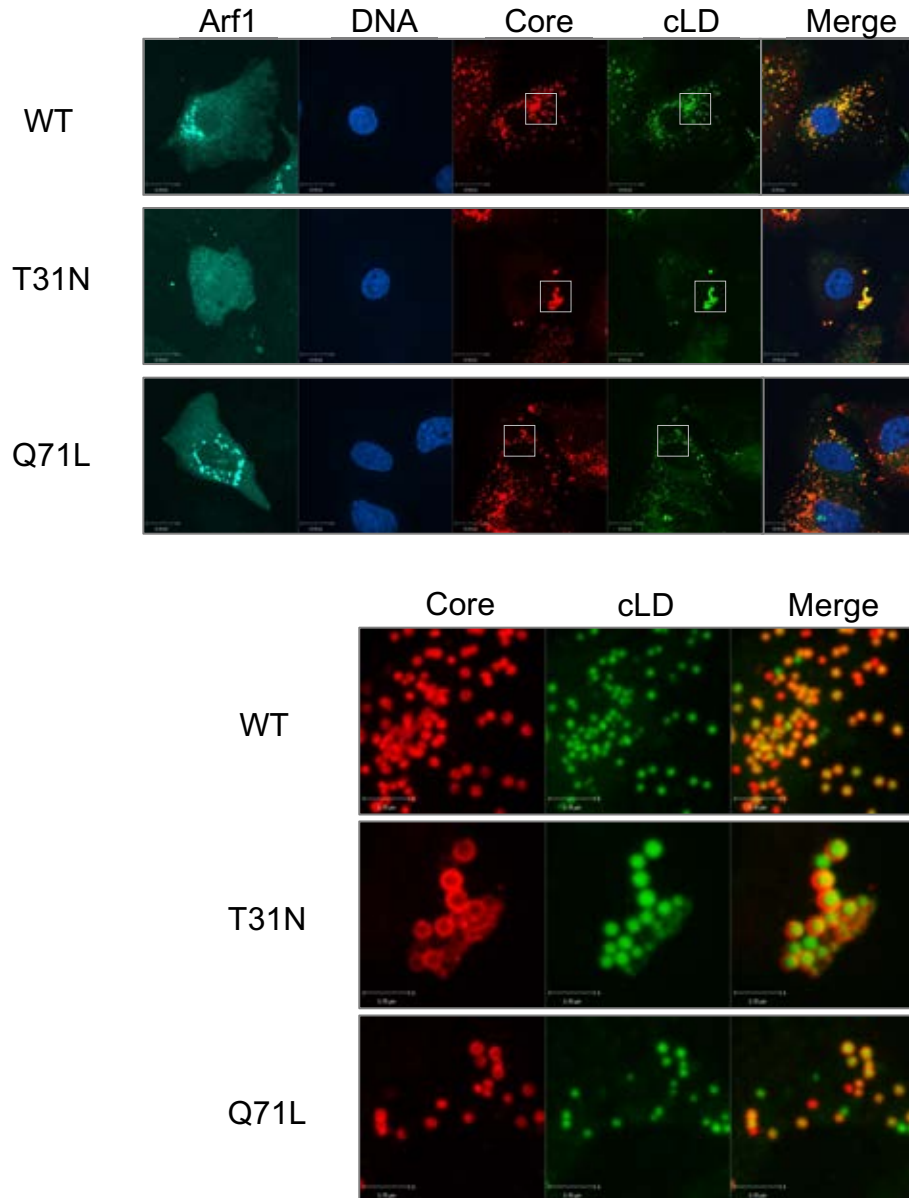


**Figure 6.9 Expression of non-cycling mutants of Arf1 affects the localization of HCV core and cLD.**

Immunofluorescence micrographs showing HCV core (red), Arf1 (cyan), and cLD (green) at 60x magnification. HCV-infected cells transfected with wild-type (top) or non-cycling mutants (middle and bottom). The areas indicated by the squares at the top showing magnification. Huh7.5 cells were co-transfected with 50 nM siRNA against endogenous Arf1 and plasmid DNA for expression of wild-type or non-cycling mutants Arf1. 24 h later, co-transfected cells were co-cultured with HCV-infected cells at ratio of 1:1 for two or three days before processing for immunofluorescence for core and evaluation by confocal microscopy (results from three independent experiments).

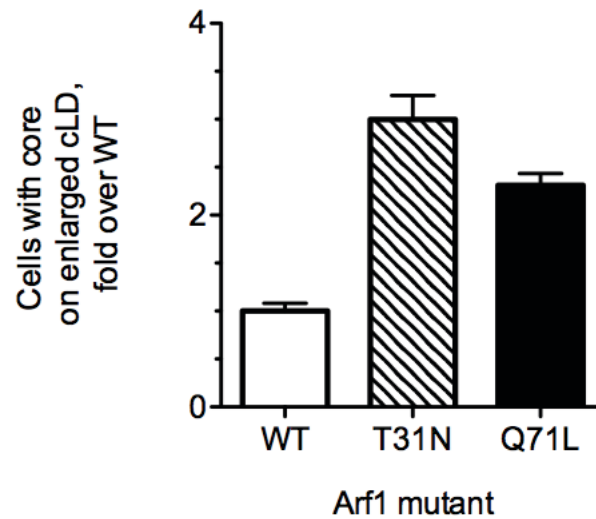


**Figure 6.10 Quantitation of localization of HCV core and cLD in the presence of non-cycling mutants of Arf1.**

Bar graph showing the fold difference of cells with enriched HCV core on the surface of enlarged cLDs. 31 infected cells, knockdowned for endogenous Arf1, and transfected with wild-type Arf1 or non-cycling mutants. The fold difference was calculated by dividing the cells showing the enriched core on enlarged cLDs of the mutants by that shown in the wild-type (results from three independent experiments).

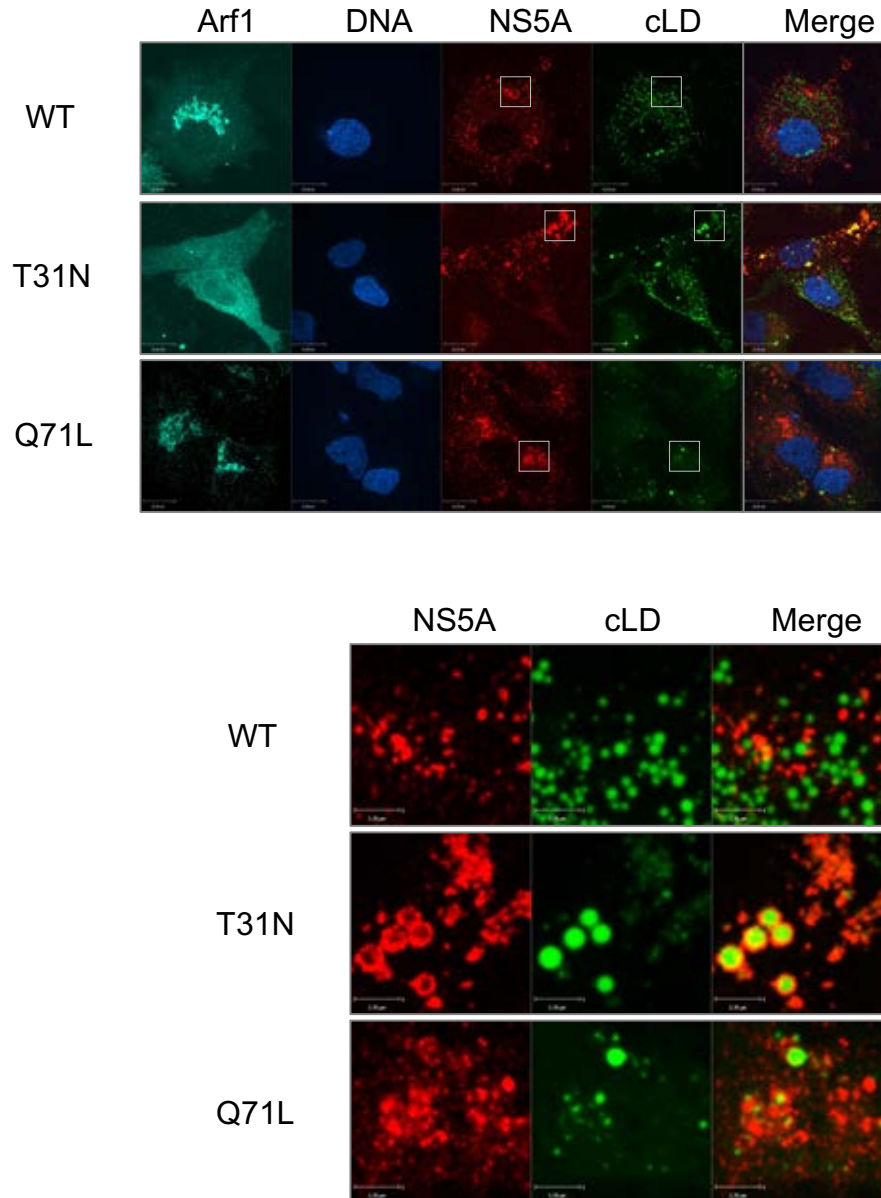


**Figure 6.11 Expression of non-cycling mutants of Arf1 affects localization of HCV NS5A and cLD.**

Immunofluorescence micrographs showing HCV NS5A (red), Arf1 (cyan), and cLD (green). Top, HCV-infected cells transfected with wild-type (top) or non-cycling mutants (middle and bottom) at 60x magnification. Bottom, the areas indicated by the squares at the top showing magnification. Huh7.5 cells were co-transfected with 50 nM siRNA against endogenous Arf1 and plasmid DNA for expression of wild-type or non-cycling mutants Arf1. Twenty-four hours later, co-transfected cells were co-cultured with HCV-infected cells at ratio of 1:1 for two or three days before processing for immunofluorescence for NS5A and evaluation by confocal microscopy (results from three independent experiments).

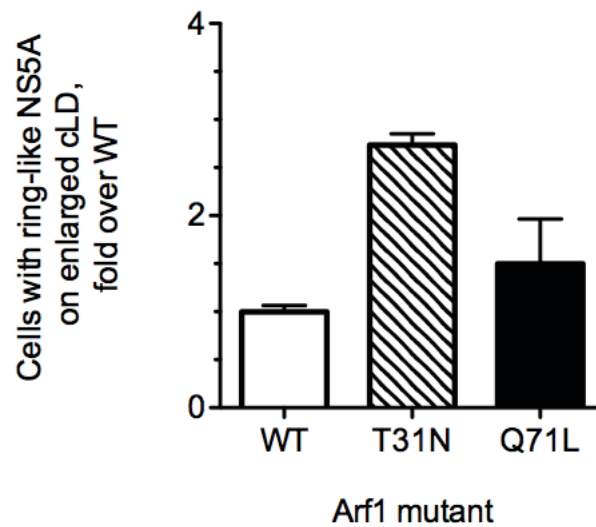


**Figure 6.12 Quantitation of non-cycling mutants of Arf1 affects localization of HCV NS5A and cLD.**

Bar graph showing the fold difference of cells with ring-like structures of HCV NS5A on the surface of enlarged cLDs. 34 infected cells, knockdowned for endogenous Arf1, and transfected with wild-type Arf1 or non-cycling mutants. The fold difference was calculated by dividing the cells showing the enriched NS5A on enlarged cLDs of the mutants by that shown in the wild-type (results from three independent experiments).

## **6.3 DISCUSSION**

### **6.3.1 Knockdown of Arf1 redistributed NS5A onto enlarged cLD**

Treatment of HCV infections by Z390 altered the level of core association of cLDs, redistributed NS5A from the ER onto the surface of cLDs, and affected the homeostasis of cLDs. Enrichment of core on the surface of cLDs has been associated with a defect in assembly. However, our analysis of the Z390 effect on HCV replication, which includes assembly, showed no difference between Z390 or vehicle-treated HCV infections. Thus, enrichment of core on cLDs was not due to defective assembly. Z390-induced enrichment of core on cLDs was associated with enlargement of cLDs. Testing the effect of Z390 on the homeostasis of cLDs in uninfected cells showed that Z390 inhibit synthesis of nascent cLDs while promoting the growth of mature ones. Thus, we concluded that Z390 effect on cLDs homeostasis resulted in the enrichment of core on cLDs. Z390 redistributed NS5A from the ER close to cLDs, onto the surface of enlarged and clustered cLDs. Although NS5A could only partially localized on the surface of cLDs, the majority is localized at the ER. siRNA knockdown of Arf1, or inhibition of its GEF GBF1 by small molecules in HCV infected cells, reversed the proportion of ER to cLD-bound NS5A and promoted the growth of mature cLDs. Thus, we proposed that Z390 could target Arf1 or its GEFs.

Huh7.5 cells were infected with HCVcc-JFH1 for 48 h, and then they were knocked down for Arf1 by siRNA for 24 h before immunostaining for NS5A and the cLDs marker ADRP. The effect of Arf1 knockdown on NS5A localization and cLDs homeostasis simulated the reported phenotype upon knockdown of Arf1 or inhibition of GBF1. Arf4 (Szul et al., 2007) and Arf5 (Claude et al., 1999), class II Arfs, are also substrates for

GBF1, while Arf3, class I Arf along with Arf1, and substrate of BIG2 GEF (Islam et al., 2007; H. W. Shin, Morinaga, Noda, & Nakayama, 2004), is not. Arf 1 and Arf3 share more than 96% sequence similarity (Moss & Vaughan, 1993) and could play a redundant role at Golgi complex (Boman et al., 1999; Cockcroft et al., 1994; Kanoh, Williger, & Exton, 1997). Thus, the phenotype obtained by inhibition of GBF1, which resembles that obtained by knockdown of Arf1, is specific for Arf1.

### **6.3.2 Knockdown of Arf1 affected cLD homeostasis and core distribution**

As an essential partner in HCV assembly, the effect of Z390 on the core prompted testing for NS5A. Similarly, the redistribution of NS5A upon knockdown of Arf1 mandated testing for the core. Huh7.5 cells were infected with HCVcc-JFH1 and knocked down for Arf1 as previously with NS5A then immunostained for the core. HCV core was still associated with homeostasis-altered cLDs, which were fewer but enlarged. Thus, knockdown of Arf1 mimicked the effect of Z390 on the distribution of NS5A and core and cLDs homeostasis.

### **6.3.3 Knockdown of Arf1 inhibit HCV cell-to-cell spread**

Knockdown of Arf1 in HCV infected cells reproduced the phenotype of Z390 and OA on the distribution of core and NS5A and cLDs homeostasis. Similarly, also, knockdown of Arf1 in the HCV donor cells 24 h before co-culture with uninfected cells inhibited the transmission of infection. It has been shown that Arf1 or GBF1 plays a role in HCV infection. siRNA knockdown of Arf1 in Huh7.5.1 or GBF1 for three days before infection with HCVcc-JFH1 for three days decreased HCV RNA by approximately 10-fold with 40% cell survival. However, knocked down of Arf1 reduces the relative infection of Huh7.5 cells with HCVcc-JFH1 as reported (Farhat et al., 2016; Goueslain et al., 2010)

and in our observation. In addition to ER-to-Golgi transport, Arf1 or Arf3 are involved in the maintenance of endosomal recycling of cell surface receptors such as TnfR (Kondo et al., 2012). Also, Arf1 is involved indirectly in the expression of occludin, a host factor required for HCV entry. HCV infection upregulates ADRP and occludin. Silencing of ADRP prevents the HCV-induced upregulation of occludin (Branche et al., 2016). Thus, Occludin upregulation in HCV infected cells is ADRP-dependent. ADRP associates with cLDs, and it is degraded upon dissociation. Expression of non-cycling mutants of Arf1 promotes dissociation and degradation of ADRP (Nakamura et al., 2004; N. Zhang, Yin, Zhou, Li, & Zhang, 2016). Arf1 upstream of ADRP regulates occludin expression. Thus, knockdown or Arf1 could reduce HCV infection by rendering cells non-susceptible to the infection by inoculation. Cell survival was analyzed in Huh7.5.1 infected HCV-Jc1FLAG2(p7-nsGluc2A) and not knocked down for Arf1 or GBF1 (L. Zhang et al., 2012). Knockdown of Arf1 (Matto et al., 2011) or GBF1 (Farhat et al., 2013; Goueslain et al., 2010) decreased HCV RNA by approximately 50%. Therefore, the role of Arf1 or GBF1 in HCV infections was assessed by infecting the cells after transfection. In our co-culture experiment, donor cells were infected first for 48 h (moi of 5), which results in a population of more than 90% infected donor cells, before transfection for 24 h before the co-culture. Infection of Huh7.5 cells with HCVcc-JFH1 at moi of 5 for 48 h produces one infectious virion per ten cells. Thus, even if knockdown of Arf1 48 h after infection would inhibit replication or production of infectious virions, the intracellular infectious virions before the transfection would enable at least one-tenth of the donor cells to transmit the infection to target adjacent cells. We co-culture 1 donor per 200 target cells for a total of  $2.0 \times 10^5$  cell per well in 24-well plate to obtain approximately 100 foci, which we found to be the

optimal number of well-dispersed foci comprised of 15-30 cells per focus. Thus, knockdown of Arf1 in HCV donor cells does not inhibit cell-to-cell spread in the co-culture assay by inhibiting intracellular infectivity before the co-culturing of donor and target cells. Infected donor cells could transmit HCV infection to target cells in a co-culture in as early as 3 h (Z. Liu & He, 2013). Thus, precluding any effect of Arf1 knockdown on intracellular infectivity after the beyond the 24 h silencing.

HCV virion exists as LVP containing several components of VLDL particles such as ApoA, ApoB, and ApoC. HCV envelope glycoproteins are glycosylated with complex glycans that are acquired by Golgi-residing enzymes. Therefore, it was suggested that HCV virions egress through the ER-to-Golgi transport pathway. Inhibition of VLDL synthesis or secretion also inhibits the release of HCV virions. Arf1 is a primary mediator of the ER-to-Golgi vesicular trafficking. Transmission of infection from donor to target cells could thus be inhibited due to interference to the ER-to-Golgi trafficking if infectious virions mediate the cell-to-cell spread. On the other hand, although Arf1 is the most studied and abundant of the Arf family (Popoff et al., 2011), functional redundancy among Arf isoforms has been demonstrated. Arf1-5 localize to the membrane when bound to GTP, while they are cytosolic when they are GDP-bound, except for Arf6, it is membrane bound in either GTP or GDP-bound form (Cavenagh et al., 1996). Depletion of individual or pairs combination of Arf1 and Arf3-5 in traffic between the ER and Golgi could not produce a discernible phenotype with knockdown of an individual Arf. However, double knockdown of pair combinations inhibited every step of the secretory pathway from ER to the plasma membrane through ERGIC, Golgi, and endosomes, regarding the integrity of the Golgi, recruitment of  $\beta$ COP, or traffic of the ts045-VSVG-GFP (Volpicelli-Daley, Li, Zhang, &



Kahn, 2005). Similarly, Arf1, or any of Arf3-5, was able to associate with, and support the formation of COPI vesicles in vitro. However, the addition of Arf1 displaces COPI-associated Arf3, suggesting the presence of competition (Popoff et al., 2011). In addition to the traffic, redundancy among Arfs in the integrity of the recycling endosomes has also been shown. Simultaneous knockdown of Arf1 and Arf3 induced tabulation of the recycling endosomes and inhibition of transferrin receptor recycling from the endosomes to the plasma membrane, while individual knockdown did not (Kondo et al., 2012). Thus, it is unlikely inhibition of HCV cell-to-cell spread upon knockdown of Arf1 in the donor cell was due to interference with the Arf1-mediated function in trafficking through the secretory pathway.

Arf1 facilitated the formation and maintenance of cLDs at REGIC and involved in the regulation of the lipid transfer proteins within Golgi. Association of Arf1 with cLDs was initially demonstrated in NIH3T3 cells after induction of cLDs formation by oleic acid (Nakamura et al., 2005). Subsequently, genome-wide RNA interference screen in *Drosophila* S2 cells (Beller et al., 2008; Guo et al., 2008) and proteomic profile of purified cLDs in CHO K2 cells, identified Arf1 and its coatmer components. Knockdown of Arf79F (*Drosophila* orthologue of mammalian Arf1) or either of seven of the eight COPI, but not COPII, components increased the lipid storage, manifested by fewer but larger cLDs (Beller et al., 2008). Similar phenotype had been obtained when Arf79F or its GEF garz were knocked down. Also, expression of Arf79F mutants, T31N (GDP-locked) or Q71L (GTP-bound), increased lipid storage, or lipolysis, respectively (Guo et al., 2008). In the proteomic study, Arf1 was identified with the proteins that are known to bind to cLDs such as ADRP and ATGL, whereas ArfGAP1 was identified among the proteins that were not

previously known to bind to cLDs. Arf1 and  $\beta$ COP were identified on cLDs fraction in the presence of GTP $\gamma$ S (non-hydrolyzable GTP) (Bartz, Li, et al., 2007). Arf1 is involved in the dissociation of ADRP from cLDs (Nakamura et al., 2004), while knockdown of GBF1 or expression of Arf1-T31N retains ADRP at the ERGIC or inhibits ATGL recruitment to cLDs, respectively, (Soni et al., 2009), leading to increased cellular lipid storage. ArfGAP1 is recruited, along with TIP47, in response to stimulation of cLDs formation by oleic acid, while it dissociates when lipolysis is stimulated by cAMP (Gannon et al., 2014). Arf1/COPI induces budding of 60-nm lipid droplets from intracellular cLDs (Wilfling et al., 2014) or reconstituted LD composed of TG and phospholipids, similar to that of the cLDs, and ArfGAP3 (Thiam et al., 2013), indicating simulation of the formation and excision of trafficking vesicles. Thus, an accumulating evidence of the involvement of Arf1 and its machinery components in the regulation of cLDs, compared to the redundancy among Arf isoforms in the secretory pathways, suggests that inhibition of HCV cell-to-cell spread by knockdown of Arf1 is likely due to the Arf1 regulatory functions in the homeostasis of cLDs.

Small GTPase, including Arf1, exist as GDP or GTP-bound, and with few exceptions, localizes in the cytosol or membranes, respectively. Guanine nucleotide exchange and hydrolysis are essential for Arf1 function in vesicular transport by allowing trafficking between the target and the destination membranes. Thus, interference to the cycling of Arf1 could also mimic the effect of Arf1 knockdown on the accumulation of HCV core and redistribution of NS5A onto cLDs. Huh7.5 cells were transfected with plasmid encoding Arf1-WT, or the mutants T31N or Q71L, which are held bound to GDP or GTP, respectively. 48 h later, transfected cells were mixed with an equal number of HCV-

infected cells, and after 48 h, co-cultured cells were processed for immunofluorescence. Core accumulated on enlarged cLD and NS5A redistributed exclusively onto cLDs, similar to the phenotype obtained in HCV-infected cells treated Z390 or oleic acid, indicating that inhibition of the nucleotide exchange or hydrolysis is sufficient to reproduce the phenotype obtained with knockdown of Arf1. Thus, Z390 could inhibit either the GDP exchange or the GTP hydrolysis. The phenotype of cLDs and HCV core and NS5A were presented sufficiently in T31N, compared to the Q71L, despite that inhibition of the GDP exchange in T31N is more efficient than the inhibition of hydrolysis in Q71L. The phenotype obtained with Q71L could be in the middle between that of the WT and T31N. The higher level of cytotoxicity noticed with Q71L could have prevented the extinct of phenotype simulation. Arf1-Q71L appears to induce an equivalent level of effect to that of Arf1-T31N with a lower level of protein expression (Wonderlich et al., 2011; N. Zhang et al., 2016). Thus, it can be speculated that both non-cycling mutants could reproduce the phenotype. Simultaneous knockdown of endogenous Arf1 during the transfection of the different Arf1 mutants increased the frequency of the observed phenotypes.

## 6.4 SUMMARY

We previously showed that treatment of HCV infected cells with Z390 induced enrichment of core and redistributed NS5A into the surface of enlarged cLDs. Treatment of uninfected cells with Z390 altered the homeostasis of the cLDs by decreasing the number of small cLDs while increasing the size of the mature cLDs. Thus, we concluded that the Z390-induced effect on the homeostasis of cLDs altered the distribution of core and NS5A in respect to the cLDs. Redistribution of NS5A from the ER into the surface of enlarged cLDs in a ring-like structures was reported by treatment of HCV-infected cell with GBF1 inhibitors BFA or GCA or knockdown of Arf1. Thus, we hypothesize that Z390 could alter the cLDs homeostasis by interference with Arf1.

We showed that genetic interference of Arf1 reproduced the phenotype of Z390 effect on the distribution of HCV core and NS5A and cLDs homeostasis and inhibited the HCV cell-to-cell spread. We concluded previously that Z390 effect on cLDs had induced the accumulation of core, and redistribution of NS5A onto the cLDs, leading to the inhibition of HCV cell-to-cell spread. This finding was supported by obtaining a similar effect on the core, NS5A, and cell-to-cell spread when infected cells were treated with oleic acid. Knockdown of Arf1 or expression of the mutant T31N, and to lesser extent Q71L, affected cLDs and distribution of core and NS5A in a similar pattern to that obtained with Z390 or oleic acid. Thus, Z390 could inhibit HCV cell-to-cell spread by interfering with either GDP exchange or GTP hydrolysis of Arf1, leading to the identification of Arf1 as a host factor involved in HCV cell-to-cell spread.

## CHAPTER SEVEN: DISCUSSION AND FUTURE DIRECTIONS

### 7.1 IDENTIFICATION OF A SMALL MOLECULE INHIBITOR OF HCV CELL-TO-CELL SPREAD

One of the main research activities in Dr. Schang lab is chemical biology applied to virology. Small molecules are used as probes to study the different steps of viral replication. The discovery and characterization of broad-spectrum fusion inhibitor with a novel mechanism of action, RAFI (St Vincent et al., 2010) as well as the characterization of EGCG (Colpitts & Schang, 2014) are successful examples of this approach. Another is the discovery of a broad-spectrum attachment inhibitor. In this thesis, I describe my own project, which also used chemical biology to study a viral life cycle. Nine selected small biologically active small molecule derivatives of 1,5-disubstituted uracil (Novikov et al., 2010) were tested for inhibition of replication for several viruses in cell culture. Of the nine small molecules tested against six viruses of different structures and which use different replication strategies, two were active, and only against HCV. Two new derivatives showed similar activity, also against HCV only, suggesting that this scaffold could produce HCV specific inhibition. A structure-activity-relationship study led to the synthesis of 64 derivatives, 21 of which inhibited HCV foci formation with different selectivities ( $EC_{50}$  1.1-40.7  $\mu$ M, SI, 1.5-45). They also had different solubilities. Z390 displayed the best combination of potency, selectivity, and solubility profile and was used in all subsequent experiments.

The specificity of the tested small molecules for HCV indicated that the HCV replication cycle includes a Z390 sensitive step that is not shared with other viruses. I

thus pursued the identification of the mechanism of inhibition of HCV foci formation. Surprisingly, Z390 did not inhibit single-step replication of HCV. In multi-step replication assays, such as foci formation, infection must spread from infected to uninfected cells, which is not required in single-step replication studies, all cells are infected at the initial time. Thus, I focused on the mechanisms of HCV infection spread. Mounting evidence show that HCV also spreads by cell-to-cell transmission without the release of cell-free virions into the extracellular space. The morphological characteristics of HCV distribution in the liver biopsies of infected individuals is characterized by focal spread, not generalized dissemination (M. Chang et al., 2000; Ming Chang et al., 2003; Gosalvez et al., 1998). HCV infected individuals cannot control the spread of the infection despite the capacity to mount strong neutralizing antibodies responses whereas antibodies confer protection by passive immunization in chimpanzee (Morin et al., 2012) or humanized mice liver (de Jong et al., 2014), and block infectivity in cell culture (Farci, Shimoda, et al., 1996). I analyzed thus whether Z390 inhibit direct HCV spread. Z390 did not inhibit infectivity of cell-free HCV virions or the permissivity of cells to HCV infection. Z390 could thus inhibit direct cell-to-cell spread. I tested if Z390 inhibits transmission from donor to target cells in the presence of HCV neutralizing antibodies. Z390 did so. I further showed that Z390 does not affect affected a virus that depends on cLDs for replication but spreads by cell lysis or a virus that spreads by cell-to-cell spread without the involvement of cLDs.

I concluded that Z390 inhibits HCV cell-to-cell spread based on the comprehensive interpretation of several assays addressing several different mechanisms that contribute to spread, virions infectivity and permissiveness of the cells yet to be infected. Either candidate agents have been applied to the co-culture throughout the assays, which

precludes the identification of the steps inhibiting donor cells prior to the co-culture (Al Olaby et al., 2014; Barretto et al., 2014). Instead, I knocked down the test protein in donor cells prior to co-culture. The current prototype strains of each genotype are chimeras containing the minimum set of proteins from JFH-1 (subtype 2a) required to replicate HCV RNA (Gottwein et al., 2009). All studies rely on the main receptors required for entry of cell-free virions. However, they vary in their efficiency for cell-to-cell spread, which could inversely correlated to the efficiency of infectious virions released (Catanese, Loureiro, et al., 2013). Thus, a subset of the receptors required for direct entry of cell-free virions is also involved in direct cell-to-cell spread. Thus far, no report yet of small molecules inhibitor specific for HCV cell-to-cell has been published. Therefore, Z390 is a valuable probe for the characterization of the mechanisms involved in direct cell-to-cell transmission. This characterization revealed a novel phenotype involving a change in the intracellular distribution of HCV proteins and homeostasis of cLDs as a determinant involved HCV cell-to-cell spread. HCV was enriched on the cLDs and redistribution of NS5A from the ER close to cLDs to the surface of cLDs. Z390 reduced the number and increased the size of mature cLDs, while inhibiting the formation.

## **7.2 HCV SPREADS PREFERENTIALLY BY DIRECT CELL-TO-CELL TRANSMISSION**

I identified a novel scaffold for small molecules that selectively inhibit HCV infection. Derivatives of this scaffold inhibited HCV foci formation without affecting replication, virion infectivity, or cell permissiveness. Inhibition was observed only in multiple-step HCV replication assays, which requires spread of infection, and not in single-step replication assays, which do not need spread of infection. Several derivatives of the main scaffold including the optimized molecule Z390 inhibited infection spread. The spread of HCV infection is characterized by focal and distant spread resulting in foci and secondary infections. The addition of neutralizing antibodies prevents secondary infections but not foci formation. Thus, I observe that Z390 inhibit the direct HCV cell-to-cell transmission in a co-culture of HCV infected and uninfected cells in the presence of neutralizing antibodies. HCV cell-to-cell spread has been proposed to be among the principal mechanisms by which HCV evade immune response, and thereby maintain persistent infection (Di Lorenzo, Angus, & Patel, 2011; T. J. Liang, 2013). Evidence for HCV spread by cell-to-cell spread has been found in vivo and in culture, but whether HCV spreads preferentially by cell-free virions or by cell-to-cell has not been evaluated. Two different assays were designed to answer this question. Two different assays were designed to answer this question. The first was monitoring infection spread across a permeable membrane with pores large enough to allow virions to pass through it. Spread of infection among the cells in the insert results from both cell-free and cell-to-cell spread. Infection of the cells in well underneath results from cell-free virions. HCV spread was compared to that of two viruses known to spread by direct cell-to-cell transmission (RSV) (Huong et



al., 2016) or by cell-free virions (Zika virus) (Chan et al., 2016). RSV spread across cells in the insert only, whereas Zika virus spread almost equally to cells in both compartments. HCV also spread to cells in both compartments, but much faster across cells in the insert, reaching approximately 90% infection in 3 days compared to ~10% of the cells in the well, HCV thus preferentially spreads by direct cell-to-cell spread.

I also monitored the persistence of infection passages by cell-free or cell-associated HCV by successive dilutions and sub-cultures. Cell-free infection was started by 1,000 infectious HCV virions. Cell-to-cell infection started by co-culturing 200 infected HCV with uninfected  $2 \times 10^5$  cells, 1/5th of the number of virions because a single infectious virion infects single cell, whereas a single infected cell contacts directly approximately 5 cells. The cell-associated infectivity was passaged in the presence of neutralizing antibodies, such that cell-free virions are neutralized. RSV and Zika virus were also used as a control for cell-to-cell or cell-free spread, respectively. The initial infections spread similarly for all three viruses' protocols. After four diluted subcultures, however, Zika virus had spread equally in both protocols. RSV infections persisted only by cell-associated passaging. HCV also persisted only by cell-associated passaging, although spread better than RSV. HCV thus preferentially spread by direct cell-to-cell transmission in this protocol. Collectively, I showed that HCV direct cell-to-cell spread is the preferential and the more efficient mechanism of HCV spread.

In addition to transmission by cell-free virions or by direct cell-to-cell spread, transfer of viral genomes between cells via exosomes has been suggested as a potential mechanism of spread of HCV infection. It was debated whether this exosome-mediated transmission was a cell-free or direct cell-to-cell mechanism. Exosomes are cell-derived

vesicles that originate from multivesicular bodies (MVBs), ranging from 40–150 nm in size and are released by most cell types. Exosome vesicles are secreted into blood circulation, urine, and other body fluids (Y. Lee, El Andaloussi, & Wood, 2012). Exosomes can modulate signal transduction, antigen presentation to T-cells, and transmission of genetic material between cells (Thery, Zitvogel, & Amigorena, 2002). Exosomes mediate several functions related to cell-to-cell communication, transfer of molecules, genomic materials, or functional proteins (Momen-Heravi et al., 2012). Exosomes recovered from the culture media of HCV infected cells could transfer infection to naïve cells. HCV envelope glycoproteins, core, and RNA were detected in exosome preparations from culture media of HCV infected cells (Bukong et al., 2014; Y. Lee et al., 2012; Ramakrishnaiah et al., 2013). Replication-competent sub-genomic replicons, which only produce viral RNA and replication but structural proteins of virions, can be transferred via exosomes. Exosome failed to transfer infection sub-genomic replicon from transfected cells plated on an insert permeable to exosome to cells underneath the insert. Therefore, exosome-mediated transmission of HCV requires direct cell-cell contact between donor and target cells (Longatti et al., 2015). The earlier studies showing exosome-mediated HCV transmission by preparation of exosomes from culture media may have had HCV virions contamination. Exosomes overlap in size and density with HCV virions (Thery et al., 2002; Wakita et al., 2005). Exosome-mediated transmission of HCV infection may be considered as a cell-mediated mechanism of transmission. Interestingly, several members of Arf family contribute in the exosome release and internalization. For example, treatment of HUVEC cells with brefeldin (BFA) inhibited the release of TNFR1 (type 1 tumor necrosis factor receptor) exosome vesicles in a BIG2, Arf1, and Arf3-dependent mechanism (Islam et al.,

2008). Arf6, on the other hand, participates in exosome internalization. Upon internalization, exosomes fuse with endosome membrane in acidic environment to deliver their contents (van der Goot & Gruenberg, 2006). Fusion requires the presence of 30% fusogenic phospholipids (Kobayashi et al., 2002), which are produced by phospholipase D2 (PLD2) (Blackwood et al., 1997) which itself can be carried within the incoming exosomes. PLD2 is activated by Arf6 (Subra et al., 2010). Moreover, exosomes also are involved in lipid metabolism and trafficking (Record, Poirot, & Silvente-Poirot, 2014). For example, exosomes transfer cholesterol from activated CD4<sup>+</sup> T cells to monocyte lipid droplets in an in vitro model of atherosclerosis (Zakharova, Svetlova, & Fomina, 2007). Exosome-mediated HCV transmission involved in HCV cell-to-cell spread, the mechanism could also have a link to the lipid metabolism and trafficking functions of the Arf family of proteins.

The HCV replication cycle has been hard to characterize as a result of the lack of experimental models. It took nearly a decade for a first cell culture HCV replication model to be developed (V. Lohmann et al., 1999). The first cell culture model that recapitulates the entire replication cycle of HCV was developed even later (Lindenbach et al., 2005; Wakita et al., 2005). The development of HCV models drove the characterization of every step in the HCV replication cycle, the mechanisms related to immune responses and pathogenicity, and for HCV antiviral agents (Catanese & Dorner, 2015; V. Lohmann & Bartenschlager, 2014). However, the direct cell-to-cell spread of HCV has not been as well studied as other replication studies. In fact, direct cell-to-cell spread was not recognized until recently. HCV infection persists and continues to spread for decades

despite the presence of neutralizing antibodies, which sometime are even cross-neutralizing to other HCV genotypes (Ball, Tarr, & McKeating, 2014).

I showed that cell-to-cell spread is likely the primary mechanism of infection transmission. I showed using two assays that cell-to-cell spread more efficient than spread by cell-free virions. Different HCV genotypes or strains could vary in their foci formation efficiency or assembly and release and spread by cell-free. For example, JFH-1 strain forms large size foci, whereas Jc1 strain forms smaller foci and releases more virions resulting in more secondary infections (Shavinskaya et al., 2007b). The assays designed here could be used to evaluate the strain differences between strains direct cell-to-cell spread versus cell-free virions spread. These differences could in turn reveal the viral factors involved in the preference spread. In summary, I showed that HCVcc-JFH1 use direct cell-to-cell transmission as the primary mechanism of spread.

### 7.3 THE ROLE OF CLDS HOMEOSTASIS IN CELL-TO-CELL SPREAD

Small molecules with a novel scaffold inhibited HCV foci formation. Inhibition was specific for HCV. An optimized derivative, Z390, has a unique mechanism of action, inhibiting the direct HCV cell-to-cell spread. By two different assays, HCV spread preferentially by direct cell-to-cell transmission over cell-free virion which was more efficient than that by cell-free transmission. Therefore, I was interested in determining the Z390 mechanism of inhibition. Evaluating HCV genome, protein expression, or certain essential host factors, would not be informative, as HCV replication is not affected in the presence of Z390. High-resolution microscopic imaging was deemed an appropriate approach to build hypothesis about the mechanisms of action of Z390. Immunofluorescence imaging revealed a mannered effect HCV core subcellular distribution. Core signal was localized to ring-like structures condensed at a juxtanuclear area. These spherical rings were localized to cLDs, as expected. NS5A, along with core is essential for the assembly of HCV virions. Immunofluorescence imaging of NS5A showed that NS5A was also redistributed from the normal speckle-like structures throughout the ER near cLDs to the surface of cLDs. Z390 also affected cLDs, resulting in fewer but larger and more homogeneously sized cLDs.

Z390 altered the phenotype of the localization of HCV proteins and that of a cellular organelle critical for the HCV virions assembly, cLDs. Z390 had no effect on any other step of the replication cycle than cell-to-cell spread including assembly. Accumulation of core on the surface of cLDs could result from inhibition of core mobilization into the assembling virions, thereby inhibiting assembly. HCV variants defective in assembly due to core mutation (Counihan et al., 2011) or p7 (Gentsch et al., 2013) protein had this phenotype, for example core also result in aberrant accumulation of cLDs in infected or

core-expressing cells. Core expression stimulates accumulation of cLDs by inducing lipogenesis and decreasing the turnover of neutral lipids, by modulating the lipogenic transcription factors SREBP (Waris et al., 2007), RXR $\alpha$  (T. Tsutsumi et al., 2002), PPAR $\alpha$ , and Par (de Gottardi et al., 2006). Core also modulates lipid metabolism by direct interactions with host factors on the surface of cLDs, such as ATGL. This interaction results in the release of free fatty acid (FFA) and decrease cLDs size (Camus et al., 2014). Thus, an increased accumulation of core on cLDs could have resulted in larger cLDs or Z390 could have an effect on cLDs size, which then leads to the accumulation of core. I then tested the effect of Z390 on cLDs in uninfected cells. Z390 induced accumulation of larger size cLDs and depletion of small size cLDs. Z390 thus alters somehow the cLDs homeostasis, which in turn modifies core and NS5A distribution. Binding of only core and NS5A to cLDs, via their cLD-binding domain, is essential for HCV productive infection. Consistently, Z390 had no effect on the localization of NS3, which has no cLD-binding domain. I propose that the alteration to cLDs homeostasis may participate in the mechanism of inhibition of HCV cell-to-cell spread. Enrichment of mature cLDs could inhibit cell-to-cell spread via modification of the distribution of core and NS5A. I thus tested the localization of ADRP. ADRP is a major cLD-associated protein, which is involved in the cLDs growth via inhibiting the lipase ATGL access to the surface of cLDs (Listenberger et al., 2007). ADRP association with cLDs is directly correlated with enrichment in mature cLDs. Z390 increases the level of ADRP on the surface of cLDs in infected and uninfected cells. Z390 could thus interfere with regulatory mechanisms that control the association or displacement of ADRP from cLDs. Z390 prevented core from displacing ADRP from the surface of cLDs, displacement which normally occurs during

HCVcc-JFH1 infection (Boulant et al., 2008; Sato et al., 2006; N. Zhang et al., 2016). cLD association with both ADRP and core could result in a synergistic effect on cLDs growth. ADRP association with cLDs regulates HCV RNA cLDs regulates HCV RNA replication and assembly. Knockdown of ADRP reduced RNA replication by 70% in multiple-step replication cycle, while increasing the extracellular infectivity by 5-fold. It could also result from a reciprocal level of cLDs with ADRP or TIP47 on cLDs. Knockdown of ADRP allowed more TIP47 to accumulate on cLDs (Branche et al., 2016). Knockdown of ADRP allowed more TIP47 to associate with cLDs, thereby enhancing assembly. It could thus be speculated that increase accumulation of ADRP could lead to the dissociation of host factors that restrict the association or promote the assembly, respectively. This concept of cLDs protein crowding as a regulator of the association and displacement of protein to surfaces of cLDs (Kory, Thiam, Farese, & Walther, 2015) might not be entirely accurate. First, addition of oleic acid induce translocation of TIP47 into cLDs, both mature and nascent (Ohsaki, Maeda, et al., 2006; Skinner et al., 2009; Wolins et al., 2005; Wolins, Rubin, & Brasaemle, 2001), and TIP47 translocation upon stimulation with oleic acid did not affect the level of ADRP (Ohsaki, Maeda, et al., 2006; Vogt et al., 2013b; Wolins et al., 2005). Translocation of TIP47 to cLDs is controlled by the metabolic lipid status in the cell. Addition of oleic acid drives the translocation of TIP47 to cLDs, whereas stimulation of lipolysis drives the dissociation (Skinner et al., 2009). Shuttling of TIP47 between cytosol, ER, and cLDs is subject to many other complex regulatory mechanisms than the reciprocal localization with ADRP on cLDs. TIP47 is under the control of species and of the localization of lipids and of the intracellular trafficking pathways. Addition of oleic acid stimulates TIP47 to translocate from the cytosol to the ER or cLDs to promote synthesis

of nascent or growth of mature cLDs, respectively. Concurrent addition of oleic acid and  $\text{AlF}_4^-$  (tetrafluoroaluminate), an inhibitor of trafficking pathways including between ER and cLDs, prevents TIP47 translocation to the cLDs. Stimulation of lipolysis slightly induced TIP47 localization to cLDs. Concurrent stimulation of lipolysis and inhibition of trafficking by  $\text{AlF}_4^-$  results in more TIP47 localizing to clads, suggesting that TIP47 shuttles between cLDs and ER during lipolysis. The rate of shuttling between ER and cLDs may result from the level of DAG on either membrane. Inhibition of DAG lipase during lipolysis accumulates DAG in cLDs and increased TIP47 on cLDs. Exogenous permeable DAG localizes to the ER and induces enrichment of TIP47 at ER (Skinner et al., 2009). Collectively, the metabolic status of cLDs and the intracellular trafficking functions are critical regulators of the association or displacement of proteins to cLDs. TIP47 enrichment of cLDs upon knockdown of ADRP could result from the action of lipases, inhibited by ADRP on cLDs, interference of trafficking, or most likely both (Skinner et al., 2009). Accumulation of ADRP on cLDs and inhibition of TIP47 translocation during oleic acid loading by Z390 mimics the effects of  $\text{AlF}_4^-$ . Z390 could thus increase ADRP on cLDs and inhibit translocation of TIP47 to them by interfering with intracellular trafficking functions. Z390 results in shift toward inhibition of nascent and the accumulation of mature cLDs, and inhibition of cell-to-cell spread. Treatment with oleic acid altered the distribution and the homeostasis of cLDs similarly to Z390 and also resulted in the inhibition of direct cell-to-cell spread. The increasing size of existing mature cLDs with increased levels of core could have increased the surface area available for assembly, and thereby rescued any assembly effect resulting from the decrease in the total number of cLDs due to the inhibition of de novo nascent cLDs synthesis. Assembly takes place



at mature cLDs, which tend to localize near the nucleus, rather than at the nascent cLDs which mostly scattered throughout cytoplasm. Live imaging of core and cLDs showed that core accumulates first stationary on juxtanuclear mature cLDs, and only then motile core puncta originating from juxtanuclear cLDs appear likely representing virions (Counihan et al., 2011).

The link between the life cycle of HCV and cellular lipid metabolism is well-established. Nearly every step of the HCV replication cycle involves factors which participate also in lipid metabolism. Host cell factors involved in lipid metabolism play important roles in entry, replication, assembly, and release of HCV. HCV utilizes the LDL receptor for the initial attachment during entry, lipid membranes for replication, cLDs for assembly, and the VLDL assembly and secretion pathways for egress (Filipe & McLauchlan, 2015; Popescu et al., 2014). Nonetheless, the roles of lipid metabolism in cell-to-cell spread, if any, remaining mostly unknown. SR-BI and NPC1L1, which are involved in lipid transfer, were proposed to participate in HCV cell-to-cell spread, although they may have been “false positives” actually involved in entry of cell-free virions.

HCV infection increases the size of existing mature, and the number of nascent, cLDs. HCV activate transcription factors that stimulate the transcription of lipogenesis and inhibits expression of lipolysis genes. De novo cLDs synthesis is required for optimal replication and spread. Inhibition of cLDs synthesis inhibits HCV replication and production of infectious virions (Camus et al., 2013; Herker et al., 2010). HCV replication is inhibited by global inhibition resulting in the depletion of most cellular pool of cLDs. Z390 affected cLDs differentially, promoting mature large cLDs while inhibiting the existing mature cLDs while inhibited synthesis of the nascent cLDs. Treatment of Huh7.5

cells with 40  $\mu$ M for 1 h before stimulation with 0.5 mM OA in the presence of Z390 for 3 h inhibited the translocation of TIP47 into cLDs and decreased the number of nascent cLDs. Inhibition of HCV cell-to-cell spread by inhibition of formation of nascent cLDs indicates that HCV cell-to-cell spread involves trafficking. Inhibition of nascent cLDs synthesis resulted from TIP47 translocation from the cytosol to the ER sites of nascent cLDs synthesis. The growth of existing mature cLDs may have been fostered by the inhibition of dissociation of ADRP from cLDs. From the phenotype, resulting from Z390 treatment appears to be a determinant factor in HCV cell-to-cell spread. This identification of cLDs homeostasis as a determinant factor in HCV cell-to-cell spread has several implications. It emphasizes the tight association of HCV life cycle and hepatic lipid metabolism, which has been researched extensively, particularly in relationship assembly and release, which rely on cLDs and lipoprotein secretion. Second, if direct cell-to-cell spread is inhibited while the release of infectious virions is not, then there is a separate mechanism for cell-to-cell spread separated from the release of cell-free infectious virions. Conversely, inhibition of release with naringenin did not affect direct cell-to-cell spread as shown using the release inhibitor (Barretto et al., 2014). The involvement of cLDs homeostasis in direct cell-to-cell could be to control spread of HCV infection in the liver. Encouragingly targeting HCV entry receptors which also played roles in direct cell-to-cell spread is in preclinical (e.g., CD81, CLDN1, NPC1L1) or clinical development (e.g., SR-BI and EGFR) (Qian, Zhu, Zhao, & Qi, 2016; Zeisel, Crouchet, Baumert, & Schuster, 2015). Inhibition of synthesis of nascent cLDs could have an additional advantage. HCV induces accumulation of cLDs in infected cells leading to steatosis, which is one of the

important complications. Concurrent inhibition of nascent cLDs synthesis and the spread of infection could thus greatly reduce the pathological impacts of the steatosis.

## 7.4 ROLE OF ARF1 IN HCV INFECTION AND CLDS HOMEOSTASIS

High-resolution immunofluorescence imaging of HCV-infected cells treated with Z390 showed an alteration of cLDs homeostasis and HCV core and NS5A localization. I identified a link between cLDs homeostasis and cell-to-cell spread. Inhibition of synthesis of nascent cLDs while promoting mature cLDs, led to inhibition of direct cell-to-cell HCV spread. This effect on cLDs was likely a result of interference with trafficking of host factors essential for cLDs homeostasis such as ADRP and TIP47. I therefore continued the characterization of mechanism inhibition of direct cell-to-cell spread by Z390 by assessing trafficking functions. However, 100 to 300 different proteins continuously associate with and dissociate from cLDs, most likely indicating a complex trafficking system through several pathways involving multiple host factors. Literature review for similar looking phenotypes led to the papers showing that NS5A translocates from the ER to the cLDs under three reported conditions. DAAs that bind to NS5A, preventing its association with HCV replication complexes, resulted in the shuttling of NS5A to the cLDs, and 80% inhibition of HCV RNA replication (Targett-Adams et al., 2011). Inhibitors of DGAT1, which is required for the interaction of NS5A and core at the assembly sites, also redistributed NS5A to cLDs and inhibits HCV RNA replication by 80% and release of infectious virions by 60% (Camus et al., 2013). Knockdown of Arf1 had resulted in a reduction of HCV RNA by 40% and infectivity titer by 70% (Matto et al., 2011). I had already concluded that inhibition of direct HCV cell-to-cell spread by Z390 had no effect on the replication cycle and resulted from an alteration to cLD homeostasis, which had affected core and NS5A localization. Core accumulated at its default localization, around cLDs, whereas NS5A has shifted to an unusual location, also around cLDs. I thus focused

on conditions that resulted in similar NS5A localization. Among the three previously reported conditions leading to similar localization, Arf1 was the ideal candidate for the major roles it plays in trafficking between ER and Golgi as well as to and from cLDs.

Previously, I concluded that the altered cLDs homeostasis induced by Z390, which affected core and NS5A localization and inhibited HCV direct cell-to-cell spread was likely a result of interference with trafficking. Based on the analysis of the literature, I thus proposed Arf1 to be involved in HCV direct cell-to-cell spread. Specifically, I envision a sequence of events such that Z390 interferes with Arf1-mediated trafficking functions related to homeostasis of cLDs, which consequently alters the core and NS5A localization resulting in inhibition of HCV cell-to-cell spread. I first reproduced the redistribution of NS5A from the ER to the surface of enlarged cLDs upon knockdown of Arf1 in HCVcc-JFH1 infected Huh7.5 cells. I then tested whether knockdown of Arf1 in the donor cells affected HCV direct cell-to-cell spread in the co-culture assay. Co-culture of infected and Arf1 knockdowned Huh7.5 cells with naïve Huh7.5 cells, inhibited cell-to-cell spread, but did not affect HCV replication.

The role of Arf proteins in the replication of HCV has not been thoroughly characterized yet. Nevertheless, the collective finding from the limited studies show that targeting several members of the Arf family or cofactors could affect HCV replication or infectivity based on the time of treatment. Interference with Arf1, 3, 4, or 5, or Arf GEF GBF1 before infection inhibits HCV replication by approximately 50% and infectivity by more than 90% (Farhat et al., 2016; Goueslain et al., 2010; Matto et al., 2011; L. Zhang et al., 2012). Using BFA (as an inhibitor of GBF1). In a time of addition assay, the inhibition appears to be at the post-entry steps. The later BFA was added, the less inhibition of

HCV replication was observed. No inhibition was observed when BFA was added 48 h after infection (Goueslain et al., 2010). These findings are in line with our own finding that knockdown of Arf1 in the donor cells used in the co-culture assay after the end of the replication cycle does not inhibit HCV replication.

As a small GTPase, Arf1 exists bound to GTP or GDP, bindings which regulate the binding and dissociation from the membrane, respectively (Rittinger, 2008). Arf1 GEFs such as GBF1 or BIG1 facilitate the exchange of GDP for GTP leading to firm attachment of Arf1-GTP to membranes (Beraud-Dufour, Paris, Chabre, & Antonny, 1999). GTP is hydrolyzed to GDP resulting in the release of Arf1-GDP from the membrane (Szafer, Rotman, & Cassel, 2001). Arf1-GTP attaches to the membrane during the assembly of cargo vesicles and it is then hydrolyzed to Arf1-GDP during the release of the vesicles and their trafficking to the destination membrane (Beck et al., 2011). Cycling between GTP and GDP is required for the trafficking function of Arf1. Interference with GDP and GTP cycling could thus more specifically inhibit the trafficking function of Arf1 than its knockdown (Dascher & Balch, 1994). I next used Arf1 non-cycling mutants to test the phenotypes of altered cLDs homeostasis and core and NS5A localization. Compared to wild-type Arf1, both non-cycling mutants affected the distribution of HCV proteins and the cLDs homeostasis in similar manners as Z390 and oleic acid. Quantitatively, the effects were more prominent by expression of T31N (GDP-locked) compared to that of Q71L (GTP-bound). The mechanism of the effects of either non-cycling mutant could account for the quantitative difference (Dascher & Balch, 1994). Expression of the T31N Arf1 mutants induced an exclusive localization of NS5A to enlarged cLDs. Localization of core to the surface of cLDs was not affected despite the altered homeostasis, fewer and

enlarged cLDs. Interruption to the Arf1-GTP-Arf1-GDP cycle is sufficient to reproduce the phenotype. Z390 could thus target Arf1 by interrupting its continuous cycling between GDP and GTP-bound forms. Reproduction of the Z390 phenotype by Arf1 knockdown or expression of non-cycling mutants suggests that Z390 could target a more specific Arf1 function or pathway than previously existing inhibitors. Consistently with this model, expression of T31N or treatment with BFA disintegrate Golgi, while treatment with Z390 did not.

The reproduction of Z390 phenotype by expression of Arf1 non-cycling mutants indicates that trafficking functions mediated by Arf1 are involved in the cLD homeostasis and core and NS5A localization. The role of Arf1 in the regulation of cLDs homeostasis has been highlighted recently. Association and dissociation of structural or enzymatic proteins to and from the cLDs are the major mechanisms regulating cLD homeostasis. For example, Arf1-GDP bind directly to ADRP promoting its dissociation from cLDs whereas Arf1-GTP did not affect the level of association of ADRP to cLDs (Nakamura et al., 2004). ADRP association with cLDs is thought to regulate lipolysis of neutral lipids, affecting cellular content of TG and cLDs homeostasis. ADRP association with cLDs also maintain cLDs growth by inhibiting the access of ATGL lipase (Listenberger et al., 2007). Knockout of ADRP in mice results in decrease of liver TG and attenuation of hepatic steatosis by high-fat feeding (B. H. Chang et al., 2006). At the cellular level, overexpression of ADRP in McA-RH 7777 cells promotes the cLDs growth and increases their TG content. siRNA knockdown of ADRP reduced cLDs and induced lipolysis and  $\beta$ -oxidation (Magnusson et al., 2006).

Z390 affected cLDs homeostasis by inhibiting the synthesis of nascent cLDs and maintaining the growth of existing mature cLDs, thus resulting in a homogenous population of mature cLDs that grow in a time-dependent manner, Z390 most likely acts by interfering with the cycling of Arf1 between GDP and GTP. Knockdown of Arf1 homolog in *Drosophila* S2 cells, or of any of the seven COPI components except  $\epsilon$ COP, shifts the cLDs population from a bimodal distribution comprised of 85% small and 15% large cLDs to a monodisperse population of medium sized cLDs (Wilfling et al., 2014). GBF1 contain a lipid-binding domain which mediates their targeting to cLDs and Golgi (Bouvet et al., 2013). Knockdown of GBF1 or expression of Arf1-T31N followed by addition of oleic acid inhibited the formation of nascent cLDs (Nakamura et al., 2004). Our findings show that treatment with Z390 for 1 h before addition of oleic acid for 3 h also inhibits the recruitment of TIP47 to the site of nascent cLDs synthesis. Addition of oleic acid without Z390 treatment induces localization of both TIP47 and ArfGAP1 to cLDs (Gannon et al., 2014). The association of ArfGAP1 with cLDs in response to oleic acid was transient, gradually increasing until reaching a peak at 4 h and then gradually dissociating by approximately 80% at 10 h and totally at 24 h. These dynamics suggest the engagement of trafficking until the incorporation of the added oleic acid pool into cLDs. Knockdown of GBF1 or ArfGAP1, or expression of Arf1-T31N, inhibited nascent cLDs. When considered together, these suggest that altering the Arf1-GDP:GTP ratio to either side result in the same effect.

Besides inhibiting the formation of nascent cLDs, knockdown of GBF1, expression of Arf1-T31N or treatment with BFA or GCA also increased the size of existing mature cLDs and of the TG and membrane phospholipids (Soni et al., 2009; Takashima et al., 2011). The underlying mechanism was inhibition of trafficking of the lipase ATGL to the



cLDs, decreasing the rate of lipolysis and promoting steady growth of mature cLDs (Soni et al., 2009). Arf1-GTP Hydrolysis results in the budding of ~60 nm vesicle from cLDs, similar to the cargo vesicles that bud from the ER by Arf1/ArfGAP1, resulting in decreasing cLDs size. Inhibition of Arf1-GTP hydrolysis by the non-hydrolyzable GTP analog, GTP $\gamma$ S, inhibits budding and, therefore, results in a net increase in the size of existing mature cLDs (Thiam et al., 2013; Wilfling et al., 2014). These findings also suggest that altering the Arf1-GTP:GDP ratio to either side similarly affects the cLDs homeostasis. Taken together, Arf1-GTP:GDP cycling mediated trafficking functions between ER and Golgi and cLDs are clearly involved in the regulation of cLDs homeostasis

The intracellular trafficking machinery is essential for replication of the intracellular pathogens (Rust et al., 2001). For example, it contributes to the recruitment of host factors to sites of pathogen replication (L. Zhang et al., 2012). The trafficking cellular machinery contributes to the mobilization of pathogen encoded factors for their interaction with the target cellular organelles (J. Li et al., 2016). The roles of Arf1 in HCV have been characterized in only few studies, mostly by targeting Arf1 GEFs or GAPs. Even fewer studies have addressed Arf1 directly. For example, knockdown of Arf1 in a cell line stably expressing full-length HCV subtype 1b (Con-1) or 2a (Jc1) reduced HCV RNA by 40% after 3 days (Matto et al., 2011). Knockdown of Arf1 or GBF1, but not of BIG1, reduced expression of HCVcc-JFH1 NS5A by 50-90% (Farhat et al., 2013; Goueslain et al., 2010; L. Zhang et al., 2012). As altering the Arf1-GTP:GDP ratio to either side similarly affected cLDs, expression of either Arf1-T31N or Arf-Q71L equally inhibited HCV infection by 80% (Farhat et al., 2016). Treatment of Huh7.5 cells with BFA during infection, or 4 h after,

resulted in >90% reduction in infection or replication, respectively (Goueslain et al., 2010). Interference of the Arf1 functions in HCV-infected cells affects HCV replication by mechanisms involving modulation of cellular lipid components. For example, PI4P, which is required for HCV replication, is translocated from Golgi to the sites of HCV replication. Treatment of HCVcc-JFH1 infected cells with ArfGAP1 small molecule inhibitor QS11, or knockdown of ArfGAP1, inhibited recruitment of PI4P to the sites of replication complexes and reduced HCV RNA by 90% or 60%, respectively (H. Li et al., 2014).

Arf1 regulates TIP47, a cLD-associated protein involved in the cLD metabolism of cLDs. TIP47 was recently found to facilitates hepatic steatosis induced by HCV core in HCV core-transgenic mice (Ferguson et al., 2017). TIP47 is upregulated in HCV infected cell, and it is involved in the assembly of HCV virion via a dual interaction with NS5A and Rab9 (Ploen, Hafirassou, Himmelsbach, Schille, et al., 2013; Vogt et al., 2013b). Silencing of TIP47 reduced production of infectious virions by ~50%, whereas overexpression increased it by 60% (Ploen, Hafirassou, Himmelsbach, Sauter, et al., 2013). HCV core inhibits the ATGL lipase on the cLDs surface (Camus et al., 2014) in a similar manner as ADRP does. Presence of core and ADRP on cLDs could have stimulated cLDs growth, resulting in their larger size, as it occurs after Z390 treatment. Association of ADRP or ATGL with cLDs is regulated by Arf1, suggesting the presence of intertwined regulatory functions on homeostasis cLDs imposed by Arf1 and HCV. HCV also upregulates ADRP, and overexpression of ADRP increases the cellular content of TG and the size of cLDs, in turn enhancing the assembly and release of infectious HCV virions. Overexpression of ADRP upregulated occludin mRNA and protein by 2-fold, resulting in >10-fold increase in the HCVpp entry (Branche et al., 2016). This

finding provides a direct evidence for the involvement of lipid metabolism, in this case ADRP, in the regulation of host factor involved in the direct cell-to-cell spread, and in entry of cell-free virions, of HCV. Although the finding presented in this paper (Branche et al., 2016) could indicate that the upregulation of occludin would increase direct HCV cell-to-cell, inconsistently with our findings, overexpression of ADRP may have also modulated the cellular distribution of occludin, to sites where it is more efficient in entry of cell-free virions than in direct cell-to-cell spread. Expression of chicken occludin in MDCK cells showed intense cytoplasmic staining close to the nucleus, and some signal at the plasma membrane, in addition to the expected staining at the cell junction sites overlapping with the endogenous MDCK occludin (McCarthy et al., 1996). Expression of Arf6 GEF EFA6 retains occludin at the cell surface and excludes it from endocytosis (Luton et al., 2004), indicating that occludin is redistributed under numbers of stimuli. I speculate a model in which HCV employs Arf1 for modulation of cLD homeostasis to favor replication and spread. Interference with Arf1, alters the HCV-mediated modulation of cLDs homeostasis pertinent to cell-to-cell spread but not that related to replication.

HCV cell-to-cell spread has been recognized as one of the mechanisms of immune evasion, and therefore, of persistence of HCV infection. The mechanisms of HCV cell-to-cell spread remain largely unknown beyond the involvement of certain host factor associated which are also associated with entry of cell-free virions. Two of these receptors, SR-BI and NPC1L1, are involved in cholesterol absorption or uptake of cholesterol from HDL, respectively. Despite, the involvement of lipid metabolism in every step of the HCV replication, its role in HCV direct cell-to-cell spread had not been investigated before. In this thesis, I identified and characterized the mechanism of action

of a small molecule that inhibited HCV cell-to-cell spread by a novel mechanism targeting Arf1-mediated trafficking functions. Interference with Arf1 function resulted in cLDs homeostasis modifications which consequently affected the localization of HCV NS5A. Arf1 and its regulators (such as GBF1 or ArfGAP1) directly interact with HCV proteins affecting entry, replication (Farhat et al., 2013; Goueslain et al., 2010; Matto et al., 2011), infectivity (Farhat et al., 2016; Goueslain et al., 2010), assembly and release (Vieyres et al., 2016). Arf1 and regulators also modulate the homeostasis of cLDs through direct interaction with host factors involved in lipid metabolism. The roles of Arf1 in both HCV life cycle and lipid metabolism likely overlap, resulting in accumulation of neutral lipids in infected hepatocytes. This study therefore identified a novel host factor that mediates critical functions in the biology of HCV infection direct cell-to-cell spread and cLDs homeostasis, and thus it is linked to one of the main HCV complications, hepatic steatosis. This study thus opens a new venue for the investigation of the role of Arf1, as a common factor involved in HCV infection, lipid metabolism, and cell-to-cell transmission.

The liver is a major organ for lipid metabolism. Dietary absorbed lipids are transported to the liver where they are processed for secretion into the blood-stream, to reach other organs that utilize lipid to produce energy or store it (adipose tissues). Dysfunction of the hepatic lipid metabolism leads to steatosis, which occurs in 40-86% of individuals with chronic HCV infection (Cheng, Torres, & Harrison, 2014). Several vital elements, including hormones and bile acids, are synthesized in the liver lipid. The metabolic processes and their regulatory mechanisms are complex and require a coordinated interaction of many host factors at several levels. These processes require the trafficking of enzymes or co-activators between organelles. Arf1 is the founding

member of Arf family proteins that play major roles in membrane trafficking, rearrangement of cytoskeleton, and cell migration. Cumulating evidence shows the involvement of Arf1 in cLDs metabolism regulation mostly by regulating the association of host factors to the cLDs. Several Arf1-mediated trafficking functions contribute to the homeostasis of cLDs by regulating the accumulation or the breakdown of neutral lipids. Thus, this study supports previous finding and emphasizes on the rising interest in the roles of Arf1-mediated trafficking functions in lipid metabolism. In this respect, Z390 represents a fine tool to further characterize hepatic cLD homeostasis.

The currently available agents interfere with Arf1 functions by targeting either an Arf1 GEF or GAP. Reviewing the mechanism of action and the morphological or functional effects of such agents identified two major issues, the substrate specificity and variable effects obtained by targeting an individual protein with different inhibitors. For example, both BFA and GCA target GBF1. However, BFA treatment results in the tubulation of endosomes and collapse of Golgi, due to inhibition of the retrograde and anterograde trafficking between ER and Golgi. These pleiotropic effects result from the inhibition of multiple GEFs that act on several Arfs (Niu, Pfeifer, Lippincott-Schwartz, & Jackson, 2005). GCA results in dispersion of cis and medial-Golgi while the trans-Golgi and its associated proteins remained unaffected, unless the treatment is prolonged in which case eventually lead to the collapse of Golgi (Saenz et al., 2009). Inhibition of BIG1 by the small molecules LM11 (Viaud et al., 2007) or LG186 (Boal et al., 2010) results in inhibition of cell migration or dissociation of COPI vesicles from the Golgi, likely by interfering with Arf5 or Arf1, respectively. Multiple Arf substrates for an individual GEF or GAP and the effects of several GEFs or GAPs on an individual Arf contribute to the lack of phenotypic

specificity of the current inhibitors. The effect of these inhibitors is mostly generalized and impact a wide range of processes, such the secretory systems resulting in the collapse of the Golgi and inhibition of protein secretion or remodeling of actin which affect cell adhesion and migration. The characterization of the interference mechanisms of Arf1-mediated trafficking by Z390 could potentially uncover unrecognized specific Arf1 regulatory pathway, which do not affect entire secretory pathway.

## 7.5 FUTURE DIRECTIONS

### 7.5.1 Evaluating the role of cLD in HCV virion release and cell-to-cell spread

I showed that localization of HCV core and NS5A proteins and cLD homeostasis have a role in HCV cell-to-cell spread. The phenotype was characterized by core localizing to clads more efficiently and NS5A being redistributed from the ER to the periphery of fewer and larger cLDs. Localization of core on the surface of cLDs was demonstrated to inversely correlates with the efficiency of assembly and release, while it directly correlates with the cell-to-cell spread. HCV-J6 core that barely associates with cLDs produces 2 to 3-log higher total infectious virions where >95% are released (Pietschmann et al., 2006; Shavinskaya et al., 2007b). In contrast, HCV-JFH1 core covers the entire surface of cLDs, resembling ring-like structures, in a time-dependent manner. HCV-JFH1 is more efficient in cell-to-cell spread, forming foci comprised of 3 to 4-fold more cells per focus than HCV-J6. Thus, the association of core with cLDs is a determinant factor as to whether assembled virions traffic through the secretory pathway to the extracellular space for infection spread by cell-free virions, or transferred to the adjacent cells for infection spread by cell-associated virions.

In contrast to the extracellular, intracellular infectious virions have higher density, which reflects assembled but not matured virions (Gastaminza et al., 2008b; Gastaminza, Kapadia, & Chisari, 2006a). As they traffic through the secretory pathway, virions are thought to fuse with pre-VLDL particles then further enriched with TG and CE from the cLDs by the activity of MTP, giving the released virions the low-density characteristic (Jones & McLauchlan, 2010; Merz et al., 2011). Digestion of glycans demonstrated that HCV virions lack glycosylation by Golgi-residing enzymes (K. Bayer et al., 2016). In

untreated co-culture, most of the actin filaments were along the boundaries of cells. Core motility to the cell periphery is blocked by cytochalasin D, an inhibitor of actin polymerization, but not with nocodazole, a microtubule depolymerization agent. Treatment with cytochalasin D induced the formation of filament aggregates in the cytoplasm and inhibited HCV cell-to-cell spread, while nocodazole disrupted microtubule without affecting cell-to-cell spread. Secretion of VLDL primarily depends on the microtubular system (Bouma et al., 1988; Le Marchand et al., 1973; Nagelkerke et al., 1991; Orci et al., 1973), although one study implicated actin microfilaments in the secretion of lipoproteins (Prentki, Chaponnier, Jeanrenaud, & Gabbiani, 1979).

Live-cell imaging of co-culture showed that during the HCV transmission, most of the mobile core puncta traffic to the areas of contact between the donor and target cell followed by transmission into the target cells in direct contacts. Inhibition of VLDL secretion inhibits the release of HCV virions but not cell-to-cell spread. Except for HCV-J6, almost all intergenotypic chimeras form foci comparable in size to that of JFH1, indicating that cell-to-cell spread is the dominant route for infection transmission. It was shown that while the majority of virions were associated with the ER opposed to cLDs, 4% of the virions were on the surface of cLDs, as visualized by electron microscopy, suggesting that assembly could occur on cLDs or assembled virions could transport into the cLDs. HCV structural and non-structural proteins involved in the assembly which includes E1E2, core, NS3, NS4A/B, and NS5A/B fractionate with cLDs. ApoE and B localize to the replication complexes on ER opposed to the cLDs. NS5A interact directly with ApoE during the early stage of assembly, suggesting that acquisition of apolipoprotein components could co-occur with assembly and does not necessarily



require virions to bud into the ER lumen. However, acquisition of lipoproteins after budding could still be the primary pathway. Thus, I propose a model that assembled virions traffic through the ER-Golgi secretory pathway for the release to the extracellular environment or traffic to adjacent cells for cell-to-cell spread. I would use the subcellular fractionation approach to isolate cytosolic, ER, Golgi, endosomes, and cLDs followed by probing for infectivity, core, envelope glycoproteins, and genomic RNA. Using this approach at times that coincide with pre-assembly, assembly, and release should provide information about the virion morphogenesis concerning subcellular distribution and infectivity. Assessment of the fractions probing should provide details about the relative kinetics of assembly and release among the fractions. These details should help us to analyze the sequential steps of assembly and release (e.g., the primary pathway of release, whether infectious virions could be obtained in cLDs fractions). For cell-to-cell spread, the aim would be to determine the time of initiation of cell-to-cell transmission and compare it to the timeline of the assembly and release. Eventually, we should be able to determine the primary pathways involved in the extracellular release or cell-to-cell transmission and whether the two mechanisms utilize similar or different pathway, or if they overlap, entirely or partially. In parallel, it would of interest to compare the characterized pathways of released or cell-to-cell transmission upon interference of Arf1, by knockdown or expression of non-cycling mutants. The expected outcome from this step is the effect of Arf1 interference to the subcellular distribution of HCV virion components in isolated organelles or their involvement in virion morphogenesis.

### **7.5.2 In vitro studies of Arf1 and Z390**

Knockdown of Arf1 or expression of non-cycling mutants reproduced the Z390 effect on the cellular distribution of HCV proteins and cLDs homeostasis. Knockdown of Arf1 inhibited HCV cell-to-cell spread. The role of Arf1 in cLDs homeostasis was established by interference to Arf1 by genetic means or to its cofactors by genetic or chemical methods. These cofactors and their inhibitors lack specificity for their substrates (Bourgoin, 2012) (Mishev, Dejonghe, & Russinova, 2013). A specific inhibitor of Arf1 is not yet available. Besides the essential role in trafficking, several roles of Arf1 have emerged such as modulation of mitochondria morphology and function (Ackema et al., 2014) or in cancer proliferation (Boulay et al., 2011), metastasis (Xie et al., 2016), and therapeutic potential (Lang, Shay, Zhao, & Teng, 2017). Thus, investigation of Z390 for a potential of a specific inhibitor could be of interest.

I would first test the effect of Z390 on the intracellular localization of Arf1 and colocalization with Golgi or ER and whether Z390 promote or inhibit activation. If the outcomes indicate interference to nucleotide loading or hydrolysis, I would use the T31N (GDP-locked) or Q71L (GTP-locked) to test if Z390 would augment or rescue into the wild-type. We should be able to determine if Z390 inhibit loading or hydrolysis. I would also attempt to conduct cell-free in vitro assays to test for GTP binding or hydrolysis and whether or not Z390 affect these reactions. If Z390 showed activity in these reactions, future follows up should include evaluation of the specificity of Z390 for Arf isoforms, binding kinetics, and structural studies.

### **7.5.3 Evaluating the role of Arf1 in HCV entry**

We noticed that Huh7.5 cells transfected with wild-type or non-cycling mutants Arf1 are refractory to HCV entry of cell-free virions, but they can be infected by adjacent infected cells in co-culture. Therefore, Arf1 may have a role in the entry of cell-free virions of HCV. Entry of HCV is mediated by clathrin-dependent endocytosis (Blanchard et al., 2006), regulation of which involve Arf1 and Arf6 (Boulakirba et al., 2014; Tanabe et al., 2005). Thus, it appears that there is a potential venue to start investigating the role Arf1 and maybe also Arf6 in the entry of cell-free virion.

## REFERENCES

- Abe, K., Ikeda, M., Dansako, H., Naka, K., & Kato, N. (2007). Cell culture-adaptive NS3 mutations required for the robust replication of genome-length hepatitis C virus RNA. *Virus Res*, 125(1), 88-97. doi:10.1016/j.virusres.2006.12.011
- Abrahamian, G. A., Cosimi, A. B., Farrell, M. L., Schoenfeld, D. A., Chung, R. T., & Pascual, M. (2000). Prevalence of hepatitis C virus-associated mixed cryoglobulinemia after liver transplantation. *Liver Transpl*, 6(2), 185-190. doi:10.1002/lt.500060224
- Ackema, K. B., Hench, J., Bockler, S., Wang, S. C., Sauder, U., Mergentaler, H., . . . Spang, A. (2014). The small GTPase Arf1 modulates mitochondrial morphology and function. *EMBO J*, 33(22), 2659-2675. doi:10.15252/embj.201489039
- Agnello, V., Abel, G., Knight, G. B., & Muchmore, E. (1998). Detection of widespread hepatocyte infection in chronic hepatitis C. *Hepatology*, 28(2), 573-584. doi:10.1002/hep.510280240
- Agosto, L. M., Zhong, P., Munro, J., & Mothes, W. (2014). Highly active antiretroviral therapies are effective against HIV-1 cell-to-cell transmission. *PLoS Pathog*, 10(2), e1003982. doi:10.1371/journal.ppat.1003982
- Ahmad, A., & Alvarez, F. (2004). Role of NK and NKT cells in the immunopathogenesis of HCV-induced hepatitis. *J Leukoc Biol*, 76(4), 743-759. doi:10.1189/jlb.0304197
- Aivazian, D., Serrano, R. L., & Pfeffer, S. (2006). TIP47 is a key effector for Rab9 localization. *J Cell Biol*, 173(6), 917-926. doi:10.1083/jcb.200510010
- Al Olaby, R. R., Cocquerel, L., Zemla, A., Saas, L., Dubuisson, J., Vielmetter, J., . . . Azzazy, H. M. (2014). Identification of a novel drug lead that inhibits HCV infection and cell-to-cell transmission by targeting the HCV E2 glycoprotein. *PloS one*, 9(10), e111333. doi:10.1371/journal.pone.0111333
- Al-Sherbiny, M., Osman, A., Mohamed, N., Shata, M. T., Abdel-Aziz, F., Abdel-Hamid, M., . . . Strickland, G. T. (2005). Exposure to hepatitis C virus induces cellular immune responses without detectable viremia or seroconversion. *Am J Trop Med Hyg*, 73(1), 44-49.
- Alimonti, J. B., Kimani, J., Matu, L., Wachihi, C., Kaul, R., Plummer, F. A., & Fowke, K. R. (2006). Characterization of CD8 T-cell responses in HIV-1-exposed seronegative commercial sex workers from Nairobi, Kenya. *Immunol Cell Biol*, 84(5), 482-485. doi:10.1111/j.1440-1711.2006.01455.x
- Allue-Guardia, A., Jofre, J., & Muniesa, M. (2012). Stability and infectivity of cytolethal distending toxin type V gene-carrying bacteriophages in a water mesocosm and under different inactivation conditions. *Appl Environ Microbiol*, 78(16), 5818-5823. doi:10.1128/AEM.00997-12
- Alter, H. J. (1980). The dominant role of non-A, non-B in the pathogenesis of post-transfusion hepatitis: a clinical assessment. *Clin Gastroenterol*, 9(1), 155-170.
- Amanzada, A., Goralczyk, A. D., Moriconi, F., van Thiel, D. H., Ramadori, G., & Mihm, S. (2013). Vitamin D status and serum ferritin concentration in chronic hepatitis C virus type 1 infection. *J Med Virol*, 85(9), 1534-1541. doi:10.1002/jmv.23632

- Andre, P., Komurian-Pradel, F., Deforges, S., Perret, M., Berland, J. L., Sodoyer, M., . . . Lotteau, V. (2002). Characterization of low- and very-low-density hepatitis C virus RNA-containing particles. *J Virol*, 76(14), 6919-6928.
- Andre, P., & Lotteau, V. (2008). Hepatitis C virus assembly: when fat makes it easier. *J Hepatol*, 49(1), 153-155. doi:10.1016/j.jhep.2008.04.005
- Anekal, S. G., Zhu, Y., Graham, M. D., & Yin, J. (2009). Dynamics of virus spread in the presence of fluid flow. *Integr Biol (Camb)*, 1(11-12), 664-671. doi:10.1039/b908197f
- Anna Godi, P. P., Rachel Meyers, Pierfrancesco Marra, Giuseppe Di Tullio, & Cristiano Iurisci, A. L., Daniela Corda and Maria Antonietta De Matteis. (1999). ARF mediates recruitment of PtdIns-4-OH kinase- $\beta$  and stimulates synthesis of PtdIns(4,5)P<sub>2</sub> on the Golgi complex. *Nature cell biology*, 1.
- Antonny, B., Huber, I., Paris, S., Chabre, M., & Cassel, D. (1997). Activation of ADP-ribosylation factor 1 GTPase-activating protein by phosphatidylcholine-derived diacylglycerols. *The Journal of biological chemistry*, 272(49), 30848-30851.
- Appel, N., Zayas, M., Miller, S., Krijnse-Locker, J., Schaller, T., Friebe, P., . . . Bartenschlager, R. (2008). Essential role of domain III of nonstructural protein 5A for hepatitis C virus infectious particle assembly. *PLoS Pathog*, 4(3), e1000035. doi:10.1371/journal.ppat.1000035
- Ariumi, Y., Kuroki, M., Maki, M., Ikeda, M., Dansako, H., Wakita, T., & Kato, N. (2011). The ESCRT system is required for hepatitis C virus production. *PloS one*, 6(1), e14517. doi:10.1371/journal.pone.0014517
- Arora, G. K., Tran, S. L., Rizzo, N., Jain, A., & Welte, M. A. (2016). Temporal control of bidirectional lipid-droplet motion in *Drosophila* depends on the ratio of kinesin-1 and its co-factor Halo. *J Cell Sci*, 129(7), 1416-1428. doi:10.1242/jcs.183426
- Auffermann-Gretzinger, S., Keeffe, E. B., & Levy, S. (2001). Impaired dendritic cell maturation in patients with chronic, but not resolved, hepatitis C virus infection. *Blood*, 97(10), 3171-3176.
- Ball, J. K., Tarr, A. W., & McKeating, J. A. (2014). The past, present and future of neutralizing antibodies for hepatitis C virus. *Antiviral research*. doi:10.1016/j.antiviral.2014.02.013
- Barber, D. L., Wherry, E. J., Masopust, D., Zhu, B., Allison, J. P., Sharpe, A. H., . . . Ahmed, R. (2006). Restoring function in exhausted CD8 T cells during chronic viral infection. *Nature*, 439(7077), 682-687. doi:10.1038/nature04444
- Barretto, N., Sainz, B., Jr., Hussain, S., & Uprichard, S. L. (2014). Determining the Involvement and Therapeutic Implications of Host Cellular Factors in Hepatitis C Virus Cell-to-Cell Spread. *Journal of virology*, 88(9), 5050-5061. doi:10.1128/JVI.03241-13
- Bartenschlager, R., Penin, F., Lohmann, V., & Andre, P. (2011). Assembly of infectious hepatitis C virus particles. *Trends Microbiol*, 19(2), 95-103. doi:10.1016/j.tim.2010.11.005
- Bartenschlager, R., & Sparacio, S. (2007). Hepatitis C virus molecular clones and their replication capacity in vivo and in cell culture. *Virus research*, 127(2), 195-207. doi:10.1016/j.virusres.2007.02.022
- Barth, H., Schafer, C., Adah, M. I., Zhang, F., Linhardt, R. J., Toyoda, H., . . . Baumert, T. F. (2003). Cellular binding of hepatitis C virus envelope glycoprotein E2 requires

- cell surface heparan sulfate. *J Biol Chem*, 278(42), 41003-41012. doi:10.1074/jbc.M302267200
- Bartlett, K., & Eaton, S. (2004). Mitochondrial beta-oxidation. *Eur J Biochem*, 271(3), 462-469.
- Bartz, R., Li, W. H., Venables, B., Zehmer, J. K., Roth, M. R., Welte, R., . . . Chapman, K. D. (2007). Lipidomics reveals that adiposomes store ether lipids and mediate phospholipid traffic. *Journal of lipid research*, 48(4), 837-847. doi:10.1194/jlr.M600413-JLR200
- Bartz, R., Zehmer, J. K., Zhu, M., Chen, Y., Serrero, G., Zhao, Y., & Liu, P. (2007). Dynamic activity of lipid droplets: protein phosphorylation and GTP-mediated protein translocation. *J Proteome Res*, 6(8), 3256-3265. doi:10.1021/pr070158j
- Bassendine, M. F., Sheridan, D. A., Felmlee, D. J., Bridge, S. H., Toms, G. L., & Neely, R. D. (2011). HCV and the hepatic lipid pathway as a potential treatment target. *Journal of hepatology*, 55(6), 1428-1440. doi:10.1016/j.jhep.2011.06.004
- Bauby, H., Lopez-Verges, S., Hoeffel, G., Delcroix-Genete, D., Janvier, K., Mammano, F., . . . Berlioz-Torrent, C. (2010). TIP47 is required for the production of infectious HIV-1 particles from primary macrophages. *Traffic*, 11(4), 455-467. doi:10.1111/j.1600-0854.2010.01036.x
- Baumeier, C., Kaiser, D., Heeren, J., Scheja, L., John, C., Weise, C., . . . Schurmann, A. (2015). Caloric restriction and intermittent fasting alter hepatic lipid droplet proteome and diacylglycerol species and prevent diabetes in NZO mice. *Biochim Biophys Acta*, 1851(5), 566-576. doi:10.1016/j.bbalip.2015.01.013
- Bayer, K., Banning, C., Bruss, V., Wiltzer-Bach, L., & Schindler, M. (2016). Hepatitis C Virus Is Released via a Noncanonical Secretory Route. *J Virol*, 90(23), 10558-10573. doi:10.1128/JVI.01615-16
- Bayer, M. E., Blumberg, B. S., & Werner, B. (1968). Particles associated with Australia antigen in the sera of patients with leukaemia, Down's Syndrome and hepatitis. *Nature*, 218(5146), 1057-1059.
- Beck, R., Prinz, S., Diestelkotter-Bachert, P., Rohling, S., Adolf, F., Hoehner, K., . . . Wieland, F. (2011). Coatamer and dimeric ADP ribosylation factor 1 promote distinct steps in membrane scission. *The Journal of cell biology*, 194(5), 765-777. doi:10.1083/jcb.201011027
- Beck, R., Sun, Z., Adolf, F., Rutz, C., Bassler, J., Wild, K., . . . Wieland, F. (2008). Membrane curvature induced by Arf1-GTP is essential for vesicle formation. *Proceedings of the National Academy of Sciences of the United States of America*, 105(33), 11731-11736. doi:10.1073/pnas.0805182105
- Becucci, L., D'Amico, M., Cinotti, S., Daniele, S., & Guidelli, R. (2011). Tethered bilayer lipid micromembranes for single-channel recording: the role of adsorbed and partially fused lipid vesicles. *Phys Chem Chem Phys*, 13(29), 13341-13348. doi:10.1039/c1cp20667b
- Belema, M., Nguyen, V. N., Romine, J. L., St Laurent, D. R., Lopez, O. D., Goodrich, J. T., . . . Snyder, L. B. (2014). Hepatitis C virus NS5A replication complex inhibitors. Part 6: Discovery of a novel and highly potent biarylimidazole chemotype with inhibitory activity toward genotypes 1a and 1b replicons. *J Med Chem*, 57(5), 1995-2012. doi:10.1021/jm4016203

- Belland, R., Ojcius, D. M., & Byrne, G. I. (2004). Chlamydia. *Nat Rev Microbiol*, 2(7), 530-531. doi:10.1038/nrmicro931
- Beller, M., Sztalryd, C., Southall, N., Bell, M., Jackle, H., Auld, D. S., & Oliver, B. (2008). COPI complex is a regulator of lipid homeostasis. *PLoS biology*, 6(11), e292. doi:10.1371/journal.pbio.0060292
- Belov, G. A., Feng, Q., Nikovics, K., Jackson, C. L., & Ehrenfeld, E. (2008). A critical role of a cellular membrane traffic protein in poliovirus RNA replication. *PLoS Pathog*, 4(11), e1000216. doi:10.1371/journal.ppat.1000216
- Benga, W. J., Krieger, S. E., Dimitrova, M., Zeisel, M. B., Parnot, M., Lupberger, J., . . . Schuster, C. (2010). Apolipoprotein E interacts with hepatitis C virus nonstructural protein 5A and determines assembly of infectious particles. *Hepatology*, 51(1), 43-53. doi:10.1002/hep.23278
- Beraud-Dufour, S., Paris, S., Chabre, M., & Antonny, B. (1999). Dual interaction of ADP ribosylation factor 1 with Sec7 domain and with lipid membranes during catalysis of guanine nucleotide exchange. *The Journal of biological chemistry*, 274(53), 37629-37636.
- Berger, K. L., Kelly, S. M., Jordan, T. X., Tartell, M. A., & Randall, G. (2011). Hepatitis C virus stimulates the phosphatidylinositol 4-kinase III alpha-dependent phosphatidylinositol 4-phosphate production that is essential for its replication. *Journal of virology*, 85(17), 8870-8883. doi:10.1128/JVI.00059-11
- Binder, M., Quinkert, D., Bochkarova, O., Klein, R., Kezmic, N., Bartenschlager, R., & Lohmann, V. (2007). Identification of determinants involved in initiation of hepatitis C virus RNA synthesis by using intergenotypic replicase chimeras. *Journal of virology*, 81(10), 5270-5283. doi:10.1128/JVI.00032-07
- Bitzegeio, J., Bankwitz, D., Hueging, K., Haid, S., Brohm, C., Zeisel, M. B., . . . Pietschmann, T. (2010). Adaptation of hepatitis C virus to mouse CD81 permits infection of mouse cells in the absence of human entry factors. *PLoS Pathog*, 6, e1000978. doi:10.1371/journal.ppat.1000978
- Blackwood, R. A., Smolen, J. E., Transue, A., Hessler, R. J., Harsh, D. M., Brower, R. C., & French, S. (1997). Phospholipase D activity facilitates Ca<sup>2+</sup>-induced aggregation and fusion of complex liposomes. *The American journal of physiology*, 272(4 Pt 1), C1279-1285.
- Blanchard, E., Belouzard, S., Goueslain, L., Wakita, T., Dubuisson, J., Wychowski, C., & Rouille, Y. (2006). Hepatitis C virus entry depends on clathrin-mediated endocytosis. *J Virol*, 80(14), 6964-6972. doi:10.1128/JVI.00024-06
- Blanchard, E., Hourieux, C., Brand, D., Ait-Goughoulte, M., Moreau, A., Trassard, S., . . . Roingeard, P. (2003). Hepatitis C virus-like particle budding: role of the core protein and importance of its Asp111. *Journal of virology*, 77(18), 10131-10138.
- Blight, K. J., Kolykhalov, A. A., & Rice, C. M. (2000). Efficient initiation of HCV RNA replication in cell culture. *Science*, 290(5498), 1972-1974.
- Blight, K. J., McKeating, J. A., & Rice, C. M. (2002). Highly permissive cell lines for subgenomic and genomic hepatitis C virus RNA replication. *Journal of virology*, 76(24), 13001-13014.
- Boal, F., Guetzoyan, L., Sessions, R. B., Zeghouf, M., Spooner, R. A., Lord, J. M., . . . Stephens, D. J. (2010). LG186: An inhibitor of GBF1 function that causes Golgi

- disassembly in human and canine cells. *Traffic*, 11(12), 1537-1551. doi:10.1111/j.1600-0854.2010.01122.x
- Bocharov, G., Meyerhans, A., Bessonov, N., Trofimchuk, S., & Volpert, V. (2016). Spatiotemporal Dynamics of Virus Infection Spreading in Tissues. *PLoS One*, 11(12), e0168576. doi:10.1371/journal.pone.0168576
- Boehm, M., Aguilar, R. C., & Bonifacino, J. S. (2001). Functional and physical interactions of the adaptor protein complex AP-4 with ADP-ribosylation factors (ARFs). *EMBO J*, 20(22), 6265-6276. doi:10.1093/emboj/20.22.6265
- Boehme, K. W., Lai, C. M., & Dermody, T. S. (2013). Mechanisms of reovirus bloodstream dissemination. *Adv Virus Res*, 87, 1-35. doi:10.1016/B978-0-12-407698-3.00001-6
- Boettler, T., Spangenberg, H. C., Neumann-Haefelin, C., Panther, E., Urbani, S., Ferrari, C., . . . Thimme, R. (2005). T cells with a CD4+CD25+ regulatory phenotype suppress in vitro proliferation of virus-specific CD8+ T cells during chronic hepatitis C virus infection. *J Virol*, 79(12), 7860-7867. doi:10.1128/JVI.79.12.7860-7867.2005
- Boman, A. L., Kuai, J., Zhu, X., Chen, J., Kuriyama, R., & Kahn, R. A. (1999). Arf proteins bind to mitotic kinesin-like protein 1 (MKLP1) in a GTP-dependent fashion. *Cell Motil Cytoskeleton*, 44(2), 119-132. doi:10.1002/(SICI)1097-0169(199910)44:2<119::AID-CM4>3.0.CO;2-C
- Bonifacino, J. S., & Glick, B. S. (2004). The mechanisms of vesicle budding and fusion. *Cell*, 116(2), 153-166.
- Bostrom, P., Rutberg, M., Ericsson, J., Holmdahl, P., Andersson, L., Frohman, M. A., . . . Olofsson, S. O. (2005). Cytosolic lipid droplets increase in size by microtubule-dependent complex formation. *Arterioscler Thromb Vasc Biol*, 25(9), 1945-1951. doi:10.1161/01.ATV.0000179676.41064.d4
- Boulakirba, S., Macia, E., Partisani, M., Lacas-Gervais, S., Brau, F., Luton, F., & Franco, M. (2014). Arf6 exchange factor EFA6 and endophilin directly interact at the plasma membrane to control clathrin-mediated endocytosis. *Proc Natl Acad Sci U S A*, 111(26), 9473-9478. doi:10.1073/pnas.1401186111
- Boulant, S., Douglas, M. W., Moody, L., Budkowska, A., Targett-Adams, P., & McLauchlan, J. (2008). Hepatitis C virus core protein induces lipid droplet redistribution in a microtubule- and dynein-dependent manner. *Traffic*, 9(8), 1268-1282. doi:10.1111/j.1600-0854.2008.00767.x
- Boulant, S., Montserret, R., Hope, R. G., Ratinier, M., Targett-Adams, P., Lavergne, J. P., . . . McLauchlan, J. (2006). Structural determinants that target the hepatitis C virus core protein to lipid droplets. *J Biol Chem*, 281(31), 22236-22247. doi:10.1074/jbc.M601031200
- Boulant, S., Targett-Adams, P., & McLauchlan, J. (2007). Disrupting the association of hepatitis C virus core protein with lipid droplets correlates with a loss in production of infectious virus. *J Gen Virol*, 88(Pt 8), 2204-2213. doi:10.1099/vir.0.82898-0
- Boulant, S., Vanbelle, C., Ebel, C., Penin, F., & Lavergne, J. P. (2005). Hepatitis C virus core protein is a dimeric alpha-helical protein exhibiting membrane protein features. *J Virol*, 79(17), 11353-11365. doi:10.1128/JVI.79.17.11353-11365.2005



- Boulay, P. L., Schlienger, S., Lewis-Saravalli, S., Vitale, N., Ferbeyre, G., & Claing, A. (2011). ARF1 controls proliferation of breast cancer cells by regulating the retinoblastoma protein. *Oncogene*, 30(36), 3846-3861. doi:10.1038/onc.2011.100
- Bouma, M. E., Pessah, M., Renaud, G., Amit, N., Catala, D., & Infante, R. (1988). Synthesis and secretion of lipoproteins by human hepatocytes in culture. *In Vitro Cell Dev Biol*, 24(2), 85-90.
- Bourgoin, S. G. (2012). Small inhibitors of ADP-ribosylation factor activation and function in mammalian cells. *World Journal of Pharmacology*, 1(4), 55. doi:10.5497/wjp.v1.i4.55
- Boutet, E., El Mourabit, H., Prot, M., Nemani, M., Khallouf, E., Colard, O., . . . Magre, J. (2009). Seipin deficiency alters fatty acid Delta9 desaturation and lipid droplet formation in Berardinelli-Seip congenital lipodystrophy. *Biochimie*, 91(6), 796-803. doi:10.1016/j.biochi.2009.01.011
- Bouvet, S., Golinelli-Cohen, M. P., Contremoulins, V., & Jackson, C. L. (2013). Targeting of the Arf-GEF GBF1 to lipid droplets and Golgi membranes. *Journal of cell science*, 126(Pt 20), 4794-4805. doi:10.1242/jcs.134254
- Boyer, A., Dumans, A., Beaumont, E., Etienne, L., Roingeard, P., & Meunier, J. C. (2014). The association of hepatitis C virus glycoproteins with apolipoproteins E and B early in assembly is conserved in lipoviral particles. *The Journal of biological chemistry*, 289(27), 18904-18913. doi:10.1074/jbc.M113.538256
- Bradley, D., McCaustland, K., Krawczynski, K., Spelbring, J., Humphrey, C., & Cook, E. H. (1991). Hepatitis C virus: buoyant density of the factor VIII-derived isolate in sucrose. *J Med Virol*, 34(3), 206-208.
- Branche, E., Conzelmann, S., Parisot, C., Bedert, L., Levy, P. L., Bartosch, B., . . . Negro, F. (2016). Hepatitis C Virus Increases Occludin Expression via the Upregulation of Adipose Differentiation-Related Protein. *PLoS One*, 11(1), e0146000. doi:10.1371/journal.pone.0146000
- Brasaemle, D. L., Dolios, G., Shapiro, L., & Wang, R. (2004). Proteomic analysis of proteins associated with lipid droplets of basal and lipolytically stimulated 3T3-L1 adipocytes. *J Biol Chem*, 279(45), 46835-46842. doi:10.1074/jbc.M409340200
- Brass, V., Bieck, E., Montserret, R., Wolk, B., Hellings, J. A., Blum, H. E., . . . Moradpour, D. (2002). An amino-terminal amphipathic alpha-helix mediates membrane association of the hepatitis C virus nonstructural protein 5A. *J Biol Chem*, 277(10), 8130-8139. doi:10.1074/jbc.M111289200
- Brazzoli, M., Bianchi, A., Filippini, S., Weiner, A., Zhu, Q., Pizza, M., & Crotta, S. (2008). CD81 is a central regulator of cellular events required for hepatitis C virus infection of human hepatocytes. *J Virol*, 82(17), 8316-8329. doi:10.1128/JVI.00665-08
- Brimacombe, C. L., Grove, J., Meredith, L. W., Hu, K., Syder, A. J., Flores, M. V., . . . McKeating, J. A. (2011a). Neutralizing antibody-resistant hepatitis C virus cell-to-cell transmission. *Journal of virology*, 85(1), 596-605. doi:10.1128/JVI.01592-10
- Brimacombe, C. L., Grove, J., Meredith, L. W., Hu, K., Syder, A. J., Flores, M. V., . . . McKeating, J. A. (2011b). Neutralizing antibody-resistant hepatitis C virus cell-to-cell transmission. *J Virol*, 85(1), 596-605. doi:10.1128/JVI.01592-10
- Brock, S. C., Goldenring, J. R., & Crowe, J. E., Jr. (2003). Apical recycling systems regulate directional budding of respiratory syncytial virus from polarized epithelial

- cells. *Proc Natl Acad Sci U S A*, 100(25), 15143-15148. doi:10.1073/pnas.2434327100
- Bronowicki, J. P., Vetter, D., Uhl, G., Hudziak, H., Uhrlacher, A., Vetter, J. M., & Doffoel, M. (1997). Lymphocyte reactivity to hepatitis C virus (HCV) antigens shows evidence for exposure to HCV in HCV-seronegative spouses of HCV-infected patients. *J Infect Dis*, 176(2), 518-522.
- Brown, F. D., Rozelle, A. L., Yin, H. L., Balla, T., & Donaldson, J. G. (2001). Phosphatidylinositol 4,5-bisphosphate and Arf6-regulated membrane traffic. *The Journal of cell biology*, 154(5), 1007-1017. doi:10.1083/jcb.200103107
- Buers, I., Robenek, H., Lorkowski, S., Nitschke, Y., Severs, N. J., & Hofnagel, O. (2009). TIP47, a lipid cargo protein involved in macrophage triglyceride metabolism. *Arterioscler Thromb Vasc Biol*, 29(5), 767-773. doi:10.1161/ATVBAHA.108.182675
- Bukh, J., Purcell, R. H., & Miller, R. H. (1992). Sequence analysis of the 5' noncoding region of hepatitis C virus. *Proc Natl Acad Sci U S A*, 89(11), 4942-4946.
- Bukong, T. N., Momen-Heravi, F., Kodys, K., Bala, S., & Szabo, G. (2014). Exosomes from hepatitis C infected patients transmit HCV infection and contain replication competent viral RNA in complex with Ago2-miR122-HSP90. *PLoS pathogens*, 10(10), e1004424. doi:10.1371/journal.ppat.1004424
- Bulankina, A. V., Deggerich, A., Wenzel, D., Mutenda, K., Wittmann, J. G., Rudolph, M. G., . . . Honing, S. (2009). TIP47 functions in the biogenesis of lipid droplets. *J Cell Biol*, 185(4), 641-655. doi:10.1083/jcb.200812042
- Bull, R. A., Leung, P., Gaudieri, S., Deshpande, P., Cameron, B., Walker, M., . . . Luciani, F. (2015). Transmitted/Founder Viruses Rapidly Escape from CD8+ T Cell Responses in Acute Hepatitis C Virus Infection. *J Virol*, 89(10), 5478-5490. doi:10.1128/JVI.03717-14
- Cabrera, R., Tu, Z., Xu, Y., Firpi, R. J., Rosen, H. R., Liu, C., & Nelson, D. R. (2004). An immunomodulatory role for CD4(+)CD25(+) regulatory T lymphocytes in hepatitis C virus infection. *Hepatology*, 40(5), 1062-1071. doi:10.1002/hep.20454
- Cacoub, P., Commarmond, C., Sadoun, D., & Desbois, A. C. (2017). Hepatitis C Virus Infection and Rheumatic Diseases: The Impact of Direct-Acting Antiviral Agents. *Rheum Dis Clin North Am*, 43(1), 123-132. doi:10.1016/j.rdc.2016.09.011
- Calisher, C. H., Childs, J. E., Field, H. E., Holmes, K. V., & Schountz, T. (2006). Bats: important reservoir hosts of emerging viruses. *Clin Microbiol Rev*, 19(3), 531-545. doi:10.1128/CMR.00017-06
- Camus, G., Herker, E., Modi, A. A., Haas, J. T., Ramage, H. R., Farese, R. V., Jr., & Ott, M. (2013). Diacylglycerol acyltransferase-1 localizes hepatitis C virus NS5A protein to lipid droplets and enhances NS5A interaction with the viral capsid core. *J Biol Chem*, 288(14), 9915-9923. doi:10.1074/jbc.M112.434910
- Camus, G., Schweiger, M., Herker, E., Harris, C., Kondratowicz, A. S., Tsou, C. L., . . . Ott, M. (2014). The hepatitis C virus core protein inhibits adipose triglyceride lipase (ATGL)-mediated lipid mobilization and enhances the ATGL interaction with comparative gene identification 58 (CGI-58) and lipid droplets. *J Biol Chem*, 289(52), 35770-35780. doi:10.1074/jbc.M114.587816

- Carabeo, R. A., Mead, D. J., & Hackstadt, T. (2003). Golgi-dependent transport of cholesterol to the Chlamydia trachomatis inclusion. *Proc Natl Acad Sci U S A*, 100(11), 6771-6776. doi:10.1073/pnas.1131289100
- Carrington, L. B., & Simmons, C. P. (2014). Human to mosquito transmission of dengue viruses. *Front Immunol*, 5, 290. doi:10.3389/fimmu.2014.00290
- Carroll, K. S., Hanna, J., Simon, I., Krise, J., Barbero, P., & Pfeffer, S. R. (2001). Role of Rab9 GTPase in facilitating receptor recruitment by TIP47. *Science*, 292(5520), 1373-1376. doi:10.1126/science.1056791
- Catanese, M. T., & Dorner, M. (2015). Advances in experimental systems to study hepatitis C virus in vitro and in vivo. *Virology*. doi:10.1016/j.virol.2015.03.014
- Catanese, M. T., Loureiro, J., Jones, C. T., Dorner, M., von Hahn, T., & Rice, C. M. (2013). Different requirements for scavenger receptor class B type I in hepatitis C virus cell-free versus cell-to-cell transmission. *Journal of virology*, 87(15), 8282-8293. doi:10.1128/JVI.01102-13
- Catanese, M. T., Uryu, K., Kopp, M., Edwards, T. J., Andrus, L., Rice, W. J., . . . Rice, C. M. (2013). Ultrastructural analysis of hepatitis C virus particles. *Proc Natl Acad Sci U S A*, 110(23), 9505-9510. doi:10.1073/pnas.1307527110
- Cavenagh, M. M., Whitney, J. A., Carroll, K., Zhang, C., Boman, A. L., Rosenwald, A. G., . . . Kahn, R. A. (1996). Intracellular distribution of Arf proteins in mammalian cells. Arf6 is uniquely localized to the plasma membrane. *J Biol Chem*, 271(36), 21767-21774.
- Cermelli, S., Guo, Y., Gross, S. P., & Welte, M. A. (2006). The lipid-droplet proteome reveals that droplets are a protein-storage depot. *Curr Biol*, 16(18), 1783-1795. doi:10.1016/j.cub.2006.07.062
- Chan, J. F., Yip, C. C., Tsang, J. O., Tee, K. M., Cai, J. P., Chik, K. K., . . . Yuen, K. Y. (2016). Differential cell line susceptibility to the emerging Zika virus: implications for disease pathogenesis, non-vector-borne human transmission and animal reservoirs. *Emerg Microbes Infect*, 5, e93. doi:10.1038/emi.2016.99
- Chang, B. H., Li, L., Paul, A., Taniguchi, S., Nannegari, V., Heird, W. C., & Chan, L. (2006). Protection against fatty liver but normal adipogenesis in mice lacking adipose differentiation-related protein. *Mol Cell Biol*, 26(3), 1063-1076. doi:10.1128/MCB.26.3.1063-1076.2006
- Chang, B. H., Li, L., Saha, P., & Chan, L. (2010). Absence of adipose differentiation related protein upregulates hepatic VLDL secretion, relieves hepatosteatosis, and improves whole body insulin resistance in leptin-deficient mice. *J Lipid Res*, 51(8), 2132-2142. doi:10.1194/jlr.M004515
- Chang, K. M., Rehmann, B., McHutchison, J. G., Pasquinelli, C., Southwood, S., Sette, A., & Chisari, F. V. (1997). Immunological significance of cytotoxic T lymphocyte epitope variants in patients chronically infected by the hepatitis C virus. *J Clin Invest*, 100(9), 2376-2385. doi:10.1172/JCI119778
- Chang, K. S., Jiang, J., Cai, Z., & Luo, G. (2007). Human apolipoprotein e is required for infectivity and production of hepatitis C virus in cell culture. *Journal of virology*, 81(24), 13783-13793. doi:10.1128/JVI.01091-07
- Chang, M., Marquardt, A. P., Wood, B. L., Williams, O., Cotler, S. J., Taylor, S. L., . . . Gretch, D. R. (2000). In situ distribution of hepatitis C virus replicative-intermediate

- RNA in hepatic tissue and its correlation with liver disease. *Journal of virology*, 74(2), 944-955.
- Chang, M., Williams, O., Mittler, J., Quintanilla, A., Carithers, R. L., Perkins, J., . . . Gretch, D. R. (2003). Dynamics of Hepatitis C Virus Replication in Human Liver. *The American journal of pathology*, 163(2), 433-444. doi:10.1016/s0002-9440(10)63673-5
- Chardin, P., Paris, S., Antonny, B., Robineau, S., Beraud-Dufour, S., Jackson, C. L., & Chabre, M. (1996). A human exchange factor for ARF contains Sec7- and pleckstrin-homology domains. *Nature*, 384(6608), 481-484. doi:10.1038/384481a0
- Chayanupatkul, M., Omino, R., Mittal, S., Kramer, J. R., Richardson, P., Thrift, A. P., . . . Kanwal, F. (2017). Hepatocellular carcinoma in the absence of cirrhosis in patients with chronic hepatitis B virus infection. *J Hepatol*, 66(2), 355-362. doi:10.1016/j.jhep.2016.09.013
- Chemello, L., Mondelli, M., Bortolotti, F., Schiavon, E., Pontisso, P., Alberti, A., . . . Realdi, G. (1986). Natural killer activity in patients with acute viral hepatitis. *Clin Exp Immunol*, 64(1), 59-64.
- Chen, J. C., Tsai, C. C., & Tzen, J. T. (1999). Cloning and secondary structure analysis of caleosin, a unique calcium-binding protein in oil bodies of plant seeds. *Plant Cell Physiol*, 40(10), 1079-1086.
- Chen, L., Zhao, H., Yang, X., Gao, J. Y., & Cheng, J. (2014). HBsAg-negative hepatitis B virus infection and hepatocellular carcinoma. *Discov Med*, 18(99), 189-193.
- Chen, P., Hubner, W., Spinelli, M. A., & Chen, B. K. (2007). Predominant mode of human immunodeficiency virus transfer between T cells is mediated by sustained Env-dependent neutralization-resistant virological synapses. *J Virol*, 81(22), 12582-12595. doi:10.1128/JVI.00381-07
- Cheng, F. K., Torres, D. M., & Harrison, S. A. (2014). Hepatitis C and lipid metabolism, hepatic steatosis, and NAFLD: still important in the era of direct acting antiviral therapy? *Journal of viral hepatitis*, 21(1), 1-8. doi:10.1111/jvh.12172
- Chevaliez, S. (2011). Antiviral activity of the new DAAs for the treatment of hepatitis C virus infection: virology and resistance. *Clin Res Hepatol Gastroenterol*, 35 Suppl 2, S46-51. doi:10.1016/S2210-7401(11)70007-9
- Chevaliez, S., & Pawlotsky, J. M. (2009). How to use virological tools for optimal management of chronic hepatitis C. *Liver Int*, 29 Suppl 1, 9-14. doi:10.1111/j.1478-3231.2008.01926.x
- Chu, C. M., Yeh, C. T., & Liaw, Y. F. (1999). Fulminant hepatic failure in acute hepatitis C: increased risk in chronic carriers of hepatitis B virus. *Gut*, 45(4), 613-617.
- Claude, A., Zhao, B. P., Kuziemy, C. E., Dahan, S., Berger, S. J., Yan, J. P., . . . Melancon, P. (1999). GBF1: A novel Golgi-associated BFA-resistant guanine nucleotide exchange factor that displays specificity for ADP-ribosylation factor 5. *J Cell Biol*, 146(1), 71-84.
- Clyde, K., Kyle, J. L., & Harris, E. (2006). Recent advances in deciphering viral and host determinants of dengue virus replication and pathogenesis. *J Virol*, 80(23), 11418-11431. doi:10.1128/JVI.01257-06
- Cocchiaro, J. L., Kumar, Y., Fischer, E. R., Hackstadt, T., & Valdivia, R. H. (2008). Cytoplasmic lipid droplets are translocated into the lumen of the Chlamydia

- trachomatis parasitophorous vacuole. *Proc Natl Acad Sci U S A*, 105(27), 9379-9384. doi:10.1073/pnas.0712241105
- Cockcroft, S., Thomas, G. M., Fensome, A., Geny, B., Cunningham, E., Gout, I., . . . Hsuan, J. J. (1994). Phospholipase D: a downstream effector of ARF in granulocytes. *Science*, 263(5146), 523-526.
- Cole, N. B., Murphy, D. D., Grider, T., Rueter, S., Brasaemle, D., & Nussbaum, R. L. (2002). Lipid droplet binding and oligomerization properties of the Parkinson's disease protein alpha-synuclein. *J Biol Chem*, 277(8), 6344-6352. doi:10.1074/jbc.M108414200
- Coller, K. E., Heaton, N. S., Berger, K. L., Cooper, J. D., Saunders, J. L., & Randall, G. (2012). Molecular determinants and dynamics of hepatitis C virus secretion. *PLoS Pathog*, 8(1), e1002466. doi:10.1371/journal.ppat.1002466
- Colpitts, C. C., & Schang, L. M. (2014). A small molecule inhibits virion attachment to heparan sulfate- or sialic acid-containing glycans. *Journal of virology*. doi:10.1128/JVI.00896-14
- Corless, L., Crump, C. M., Griffin, S. D., & Harris, M. (2010). Vps4 and the ESCRT-III complex are required for the release of infectious hepatitis C virus particles. *J Gen Virol*, 91(Pt 2), 362-372. doi:10.1099/vir.0.017285-0
- Counihan, N. A., Rawlinson, S. M., & Lindenbach, B. D. (2011). Trafficking of hepatitis C virus core protein during virus particle assembly. *PLoS Pathog*, 7(10), e1002302. doi:10.1371/journal.ppat.1002302
- Crossingham, J. L., Jenkinson, J., Woolridge, N., Gallinger, S., Tait, G. A., & Moulton, C. A. (2009). Interpreting three-dimensional structures from two-dimensional images: a web-based interactive 3D teaching model of surgical liver anatomy. *HPB (Oxford)*, 11(6), 523-528. doi:10.1111/j.1477-2574.2009.00097.x
- Crunk, A. E., Monks, J., Murakami, A., Jackman, M., Maclean, P. S., Ladinsky, M., . . . McManaman, J. L. (2013). Dynamic regulation of hepatic lipid droplet properties by diet. *PLoS One*, 8(7), e67631. doi:10.1371/journal.pone.0067631
- Cukierman, E., Huber, I., Rotman, M., & Cassel, D. (1995). The ARF1 GTPase-activating protein: zinc finger motif and Golgi complex localization. *Science*, 270(5244), 1999-2002.
- Cun, W., Jiang, J., & Luo, G. (2010). The C-terminal alpha-helix domain of apolipoprotein E is required for interaction with nonstructural protein 5A and assembly of hepatitis C virus. *J Virol*, 84(21), 11532-11541. doi:10.1128/JVI.01021-10
- D'Angelo, G., Polishchuk, E., Di Tullio, G., Santoro, M., Di Campli, A., Godi, A., . . . De Matteis, M. A. (2007). Glycosphingolipid synthesis requires FAPP2 transfer of glucosylceramide. *Nature*, 449(7158), 62-67. doi:10.1038/nature06097
- D'Aquila, T., Sirohi, D., Grabowski, J. M., Hedrick, V. E., Paul, L. N., Greenberg, A. S., . . . Buhman, K. K. (2015). Characterization of the proteome of cytoplasmic lipid droplets in mouse enterocytes after a dietary fat challenge. *PLoS One*, 10(5), e0126823. doi:10.1371/journal.pone.0126823
- D'Souza-Schorey, C., Li, G., Colombo, M. I., & Stahl, P. D. (1995). A regulatory role for ARF6 in receptor-mediated endocytosis. *Science*, 267(5201), 1175-1178.
- Dahlhoff, M., Frohlich, T., Arnold, G. J., Muller, U., Leonhardt, H., Zouboulis, C. C., & Schneider, M. R. (2015). Characterization of the sebocyte lipid droplet proteome

- reveals novel potential regulators of sebaceous lipogenesis. *Exp Cell Res*, 332(1), 146-155. doi:10.1016/j.yexcr.2014.12.004
- Daniel, J., Deb, C., Dubey, V. S., Sirakova, T. D., Abomoelak, B., Morbidoni, H. R., & Kolattukudy, P. E. (2004). Induction of a novel class of diacylglycerol acyltransferases and triacylglycerol accumulation in *Mycobacterium tuberculosis* as it goes into a dormancy-like state in culture. *J Bacteriol*, 186(15), 5017-5030. doi:10.1128/JB.186.15.5017-5030.2004
- Danielsson, A., Palanisamy, N., Golbob, S., Yin, H., Blomberg, J., Hedlund, J., . . . Lennerstrand, J. (2014). Transmission of hepatitis C virus among intravenous drug users in the Uppsala region of Sweden. *Infect Ecol Epidemiol*, 4. doi:10.3402/iee.v4.22251
- Dascher, C., & Balch, W. E. (1994). Dominant inhibitory mutants of ARF1 block endoplasmic reticulum to Golgi transport and trigger disassembly of the Golgi apparatus. *J Biol Chem*, 269(2), 1437-1448.
- de Gottardi, A., Paziienza, V., Pugnale, P., Bruttin, F., Rubbia-Brandt, L., Juge-Aubry, C. E., . . . Negro, F. (2006). Peroxisome proliferator-activated receptor-alpha and -gamma mRNA levels are reduced in chronic hepatitis C with steatosis and genotype 3 infection. *Alimentary pharmacology & therapeutics*, 23(1), 107-114. doi:10.1111/j.1365-2036.2006.02729.x
- de Jong, Y. P., Dorner, M., Mommersteeg, M. C., Xiao, J. W., Balazs, A. B., Robbins, J. B., . . . Ploss, A. (2014). Broadly neutralizing antibodies abrogate established hepatitis C virus infection. *Sci Transl Med*, 6(254), 254ra129. doi:10.1126/scitranslmed.3009512
- De Maria, A., Fogli, M., Mazza, S., Basso, M., Picciotto, A., Costa, P., . . . Moretta, L. (2007). Increased natural cytotoxicity receptor expression and relevant IL-10 production in NK cells from chronically infected viremic HCV patients. *Eur J Immunol*, 37(2), 445-455. doi:10.1002/eji.200635989
- De Matteis, M. A., & Godi, A. (2004). Protein-lipid interactions in membrane trafficking at the Golgi complex. *Biochim Biophys Acta*, 1666(1-2), 264-274. doi:10.1016/j.bbamem.2004.07.002
- De Miranda, M. A., Jr., Schlater, A. E., Green, T. L., & Kanatous, S. B. (2012). In the face of hypoxia: myoglobin increases in response to hypoxic conditions and lipid supplementation in cultured Weddell seal skeletal muscle cells. *J Exp Biol*, 215(Pt 5), 806-813. doi:10.1242/jeb.060681
- Debiaggi, M., Spinillo, A., Zara, F., Santolo, A., Brerra, R., Maserati, R., . . . Filice, G. (1999). Quantitative assessment of cell-associated and cell-free virus in cervicovaginal samples of HIV-1-infected women. *Clin Microbiol Infect*, 5(10), 605-611. doi:10.1111/j.1469-0691.1999.tb00416.x
- Decaens, C., Durand, M., Grosse, B., & Cassio, D. (2008). Which in vitro models could be best used to study hepatocyte polarity? *Biol Cell*, 100(7), 387-398. doi:10.1042/BC20070127
- Devhare, P. B., Sasaki, R., Shrivastava, S., Di Bisceglie, A. M., Ray, R., & Ray, R. B. (2017). Exosome-Mediated Intercellular Communication between Hepatitis C Virus-Infected Hepatocytes and Hepatic Stellate Cells. *Journal of virology*, 91(6). doi:10.1128/JVI.02225-16

- Di Lorenzo, C., Angus, A. G., & Patel, A. H. (2011). Hepatitis C virus evasion mechanisms from neutralizing antibodies. *Viruses*, 3(11), 2280-2300. doi:10.3390/v3112280
- Diamond, D. L., Syder, A. J., Jacobs, J. M., Sorensen, C. M., Walters, K. A., Prohl, S. C., . . . Katze, M. G. (2010). Temporal proteome and lipidome profiles reveal hepatitis C virus-associated reprogramming of hepatocellular metabolism and bioenergetics. *PLoS pathogens*, 6(1), e1000719. doi:10.1371/journal.ppat.1000719
- Diao, J., Pantua, H., Ngu, H., Komuves, L., Diehl, L., Schaefer, G., & Kapadia, S. B. (2012). Hepatitis C virus induces epidermal growth factor receptor activation via CD81 binding for viral internalization and entry. *J Virol*, 86(20), 10935-10949. doi:10.1128/JVI.00750-12
- Diaz, E., & Pfeffer, S. R. (1998). TIP47: a cargo selection device for mannose 6-phosphate receptor trafficking. *Cell*, 93(3), 433-443.
- Dienstag, J. L., & Alter, H. J. (1986). Non-A, non-B hepatitis: evolving epidemiologic and clinical perspective. *Semin Liver Dis*, 6(1), 67-81. doi:10.1055/s-2008-1040795
- Diepolder, H. M., Zachoval, R., Hoffmann, R. M., Wierenga, E. A., Santantonio, T., Jung, M. C., . . . Pape, G. R. (1995). Possible mechanism involving T-lymphocyte response to non-structural protein 3 in viral clearance in acute hepatitis C virus infection. *Lancet*, 346(8981), 1006-1007.
- Dimitrova, M., Imbert, I., Kieny, M. P., & Schuster, C. (2003). Protein-protein interactions between hepatitis C virus nonstructural proteins. *J Virol*, 77(9), 5401-5414.
- Ding, Q., Huang, B., Lu, J., Liu, Y. J., & Zhong, J. (2012). Hepatitis C virus NS3/4A protease blocks IL-28 production. *Eur J Immunol*, 42(9), 2374-2382. doi:10.1002/eji.201242388
- Dolganiuc, A., Garcia, C., Kodys, K., & Szabo, G. (2006). Distinct Toll-like receptor expression in monocytes and T cells in chronic HCV infection. *World J Gastroenterol*, 12(8), 1198-1204.
- Donaldson, J. G., & Jackson, C. L. (2011). ARF family G proteins and their regulators: roles in membrane transport, development and disease. *Nature reviews. Molecular cell biology*, 12(6), 362-375. doi:10.1038/nrm3117
- Dorner, M., & Ploss, A. (2011). Deconstructing hepatitis C virus infection in humanized mice. *Ann N Y Acad Sci*, 1245, 59-62. doi:10.1111/j.1749-6632.2011.06317.x
- Dorner, M., Rice, C. M., & Ploss, A. (2013). Study of hepatitis C virus entry in genetically humanized mice. *Methods*, 59(2), 249-257. doi:10.1016/j.ymeth.2012.05.010
- Dowd, K. A., Netski, D. M., Wang, X. H., Cox, A. L., & Ray, S. C. (2009). Selection pressure from neutralizing antibodies drives sequence evolution during acute infection with hepatitis C virus. *Gastroenterology*, 136(7), 2377-2386. doi:10.1053/j.gastro.2009.02.080
- Doyle, J. S., Hellard, M. E., & Thompson, A. J. (2012). The role of viral and host genetics in natural history and treatment of chronic HCV infection. *Best Pract Res Clin Gastroenterol*, 26(4), 413-427. doi:10.1016/j.bpg.2012.09.004
- Ducharme, N. A., & Bickel, P. E. (2008). Lipid droplets in lipogenesis and lipolysis. *Endocrinology*, 149(3), 942-949. doi:10.1210/en.2007-1713
- Durham, N. D., & Chen, B. K. (2015). HIV-1 Cell-Free and Cell-to-Cell Infections Are Differentially Regulated by Distinct Determinants in the Env gp41 Cytoplasmic Tail. *J Virol*, 89(18), 9324-9337. doi:10.1128/JVI.00655-15

- Egger, D., Wolk, B., Gosert, R., Bianchi, L., Blum, H. E., Moradpour, D., & Bienz, K. (2002). Expression of hepatitis C virus proteins induces distinct membrane alterations including a candidate viral replication complex. *Journal of virology*, 76(12), 5974-5984.
- Eggert, D., Rosch, K., Reimer, R., & Herker, E. (2014). Visualization and analysis of hepatitis C virus structural proteins at lipid droplets by super-resolution microscopy. *PLoS One*, 9(7), e102511. doi:10.1371/journal.pone.0102511
- Eichmann, T. O., Grumet, L., Taschler, U., Hartler, J., Heier, C., Woblistin, A., . . . Lass, A. (2015). ATGL and CGI-58 are lipid droplet proteins of the hepatic stellate cell line HSC-T6. *J Lipid Res*, 56(10), 1972-1984. doi:10.1194/jlr.M062372
- El-Hage, N., & Luo, G. (2003). Replication of hepatitis C virus RNA occurs in a membrane-bound replication complex containing nonstructural viral proteins and RNA. *J Gen Virol*, 84(Pt 10), 2761-2769. doi:10.1099/vir.0.19305-0
- El-Kamary, S. S., Hashem, M., Saleh, D. A., Abdelwahab, S. F., Sobhy, M., Shebl, F. M., . . . Shata, M. T. (2013). Hepatitis C virus-specific cell-mediated immune responses in children born to mothers infected with hepatitis C virus. *J Pediatr*, 162(1), 148-154. doi:10.1016/j.jpeds.2012.06.057
- El-Serag, H. B. (2012). Epidemiology of viral hepatitis and hepatocellular carcinoma. *Gastroenterology*, 142(6), 1264-1273 e1261. doi:10.1053/j.gastro.2011.12.061
- Elong, E. N., Soni, K. G., Bui, Q. T., Sougrat, R., Golinelli-Cohen, M. P., & Jackson, C. L. (2011). Interaction between the triglyceride lipase ATGL and the Arf1 activator GBF1. *PloS one*, 6(7), e21889. doi:10.1371/journal.pone.0021889
- Evans, M. J., Rice, C. M., & Goff, S. P. (2004). Phosphorylation of hepatitis C virus nonstructural protein 5A modulates its protein interactions and viral RNA replication. *Proceedings of the National Academy of Sciences of the United States of America*, 101(35), 13038-13043. doi:10.1073/pnas.0405152101
- Evans, M. J., von Hahn, T., Tscherne, D. M., Syder, A. J., Panis, M., Wolk, B., . . . Rice, C. M. (2007). Claudin-1 is a hepatitis C virus co-receptor required for a late step in entry. *Nature*, 446(7137), 801-805. doi:10.1038/nature05654
- Falade-Nwulia, O., Suarez-Cuervo, C., Nelson, D. R., Fried, M. W., Segal, J. B., & Sulkowski, M. S. (2017). Oral Direct-Acting Agent Therapy for Hepatitis C Virus Infection: A Systematic Review. *Ann Intern Med*, 166(9), 637-648. doi:10.7326/M16-2575
- Fan, H., Qiao, L., Kang, K. D., Fan, J., Wei, W., & Luo, G. (2017a). Attachment and Post-Attachment Receptors Important for Hepatitis C Virus Infection and Cell-to-Cell Transmission. *Journal of virology*. doi:10.1128/JVI.00280-17
- Fan, H., Qiao, L., Kang, K. D., Fan, J., Wei, W., & Luo, G. (2017b). Attachment and Postattachment Receptors Important for Hepatitis C Virus Infection and Cell-to-Cell Transmission. *Journal of virology*, 91(13). doi:10.1128/JVI.00280-17
- Farci, P., Alter, H. J., Shimoda, A., Govindarajan, S., Cheung, L. C., Melpolder, J. C., . . . Purcell, R. H. (1996). Hepatitis C virus-associated fulminant hepatic failure. *N Engl J Med*, 335(9), 631-634. doi:10.1056/NEJM199608293350904
- Farci, P., Shimoda, A., Wong, D., Cabezon, T., De Gioannis, D., Strazzer, A., . . . Purcell, R. H. (1996). Prevention of hepatitis C virus infection in chimpanzees by hyperimmune serum against the hypervariable region 1 of the envelope 2 protein. *Proc Natl Acad Sci U S A*, 93(26), 15394-15399.



- Farhat, R., Goueslain, L., Wychowski, C., Belouzard, S., Feneant, L., Jackson, C. L., . . . Rouille, Y. (2013). Hepatitis C virus replication and Golgi function in brefeldin A-resistant hepatoma-derived cells. *PloS one*, 8(9), e74491. doi:10.1371/journal.pone.0074491
- Farhat, R., Seron, K., Ferlin, J., Feneant, L., Belouzard, S., Goueslain, L., . . . Rouille, Y. (2016). Identification of class II ADP-ribosylation factors as cellular factors required for hepatitis C virus replication. *Cellular microbiology*, 18(8), 1121-1133. doi:10.1111/cmi.12572
- Fauny, J. D., Silber, J., & Zider, A. (2005). Drosophila Lipid Storage Droplet 2 gene (Lsd-2) is expressed and controls lipid storage in wing imaginal discs. *Dev Dyn*, 232(3), 725-732. doi:10.1002/dvdy.20277
- Fei, W., Shui, G., Zhang, Y., Krahmer, N., Ferguson, C., Kapterian, T. S., . . . Yang, H. (2011). A role for phosphatidic acid in the formation of "supersized" lipid droplets. *PLoS Genet*, 7(7), e1002201. doi:10.1371/journal.pgen.1002201
- Feinstone, S. M., Kapikian, A. Z., & Purceli, R. H. (1973). Hepatitis A: detection by immune electron microscopy of a viruslike antigen associated with acute illness. *Science*, 182(4116), 1026-1028.
- Ferguson, D., Zhang, J., Davis, M. A., Helsley, R. N., Vedin, L. L., Lee, R. G., . . . Brown, J. M. (2017). The lipid droplet-associated protein perilipin 3 facilitates hepatitis C virus-driven hepatic steatosis. *Journal of lipid research*, 58(2), 420-432. doi:10.1194/jlr.M073734
- Ferraris, P., Blanchard, E., & Roingeard, P. (2010). Ultrastructural and biochemical analyses of hepatitis C virus-associated host cell membranes. *The Journal of general virology*, 91(Pt 9), 2230-2237. doi:10.1099/vir.0.022186-0
- Ferreira, T., Regnacq, M., Alimardani, P., Moreau-Vauzelle, C., & Berges, T. (2004). Lipid dynamics in yeast under haem-induced unsaturated fatty acid and/or sterol depletion. *Biochem J*, 378(Pt 3), 899-908. doi:10.1042/BJ20031064
- Fields, K. A., & Hackstadt, T. (2002). The chlamydial inclusion: escape from the endocytic pathway. *Annu Rev Cell Dev Biol*, 18, 221-245. doi:10.1146/annurev.cellbio.18.012502.105845
- Filipe, A., & McLauchlan, J. (2015). Hepatitis C virus and lipid droplets: finding a niche. *Trends in molecular medicine*, 21(1), 34-42. doi:10.1016/j.molmed.2014.11.003
- Flisiak, R., Jaroszewicz, J., & Parfieniuk-Kowerda, A. (2013). Emerging treatments for hepatitis C. *Expert Opin Emerg Drugs*, 18(4), 461-475. doi:10.1517/14728214.2013.847089
- Fofana, I., Xiao, F., Thumann, C., Turek, M., Zona, L., Tawar, R. G., . . . Baumert, T. F. (2013). A novel monoclonal anti-CD81 antibody produced by genetic immunization efficiently inhibits Hepatitis C virus cell-cell transmission. *PloS one*, 8(5), e64221. doi:10.1371/journal.pone.0064221
- Forton, D. M., Thomas, H. C., & Taylor-Robinson, S. D. (2004). Central nervous system involvement in hepatitis C virus infection. *Metab Brain Dis*, 19(3-4), 383-391.
- Fowke, K. R., Nagelkerke, N. J., Kimani, J., Simonsen, J. N., Anzala, A. O., Bwayo, J. J., . . . Plummer, F. A. (1996). Resistance to HIV-1 infection among persistently seronegative prostitutes in Nairobi, Kenya. *Lancet*, 348(9038), 1347-1351. doi:10.1016/S0140-6736(95)12269-2

- Foxton, M. R., Quaglia, A., Muiesan, P., Heneghan, M. A., Portmann, B., Norris, S., . . . O'Grady, J. G. (2006). The impact of diabetes mellitus on fibrosis progression in patients transplanted for hepatitis C. *Am J Transplant*, 6(8), 1922-1929. doi:10.1111/j.1600-6143.2006.01408.x
- Foy, E., Li, K., Sumpter, R., Jr., Loo, Y. M., Johnson, C. L., Wang, C., . . . Gale, M., Jr. (2005). Control of antiviral defenses through hepatitis C virus disruption of retinoic acid-inducible gene-I signaling. *Proc Natl Acad Sci U S A*, 102(8), 2986-2991. doi:10.1073/pnas.0408707102
- Freeman, A. J., Dore, G. J., Law, M. G., Thorpe, M., Von Overbeck, J., Lloyd, A. R., . . . Kaldor, J. M. (2001). Estimating progression to cirrhosis in chronic hepatitis C virus infection. *Hepatology*, 34(4 Pt 1), 809-816. doi:10.1053/jhep.2001.27831
- Freeman, A. J., Ffrench, R. A., Post, J. J., Harvey, C. E., Gilmour, S. J., White, P. A., . . . Lloyd, A. R. (2004). Prevalence of production of virus-specific interferon-gamma among seronegative hepatitis C-resistant subjects reporting injection drug use. *J Infect Dis*, 190(6), 1093-1097. doi:10.1086/422605
- Fridell, R. A., Qiu, D., Valera, L., Wang, C., Rose, R. E., & Gao, M. (2011). Distinct functions of NS5A in hepatitis C virus RNA replication uncovered by studies with the NS5A inhibitor BMS-790052. *J Virol*, 85(14), 7312-7320. doi:10.1128/JVI.00253-11
- Friebe, P., Boudet, J., Simorre, J. P., & Bartenschlager, R. (2005). Kissing-loop interaction in the 3' end of the hepatitis C virus genome essential for RNA replication. *J Virol*, 79(1), 380-392. doi:10.1128/JVI.79.1.380-392.2005
- Gale, M., Jr., Blakely, C. M., Kwieciszewski, B., Tan, S. L., Dossett, M., Tang, N. M., . . . Katze, M. G. (1998). Control of PKR protein kinase by hepatitis C virus nonstructural 5A protein: molecular mechanisms of kinase regulation. *Molecular and cellular biology*, 18(9), 5208-5218.
- Galossi, A., Guarisco, R., Bellis, L., & Puoti, C. (2007). Extrahepatic manifestations of chronic HCV infection. *J Gastrointest Liver Dis*, 16(1), 65-73.
- Gannon, J., Fernandez-Rodriguez, J., Alamri, H., Feng, S. B., Kalantari, F., Negi, S., . . . Nilsson, T. (2014). ARFGAP1 Is Dynamically Associated with Lipid Droplets in Hepatocytes. *PLoS one*, 9(11), e111309. doi:10.1371/journal.pone.0111309
- Garcia, A., Sekowski, A., Subramanian, V., & Brasaemle, D. L. (2003). The central domain is required to target and anchor perilipin A to lipid droplets. *The Journal of biological chemistry*, 278(1), 625-635. doi:10.1074/jbc.M206602200
- Gastaminza, P., Cheng, G., Wieland, S., Zhong, J., Liao, W., & Chisari, F. V. (2008a). Cellular determinants of hepatitis C virus assembly, maturation, degradation, and secretion. *J Virol*, 82(5), 2120-2129. doi:10.1128/JVI.02053-07
- Gastaminza, P., Cheng, G., Wieland, S., Zhong, J., Liao, W., & Chisari, F. V. (2008b). Cellular determinants of hepatitis C virus assembly, maturation, degradation, and secretion. *Journal of virology*, 82(5), 2120-2129. doi:10.1128/JVI.02053-07
- Gastaminza, P., Dryden, K. A., Boyd, B., Wood, M. R., Law, M., Yeager, M., & Chisari, F. V. (2010). Ultrastructural and biophysical characterization of hepatitis C virus particles produced in cell culture. *J Virol*, 84(21), 10999-11009. doi:10.1128/JVI.00526-10

- Gastaminza, P., Kapadia, S. B., & Chisari, F. V. (2006a). Differential biophysical properties of infectious intracellular and secreted hepatitis C virus particles. *Journal of virology*, 80(22), 11074-11081. doi:10.1128/JVI.01150-06
- Gastaminza, P., Kapadia, S. B., & Chisari, F. V. (2006b). Differential biophysical properties of infectious intracellular and secreted hepatitis C virus particles. *J Virol*, 80(22), 11074-11081. doi:10.1128/JVI.01150-06
- Gentzsch, J., Brohm, C., Steinmann, E., Friesland, M., Menzel, N., Vieyres, G., . . . Pietschmann, T. (2013). hepatitis c Virus p7 is critical for capsid assembly and envelopment. *PLoS Pathog*, 9(5), e1003355. doi:10.1371/journal.ppat.1003355
- Gerlach, J. T., Diepolder, H., & Pape, G. R. (1999). Determination of Hepatitis C Virus-Specific CD4(+) T-Cell Activity in PBMC. *Methods Mol Med*, 19, 413-422. doi:10.1385/0-89603-521-2:413
- Gibbons, H. S., Lin, S., Cotter, R. J., & Raetz, C. R. (2000). Oxygen requirement for the biosynthesis of the S-2-hydroxymyristate moiety in Salmonella typhimurium lipid A. Function of LpxO, A new Fe<sup>2+</sup>/alpha-ketoglutarate-dependent dioxygenase homologue. *J Biol Chem*, 275(42), 32940-32949. doi:10.1074/jbc.M005779200
- Goffard, A., Callens, N., Bartosch, B., Wychowski, C., Cosset, F. L., Montpellier, C., & Dubuisson, J. (2005). Role of N-linked glycans in the functions of hepatitis C virus envelope glycoproteins. *J Virol*, 79(13), 8400-8409. doi:10.1128/JVI.79.13.8400-8409.2005
- Goldberg, J. (1998). Structural basis for activation of ARF GTPase: mechanisms of guanine nucleotide exchange and GTP-myristoyl switching. *Cell*, 95(2), 237-248.
- Golden-Mason, L., Cox, A. L., Randall, J. A., Cheng, L., & Rosen, H. R. (2010). Increased natural killer cell cytotoxicity and NKp30 expression protects against hepatitis C virus infection in high-risk individuals and inhibits replication in vitro. *Hepatology*, 52(5), 1581-1589. doi:10.1002/hep.23896
- Gommel, D. U., Memon, A. R., Heiss, A., Lottspeich, F., Pfannstiel, J., Lechner, J., . . . Wieland, F. T. (2001). Recruitment to Golgi membranes of ADP-ribosylation factor 1 is mediated by the cytoplasmic domain of p23. *EMBO J*, 20(23), 6751-6760. doi:10.1093/emboj/20.23.6751
- Gondar, V., Molina-Jimenez, F., Hishiki, T., Garcia-Buey, L., Koutsoudakis, G., Shimotohno, K., . . . Majano, P. L. (2015). Apolipoprotein E, but not Apolipoprotein B, is essential for efficient HCV cell-to-cell transmission. *Journal of virology*. doi:10.1128/JVI.00577-15
- Gosálvez, J., Rodríguez-Inigo, E., Ramiro-Díaz, J. L., Bartolomé, J., Tomás, J. F., Oliva, H., & Carreno, V. (1998). Relative quantification and mapping of hepatitis C virus by in situ hybridization and digital image analysis. *Hepatology*, 27(5), 1428-1434. doi:10.1002/hep.510270534
- Gottwein, J. M., Scheel, T. K., Jensen, T. B., Lademann, J. B., Prentoe, J. C., Knudsen, M. L., . . . Bukh, J. (2009). Development and characterization of hepatitis C virus genotype 1-7 cell culture systems: role of CD81 and scavenger receptor class B type I and effect of antiviral drugs. *Hepatology*, 49(2), 364-377. doi:10.1002/hep.22673
- Goueslain, L., Alsaleh, K., Horellou, P., Roingeard, P., Descamps, V., Duverlie, G., . . . Rouille, Y. (2010). Identification of GBF1 as a cellular factor required for hepatitis

- C virus RNA replication. *Journal of virology*, 84(2), 773-787. doi:10.1128/JVI.01190-09
- Granneman, J. G., Moore, H. P., Krishnamoorthy, R., & Rathod, M. (2009). Perilipin controls lipolysis by regulating the interactions of AB-hydrolase containing 5 (Abhd5) and adipose triglyceride lipase (Atgl). *The Journal of biological chemistry*, 284(50), 34538-34544. doi:10.1074/jbc.M109.068478
- Grant, B. D., & Donaldson, J. G. (2009). Pathways and mechanisms of endocytic recycling. *Nat Rev Mol Cell Biol*, 10(9), 597-608. doi:10.1038/nrm2755
- Grebely, J., Petoumenos, K., Hellard, M., Matthews, G. V., Suppiah, V., Applegate, T., . . . Group, A. S. (2010). Potential role for interleukin-28B genotype in treatment decision-making in recent hepatitis C virus infection. *Hepatology*, 52(4), 1216-1224. doi:10.1002/hep.23850
- Grippa, A., Buxo, L., Mora, G., Funaya, C., Idrissi, F. Z., Mancuso, F., . . . Carvalho, P. (2015). The seipin complex Fld1/Ldb16 stabilizes ER-lipid droplet contact sites. *J Cell Biol*, 211(4), 829-844. doi:10.1083/jcb.201502070
- Gross, D. A., Zhan, C., & Silver, D. L. (2011). Direct binding of triglyceride to fat storage-inducing transmembrane proteins 1 and 2 is important for lipid droplet formation. *Proceedings of the National Academy of Sciences of the United States of America*, 108(49), 19581-19586. doi:10.1073/pnas.1110817108
- Grove, J., Nielsen, S., Zhong, J., Bassendine, M. F., Drummer, H. E., Balfe, P., & McKeating, J. A. (2008). Identification of a residue in hepatitis C virus E2 glycoprotein that determines scavenger receptor BI and CD81 receptor dependency and sensitivity to neutralizing antibodies. *J Virol*, 82(24), 12020-12029. doi:10.1128/JVI.01569-08
- Gruner, N. H., Gerlach, T. J., Jung, M. C., Diepolder, H. M., Schirren, C. A., Schraut, W. W., . . . Pape, G. R. (2000). Association of hepatitis C virus-specific CD8+ T cells with viral clearance in acute hepatitis C. *J Infect Dis*, 181(5), 1528-1536. doi:10.1086/315450
- Guo, Y., Walther, T. C., Rao, M., Stuurman, N., Goshima, G., Terayama, K., . . . Farese, R. V. (2008). Functional genomic screen reveals genes involved in lipid-droplet formation and utilization. *Nature*, 453(7195), 657-661. doi:10.1038/nature06928
- Gutti, T. L., Knibbe, J. S., Makarov, E., Zhang, J., Yannam, G. R., Gorantla, S., . . . Poluektova, L. Y. (2014). Human hepatocytes and hematolymphoid dual reconstitution in treosulfan-conditioned uPA-NOG mice. *Am J Pathol*, 184(1), 101-109. doi:10.1016/j.ajpath.2013.09.008
- Haas, A. K., Yoshimura, S., Stephens, D. J., Preisinger, C., Fuchs, E., & Barr, F. A. (2007). Analysis of GTPase-activating proteins: Rab1 and Rab43 are key Rabs required to maintain a functional Golgi complex in human cells. *J Cell Sci*, 120(Pt 17), 2997-3010. doi:10.1242/jcs.014225
- Hajarizadeh, B., Grebely, J., Applegate, T., Matthews, G. V., Amin, J., Petoumenos, K., . . . group, A. s. (2014). Dynamics of HCV RNA levels during acute hepatitis C virus infection. *Journal of medical virology*, 86(10), 1722-1729. doi:10.1002/jmv.24010
- Hall, A. J. (2010). Boosters for hepatitis B vaccination? Need for an evidence-based policy. *Hepatology*, 51(5), 1485-1486. doi:10.1002/hep.23674

- Hall, A. M., Brunt, E. M., Chen, Z., Viswakarma, N., Reddy, J. K., Wolins, N. E., & Finck, B. N. (2010). Dynamic and differential regulation of proteins that coat lipid droplets in fatty liver dystrophic mice. *J Lipid Res*, 51(3), 554-563. doi:10.1194/jlr.M000976
- Hamamoto, I., Nishimura, Y., Okamoto, T., Aizaki, H., Liu, M., Mori, Y., . . . Matsuura, Y. (2005). Human VAP-B is involved in hepatitis C virus replication through interaction with NS5A and NS5B. *Journal of virology*, 79(21), 13473-13482. doi:10.1128/JVI.79.21.13473-13482.2005
- Han, Y., Niu, J., Wang, D., & Li, Y. (2016). Hepatitis C Virus Protein Interaction Network Analysis Based on Hepatocellular Carcinoma. *PLoS One*, 11(4), e0153882. doi:10.1371/journal.pone.0153882
- Hanna, J., Carroll, K., & Pfeffer, S. R. (2002). Identification of residues in TIP47 essential for Rab9 binding. *Proc Natl Acad Sci U S A*, 99(11), 7450-7454. doi:10.1073/pnas.112198799
- Hansen, J. P., Falconer, J. A., Hamilton, J. D., & Herpok, F. J. (1981). Hepatitis B in a medical center. *J Occup Med*, 23(5), 338-342.
- Hansurabhanon, T., Jiraphongsa, C., Tunsakun, P., Sukbunsung, R., Bunyamanee, B., Kuirat, P., . . . Poovorawan, Y. (2002). Infection with hepatitis C virus among intravenous-drug users: prevalence, genotypes and risk-factor-associated behaviour patterns in Thailand. *Ann Trop Med Parasitol*, 96(6), 615-625. doi:10.1179/000349802125001465
- Harris, H. J., Farquhar, M. J., Mee, C. J., Davis, C., Reynolds, G. M., Jennings, A., . . . McKeating, J. A. (2008). CD81 and claudin 1 coreceptor association: role in hepatitis C virus entry. *Journal of virology*, 82(10), 5007-5020. doi:10.1128/JVI.02286-07
- Hartler, J., Kofeler, H. C., Trotschmuller, M., Thallinger, G. G., & Spener, F. (2014). Assessment of lipidomic species in hepatocyte lipid droplets from stressed mouse models. *Sci Data*, 1, 140051. doi:10.1038/sdata.2014.51
- Haruna, Y., Hayashi, N., Hiramatsu, N., Takehara, T., Hagiwara, H., Sasaki, Y., . . . Kamada, T. (1993). Detection of hepatitis C virus RNA in liver tissues by an in situ hybridization technique. *J Hepatol*, 18(1), 96-100.
- Hasebe, R., Suzuki, T., Makino, Y., Igarashi, M., Yamanouchi, S., Maeda, A., . . . Kimura, T. (2010). Transcellular transport of West Nile virus-like particles across human endothelial cells depends on residues 156 and 159 of envelope protein. *BMC Microbiol*, 10, 165. doi:10.1186/1471-2180-10-165
- Hashem, M., El-Karaksy, H., Shata, M. T., Sobhy, M., Helmy, H., El-Naghi, S., . . . El-Kamary, S. S. (2011). Strong hepatitis C virus (HCV)-specific cell-mediated immune responses in the absence of viremia or antibodies among uninfected siblings of HCV chronically infected children. *J Infect Dis*, 203(6), 854-861. doi:10.1093/infdis/jiq123
- Hayashi, N., & Takehara, T. (2006). Antiviral therapy for chronic hepatitis C: past, present, and future. *Journal of gastroenterology*, 41(1), 17-27. doi:10.1007/s00535-005-1740-7
- Heaton, N. S., Perera, R., Berger, K. L., Khadka, S., Lacount, D. J., Kuhn, R. J., & Randall, G. (2010). Dengue virus nonstructural protein 3 redistributes fatty acid synthase to sites of viral replication and increases cellular fatty acid synthesis. *Proc Natl Acad Sci U S A*, 107(40), 17345-17350. doi:10.1073/pnas.1010811107

- Helenius, A., Kartenbeck, J., Simons, K., & Fries, E. (1980). On the entry of Semliki forest virus into BHK-21 cells. *J Cell Biol*, 84(2), 404-420.
- Henderson, D. K. (2003). Managing occupational risks for hepatitis C transmission in the health care setting. *Clin Microbiol Rev*, 16(3), 546-568.
- Herker, E., Harris, C., Hernandez, C., Carpentier, A., Kaehlcke, K., Rosenberg, A. R., . . . Ott, M. (2010). Efficient hepatitis C virus particle formation requires diacylglycerol acyltransferase-1. *Nat Med*, 16(11), 1295-1298. doi:10.1038/nm.2238
- Hickenbottom, S. J., Kimmel, A. R., Londos, C., & Hurley, J. H. (2004). Structure of a lipid droplet protein; the PAT family member TIP47. *Structure*, 12(7), 1199-1207. doi:10.1016/j.str.2004.04.021
- Hinrichsen, L., Meyerholz, A., Groos, S., & Ungewickell, E. J. (2006). Bending a membrane: how clathrin affects budding. *Proc Natl Acad Sci U S A*, 103(23), 8715-8720. doi:10.1073/pnas.0600312103
- Hiramatsu, N., Hayashi, N., Haruna, Y., Kasahara, A., Fusamoto, H., Mori, C., . . . Kamada, T. (1992). Immunohistochemical detection of hepatitis C virus-infected hepatocytes in chronic liver disease with monoclonal antibodies to core, envelope and NS3 regions of the hepatitis C virus genome. *Hepatology*, 16(2), 306-311.
- Hoffmann, R. M., Diepolder, H. M., Zachoval, R., Zwiebel, F. M., Jung, M. C., Scholz, S., . . . Pape, G. R. (1995). Mapping of immunodominant CD4+ T lymphocyte epitopes of hepatitis C virus antigens and their relevance during the course of chronic infection. *Hepatology*, 21(3), 632-638.
- Hoftberger, R., Garzuly, F., Dienes, H. P., Grubits, J., Rohonyi, B., Fischer, G., . . . Budka, H. (2007). Fulminant central nervous system demyelination associated with interferon-alpha therapy and hepatitis C virus infection. *Mult Scler*, 13(9), 1100-1106. doi:10.1177/1352458507078684
- Hollederer, A., Braun, G. E., Dahlhoff, G., Drexler, H., Engel, J., Grassel, E., . . . Zellner, A. (2015). [Memorandum 'Development of health services research in Bavaria from the perspective of the Bavarian State Working Group 'Health Services Research (LAGeV)': status quo - potential - strategies']. *Gesundheitswesen*, 77(3), 180-185. doi:10.1055/s-0034-1389915
- Hong, J. X., Lee, F. J., Patton, W. A., Lin, C. Y., Moss, J., & Vaughan, M. (1998). Phospholipid- and GTP-dependent activation of cholera toxin and phospholipase D by human ADP-ribosylation factor-like protein 1 (HARL1). *J Biol Chem*, 273(25), 15872-15876.
- Hope, R. G., Murphy, D. J., & McLauchlan, J. (2002). The domains required to direct core proteins of hepatitis C virus and GB virus-B to lipid droplets share common features with plant oleosin proteins. *J Biol Chem*, 277(6), 4261-4270. doi:10.1074/jbc.M108798200
- Houghton, M., Selby, M., Weiner, A., & Choo, Q. L. (1994). Hepatitis C virus: structure, protein products and processing of the polyprotein precursor. *Curr Stud Hematol Blood Transfus*(61), 1-11.
- Howes, D. W., Melnick, J. L., & Reissig, M. (1956). Sequence of morphological changes in epithelial cell cultures infected with poliovirus. *J Exp Med*, 104(3), 289-304.
- Huang, H., Sun, F., Owen, D. M., Li, W., Chen, Y., Gale, M., Jr., & Ye, J. (2007). Hepatitis C virus production by human hepatocytes dependent on assembly and secretion of very low-density lipoproteins. *Proceedings of the National Academy of Sciences*

- of the United States of America, 104(14), 5848-5853. doi:10.1073/pnas.0700760104
- Huang, L., Hwang, J., Sharma, S. D., Hargittai, M. R., Chen, Y., Arnold, J. J., . . . Cameron, C. E. (2005). Hepatitis C virus nonstructural protein 5A (NS5A) is an RNA-binding protein. *J Biol Chem*, 280(43), 36417-36428. doi:10.1074/jbc.M508175200
- Hueging, K., Doepke, M., Vieyres, G., Bankwitz, D., Frentzen, A., Doerrbecker, J., . . . Pietschmann, T. (2014). Apolipoprotein E codetermines tissue tropism of hepatitis C virus and is crucial for viral cell-to-cell transmission by contributing to a postenvelopment step of assembly. *Journal of virology*, 88(3), 1433-1446. doi:10.1128/JVI.01815-13
- Huong, T. N., Iyer Ravi, L., Tan, B. H., & Sugrue, R. J. (2016). Evidence for a biphasic mode of respiratory syncytial virus transmission in permissive HEP2 cell monolayers. *Virol J*, 13, 12. doi:10.1186/s12985-016-0467-9
- Ikeda, M., Yi, M., Li, K., & Lemon, S. M. (2002). Selectable subgenomic and genome-length dicistronic RNAs derived from an infectious molecular clone of the HCV-N strain of hepatitis C virus replicate efficiently in cultured Huh7 cells. *J Virol*, 76(6), 2997-3006.
- Imai, Y., Varela, G. M., Jackson, M. B., Graham, M. J., Crooke, R. M., & Ahima, R. S. (2007). Reduction of hepatosteatosis and lipid levels by an adipose differentiation-related protein antisense oligonucleotide. *Gastroenterology*, 132(5), 1947-1954. doi:10.1053/j.gastro.2007.02.046
- Imamura, M., Inoguchi, T., Ikuyama, S., Taniguchi, S., Kobayashi, K., Nakashima, N., & Nawata, H. (2002). ADRP stimulates lipid accumulation and lipid droplet formation in murine fibroblasts. *Am J Physiol Endocrinol Metab*, 283(4), E775-783. doi:10.1152/ajpendo.00040.2002
- Ingelmo-Torres, M., Gonzalez-Moreno, E., Kassan, A., Hanzal-Bayer, M., Tebar, F., Herms, A., . . . Pol, A. (2009). Hydrophobic and basic domains target proteins to lipid droplets. *Traffic*, 10(12), 1785-1801. doi:10.1111/j.1600-0854.2009.00994.x
- Ishigami, K., Zhang, Y., Rayhill, S., Katz, D., & Stolpen, A. (2004). Does variant hepatic artery anatomy in a liver transplant recipient increase the risk of hepatic artery complications after transplantation? *AJR Am J Roentgenol*, 183(6), 1577-1584. doi:10.2214/ajr.183.6.01831577
- Ishizaki, R., Shin, H. W., Mitsuhashi, H., & Nakayama, K. (2008). Redundant roles of BIG2 and BIG1, guanine-nucleotide exchange factors for ADP-ribosylation factors in membrane traffic between the trans-Golgi network and endosomes. *Mol Biol Cell*, 19(6), 2650-2660. doi:10.1091/mbc.E07-10-1067
- Islam, A., Jones, H., Hiroi, T., Lam, J., Zhang, J., Moss, J., . . . Levine, S. J. (2008). cAMP-dependent protein kinase A (PKA) signaling induces TNFR1 exosome-like vesicle release via anchoring of PKA regulatory subunit RIIbeta to BIG2. *The Journal of biological chemistry*, 283(37), 25364-25371. doi:10.1074/jbc.M804966200
- Islam, A., Shen, X., Hiroi, T., Moss, J., Vaughan, M., & Levine, S. J. (2007). The brefeldin A-inhibited guanine nucleotide-exchange protein, BIG2, regulates the constitutive release of TNFR1 exosome-like vesicles. *J Biol Chem*, 282(13), 9591-9599. doi:10.1074/jbc.M607122200

- Israelow, B., Narbus, C. M., Sourisseau, M., & Evans, M. J. (2014). HepG2 cells mount an effective antiviral interferon-lambda based innate immune response to hepatitis C virus infection. *Hepatology*, 60(4), 1170-1179. doi:10.1002/hep.27227
- Iwami, S., Takeuchi, J. S., Nakaoka, S., Mammano, F., Clavel, F., Inaba, H., . . . Sato, K. (2015). Cell-to-cell infection by HIV contributes over half of virus infection. *Elife*, 4. doi:10.7554/eLife.08150
- Jambunathan, S., Yin, J., Khan, W., Tamori, Y., & Puri, V. (2011). FSP27 promotes lipid droplet clustering and then fusion to regulate triglyceride accumulation. *PLoS One*, 6(12), e28614. doi:10.1371/journal.pone.0028614
- Ji, C., Liu, Y., Pamulapati, C., Bohini, S., Fertig, G., Schraeml, M., . . . Klumpp, K. (2014). Prevention of hepatitis C virus infection and spread in human liver chimeric mice by an anti-CD81 monoclonal antibody. *Hepatology*. doi:10.1002/hep.27603
- Jiang, J., & Luo, G. (2009). Apolipoprotein E but not B is required for the formation of infectious hepatitis C virus particles. *J Virol*, 83(24), 12680-12691. doi:10.1128/JVI.01476-09
- Jiang, J., Wu, X., Tang, H., & Luo, G. (2013). Apolipoprotein E mediates attachment of clinical hepatitis C virus to hepatocytes by binding to cell surface heparan sulfate proteoglycan receptors. *PLoS One*, 8(7), e67982. doi:10.1371/journal.pone.0067982
- Jirasko, V., Montserret, R., Lee, J. Y., Gouttenoire, J., Moradpour, D., Penin, F., & Bartenschlager, R. (2010). Structural and functional studies of nonstructural protein 2 of the hepatitis C virus reveal its key role as organizer of virion assembly. *PLoS Pathog*, 6(12), e1001233. doi:10.1371/journal.ppat.1001233
- Johnson, D. C., & Huber, M. T. (2002). Directed Egress of Animal Viruses Promotes Cell-to-Cell Spread. *Journal of virology*, 76(1), 1-8. doi:10.1128/jvi.76.1.1-8.2002
- Johnson, R. J., Gretch, D. R., Yamabe, H., Hart, J., Bacchi, C. E., Hartwell, P., . . . et al. (1993). Membranoproliferative glomerulonephritis associated with hepatitis C virus infection. *The New England journal of medicine*, 328(7), 465-470. doi:10.1056/NEJM199302183280703
- Jones, D. M., & McLauchlan, J. (2010). Hepatitis C virus: assembly and release of virus particles. *J Biol Chem*, 285(30), 22733-22739. doi:10.1074/jbc.R110.133017
- Jones, D. M., Patel, A. H., Targett-Adams, P., & McLauchlan, J. (2009). The hepatitis C virus NS4B protein can trans-complement viral RNA replication and modulates production of infectious virus. *J Virol*, 83(5), 2163-2177. doi:10.1128/JVI.01885-08
- Kaczor, M. P., Seczynska, M., Szczeklik, W., & Sanak, M. (2015). IL28B polymorphism (rs12979860) associated with clearance of HCV infection in Poland: systematic review of its prevalence in chronic hepatitis C patients and general population frequency. *Pharmacol Rep*, 67(2), 260-266. doi:10.1016/j.pharep.2014.10.006
- Kahn, R. A., Cherfils, J., Elias, M., Lovering, R. C., Munro, S., & Schurmann, A. (2006). Nomenclature for the human Arf family of GTP-binding proteins: ARF, ARL, and SAR proteins. *J Cell Biol*, 172(5), 645-650. doi:10.1083/jcb.200512057
- Kamal, S. M., Amin, A., Madwar, M., Graham, C. S., He, Q., Al Tawil, A., . . . Koziel, M. J. (2004). Cellular immune responses in seronegative sexual contacts of acute hepatitis C patients. *J Virol*, 78(22), 12252-12258. doi:10.1128/JVI.78.22.12252-12258.2004



- Kaneko, T., Tanji, Y., Satoh, S., Hijikata, M., Asabe, S., Kimura, K., & Shimotohno, K. (1994). Production of two phosphoproteins from the NS5A region of the hepatitis C viral genome. *Biochem Biophys Res Commun*, 205(1), 320-326. doi:10.1006/bbrc.1994.2667
- Kanoh, H., Williger, B. T., & Exton, J. H. (1997). Arfaptin 1, a putative cytosolic target protein of ADP-ribosylation factor, is recruited to Golgi membranes. *J Biol Chem*, 272(9), 5421-5429.
- Kaser, A., Vogel, W., & Tilg, H. (1999). Plasma levels of soluble Fas during treatment of chronic hepatitis C patients with interferon alpha. *J Hepatol*, 31(3), 575.
- Kato, N., Ootsuyama, Y., Ohkoshi, S., Nakazawa, T., Sekiya, H., Hijikata, M., & Shimotohno, K. (1992). Characterization of hypervariable regions in the putative envelope protein of hepatitis C virus. *Biochem Biophys Res Commun*, 189(1), 119-127.
- Kaul, R., Rutherford, J., Rowland-Jones, S. L., Kimani, J., Onyango, J. I., Fowke, K., . . . Plummer, F. A. (2004). HIV-1 Env-specific cytotoxic T-lymphocyte responses in exposed, uninfected Kenyan sex workers: a prospective analysis. *AIDS*, 18(15), 2087-2089.
- Kaushik, S., & Cuervo, A. M. (2015). Degradation of lipid droplet-associated proteins by chaperone-mediated autophagy facilitates lipolysis. *Nat Cell Biol*, 17(6), 759-770. doi:10.1038/ncb3166
- Kawamoto, K., Yoshida, Y., Tamaki, H., Torii, S., Shinotsuka, C., Yamashina, S., & Nakayama, K. (2002). GBF1, a guanine nucleotide exchange factor for ADP-ribosylation factors, is localized to the cis-Golgi and involved in membrane association of the COPI coat. *Traffic*, 3(7), 483-495.
- Khaldoun, S. A., Emond-Boisjoly, M. A., Chateau, D., Carriere, V., Lacasa, M., Rousset, M., . . . Morel, E. (2014). Autophagosomes contribute to intracellular lipid distribution in enterocytes. *Mol Biol Cell*, 25(1), 118-132. doi:10.1091/mbc.E13-06-0324
- Khan, I., Katikaneni, D. S., Han, Q., Sanchez-Felipe, L., Hanada, K., Ambrose, R. L., . . . Konan, K. V. (2014). Modulation of hepatitis C virus genome replication by glycosphingolipids and FAPP2 protein. *Journal of virology*. doi:10.1128/JVI.00970-14
- Khandelia, H., Duelund, L., Pakkanen, K. I., & Ipsen, J. H. (2010). Triglyceride blisters in lipid bilayers: implications for lipid droplet biogenesis and the mobile lipid signal in cancer cell membranes. *PLoS One*, 5(9), e12811. doi:10.1371/journal.pone.0012811
- King, R. W., Zecher, M., Jeffries, M. W., Carroll, D. R., Parisi, J. M., & Pasquinelli, C. (2002). A cell-based model of HCV-negative-strand RNA replication utilizing a chimeric hepatitis C virus/reporter RNA template. *Antiviral chemistry & chemotherapy*, 13(6), 353-362. doi:10.1177/095632020201300603
- Kiyosawa, K., Akahane, Y., Nagata, A., & Furuta, S. (1984). Hepatocellular carcinoma after non-A, non-B posttransfusion hepatitis. *Am J Gastroenterol*, 79(10), 777-781.
- Klemm, R. W., Norton, J. P., Cole, R. A., Li, C. S., Park, S. H., Crane, M. M., . . . Mak, H. Y. (2013). A conserved role for atlastin GTPases in regulating lipid droplet size. *Cell Rep*, 3(5), 1465-1475. doi:10.1016/j.celrep.2013.04.015

- Kobayashi, T., Beuchat, M. H., Chevallier, J., Makino, A., Mayran, N., Escola, J. M., . . . Gruenberg, J. (2002). Separation and characterization of late endosomal membrane domains. *The Journal of biological chemistry*, 277(35), 32157-32164. doi:10.1074/jbc.M202838200
- Koerner, K., Cardoso, M., Dengler, T., Kerowgan, M., & Kubanek, B. (1998). Estimated risk of transmission of hepatitis C virus by blood transfusion. *Vox Sang*, 74(4), 213-216.
- Kokordelis, P., Kramer, B., Korner, C., Boesecke, C., Voigt, E., Ingiliz, P., . . . Nattermann, J. (2014). An effective interferon-gamma-mediated inhibition of hepatitis C virus replication by natural killer cells is associated with spontaneous clearance of acute hepatitis C in human immunodeficiency virus-positive patients. *Hepatology*, 59(3), 814-827. doi:10.1002/hep.26782
- Kolykhalov, A. A., Agapov, E. V., Blight, K. J., Mihalik, K., Feinstone, S. M., & Rice, C. M. (1997). Transmission of hepatitis C by intrahepatic inoculation with transcribed RNA. *Science*, 277(5325), 570-574.
- Kondo, Y., Hanai, A., Nakai, W., Katoh, Y., Nakayama, K., & Shin, H. W. (2012). ARF1 and ARF3 are required for the integrity of recycling endosomes and the recycling pathway. *Cell Struct Funct*, 37(2), 141-154.
- Kory, N., Farese, R. V., Jr., & Walther, T. C. (2016). Targeting Fat: Mechanisms of Protein Localization to Lipid Droplets. *Trends in cell biology*, 26(7), 535-546. doi:10.1016/j.tcb.2016.02.007
- Kory, N., Thiam, A. R., Farese, R. V., Jr., & Walther, T. C. (2015). Protein Crowding Is a Determinant of Lipid Droplet Protein Composition. *Developmental cell*, 34(3), 351-363. doi:10.1016/j.devcel.2015.06.007
- Koumandou, V. L., Wickstead, B., Ginger, M. L., van der Giezen, M., Dacks, J. B., & Field, M. C. (2013). Molecular paleontology and complexity in the last eukaryotic common ancestor. *Crit Rev Biochem Mol Biol*, 48(4), 373-396. doi:10.3109/10409238.2013.821444
- Koutsoudakis, G., Herrmann, E., Kallis, S., Bartenschlager, R., & Pietschmann, T. (2007). The level of CD81 cell surface expression is a key determinant for productive entry of hepatitis C virus into host cells. *J Virol*, 81(2), 588-598. doi:10.1128/JVI.01534-06
- Koutsoudakis, G., Kaul, A., Steinmann, E., Kallis, S., Lohmann, V., Pietschmann, T., & Bartenschlager, R. (2006). Characterization of the early steps of hepatitis C virus infection by using luciferase reporter viruses. *Journal of virology*, 80(11), 5308-5320. doi:10.1128/JVI.02460-05
- Kovsan, J., Ben-Romano, R., Souza, S. C., Greenberg, A. S., & Rudich, A. (2007). Regulation of adipocyte lipolysis by degradation of the perilipin protein: nelfinavir enhances lysosome-mediated perilipin proteolysis. *J Biol Chem*, 282(30), 21704-21711. doi:10.1074/jbc.M702223200
- Koziel, M. J., Wong, D. K., Dudley, D., Houghton, M., & Walker, B. D. (1997). Hepatitis C virus-specific cytolytic T lymphocyte and T helper cell responses in seronegative persons. *J Infect Dis*, 176(4), 859-866.
- Krahmer, N., Guo, Y., Wilfling, F., Hilger, M., Lingrell, S., Heger, K., . . . Walther, T. C. (2011). Phosphatidylcholine synthesis for lipid droplet expansion is mediated by

- localized activation of CTP:phosphocholine cytidyltransferase. *Cell Metab*, 14(4), 504-515. doi:10.1016/j.cmet.2011.07.013
- Krieger, N., Lohmann, V., & Bartenschlager, R. (2001). Enhancement of hepatitis C virus RNA replication by cell culture-adaptive mutations. *J Virol*, 75(10), 4614-4624. doi:10.1128/JVI.75.10.4614-4624.2001
- Kumar, Y., Cocchiaro, J., & Valdivia, R. H. (2006). The obligate intracellular pathogen *Chlamydia trachomatis* targets host lipid droplets. *Curr Biol*, 16(16), 1646-1651. doi:10.1016/j.cub.2006.06.060
- Kuno, G., & Chang, G. J. (2005). Biological transmission of arboviruses: reexamination of and new insights into components, mechanisms, and unique traits as well as their evolutionary trends. *Clin Microbiol Rev*, 18(4), 608-637. doi:10.1128/CMR.18.4.608-637.2005
- Kuppast, B., & Fahmy, H. (2016). Thiazolo[4,5-d]pyrimidines as a privileged scaffold in drug discovery. *Eur J Med Chem*, 113, 198-213. doi:10.1016/j.ejmech.2016.02.031
- Kuramoto, K., Sakai, F., Yoshinori, N., Nakamura, T. Y., Wakabayashi, S., Kojidani, T., . . . Osumi, T. (2014). Deficiency of a lipid droplet protein, perilipin 5, suppresses myocardial lipid accumulation, thereby preventing type 1 diabetes-induced heart malfunction. *Mol Cell Biol*, 34(14), 2721-2731. doi:10.1128/MCB.00133-14
- Lagoja, I. M. (2005). Pyrimidine as constituent of natural biologically active compounds. *Chem Biodivers*, 2(1), 1-50. doi:10.1002/cbdv.200490173
- Lamas, E., Baccarini, P., Housset, C., Kremsdorf, D., & Brechot, C. (1992). Detection of hepatitis C virus (HCV) RNA sequences in liver tissue by in situ hybridization. *J Hepatol*, 16(1-2), 219-223.
- Lang, L., Shay, C., Zhao, X., & Teng, Y. (2017). Combined targeting of Arf1 and Ras potentiates anticancer activity for prostate cancer therapeutics. *J Exp Clin Cancer Res*, 36(1), 112. doi:10.1186/s13046-017-0583-4
- Larigauderie, G., Cuaz-Perolin, C., Younes, A. B., Furman, C., Lasselin, C., Copin, C., . . . Rouis, M. (2006). Adipophilin increases triglyceride storage in human macrophages by stimulation of biosynthesis and inhibition of beta-oxidation. *FEBS J*, 273(15), 3498-3510. doi:10.1111/j.1742-4658.2006.05357.x
- Larigauderie, G., Furman, C., Jaye, M., Lasselin, C., Copin, C., Fruchart, J. C., . . . Rouis, M. (2004). Adipophilin enhances lipid accumulation and prevents lipid efflux from THP-1 macrophages: potential role in atherogenesis. *Arterioscler Thromb Vasc Biol*, 24(3), 504-510. doi:10.1161/01.ATV.0000115638.27381.97
- Lass, A., Zimmermann, R., Haemmerle, G., Riederer, M., Schoiswohl, G., Schweiger, M., . . . Zechner, R. (2006). Adipose triglyceride lipase-mediated lipolysis of cellular fat stores is activated by CGI-58 and defective in Chanarin-Dorfman Syndrome. *Cell Metab*, 3(5), 309-319. doi:10.1016/j.cmet.2006.03.005
- Lass, A., Zimmermann, R., Oberer, M., & Zechner, R. (2011). Lipolysis - a highly regulated multi-enzyme complex mediates the catabolism of cellular fat stores. *Prog Lipid Res*, 50(1), 14-27. doi:10.1016/j.plipres.2010.10.004
- Lau, J. Y., & Davis, G. L. (1994). Detection of hepatitis C virus RNA genome in liver tissue by nonisotopic in situ hybridization. *J Med Virol*, 42(3), 268-271.

- Laurens, C., Bourlier, V., Mairal, A., Louche, K., Badin, P. M., Mouisel, E., . . . Moro, C. (2016). Perilipin 5 fine-tunes lipid oxidation to metabolic demand and protects against lipotoxicity in skeletal muscle. *Sci Rep*, 6, 38310. doi:10.1038/srep38310
- Law, M., Maruyama, T., Lewis, J., Giang, E., Tarr, A. W., Stamatakis, Z., . . . Burton, D. R. (2008). Broadly neutralizing antibodies protect against hepatitis C virus quasispecies challenge. *Nature medicine*, 14(1), 25-27. doi:10.1038/nm1698
- Lawson, A., & Ryder, S. D. (2006). Progression of hepatic fibrosis in chronic hepatitis C and the need for treatment in mild disease. *Eur J Gastroenterol Hepatol*, 18(4), 343-347.
- Le Borgne, R., & Hoflack, B. (1998). Protein transport from the secretory to the endocytic pathway in mammalian cells. *Biochim Biophys Acta*, 1404(1-2), 195-209.
- Le Marchand, Y., Singh, A., Assimacopoulos-Jeannet, F., Orci, L., Rouiller, C., & Jeanrenaud, B. (1973). A role for the microtubular system in the release of very low density lipoproteins by perfused mouse livers. *J Biol Chem*, 248(19), 6862-6870.
- Lee, B., Zhu, J., Wolins, N. E., Cheng, J. X., & Buhman, K. K. (2009). Differential association of adipophilin and TIP47 proteins with cytoplasmic lipid droplets in mouse enterocytes during dietary fat absorption. *Biochim Biophys Acta*, 1791(12), 1173-1180. doi:10.1016/j.bbaliip.2009.08.002
- Lee, Y., El Andaloussi, S., & Wood, M. J. (2012). Exosomes and microvesicles: extracellular vesicles for genetic information transfer and gene therapy. *Human molecular genetics*, 21(R1), R125-134. doi:10.1093/hmg/ddc317
- Lefevre, M., Felmlee, D. J., Parnot, M., Baumert, T. F., & Schuster, C. (2014). Syndecan 4 Is Involved in Mediating HCV Entry through Interaction with Lipoviral Particle-Associated Apolipoprotein E. *PloS one*, 9(4), e95550. doi:10.1371/journal.pone.0095550
- Levin, A., Neufeldt, C. J., Pang, D., Wilson, K., Loewen-Dobler, D., Joyce, M. A., . . . Tyrrell, D. L. (2014). Functional characterization of nuclear localization and export signals in hepatitis C virus proteins and their role in the membranous web. *PloS one*, 9(12), e114629. doi:10.1371/journal.pone.0114629
- Levings, M. K., Sangregorio, R., & Roncarolo, M. G. (2001). Human cd25(+)cd4(+) t regulatory cells suppress naive and memory T cell proliferation and can be expanded in vitro without loss of function. *J Exp Med*, 193(11), 1295-1302.
- Li, G., Li, K., Lea, A. S., Li, N. L., Abdulla, N. E., Eltorky, M. A., & Ferguson, M. R. (2013). In situ hybridization for the detection of hepatitis C virus RNA in human liver tissue. *Journal of viral hepatitis*, 20(3), 183-192. doi:10.1111/j.1365-2893.2012.01642.x
- Li, H., Hughes, A. L., Bano, N., McArdle, S., Livingston, S., Deubner, H., . . . Gretch, D. R. (2011). Genetic diversity of near genome-wide hepatitis C virus sequences during chronic infection: evidence for protein structural conservation over time. *PloS one*, 6(5), e19562. doi:10.1371/journal.pone.0019562
- Li, H., Yang, X., Yang, G., Hong, Z., Zhou, L., Yin, P., . . . Zhang, L. (2014). Hepatitis C virus NS5A hijacks ARFGAP1 to maintain a phosphatidylinositol 4-phosphate-enriched microenvironment. *Journal of virology*, 88(11), 5956-5966. doi:10.1128/JVI.03738-13

- Li, H. F., Huang, C. H., Ai, L. S., Chuang, C. K., & Chen, S. S. (2009). Mutagenesis of the fusion peptide-like domain of hepatitis C virus E1 glycoprotein: involvement in cell fusion and virus entry. *J Biomed Sci*, 16, 89. doi:10.1186/1423-0127-16-89
- Li, J., Fuchs, S., Zhang, J., Wellford, S., Schuldiner, M., & Wang, X. (2016). An unrecognized function for COPII components in recruiting the viral replication protein BMV 1a to the perinuclear ER. *Journal of cell science*, 129(19), 3597-3608. doi:10.1242/jcs.190082
- Li, K., Foy, E., Ferreon, J. C., Nakamura, M., Ferreon, A. C., Ikeda, M., . . . Lemon, S. M. (2005). Immune evasion by hepatitis C virus NS3/4A protease-mediated cleavage of the Toll-like receptor 3 adaptor protein TRIF. *Proc Natl Acad Sci U S A*, 102(8), 2992-2997. doi:10.1073/pnas.0408824102
- Li, S., Ye, L., Yu, X., Xu, B., Li, K., Zhu, X., . . . Kong, L. (2009). Hepatitis C virus NS4B induces unfolded protein response and endoplasmic reticulum overload response-dependent NF-kappaB activation. *Virology*, 391(2), 257-264. doi:10.1016/j.virol.2009.06.039
- Li, Y., Han, D., Hu, G., Sommerfeld, M., & Hu, Q. (2010). Inhibition of starch synthesis results in overproduction of lipids in *Chlamydomonas reinhardtii*. *Biotechnol Bioeng*, 107(2), 258-268. doi:10.1002/bit.22807
- Liang, T. J. (2013). Current progress in development of hepatitis C virus vaccines. *Nature medicine*, 19(7), 869-878. doi:10.1038/nm.3183
- Liang, Y., Shilagard, T., Xiao, S. Y., Snyder, N., Lau, D., Cicalese, L., . . . Lemon, S. M. (2009). Visualizing hepatitis C virus infections in human liver by two-photon microscopy. *Gastroenterology*, 137(4), 1448-1458. doi:10.1053/j.gastro.2009.07.050
- Lidove, O., Cacoub, P., Maisonneuve, T., Servan, J., Thibault, V., Piette, J. C., & Leger, J. M. (2001). Hepatitis C virus infection with peripheral neuropathy is not always associated with cryoglobulinaemia. *Ann Rheum Dis*, 60(3), 290-292.
- Liefhebber, J. M., Hague, C. V., Zhang, Q., Wakelam, M. J., & McLauchlan, J. (2014). Modulation of Triglyceride and Cholesterol Ester Synthesis Impairs Assembly of Infectious Hepatitis C Virus. *The Journal of biological chemistry*. doi:10.1074/jbc.M114.582999
- Liefhebber, J. M., Hensbergen, P. J., Deelder, A. M., Spaan, W. J., & van Leeuwen, H. C. (2010). Characterization of hepatitis C virus NS3 modifications in the context of replication. *J Gen Virol*, 91(Pt 4), 1013-1018. doi:10.1099/vir.0.016881-0
- Lin, R. J., Chang, B. L., Yu, H. P., Liao, C. L., & Lin, Y. L. (2006). Blocking of interferon-induced Jak-Stat signaling by Japanese encephalitis virus NS5 through a protein tyrosine phosphatase-mediated mechanism. *J Virol*, 80(12), 5908-5918. doi:10.1128/JVI.02714-05
- Lindenbach, B. D., Evans, M. J., Syder, A. J., Wolk, B., Tellinghuisen, T. L., Liu, C. C., . . . Rice, C. M. (2005). Complete replication of hepatitis C virus in cell culture. *Science*, 309(5734), 623-626. doi:10.1126/science.1114016
- Listenberger, L. L., Han, X., Lewis, S. E., Cases, S., Farese, R. V., Jr., Ory, D. S., & Schaffer, J. E. (2003). Triglyceride accumulation protects against fatty acid-induced lipotoxicity. *Proc Natl Acad Sci U S A*, 100(6), 3077-3082. doi:10.1073/pnas.0630588100

- Listenberger, L. L., Ostermeyer-Fay, A. G., Goldberg, E. B., Brown, W. J., & Brown, D. A. (2007). Adipocyte differentiation-related protein reduces the lipid droplet association of adipose triglyceride lipase and slows triacylglycerol turnover. *J Lipid Res*, 48(12), 2751-2761. doi:10.1194/jlr.M700359-JLR200
- Liu, K., & Czaja, M. J. (2013). Regulation of lipid stores and metabolism by lipophagy. *Cell Death Differ*, 20(1), 3-11. doi:10.1038/cdd.2012.63
- Liu, Y., Kahn, R. A., & Prestegard, J. H. (2010). Dynamic structure of membrane-anchored Arf\*GTP. *Nat Struct Mol Biol*, 17(7), 876-881. doi:10.1038/nsmb.1853
- Liu, Z., & He, J. J. (2013). Cell-cell contact-mediated hepatitis C virus (HCV) transfer, productive infection, and replication and their requirement for HCV receptors. *Journal of virology*, 87(15), 8545-8558. doi:10.1128/JVI.01062-13
- Lohmann, D., Spandl, J., Stevanovic, A., Schoene, M., Philippou-Massier, J., & Thiele, C. (2013). Monoubiquitination of ancient ubiquitous protein 1 promotes lipid droplet clustering. *PLoS one*, 8(9), e72453. doi:10.1371/journal.pone.0072453
- Lohmann, V., & Bartenschlager, R. (2014). On the history of hepatitis C virus cell culture systems. *Journal of medicinal chemistry*, 57(5), 1627-1642. doi:10.1021/jm401401n
- Lohmann, V., Korner, F., Koch, J., Herian, U., Theilmann, L., & Bartenschlager, R. (1999). Replication of subgenomic hepatitis C virus RNAs in a hepatoma cell line. *Science*, 285(5424), 110-113.
- Longatti, A., Boyd, B., & Chisari, F. V. (2015). Virion-independent transfer of replication-competent hepatitis C virus RNA between permissive cells. *Journal of virology*, 89(5), 2956-2961. doi:10.1128/JVI.02721-14
- Longley, D. B., Harkin, D. P., & Johnston, P. G. (2003). 5-fluorouracil: mechanisms of action and clinical strategies. *Nat Rev Cancer*, 3(5), 330-338. doi:10.1038/nrc1074
- Loo, Y. M., Owen, D. M., Li, K., Erickson, A. K., Johnson, C. L., Fish, P. M., . . . Gale, M., Jr. (2006). Viral and therapeutic control of IFN-beta promoter stimulator 1 during hepatitis C virus infection. *Proc Natl Acad Sci U S A*, 103(15), 6001-6006. doi:10.1073/pnas.0601523103
- Lopez-Verges, S., Camus, G., Blot, G., Beauvoir, R., Benarous, R., & Berlioz-Torrent, C. (2006). Tail-interacting protein TIP47 is a connector between Gag and Env and is required for Env incorporation into HIV-1 virions. *Proc Natl Acad Sci U S A*, 103(40), 14947-14952. doi:10.1073/pnas.0602941103
- Lorizate, M., & Krausslich, H. G. (2011). Role of lipids in virus replication. *Cold Spring Harb Perspect Biol*, 3(10), a004820. doi:10.1101/cshperspect.a004820
- Lu, L., Nakano, T., Orito, E., Mizokami, M., & Robertson, B. H. (2001). Evaluation of accumulation of hepatitis C virus mutations in a chronically infected chimpanzee: comparison of the core, E1, HVR1, and NS5b regions. *J Virol*, 75(6), 3004-3009. doi:10.1128/JVI.75.6.3004-3009.2001
- Lu, X., Gruia-Gray, J., Copeland, N. G., Gilbert, D. J., Jenkins, N. A., Londos, C., & Kimmel, A. R. (2001). The murine perilipin gene: the lipid droplet-associated perilipins derive from tissue-specific, mRNA splice variants and define a gene family of ancient origin. *Mamm Genome*, 12(9), 741-749.
- Lupberger, J., Zeisel, M. B., Xiao, F., Thumann, C., Fofana, I., Zona, L., . . . Baumert, T. F. (2011). EGFR and EphA2 are host factors for hepatitis C virus entry and

- possible targets for antiviral therapy. *Nature medicine*, 17(5), 589-595. doi:10.1038/nm.2341
- Luton, F., Klein, S., Chauvin, J. P., Le Bivic, A., Bourgoïn, S., Franco, M., & Chardin, P. (2004). EFA6, exchange factor for ARF6, regulates the actin cytoskeleton and associated tight junction in response to E-cadherin engagement. *Molecular biology of the cell*, 15(3), 1134-1145. doi:10.1091/mbc.E03-10-0751
- Lyn, R. K., Kennedy, D. C., Stolor, A., Ridsdale, A., & Pezacki, J. P. (2010). Dynamics of lipid droplets induced by the hepatitis C virus core protein. *Biochemical and biophysical research communications*, 399(4), 518-524. doi:10.1016/j.bbrc.2010.07.101
- Ma, Y., Yates, J., Liang, Y., Lemon, S. M., & Yi, M. (2008). NS3 helicase domains involved in infectious intracellular hepatitis C virus particle assembly. *J Virol*, 82(15), 7624-7639. doi:10.1128/JVI.00724-08
- MacDonald, A. J., Duffy, M., Brady, M. T., McKiernan, S., Hall, W., Hegarty, J., . . . Mills, K. H. (2002). CD4 T helper type 1 and regulatory T cells induced against the same epitopes on the core protein in hepatitis C virus-infected persons. *J Infect Dis*, 185(6), 720-727. doi:10.1086/339340
- Mackinnon, W. B., May, G. L., & Mountford, C. E. (1992). Esterified cholesterol and triglyceride are present in plasma membranes of Chinese hamster ovary cells. *Eur J Biochem*, 205(2), 827-839.
- Magnusson, B., Asp, L., Bostrom, P., Ruiz, M., Stillemark-Billton, P., Linden, D., . . . Olofsson, S. O. (2006). Adipocyte differentiation-related protein promotes fatty acid storage in cytosolic triglycerides and inhibits secretion of very low-density lipoproteins. *Arteriosclerosis, thrombosis, and vascular biology*, 26(7), 1566-1571. doi:10.1161/01.ATV.0000223345.11820.da
- Mahnert, N., Lim, C., Mowers, E., Bethany, S., Neil, K., Daniel, M., & As-Sanie, S. (2015). Risk Factors Associated With Emergency Room Visits and Hospital Readmission Following Benign Hysterectomy. *J Minim Invasive Gynecol*, 22(6S), S80. doi:10.1016/j.jmig.2015.08.215
- Mak, K. M., Ren, C., Ponomarenko, A., Cao, Q., & Lieber, C. S. (2008). Adipose differentiation-related protein is a reliable lipid droplet marker in alcoholic fatty liver of rats. *Alcohol Clin Exp Res*, 32(4), 683-689. doi:10.1111/j.1530-0277.2008.00624.x
- Makowska, Z., Duong, F. H., Trincucci, G., Tough, D. F., & Heim, M. H. (2011). Interferon-beta and interferon-lambda signaling is not affected by interferon-induced refractoriness to interferon-alpha in vivo. *Hepatology*, 53(4), 1154-1163. doi:10.1002/hep.24189
- Malsam, J., Gommel, D., Wieland, F. T., & Nickel, W. (1999). A role for ADP ribosylation factor in the control of cargo uptake during COPI-coated vesicle biogenesis. *FEBS Lett*, 462(3), 267-272.
- Marcellin, P., Asselah, T., & Boyer, N. (2002). Fibrosis and disease progression in hepatitis C. *Hepatology*, 36(5 Suppl 1), S47-56. doi:10.1053/jhep.2002.36993
- Marcinkiewicz, A., Gauthier, D., Garcia, A., & Brasaemle, D. L. (2006). The phosphorylation of serine 492 of perilipin a directs lipid droplet fragmentation and dispersion. *The Journal of biological chemistry*, 281(17), 11901-11909. doi:10.1074/jbc.M600171200

- Martin, S., Driessen, K., Nixon, S. J., Zerial, M., & Parton, R. G. (2005). Regulated localization of Rab18 to lipid droplets: effects of lipolytic stimulation and inhibition of lipid droplet catabolism. *The Journal of biological chemistry*, 280(51), 42325-42335. doi:10.1074/jbc.M506651200
- Martin, S. W., & Konopka, J. B. (2004). Lipid raft polarization contributes to hyphal growth in *Candida albicans*. *Eukaryot Cell*, 3(3), 675-684. doi:10.1128/EC.3.3.675-684.2004
- Maruyama, T., Demizu, Y., Kozai, S., Witvrouw, M., Pannecouque, C., Balzarini, J., . . . De Clercq, E. (2007). Antiviral activity of 3-(3,5-dimethylbenzyl)uracil derivatives against HIV-1 and HCMV. *Nucleosides, nucleotides & nucleic acids*, 26(10-12), 1553-1558. doi:10.1080/15257770701545424
- Maruyama, T., Kozai, S., Demizu, Y., Witvrouw, M., Pannecouque, C., Balzarini, J., . . . De Clercq, E. (2004). Synthesis and antiviral activity of 1-substituted 3-(3,5-dimethylbenzyl)uracil against HIV-1. *Nucleic acids symposium series*(48), 3-4. doi:10.1093/nass/48.1.3
- Masaki, T., Matsunaga, S., Takahashi, H., Nakashima, K., Kimura, Y., Ito, M., . . . Suzuki, T. (2014). Involvement of hepatitis C virus NS5A hyperphosphorylation mediated by casein kinase I-alpha in infectious virus production. *J Virol*, 88(13), 7541-7555. doi:10.1128/JVI.03170-13
- Masaki, T., Suzuki, R., Murakami, K., Aizaki, H., Ishii, K., Murayama, A., . . . Suzuki, T. (2008). Interaction of hepatitis C virus nonstructural protein 5A with core protein is critical for the production of infectious virus particles. *J Virol*, 82(16), 7964-7976. doi:10.1128/JVI.00826-08
- Mathiesen, C. K., Prentoe, J., Meredith, L. W., Jensen, T. B., Krarup, H., McKeating, J. A., . . . Bukh, J. (2015). Adaptive mutations enhance assembly and cell-to-cell transmission of a high-titer hepatitis C virus genotype 5a Core-NS2 JFH1-based recombinant. *Journal of virology*. doi:10.1128/JVI.00039-15
- Matto, M., Sklan, E. H., David, N., Melamed-Book, N., Casanova, J. E., Glenn, J. S., & Aroeti, B. (2011). Role for ADP ribosylation factor 1 in the regulation of hepatitis C virus replication. *Journal of virology*, 85(2), 946-956. doi:10.1128/JVI.00753-10
- McCarthy, K. M., Skare, I. B., Stankewich, M. C., Furuse, M., Tsukita, S., Rogers, R. A., . . . Schneeberger, E. E. (1996). Occludin is a functional component of the tight junction. *Journal of cell science*, 109 ( Pt 9), 2287-2298.
- McCaughan, G. W., & Zekry, A. (2000). Effects of immunosuppression and organ transplantation on the natural history and immunopathogenesis of hepatitis C virus infection. *Transpl Infect Dis*, 2(4), 166-185.
- McHutchison, J. G., Kuo, G., Houghton, M., Choo, Q. L., & Redeker, A. G. (1991). Hepatitis C virus antibodies in acute icteric and chronic non-A, non-B hepatitis. *Gastroenterology*, 101(4), 1117-1119.
- McLauchlan, J., Lemberg, M. K., Hope, G., & Martoglio, B. (2002). Intramembrane proteolysis promotes trafficking of hepatitis C virus core protein to lipid droplets. *EMBO J*, 21(15), 3980-3988. doi:10.1093/emboj/cdf414
- McManaman, J. L., Bales, E. S., Orlicky, D. J., Jackman, M., MacLean, P. S., Cain, S., . . . Greenberg, A. S. (2013). Perilipin-2-null mice are protected against diet-induced obesity, adipose inflammation, and fatty liver disease. *J Lipid Res*, 54(5), 1346-1359. doi:10.1194/jlr.M035063



- McManaman, J. L., Zabaronick, W., Schaack, J., & Orlicky, D. J. (2003). Lipid droplet targeting domains of adipophilin. *J Lipid Res*, 44(4), 668-673. doi:10.1194/jlr.C200021-JLR200
- Mee, C. J., Harris, H. J., Farquhar, M. J., Wilson, G., Reynolds, G., Davis, C., . . . McKeating, J. A. (2009). Polarization restricts hepatitis C virus entry into HepG2 hepatoma cells. *Journal of virology*, 83(12), 6211-6221. doi:10.1128/JVI.00246-09
- Mehedi, M., Collins, P. L., & Buchholz, U. J. (2017). A novel host factor for human respiratory syncytial virus. *Commun Integr Biol*, 10(3), e1319025. doi:10.1080/19420889.2017.1319025
- Melis, R., Fauron, C., McMillin, G., Lyon, E., Shirts, B., Hubley, L. M., & Slev, P. R. (2011). Simultaneous genotyping of rs12979860 and rs8099917 variants near the IL28B locus associated with HCV clearance and treatment response. *J Mol Diagn*, 13(4), 446-451. doi:10.1016/j.jmoldx.2011.03.008
- Mercer, D. F., Schiller, D. E., Elliott, J. F., Douglas, D. N., Hao, C., Rinfret, A., . . . Kneteman, N. M. (2001). Hepatitis C virus replication in mice with chimeric human livers. *Nature medicine*, 7(8), 927-933. doi:10.1038/90968
- Meredith, L. W., Zitzmann, N., & McKeating, J. A. (2013). Differential effect of p7 inhibitors on hepatitis C virus cell-to-cell transmission. *Antiviral research*, 100(3), 636-639. doi:10.1016/j.antiviral.2013.10.006
- Mertz, G. J. (2008). Asymptomatic shedding of herpes simplex virus 1 and 2: implications for prevention of transmission. *J Infect Dis*, 198(8), 1098-1100. doi:10.1086/591914
- Merz, A., Long, G., Hiet, M. S., Brugger, B., Chlanda, P., Andre, P., . . . Bartenschlager, R. (2011). Biochemical and morphological properties of hepatitis C virus particles and determination of their lipidome. *J Biol Chem*, 286(4), 3018-3032. doi:10.1074/jbc.M110.175018
- Mesmin, B., Bigay, J., Moser von Filseck, J., Lacas-Gervais, S., Drin, G., & Antonny, B. (2013). A four-step cycle driven by PI(4)P hydrolysis directs sterol/PI(4)P exchange by the ER-Golgi tether OSBP. *Cell*, 155(4), 830-843. doi:10.1016/j.cell.2013.09.056
- Metz, P., Dazert, E., Ruggieri, A., Mazur, J., Kaderali, L., Kaul, A., . . . Bartenschlager, R. (2012). Identification of type I and type II interferon-induced effectors controlling hepatitis C virus replication. *Hepatology*, 56(6), 2082-2093. doi:10.1002/hep.25908
- Meuleman, P., Bukh, J., Verhoye, L., Farhoudi, A., Vanwolleghem, T., Wang, R. Y., . . . Leroux-Roels, G. (2011). In vivo evaluation of the cross-genotype neutralizing activity of polyclonal antibodies against hepatitis C virus. *Hepatology*, 53(3), 755-762. doi:10.1002/hep.24171
- Meunier, J. C., Fournillier, A., Choukhi, A., Cahour, A., Cocquerel, L., Dubuisson, J., & Wychowski, C. (1999). Analysis of the glycosylation sites of hepatitis C virus (HCV) glycoprotein E1 and the influence of E1 glycans on the formation of the HCV glycoprotein complex. *J Gen Virol*, 80 ( Pt 4), 887-896. doi:10.1099/0022-1317-80-4-887
- Meunier, J. C., Russell, R. S., Engle, R. E., Faulk, K. N., Purcell, R. H., & Emerson, S. U. (2008). Apolipoprotein c1 association with hepatitis C virus. *J Virol*, 82(19), 9647-9656. doi:10.1128/JVI.00914-08

- Miller, R. H., & Purcell, R. H. (1990). Hepatitis C virus shares amino acid sequence similarity with pestiviruses and flaviviruses as well as members of two plant virus supergroups. *Proc Natl Acad Sci U S A*, 87(6), 2057-2061.
- Miller, S., & Krijnse-Locker, J. (2008). Modification of intracellular membrane structures for virus replication. *Nature reviews. Microbiology*, 6(5), 363-374. doi:10.1038/nrmicro1890
- Miranda, D. A., Kim, J. H., Nguyen, L. N., Cheng, W., Tan, B. C., Goh, V. J., . . . Silver, D. L. (2014). Fat storage-inducing transmembrane protein 2 is required for normal fat storage in adipose tissue. *J Biol Chem*, 289(14), 9560-9572. doi:10.1074/jbc.M114.547687
- Mishev, K., Dejonghe, W., & Russinova, E. (2013). Small molecules for dissecting endomembrane trafficking: a cross-systems view. *Chem Biol*, 20(4), 475-486. doi:10.1016/j.chembiol.2013.03.009
- Mishiba, K., Nagashima, Y., Suzuki, E., Hayashi, N., Ogata, Y., Shimada, Y., & Koizumi, N. (2013). Defects in IRE1 enhance cell death and fail to degrade mRNAs encoding secretory pathway proteins in the Arabidopsis unfolded protein response. *Proceedings of the National Academy of Sciences of the United States of America*, 110(14), 5713-5718. doi:10.1073/pnas.1219047110
- Mishra, G. R., Suresh, M., Kumaran, K., Kannabiran, N., Suresh, S., Bala, P., . . . Pandey, A. (2006). Human protein reference database--2006 update. *Nucleic Acids Res*, 34(Database issue), D411-414. doi:10.1093/nar/gkj141
- Missale, G., Bertoni, R., Lamonaca, V., Valli, A., Massari, M., Mori, C., . . . Ferrari, C. (1996). Different clinical behaviors of acute hepatitis C virus infection are associated with different vigor of the anti-viral cell-mediated immune response. *J Clin Invest*, 98(3), 706-714. doi:10.1172/JCI118842
- Missiha, S. B., Ostrowski, M., & Heathcote, E. J. (2008). Disease progression in chronic hepatitis C: modifiable and nonmodifiable factors. *Gastroenterology*, 134(6), 1699-1714. doi:10.1053/j.gastro.2008.02.069
- Mittelbrunn, M., & Sanchez-Madrid, F. (2012). Intercellular communication: diverse structures for exchange of genetic information. *Nat Rev Mol Cell Biol*, 13(5), 328-335. doi:10.1038/nrm3335
- Miyanari, Y., Atsuzawa, K., Usuda, N., Watashi, K., Hishiki, T., Zayas, M., . . . Shimotohno, K. (2007). The lipid droplet is an important organelle for hepatitis C virus production. *Nature cell biology*, 9(9), 1089-1097. doi:10.1038/ncb1631
- Miyoshi, H., Perfield, J. W., 2nd, Souza, S. C., Shen, W. J., Zhang, H. H., Stancheva, Z. S., . . . Greenberg, A. S. (2007). Control of adipose triglyceride lipase action by serine 517 of perilipin A globally regulates protein kinase A-stimulated lipolysis in adipocytes. *J Biol Chem*, 282(2), 996-1002. doi:10.1074/jbc.M605770200
- Mizukoshi, E., Eisenbach, C., Edlin, B. R., Newton, K. P., Raghuraman, S., Weiler-Normann, C., . . . Rehermann, B. (2008). Hepatitis C virus (HCV)-specific immune responses of long-term injection drug users frequently exposed to HCV. *J Infect Dis*, 198(2), 203-212. doi:10.1086/589510
- Momen-Heravi, F., Balaj, L., Alian, S., Tigges, J., Toxavidis, V., Ericsson, M., . . . Kuo, W. P. (2012). Alternative methods for characterization of extracellular vesicles. *Front Physiol*, 3, 354. doi:10.3389/fphys.2012.00354

- Moore, M. D., McGarvey, M. J., Russell, R. A., Cullen, B. R., & McClure, M. O. (2005). Stable inhibition of hepatitis B virus proteins by small interfering RNA expressed from viral vectors. *J Gene Med*, 7(7), 918-925. doi:10.1002/jgm.739
- Moradpour, D., Brass, V., Bieck, E., Friebe, P., Gosert, R., Blum, H. E., . . . Lohmann, V. (2004). Membrane association of the RNA-dependent RNA polymerase is essential for hepatitis C virus RNA replication. *J Virol*, 78(23), 13278-13284. doi:10.1128/JVI.78.23.13278-13284.2004
- Moradpour, D., Evans, M. J., Gosert, R., Yuan, Z., Blum, H. E., Goff, S. P., . . . Rice, C. M. (2004). Insertion of green fluorescent protein into nonstructural protein 5A allows direct visualization of functional hepatitis C virus replication complexes. *Journal of virology*, 78(14), 7400-7409. doi:10.1128/JVI.78.14.7400-7409.2004
- Moradpour, D., & Penin, F. (2013). Hepatitis C virus proteins: from structure to function. *Current topics in microbiology and immunology*, 369, 113-142. doi:10.1007/978-3-642-27340-7\_5
- Morin, T. J., Broering, T. J., Leav, B. A., Blair, B. M., Rowley, K. J., Boucher, E. N., . . . Babcock, G. J. (2012). Human monoclonal antibody HCV1 effectively prevents and treats HCV infection in chimpanzees. *PLoS pathogens*, 8(8), e1002895. doi:10.1371/journal.ppat.1002895
- Morishima, C., Polyak, S. J., Ray, R., Doherty, M. C., Di Bisceglie, A. M., Malet, P. F., . . . Hepatitis, C. A. L.-T. T. A. C. T. G. (2006). Hepatitis C virus-specific immune responses and quasi-species variability at baseline are associated with nonresponse to antiviral therapy during advanced hepatitis C. *The Journal of infectious diseases*, 193(7), 931-940. doi:10.1086/500952
- Moss, J., & Vaughan, M. (1993). ADP-ribosylation factors, 20,000 M(r) guanine nucleotide-binding protein activators of cholera toxin and components of intracellular vesicular transport systems. *Cell Signal*, 5(4), 367-379.
- Mothes, W., Sherer, N. M., Jin, J., & Zhong, P. (2010). Virus cell-to-cell transmission. *Journal of virology*, 84(17), 8360-8368. doi:10.1128/JVI.00443-10
- Murphy, D. J., & Vance, J. (1999). Mechanisms of lipid-body formation. *Trends Biochem Sci*, 24(3), 109-115.
- Na, T. Y., Shin, Y. K., Roh, K. J., Kang, S. A., Hong, I., Oh, S. J., . . . Lee, M. O. (2009). Liver X receptor mediates hepatitis B virus X protein-induced lipogenesis in hepatitis B virus-associated hepatocellular carcinoma. *Hepatology*, 49(4), 1122-1131. doi:10.1002/hep.22740
- Nagelkerke, J. F., van de Water, B., Twiss, I. M., Zoetewey, J. P., de Bont, H. J., Dogterom, P., & Mulder, G. J. (1991). Role of microtubuli in secretion of very-low-density lipoprotein in isolated rat hepatocytes: early effects of thiol reagents. *Hepatology*, 14(6), 1259-1268.
- Nahmias, Y., Goldwasser, J., Casali, M., van Poll, D., Wakita, T., Chung, R. T., & Yarmush, M. L. (2008). Apolipoprotein B-dependent hepatitis C virus secretion is inhibited by the grapefruit flavonoid naringenin. *Hepatology*, 47(5), 1437-1445. doi:10.1002/hep.22197
- Nair, V., Uchil, V., Chi, G., Dams, I., Cox, A., & Seo, B. (2007). Biologically-validated HIV integrase inhibitors with nucleobase scaffolds: structure, synthesis, chemical biology, molecular modeling, and antiviral activity. *Nucleosides, nucleotides & nucleic acids*, 26(6-7), 665-668. doi:10.1080/15257770701490563

- Nakamura, N., Akashi, T., Taneda, T., Kogo, H., Kikuchi, A., & Fujimoto, T. (2004). ADRP is dissociated from lipid droplets by ARF1-dependent mechanism. *Biochemical and biophysical research communications*, 322(3), 957-965. doi:10.1016/j.bbrc.2004.08.010
- Nakamura, N., Banno, Y., & Tamiya-Koizumi, K. (2005). Arf1-dependent PLD1 is localized to oleic acid-induced lipid droplets in NIH3T3 cells. *Biochemical and biophysical research communications*, 335(1), 117-123. doi:10.1016/j.bbrc.2005.07.050
- Nan, X., Potma, E. O., & Xie, X. S. (2006). Nonperturbative chemical imaging of organelle transport in living cells with coherent anti-stokes Raman scattering microscopy. *Biophys J*, 91(2), 728-735. doi:10.1529/biophysj.105.074534
- Narciso-Schiavon, J. L., Schiavon Lde, L., Carvalho-Filho, R. J., Sampaio, J. P., Batah, P. N., Barbosa, D. V., . . . Silva, A. E. (2010). Gender influence on treatment of chronic hepatitis C genotype 1. *Rev Soc Bras Med Trop*, 43(3), 217-223.
- Nasheri, N., Joyce, M., Rouleau, Y., Yang, P., Yao, S., Tyrrell, D. L., & Pezacki, J. P. (2013). Modulation of fatty acid synthase enzyme activity and expression during hepatitis C virus replication. *Chem Biol*, 20(4), 570-582. doi:10.1016/j.chembiol.2013.03.014
- Nattermann, J., Schneiders, A. M., Leifeld, L., Langhans, B., Schulz, M., Inchauspe, G., . . . Spengler, U. (2005). Serum antibodies against the hepatitis C virus E2 protein mediate antibody-dependent cellular cytotoxicity (ADCC). *J Hepatol*, 42(4), 499-504. doi:10.1016/j.jhep.2004.12.018
- Negro, F., Giostra, E., Krawczynski, K., Quadri, R., Rubbia-Brandt, L., Mentha, G., . . . Hadengue, A. (1998). Detection of intrahepatic hepatitis C virus replication by strand-specific semi-quantitative RT-PCR: preliminary application to the liver transplantation model. *J Hepatol*, 29(1), 1-11.
- Netski, D. M., Mosbrugger, T., Depla, E., Maertens, G., Ray, S. C., Hamilton, R. G., . . . Cox, A. (2005). Humoral immune response in acute hepatitis C virus infection. *Clin Infect Dis*, 41(5), 667-675. doi:10.1086/432478
- Neveu, G., Barouch-Bentov, R., Ziv-Av, A., Gerber, D., Jacob, Y., & Einav, S. (2012). Identification and targeting of an interaction between a tyrosine motif within hepatitis C virus core protein and AP2M1 essential for viral assembly. *PLoS Pathog*, 8(8), e1002845. doi:10.1371/journal.ppat.1002845
- Nevo-Yassaf, I., Yaffe, Y., Asher, M., Ravid, O., Eizenberg, S., Henis, Y. I., . . . Sklan, E. H. (2012). Role for TBC1D20 and Rab1 in hepatitis C virus replication via interaction with lipid droplet-bound nonstructural protein 5A. *J Virol*, 86(12), 6491-6502. doi:10.1128/JVI.00496-12
- Nickel, W., & Wieland, F. T. (1997). Biogenesis of COPI-coated transport vesicles. *FEBS Lett*, 413(3), 395-400.
- Nielsen, S. U., Bassendine, M. F., Burt, A. D., Martin, C., Pumeekochchai, W., & Toms, G. L. (2006). Association between hepatitis C virus and very-low-density lipoprotein (VLDL)/LDL analyzed in iodixanol density gradients. *J Virol*, 80(5), 2418-2428. doi:10.1128/JVI.80.5.2418-2428.2006
- Nishimoto, Y., & Tamori, Y. (2017). CIDE Family-Mediated Unique Lipid Droplet Morphology in White Adipose Tissue and Brown Adipose Tissue Determines the

- Adipocyte Energy Metabolism. *J Atheroscler Thromb*, 24(10), 989-998. doi:10.5551/jat.RV17011
- Niu, T. K., Pfeifer, A. C., Lippincott-Schwartz, J., & Jackson, C. L. (2005). Dynamics of GBF1, a Brefeldin A-sensitive Arf1 exchange factor at the Golgi. *Molecular biology of the cell*, 16(3), 1213-1222. doi:10.1091/mbc.E04-07-0599
- Noppornpanth, S., Smits, S. L., Lien, T. X., Poovorawan, Y., Osterhaus, A. D., & Haagmans, B. L. (2007). Characterization of hepatitis C virus deletion mutants circulating in chronically infected patients. *J Virol*, 81(22), 12496-12503. doi:10.1128/JVI.01059-07
- Nose, F., Yamaguchi, T., Kato, R., Aiuchi, T., Obama, T., Hara, S., . . . Itabe, H. (2013). Crucial role of perilipin-3 (TIP47) in formation of lipid droplets and PGE2 production in HL-60-derived neutrophils. *PLoS One*, 8(8), e71542. doi:10.1371/journal.pone.0071542
- Nouri Aria, K. T., Sallie, R., Sangar, D., Alexander, G. J., Smith, H., Byrne, J., . . . Williams, R. (1993). Detection of genomic and intermediate replicative strands of hepatitis C virus in liver tissue by in situ hybridization. *J Clin Invest*, 91(5), 2226-2234. doi:10.1172/JCI116449
- Novikov, M. S., Buckheit, R. W., Jr., Temburnikar, K., Khandazhinskaya, A. L., Ivanov, A. V., & Seley-Radtke, K. L. (2010). 1-Benzyl derivatives of 5-(arylamino)uracils as anti-HIV-1 and anti-EBV agents. *Bioorganic & medicinal chemistry*, 18(23), 8310-8314. doi:10.1016/j.bmc.2010.09.070
- O'Beirne, J., Mitchell, J., Farzaneh, F., & Harrison, P. M. (2009). Inhibition of major histocompatibility complex Class I antigen presentation by hepatitis C virus core protein in myeloid dendritic cells. *Virology*, 389(1-2), 1-7. doi:10.1016/j.virol.2009.03.035
- Ohsaki, Y., Cheng, J., Fujita, A., Tokumoto, T., & Fujimoto, T. (2006). Cytoplasmic lipid droplets are sites of convergence of proteasomal and autophagic degradation of apolipoprotein B. *Mol Biol Cell*, 17(6), 2674-2683. doi:10.1091/mbc.E05-07-0659
- Ohsaki, Y., Maeda, T., Maeda, M., Tauchi-Sato, K., & Fujimoto, T. (2006). Recruitment of TIP47 to lipid droplets is controlled by the putative hydrophobic cleft. *Biochem Biophys Res Commun*, 347(1), 279-287. doi:10.1016/j.bbrc.2006.06.074
- Oliviero, B., Varchetta, S., Paudice, E., Michelone, G., Zaramella, M., Mavilio, D., . . . Mondelli, M. U. (2009). Natural killer cell functional dichotomy in chronic hepatitis B and chronic hepatitis C virus infections. *Gastroenterology*, 137(3), 1151-1160, 1160 e1151-1157. doi:10.1053/j.gastro.2009.05.047
- Olofsson, S.-O., Boström, P., Lagerstedt, J., Andersson, L., Adiels, M., Perman, J., . . . Borén, J. (2009). The Lipid Droplet: a Dynamic Organelle, not only Involved in the Storage and Turnover of Lipids. 1-26. doi:10.1007/978-3-642-00300-4\_1
- Onlamoon, N., Das Gupta, J., Sharma, P., Rogers, K., Suppiah, S., Rhea, J., . . . Villinger, F. (2011). Infection, viral dissemination, and antibody responses of rhesus macaques exposed to the human gammaretrovirus XMRV. *J Virol*, 85(9), 4547-4557. doi:10.1128/JVI.02411-10
- Orci, L., Le Marchand, Y., Singh, A., Assimacopoulos-Jeannet, F., Rouiller, C., & Jeanrenaud, B. (1973). Letter: Role of microtubules in lipoprotein secretion by the liver. *Nature*, 244(5410), 30-32.

- Orlicky, D. J., Monks, J., Stefanski, A. L., & McManaman, J. L. (2013). Dynamics and molecular determinants of cytoplasmic lipid droplet clustering and dispersion. *PLoS one*, 8(6), e66837. doi:10.1371/journal.pone.0066837
- Owen, D. M., Huang, H., Ye, J., & Gale, M., Jr. (2009). Apolipoprotein E on hepatitis C virion facilitates infection through interaction with low-density lipoprotein receptor. *Virology*, 394(1), 99-108. doi:10.1016/j.virol.2009.08.037
- Ozeki, S., Cheng, J., Tauchi-Sato, K., Hatano, N., Taniguchi, H., & Fujimoto, T. (2005). Rab18 localizes to lipid droplets and induces their close apposition to the endoplasmic reticulum-derived membrane. *J Cell Sci*, 118(Pt 12), 2601-2611. doi:10.1242/jcs.02401
- Ozkok, A., & Yildiz, A. (2014). Hepatitis C virus associated glomerulopathies. *World J Gastroenterol*, 20(24), 7544-7554. doi:10.3748/wjg.v20.i24.7544
- Paar, M., Jungst, C., Steiner, N. A., Magnes, C., Sinner, F., Kolb, D., . . . Wolinski, H. (2012). Remodeling of lipid droplets during lipolysis and growth in adipocytes. *J Biol Chem*, 287(14), 11164-11173. doi:10.1074/jbc.M111.316794
- Pagac, M., Cooper, D. E., Qi, Y., Lukmantara, I. E., Mak, H. Y., Wu, Z., . . . Yang, H. (2016). SEIPIN Regulates Lipid Droplet Expansion and Adipocyte Development by Modulating the Activity of Glycerol-3-phosphate Acyltransferase. *Cell Rep*, 17(6), 1546-1559. doi:10.1016/j.celrep.2016.10.037
- Pal, S., Shuhart, M. C., Thomassen, L., Emerson, S. S., Su, T., Feuerborn, N., . . . Gretsch, D. R. (2006). Intrahepatic hepatitis C virus replication correlates with chronic hepatitis C disease severity in vivo. *Journal of virology*, 80(5), 2280-2290. doi:10.1128/JVI.80.5.2280-2290.2006
- Palapac, N. M., Hiramane, Y., Seto, S., Hiramatsu, R., Horii, T., & Mitamura, T. (2004). Evidence that Plasmodium falciparum diacylglycerol acyltransferase is essential for intraerythrocytic proliferation. *Biochem Biophys Res Commun*, 321(4), 1062-1068. doi:10.1016/j.bbrc.2004.07.070
- Paladino, N., Fainboim, H., Theiler, G., Schroder, T., Munoz, A. E., Flores, A. C., . . . Fainboim, L. (2006). Gender susceptibility to chronic hepatitis C virus infection associated with interleukin 10 promoter polymorphism. *J Virol*, 80(18), 9144-9150. doi:10.1128/JVI.00339-06
- Parashar, U. D., Gibson, C. J., Bresee, J. S., & Glass, R. I. (2006). Rotavirus and severe childhood diarrhea. *Emerg Infect Dis*, 12(2), 304-306. doi:10.3201/eid1202.050006
- Paredes, A. M., & Blight, K. J. (2008). A genetic interaction between hepatitis C virus NS4B and NS3 is important for RNA replication. *J Virol*, 82(21), 10671-10683. doi:10.1128/JVI.00875-08
- Parrish, C. R., Holmes, E. C., Morens, D. M., Park, E. C., Burke, D. S., Calisher, C. H., . . . Daszak, P. (2008). Cross-species virus transmission and the emergence of new epidemic diseases. *Microbiol Mol Biol Rev*, 72(3), 457-470. doi:10.1128/MMBR.00004-08
- Patton, J. T., Silvestri, L. S., Tortorici, M. A., Vasquez-Del Carpio, R., & Taraporewala, Z. F. (2006). Rotavirus genome replication and morphogenesis: role of the viroplasm. *Curr Top Microbiol Immunol*, 309, 169-187.

- Paul, D., Madan, V., & Bartenschlager, R. (2014). Hepatitis C Virus RNA Replication and Assembly: Living on the Fat of the Land. *Cell host & microbe*, 16(5), 569-579. doi:10.1016/j.chom.2014.10.008
- Paul, D., Romero-Brey, I., Gouttenoire, J., Stoitsova, S., Krijnse-Locker, J., Moradpour, D., & Bartenschlager, R. (2011). NS4B self-interaction through conserved C-terminal elements is required for the establishment of functional hepatitis C virus replication complexes. *Journal of virology*, 85(14), 6963-6976. doi:10.1128/JVI.00502-11
- Pelletier, S., Drouin, C., Bedard, N., Khakoo, S. I., Bruneau, J., & Shoukry, N. H. (2010). Increased degranulation of natural killer cells during acute HCV correlates with the magnitude of virus-specific T cell responses. *J Hepatol*, 53(5), 805-816. doi:10.1016/j.jhep.2010.05.013
- Perlemuter, G., Sabile, A., Letteron, P., Vona, G., Topilco, A., Chretien, Y., . . . Brechot, C. (2002). Hepatitis C virus core protein inhibits microsomal triglyceride transfer protein activity and very low density lipoprotein secretion: a model of viral-related steatosis. *The FASEB journal : official publication of the Federation of American Societies for Experimental Biology*, 16(2), 185-194. doi:10.1096/fj.01-0396com
- Pesavento, J. B., Crawford, S. E., Estes, M. K., & Prasad, B. V. (2006). Rotavirus proteins: structure and assembly. *Curr Top Microbiol Immunol*, 309, 189-219.
- Pestka, J. M., Zeisel, M. B., Blaser, E., Schurmann, P., Bartosch, B., Cosset, F. L., . . . Baumert, T. F. (2007). Rapid induction of virus-neutralizing antibodies and viral clearance in a single-source outbreak of hepatitis C. *Proc Natl Acad Sci U S A*, 104(14), 6025-6030. doi:10.1073/pnas.0607026104
- Peters, T., Mohr, L., Scheiffele, F., Schlayer, H. J., Preisler, S., Berthold, H., . . . Rasenack, J. (1994). Antibodies and viremia in acute post-transfusion hepatitis C: a prospective study. *J Med Virol*, 42(4), 420-427.
- Petersen, L. R., Brault, A. C., & Nasci, R. S. (2013). West Nile virus: review of the literature. *JAMA*, 310(3), 308-315. doi:10.1001/jama.2013.8042
- Pham, T. M., Tran, S. C., Lim, Y. S., & Hwang, S. B. (2016). Hepatitis C Virus-Induced Rab32 Aggregation and its Implication in Virion Assembly. *Journal of virology*. doi:10.1128/JVI.01662-16
- Phan, T., Kohlway, A., Dimberu, P., Pyle, A. M., & Lindenbach, B. D. (2011). The acidic domain of hepatitis C virus NS4A contributes to RNA replication and virus particle assembly. *J Virol*, 85(3), 1193-1204. doi:10.1128/JVI.01889-10
- Pietschmann, T., Kaul, A., Koutsoudakis, G., Shavinskaya, A., Kallis, S., Steinmann, E., . . . Bartenschlager, R. (2006). Construction and characterization of infectious intragenotypic and intergenotypic hepatitis C virus chimeras. *Proc Natl Acad Sci U S A*, 103(19), 7408-7413. doi:10.1073/pnas.0504877103
- Pileri, P., Uematsu, Y., Campagnoli, S., Galli, G., Falugi, F., Petracca, R., . . . Abrignani, S. (1998). Binding of hepatitis C virus to CD81. *Science*, 282(5390), 938-941.
- Pineiro, D., & Martinez-Salas, E. (2012). RNA structural elements of hepatitis C virus controlling viral RNA translation and the implications for viral pathogenesis. *Viruses*, 4(10), 2233-2250. doi:10.3390/v4102233
- Ploen, D., Hafirassou, M. L., Himmelsbach, K., Sauter, D., Biniossek, M. L., Weiss, T. S., . . . Hildt, E. (2013). TIP47 plays a crucial role in the life cycle of hepatitis C virus. *Journal of hepatology*, 58(6), 1081-1088. doi:10.1016/j.jhep.2013.01.022

- Ploen, D., Hafirassou, M. L., Himmelsbach, K., Schille, S. A., Biniossek, M. L., Baumert, T. F., . . . Hildt, E. (2013). TIP47 is associated with the hepatitis C virus and its interaction with Rab9 is required for release of viral particles. *Eur J Cell Biol*, 92(12), 374-382. doi:10.1016/j.ejcb.2013.12.003
- Ploss, A., Evans, M. J., Gaysinskaya, V. A., Panis, M., You, H., de Jong, Y. P., & Rice, C. M. (2009). Human occludin is a hepatitis C virus entry factor required for infection of mouse cells. *Nature*, 457(7231), 882-886. doi:10.1038/nature07684
- Popescu, C. I., Callens, N., Trinel, D., Roingeard, P., Moradpour, D., Descamps, V., . . . Dubuisson, J. (2011). NS2 protein of hepatitis C virus interacts with structural and non-structural proteins towards virus assembly. *PLoS Pathog*, 7(2), e1001278. doi:10.1371/journal.ppat.1001278
- Popescu, C. I., Riva, L., Vlaicu, O., Farhat, R., Rouille, Y., & Dubuisson, J. (2014). Hepatitis C virus life cycle and lipid metabolism. *Biology (Basel)*, 3(4), 892-921. doi:10.3390/biology3040892
- Popoff, V., Langer, J. D., Reckmann, I., Hellwig, A., Kahn, R. A., Brugger, B., & Wieland, F. T. (2011). Several ADP-ribosylation factor (Arf) isoforms support COPI vesicle formation. *The Journal of biological chemistry*, 286(41), 35634-35642. doi:10.1074/jbc.M111.261800
- Poppelreuther, M., Rudolph, B., Du, C., Grossmann, R., Becker, M., Thiele, C., . . . Fullekrug, J. (2012). The N-terminal region of acyl-CoA synthetase 3 is essential for both the localization on lipid droplets and the function in fatty acid uptake. *J Lipid Res*, 53(5), 888-900. doi:10.1194/jlr.M024562
- Post, J. J., Pan, Y., Freeman, A. J., Harvey, C. E., White, P. A., Palladinetti, P., . . . Transmission in Prisons Study, G. (2004). Clearance of hepatitis C viremia associated with cellular immunity in the absence of seroconversion in the hepatitis C incidence and transmission in prisons study cohort. *J Infect Dis*, 189(10), 1846-1855. doi:10.1086/383279
- Pourteymour, S., Lee, S., Langleite, T. M., Eckardt, K., Hjorth, M., Bindesboll, C., . . . Norheim, F. (2015). Perilipin 4 in human skeletal muscle: localization and effect of physical activity. *Physiol Rep*, 3(8). doi:10.14814/phy2.12481
- Prentki, M., Chaponnier, C., Jeanrenaud, B., & Gabbiani, G. (1979). Actin microfilaments, cell shape, and secretory processes in isolated rat hepatocytes. Effect of phalloidin and cytochalasin D. *J Cell Biol*, 81(3), 592-607.
- Prince, A. M., Brotman, B., Grady, G. F., Kuhns, W. J., Hazzi, C., Levine, R. W., & Millian, S. J. (1974). Long-incubation post-transfusion hepatitis without serological evidence of exposure to hepatitis-B virus. *Lancet*, 2(7875), 241-246.
- Qian, X. J., Zhu, Y. Z., Zhao, P., & Qi, Z. T. (2016). Entry inhibitors: New advances in HCV treatment. *Emerg Microbes Infect*, 5, e3. doi:10.1038/emi.2016.3
- Qu, R. D., & Huang, A. H. (1990). Oleosin KD 18 on the surface of oil bodies in maize. Genomic and cDNA sequences and the deduced protein structure. *J Biol Chem*, 265(4), 2238-2243.
- Radziejewicz, H., Ibegbu, C. C., Fernandez, M. L., Workowski, K. A., Obideen, K., Wehbi, M., . . . Grakoui, A. (2007). Liver-infiltrating lymphocytes in chronic human hepatitis C virus infection display an exhausted phenotype with high levels of PD-1 and low levels of CD127 expression. *J Virol*, 81(6), 2545-2553. doi:10.1128/JVI.02021-06



- Ramaen, O., Joubert, A., Simister, P., Belgareh-Touze, N., Olivares-Sanchez, M. C., Zeeh, J. C., . . . Cherfils, J. (2007). Interactions between conserved domains within homodimers in the BIG1, BIG2, and GBF1 Arf guanine nucleotide exchange factors. *The Journal of biological chemistry*, 282(39), 28834-28842. doi:10.1074/jbc.M705525200
- Ramakrishnaiah, V., Thumann, C., Fofana, I., Habersetzer, F., Pan, Q., de Ruiter, P. E., . . . van der Laan, L. J. (2013). Exosome-mediated transmission of hepatitis C virus between human hepatoma Huh7.5 cells. *Proceedings of the National Academy of Sciences of the United States of America*, 110(32), 13109-13113. doi:10.1073/pnas.1221899110
- Record, M., Poirot, M., & Silvente-Poirot, S. (2014). Emerging concepts on the role of exosomes in lipid metabolic diseases. *Biochimie*, 96, 67-74. doi:10.1016/j.biochi.2013.06.016
- Reiss, S., Rebhan, I., Backes, P., Romero-Brey, I., Erfle, H., Matula, P., . . . Bartenschlager, R. (2011). Recruitment and activation of a lipid kinase by hepatitis C virus NS5A is essential for integrity of the membranous replication compartment. *Cell Host Microbe*, 9(1), 32-45. doi:10.1016/j.chom.2010.12.002
- Richards, A. L., Soares-Martins, J. A., Riddell, G. T., & Jackson, W. T. (2014). Generation of unique poliovirus RNA replication organelles. *MBio*, 5(2), e00833-00813. doi:10.1128/mBio.00833-13
- Richards, S. L., Anderson, S. L., Lord, C. C., Smartt, C. T., & Tabachnick, W. J. (2012). Relationships between infection, dissemination, and transmission of West Nile virus RNA in *Culex pipiens quinquefasciatus* (Diptera: Culicidae). *J Med Entomol*, 49(1), 132-142.
- Rigamonti, C., Andorno, S., Maduli, E., Capelli, F., Boldorini, R., & Sartori, M. (2005). Gender and liver fibrosis in chronic hepatitis: the role of iron status. *Aliment Pharmacol Ther*, 21(12), 1445-1451. doi:10.1111/j.1365-2036.2005.02517.x
- Rittinger, K. (2008). Snapshots Form a Big Picture of Guanine Nucleotide Exchange.
- Robbins, F. C., Enders, J. F., & Weller, T. H. (1950). Cytopathogenic effect of poliomyelitis viruses in vitro on human embryonic tissues. *Proc Soc Exp Biol Med*, 75(2), 370-374.
- Robenek, H., Hofnagel, O., Buers, I., Robenek, M. J., Troyer, D., & Severs, N. J. (2006). Adipophilin-enriched domains in the ER membrane are sites of lipid droplet biogenesis. *J Cell Sci*, 119(Pt 20), 4215-4224. doi:10.1242/jcs.03191
- Robenek, H., Lorkowski, S., Schnoor, M., & Troyer, D. (2005). Spatial integration of TIP47 and adipophilin in macrophage lipid bodies. *J Biol Chem*, 280(7), 5789-5794. doi:10.1074/jbc.M407194200
- Roberts, S. R., Compans, R. W., & Wertz, G. W. (1995). Respiratory syncytial virus matures at the apical surfaces of polarized epithelial cells. *J Virol*, 69(4), 2667-2673.
- Rodenhuis-Zybert, I. A., Wilschut, J., & Smit, J. M. (2010). Dengue virus life cycle: viral and host factors modulating infectivity. *Cell Mol Life Sci*, 67(16), 2773-2786. doi:10.1007/s00018-010-0357-z
- Rohwedder, A., Zhang, Q., Rudge, S. A., & Wakelam, M. J. (2014). Lipid droplet formation in response to oleic acid in Huh-7 cells is mediated by the fatty acid receptor FFAR4. *Journal of cell science*, 127(Pt 14), 3104-3115. doi:10.1242/jcs.145854

- Rosch, K., Kwiatkowski, M., Hofmann, S., Schobel, A., Gruttner, C., Wurlitzer, M., . . . Herker, E. (2016). Quantitative Lipid Droplet Proteome Analysis Identifies Annexin A3 as a Cofactor for HCV Particle Production. *Cell Rep*, 16(12), 3219-3231. doi:10.1016/j.celrep.2016.08.052
- Ross-Thriepland, D., Amako, Y., & Harris, M. (2013). The C terminus of NS5A domain II is a key determinant of hepatitis C virus genome replication, but is not required for virion assembly and release. *J Gen Virol*, 94(Pt 5), 1009-1018. doi:10.1099/vir.0.050633-0
- Rothman, J. E., & Wieland, F. T. (1996). Protein sorting by transport vesicles. *Science*, 272(5259), 227-234.
- Rouille, Y., Helle, F., Delgrange, D., Roingeard, P., Voisset, C., Blanchard, E., . . . Dubuisson, J. (2006). Subcellular localization of hepatitis C virus structural proteins in a cell culture system that efficiently replicates the virus. *Journal of virology*, 80(6), 2832-2841. doi:10.1128/JVI.80.6.2832-2841.2006
- Rueger, S., Bochud, P. Y., Dufour, J. F., Mullhaupt, B., Semela, D., Heim, M. H., . . . Negro, F. (2015). Impact of common risk factors of fibrosis progression in chronic hepatitis C. *Gut*, 64(10), 1605-1615. doi:10.1136/gutjnl-2014-306997
- Russell, T. D., Schaack, J., Orlicky, D. J., Palmer, C., Chang, B. H., Chan, L., & McManaman, J. L. (2011). Adipophilin regulates maturation of cytoplasmic lipid droplets and alveolae in differentiating mammary glands. *J Cell Sci*, 124(Pt 19), 3247-3253. doi:10.1242/jcs.082974
- Rust, R. C., Landmann, L., Gosert, R., Tang, B. L., Hong, W., Hauri, H. P., . . . Bienz, K. (2001). Cellular COPII proteins are involved in production of the vesicles that form the poliovirus replication complex. *Journal of virology*, 75(20), 9808-9818. doi:10.1128/JVI.75.20.9808-9818.2001
- Sabahi, A., Marsh, K. A., Dahari, H., Corcoran, P., Lamora, J. M., Yu, X., . . . Uprichard, S. L. (2010). The rate of hepatitis C virus infection initiation in vitro is directly related to particle density. *Virology*, 407(1), 110-119. doi:10.1016/j.virol.2010.07.026
- Saenz, J. B., Sun, W. J., Chang, J. W., Li, J., Bursulaya, B., Gray, N. S., & Haslam, D. B. (2009). Golgicide A reveals essential roles for GBF1 in Golgi assembly and function. *Nature chemical biology*, 5(3), 157-165. doi:10.1038/nchembio.144
- Sainz, B., Jr., Barretto, N., Martin, D. N., Hiraga, N., Imamura, M., Hussain, S., . . . Uprichard, S. L. (2012). Identification of the Niemann-Pick C1-like 1 cholesterol absorption receptor as a new hepatitis C virus entry factor. *Nat Med*, 18(2), 281-285. doi:10.1038/nm.2581
- Saito, T., & Gale, M., Jr. (2008). Regulation of innate immunity against hepatitis C virus infection. *Hepatol Res*, 38(2), 115-122. doi:10.1111/j.1872-034X.2007.00283.x
- Saito, T., Owen, D. M., Jiang, F., Marcotrigiano, J., & Gale, M., Jr. (2008). Innate immunity induced by composition-dependent RIG-I recognition of hepatitis C virus RNA. *Nature*, 454(7203), 523-527. doi:10.1038/nature07106
- Salloum, S., Wang, H., Ferguson, C., Parton, R. G., & Tai, A. W. (2013). Rab18 binds to hepatitis C virus NS5A and promotes interaction between sites of viral replication and lipid droplets. *PLoS Pathog*, 9(8), e1003513. doi:10.1371/journal.ppat.1003513
- Samsa, M. M., Mondotte, J. A., Iglesias, N. G., Assuncao-Miranda, I., Barbosa-Lima, G., Da Poian, A. T., . . . Gamarnik, A. V. (2009). Dengue virus capsid protein usurps

- lipid droplets for viral particle formation. *PLoS Pathog*, 5(10), e1000632. doi:10.1371/journal.ppat.1000632
- Sarasin-Filipowicz, M., Oakeley, E. J., Duong, F. H., Christen, V., Terracciano, L., Filipowicz, W., & Heim, M. H. (2008). Interferon signaling and treatment outcome in chronic hepatitis C. *Proc Natl Acad Sci U S A*, 105(19), 7034-7039. doi:10.1073/pnas.0707882105
- Sato, S., Fukasawa, M., Yamakawa, Y., Natsume, T., Suzuki, T., Shoji, I., . . . Nishijima, M. (2006). Proteomic profiling of lipid droplet proteins in hepatoma cell lines expressing hepatitis C virus core protein. *Journal of biochemistry*, 139(5), 921-930. doi:10.1093/jb/mvj104
- Scarselli, E., Ansuini, H., Cerino, R., Roccasecca, R. M., Acali, S., Filocamo, G., . . . Vitelli, A. (2002). The human scavenger receptor class B type I is a novel candidate receptor for the hepatitis C virus. *The EMBO journal*, 21(19), 5017-5025.
- Schaffer, J. E. (2003). Lipotoxicity: when tissues overeat. *Curr Opin Lipidol*, 14(3), 281-287. doi:10.1097/01.mol.0000073508.41685.7f
- Schmidt-Mende, J., Bieck, E., Hugle, T., Penin, F., Rice, C. M., Blum, H. E., & Moradpour, D. (2001). Determinants for membrane association of the hepatitis C virus RNA-dependent RNA polymerase. *J Biol Chem*, 276(47), 44052-44063. doi:10.1074/jbc.M103358200
- Schmitt, M., Scrima, N., Radujkovic, D., Caillet-Saguy, C., Simister, P. C., Friebe, P., . . . Bressanelli, S. (2011). A comprehensive structure-function comparison of hepatitis C virus strain JFH1 and J6 polymerases reveals a key residue stimulating replication in cell culture across genotypes. *J Virol*, 85(6), 2565-2581. doi:10.1128/JVI.02177-10
- Schulze, R. J., Weller, S. G., Schroeder, B., Krueger, E. W., Chi, S., Casey, C. A., & McNiven, M. A. (2013). Lipid droplet breakdown requires dynamin 2 for vesiculation of autolysosomal tubules in hepatocytes. *The Journal of cell biology*, 203(2), 315-326. doi:10.1083/jcb.201306140
- Scognamiglio, P., Accapezzato, D., Casciaro, M. A., Cacciani, A., Artini, M., Bruno, G., . . . Barnaba, V. (1999). Presence of effector CD8+ T cells in hepatitis C virus-exposed healthy seronegative donors. *J Immunol*, 162(11), 6681-6689.
- Scott, R. M., Snitbhan, R., Bancroft, W. H., Alter, H. J., & Tingpalapong, M. (1980). Experimental transmission of hepatitis B virus by semen and saliva. *J Infect Dis*, 142(1), 67-71.
- Shanmugam, S., Saravanabalaji, D., & Yi, M. (2015). Detergent-resistant membrane association of NS2 and E2 during hepatitis C virus replication. *J Virol*, 89(8), 4562-4574. doi:10.1128/JVI.00123-15
- Sharma, V., Chitranshi, N., & Agarwal, A. K. (2014). Significance and biological importance of pyrimidine in the microbial world. *Int J Med Chem*, 2014, 202784. doi:10.1155/2014/202784
- Shata, M. T., Tricoche, N., Perkus, M., Tom, D., Brotman, B., McCormack, P., . . . Prince, A. M. (2003). Exposure to low infective doses of HCV induces cellular immune responses without consistently detectable viremia or seroconversion in chimpanzees. *Virology*, 314(2), 601-616.
- Shavinskaya, A., Boulant, S., Penin, F., McLauchlan, J., & Bartenschlager, R. (2007a). The lipid droplet binding domain of hepatitis C virus core protein is a major

- determinant for efficient virus assembly. *J Biol Chem*, 282(51), 37158-37169. doi:10.1074/jbc.M707329200
- Shavinskaya, A., Boulant, S., Penin, F., McLauchlan, J., & Bartenschlager, R. (2007b). The lipid droplet binding domain of hepatitis C virus core protein is a major determinant for efficient virus assembly. *The Journal of biological chemistry*, 282(51), 37158-37169. doi:10.1074/jbc.M707329200
- Shen, W. J., Hu, J., Hu, Z., Kraemer, F. B., & Azhar, S. (2014). Scavenger receptor class B type I (SR-BI): a versatile receptor with multiple functions and actions. *Metabolism*, 63(7), 875-886. doi:10.1016/j.metabol.2014.03.011
- Sherman, A. C., & Sherman, K. E. (2015). Extrahepatic manifestations of hepatitis C infection: navigating CHASM. *Curr HIV/AIDS Rep*, 12(3), 353-361. doi:10.1007/s11904-015-0274-8
- Shi, Q., Jiang, J., & Luo, G. (2013). Syndecan-1 serves as the major receptor for attachment of hepatitis C virus to the surfaces of hepatocytes. *J Virol*, 87(12), 6866-6875. doi:10.1128/JVI.03475-12
- Shi, S. T., Polyak, S. J., Tu, H., Taylor, D. R., Gretch, D. R., & Lai, M. M. (2002). Hepatitis C virus NS5A colocalizes with the core protein on lipid droplets and interacts with apolipoproteins. *Virology*, 292(2), 198-210. doi:10.1006/viro.2001.1225
- Shih, J. W., Mur, J. I., & Alter, H. J. (1986). Non-A, non-B hepatitis: advances and unfulfilled expectations of the first decade. *Prog Liver Dis*, 8, 433-452.
- Shimakami, T., Hijikata, M., Luo, H., Ma, Y. Y., Kaneko, S., Shimotohno, K., & Murakami, S. (2004). Effect of interaction between hepatitis C virus NS5A and NS5B on hepatitis C virus RNA replication with the hepatitis C virus replicon. *J Virol*, 78(6), 2738-2748.
- Shimotohno, K., Tanji, Y., Hirowatari, Y., Komoda, Y., Kato, N., & Hijikata, M. (1995). Processing of the hepatitis C virus precursor protein. *J Hepatol*, 22(1 Suppl), 87-92.
- Shin, E. C., Capone, S., Cortese, R., Colloca, S., Nicosia, A., Folgori, A., & Rehmann, B. (2008). The kinetics of hepatitis C virus-specific CD8 T-cell responses in the blood mirror those in the liver in acute hepatitis C virus infection. *J Virol*, 82(19), 9782-9788. doi:10.1128/JVI.00475-08
- Shin, H. W., Morinaga, N., Noda, M., & Nakayama, K. (2004). BIG2, a guanine nucleotide exchange factor for ADP-ribosylation factors: its localization to recycling endosomes and implication in the endosome integrity. *Mol Biol Cell*, 15(12), 5283-5294. doi:10.1091/mbc.E04-05-0388
- Shin, H. W., & Nakayama, K. (2004). Guanine nucleotide-exchange factors for arf GTPases: their diverse functions in membrane traffic. *J Biochem*, 136(6), 761-767. doi:10.1093/jb/mvh185
- Shoukry, N. H., Grakoui, A., Houghton, M., Chien, D. Y., Ghayeb, J., Reimann, K. A., & Walker, C. M. (2003). Memory CD8+ T cells are required for protection from persistent hepatitis C virus infection. *J Exp Med*, 197(12), 1645-1655. doi:10.1084/jem.20030239
- Shubeita, G. T., Tran, S. L., Xu, J., Vershinin, M., Cermelli, S., Cotton, S. L., . . . Gross, S. P. (2008). Consequences of motor copy number on the intracellular transport of kinesin-1-driven lipid droplets. *Cell*, 135(6), 1098-1107. doi:10.1016/j.cell.2008.10.021

- Shulla, A., & Randall, G. (2015). Spatiotemporal analysis of hepatitis C virus infection. *PLoS pathogens*, 11(3), e1004758. doi:10.1371/journal.ppat.1004758
- Sigal, A., Kim, J. T., Balazs, A. B., Dekel, E., Mayo, A., Milo, R., & Baltimore, D. (2011). Cell-to-cell spread of HIV permits ongoing replication despite antiretroviral therapy. *Nature*, 477(7362), 95-98. doi:10.1038/nature10347
- Simha, V., & Garg, A. (2003). Phenotypic heterogeneity in body fat distribution in patients with congenital generalized lipodystrophy caused by mutations in the AGPAT2 or seipin genes. *J Clin Endocrinol Metab*, 88(11), 5433-5437. doi:10.1210/jc.2003-030835
- Simister, P., Schmitt, M., Geitmann, M., Wicht, O., Danielson, U. H., Klein, R., . . . Lohmann, V. (2009). Structural and functional analysis of hepatitis C virus strain JFH1 polymerase. *Journal of virology*, 83(22), 11926-11939. doi:10.1128/JVI.01008-09
- Simmonds, P. (1995). Variability of hepatitis C virus. *Hepatology*, 21(2), 570-583.
- Simmonds, P. (2004). Genetic diversity and evolution of hepatitis C virus--15 years on. *The Journal of general virology*, 85(Pt 11), 3173-3188. doi:10.1099/vir.0.80401-0
- Skinner, J. R., Shew, T. M., Schwartz, D. M., Tzekov, A., Lepus, C. M., Abumrad, N. A., & Wolins, N. E. (2009). Diacylglycerol enrichment of endoplasmic reticulum or lipid droplets recruits perilipin 3/TIP47 during lipid storage and mobilization. *J Biol Chem*, 284(45), 30941-30948. doi:10.1074/jbc.M109.013995
- Sklan, E. H., Staschke, K., Oakes, T. M., Elazar, M., Winters, M., Aroeti, B., . . . Glenn, J. S. (2007). A Rab-GAP TBC domain protein binds hepatitis C virus NS5A and mediates viral replication. *J Virol*, 81(20), 11096-11105. doi:10.1128/JVI.01249-07
- Slater-Handshy, T., Droll, D. A., Fan, X., Di Bisceglie, A. M., & Chambers, T. J. (2004). HCV E2 glycoprotein: mutagenesis of N-linked glycosylation sites and its effects on E2 expression and processing. *Virology*, 319(1), 36-48. doi:10.1016/j.virol.2003.10.008
- Smith, R. M., & Wu, G. Y. (2003). Structure-based design of hepatitis C virus inhibitors. *J Viral Hepat*, 10(6), 405-412.
- Soni, K. G., Mardones, G. A., Sougrat, R., Smirnova, E., Jackson, C. L., & Bonifacio, J. S. (2009). Coatomer-dependent protein delivery to lipid droplets. *Journal of cell science*, 122(Pt 11), 1834-1841. doi:10.1242/jcs.045849
- Sourisseau, M., Sol-Foulon, N., Porrot, F., Blanchet, F., & Schwartz, O. (2007). Inefficient human immunodeficiency virus replication in mobile lymphocytes. *J Virol*, 81(2), 1000-1012. doi:10.1128/JVI.01629-06
- St Vincent, M. R., Colpitts, C. C., Ustinov, A. V., Muqadas, M., Joyce, M. A., Barsby, N. L., . . . Schang, L. M. (2010). Rigid amphipathic fusion inhibitors, small molecule antiviral compounds against enveloped viruses. *Proceedings of the National Academy of Sciences of the United States of America*, 107(40), 17339-17344. doi:10.1073/pnas.1010026107
- Stapleford, K. A., & Miller, D. J. (2010). Role of cellular lipids in positive-sense RNA virus replication complex assembly and function. *Viruses*, 2(5), 1055-1068. doi:10.3390/v2051055
- Steinmann, E., Penin, F., Kallis, S., Patel, A. H., Bartenschlager, R., & Pietschmann, T. (2007). Hepatitis C virus p7 protein is crucial for assembly and release of infectious virions. *PLoS pathogens*, 3(7), e103. doi:10.1371/journal.ppat.0030103

- Stenmark, H. (2009). Rab GTPases as coordinators of vesicle traffic. *Nature reviews. Molecular cell biology*, 10(8), 513-525. doi:10.1038/nrm2728
- Stephens, D. J., & Pepperkok, R. (2001). Illuminating the secretory pathway: when do we need vesicles? *J Cell Sci*, 114(Pt 6), 1053-1059.
- Stetson, D. B., & Medzhitov, R. (2006). Antiviral defense: interferons and beyond. *J Exp Med*, 203(8), 1837-1841. doi:10.1084/jem.20061377
- Straub, B. K., Stoeffel, P., Heid, H., Zimbelmann, R., & Schirmacher, P. (2008). Differential pattern of lipid droplet-associated proteins and de novo perilipin expression in hepatocyte steatogenesis. *Hepatology*, 47(6), 1936-1946. doi:10.1002/hep.22268
- Sturmey, R. G., O'Toole, P. J., & Leese, H. J. (2006). Fluorescence resonance energy transfer analysis of mitochondrial:lipid association in the porcine oocyte. *Reproduction*, 132(6), 829-837. doi:10.1530/REP-06-0073
- Su, A. I., Pezacki, J. P., Wodicka, L., Brideau, A. D., Supekova, L., Thimme, R., . . . Chisari, F. V. (2002). Genomic analysis of the host response to hepatitis C virus infection. *Proc Natl Acad Sci U S A*, 99(24), 15669-15674. doi:10.1073/pnas.202608199
- Subra, C., Grand, D., Laulagnier, K., Stella, A., Lambeau, G., Paillasse, M., . . . Record, M. (2010). Exosomes account for vesicle-mediated transcellular transport of activatable phospholipases and prostaglandins. *Journal of lipid research*, 51(8), 2105-2120. doi:10.1194/jlr.M003657
- Sumpter, R., Jr., Loo, Y. M., Foy, E., Li, K., Yoneyama, M., Fujita, T., . . . Gale, M., Jr. (2005). Regulating intracellular antiviral defense and permissiveness to hepatitis C virus RNA replication through a cellular RNA helicase, RIG-I. *J Virol*, 79(5), 2689-2699. doi:10.1128/JVI.79.5.2689-2699.2005
- Sundstedt, A., O'Neill, E. J., Nicolson, K. S., & Wraith, D. C. (2003). Role for IL-10 in suppression mediated by peptide-induced regulatory T cells in vivo. *J Immunol*, 170(3), 1240-1248.
- Suzuki, R., Matsuda, M., Watashi, K., Aizaki, H., Matsuura, Y., Wakita, T., & Suzuki, T. (2013). Signal peptidase complex subunit 1 participates in the assembly of hepatitis C virus through an interaction with E2 and NS2. *PLoS Pathog*, 9(8), e1003589. doi:10.1371/journal.ppat.1003589
- Syed, G. H., Khan, M., Yang, S., & Siddiqui, A. (2017). Hepatitis C virus lipovirions (HCV-LVP) assemble in the endoplasmic reticulum (ER) and bud off from the ER to Golgi in COPII vesicles. *Journal of virology*. doi:10.1128/JVI.00499-17
- Szafer, E., Rotman, M., & Cassel, D. (2001). Regulation of GTP hydrolysis on ADP-ribosylation factor-1 at the Golgi membrane. *The Journal of biological chemistry*, 276(51), 47834-47839. doi:10.1074/jbc.M106000200
- Szigeti, A., Minik, O., Hocsak, E., Pozsgai, E., Boronkai, A., Farkas, R., . . . Bellyei, S. (2009). Preliminary study of TIP47 as a possible new biomarker of cervical dysplasia and invasive carcinoma. *Anticancer Res*, 29(2), 717-724.
- Sztalryd, C., Bell, M., Lu, X., Mertz, P., Hickenbottom, S., Chang, B. H., . . . Londos, C. (2006). Functional compensation for adipose differentiation-related protein (ADFP) by Tip47 in an ADFP null embryonic cell line. *J Biol Chem*, 281(45), 34341-34348. doi:10.1074/jbc.M602497200

- Szul, T., Grabski, R., Lyons, S., Morohashi, Y., Shestopal, S., Lowe, M., & Sztul, E. (2007). Dissecting the role of the ARF guanine nucleotide exchange factor GBF1 in Golgi biogenesis and protein trafficking. *J Cell Sci*, 120(Pt 22), 3929-3940. doi:10.1242/jcs.010769
- Szymanski, K. M., Binns, D., Bartz, R., Grishin, N. V., Li, W. P., Agarwal, A. K., . . . Goodman, J. M. (2007). The lipodystrophy protein seipin is found at endoplasmic reticulum lipid droplet junctions and is important for droplet morphology. *Proc Natl Acad Sci U S A*, 104(52), 20890-20895. doi:10.1073/pnas.0704154104
- Takahashi, Y., Hori, Y., Yamamoto, T., Urashima, T., Ohara, Y., & Tanaka, H. (2015). Three-dimensional (3D) spheroid cultures improve the metabolic gene expression profiles of HepaRG cells. *Bioscience reports*. doi:10.1042/bsr20150034
- Takahashi, Y., Shinoda, A., Furuya, N., Harada, E., Arimura, N., Ichi, I., . . . Sato, R. (2013). Perilipin-mediated lipid droplet formation in adipocytes promotes sterol regulatory element-binding protein-1 processing and triacylglyceride accumulation. *PLoS One*, 8(5), e64605. doi:10.1371/journal.pone.0064605
- Takaki, A., Wiese, M., Maertens, G., Depla, E., Seifert, U., Liebetrau, A., . . . Rehmann, B. (2000). Cellular immune responses persist and humoral responses decrease two decades after recovery from a single-source outbreak of hepatitis C. *Nat Med*, 6(5), 578-582. doi:10.1038/75063
- Takashima, K., Saitoh, A., Hirose, S., Nakai, W., Kondo, Y., Takasu, Y., . . . Nakayama, K. (2011). GBF1-Arf-COPI-ArfGAP-mediated Golgi-to-ER transport involved in regulation of lipid homeostasis. *Cell Struct Funct*, 36(2), 223-235.
- Tanabe, K., Torii, T., Natsume, W., Braesch-Andersen, S., Watanabe, T., & Satake, M. (2005). A novel GTPase-activating protein for ARF6 directly interacts with clathrin and regulates clathrin-dependent endocytosis. *Mol Biol Cell*, 16(4), 1617-1628. doi:10.1091/mbc.E04-08-0683
- Tanaka, Y., Enomoto, N., Kojima, S., Tang, L., Goto, M., Marumo, F., & Sato, C. (1993). Detection of hepatitis C virus RNA in the liver by in situ hybridization. *Liver*, 13(4), 203-208.
- Tang, L. I., Ling, A. P., Koh, R. Y., Chye, S. M., & Voon, K. G. (2012). Screening of anti-dengue activity in methanolic extracts of medicinal plants. *BMC Complement Altern Med*, 12, 3. doi:10.1186/1472-6882-12-3
- Tang, W., Tam, J. H., Seah, C., Chiu, J., Tyrer, A., Cregan, S. P., . . . Pasternak, S. H. (2015). Arf6 controls beta-amyloid production by regulating macropinocytosis of the Amyloid Precursor Protein to lysosomes. *Mol Brain*, 8, 41. doi:10.1186/s13041-015-0129-7
- Tanji, Y., Kaneko, T., Satoh, S., & Shimotohno, K. (1995). Phosphorylation of hepatitis C virus-encoded nonstructural protein NS5A. *J Virol*, 69(7), 3980-3986.
- Targett-Adams, P., Chambers, D., Gledhill, S., Hope, R. G., Coy, J. F., Girod, A., & McLauchlan, J. (2003). Live cell analysis and targeting of the lipid droplet-binding adipocyte differentiation-related protein. *The Journal of biological chemistry*, 278(18), 15998-16007. doi:10.1074/jbc.M211289200
- Targett-Adams, P., Graham, E. J., Middleton, J., Palmer, A., Shaw, S. M., Lavender, H., . . . Westby, M. (2011). Small molecules targeting hepatitis C virus-encoded NS5A cause subcellular redistribution of their target: insights into compound modes of action. *Journal of virology*, 85(13), 6353-6368. doi:10.1128/JVI.00215-11

- Targett-Adams, P., Hope, G., Boulant, S., & McLauchlan, J. (2008). Maturation of hepatitis C virus core protein by signal peptide peptidase is required for virus production. *The Journal of biological chemistry*, 283(24), 16850-16859. doi:10.1074/jbc.M802273200
- Targett-Adams, P., & McLauchlan, J. (2005). Development and characterization of a transient-replication assay for the genotype 2a hepatitis C virus subgenomic replicon. *J Gen Virol*, 86(Pt 11), 3075-3080. doi:10.1099/vir.0.81334-0
- Tarr, A. W., Urbanowicz, R. A., Hamed, M. R., Albecka, A., McClure, C. P., Brown, R. J., . . . Ball, J. K. (2011). Hepatitis C patient-derived glycoproteins exhibit marked differences in susceptibility to serum neutralizing antibodies: genetic subtype defines antigenic but not neutralization serotype. *J Virol*, 85(9), 4246-4257. doi:10.1128/JVI.01332-10
- Tauchi-Sato, K., Ozeki, S., Houjou, T., Taguchi, R., & Fujimoto, T. (2002). The surface of lipid droplets is a phospholipid monolayer with a unique Fatty Acid composition. *J Biol Chem*, 277(46), 44507-44512. doi:10.1074/jbc.M207712200
- Taylor, D. R., Shi, S. T., Romano, P. R., Barber, G. N., & Lai, M. M. (1999). Inhibition of the interferon-inducible protein kinase PKR by HCV E2 protein. *Science*, 285(5424), 107-110.
- Teixeira, L., Rabouille, C., Rorth, P., Ephrussi, A., & Vanzo, N. F. (2003). Drosophila Perilipin/ADRP homologue Lsd2 regulates lipid metabolism. *Mech Dev*, 120(9), 1071-1081.
- Tellinghuisen, T. L., Marcotrigiano, J., Gorbalenya, A. E., & Rice, C. M. (2004). The NS5A protein of hepatitis C virus is a zinc metalloprotein. *J Biol Chem*, 279(47), 48576-48587. doi:10.1074/jbc.M407787200
- Terczynska-Dyla, E., Bibert, S., Duong, F. H., Krol, I., Jorgensen, S., Collinet, E., . . . Hartmann, R. (2014). Reduced IFNlambda4 activity is associated with improved HCV clearance and reduced expression of interferon-stimulated genes. *Nat Commun*, 5, 5699. doi:10.1038/ncomms6699
- Thein, H. H., Yi, Q., Dore, G. J., & Krahn, M. D. (2008). Estimation of stage-specific fibrosis progression rates in chronic hepatitis C virus infection: a meta-analysis and meta-regression. *Hepatology*, 48(2), 418-431. doi:10.1002/hep.22375
- Thery, C., Zitvogel, L., & Amigorena, S. (2002). Exosomes: composition, biogenesis and function. *Nature reviews. Immunology*, 2(8), 569-579. doi:10.1038/nri855
- Thiam, A. R., Antonny, B., Wang, J., Delacotte, J., Wilfling, F., Walther, T. C., . . . Pincet, F. (2013). COPI buds 60-nm lipid droplets from reconstituted water-phospholipid-triacylglyceride interfaces, suggesting a tension clamp function. *Proceedings of the National Academy of Sciences of the United States of America*, 110(33), 13244-13249. doi:10.1073/pnas.1307685110
- Thimme, R., Bukh, J., Spangenberg, H. C., Wieland, S., Pemberton, J., Steiger, C., . . . Chisari, F. V. (2002). Viral and immunological determinants of hepatitis C virus clearance, persistence, and disease. *Proc Natl Acad Sci U S A*, 99(24), 15661-15668. doi:10.1073/pnas.202608299
- Thimme, R., Chang, K. M., Pemberton, J., Sette, A., & Chisari, F. V. (2001). Degenerate immunogenicity of an HLA-A2-restricted hepatitis B virus nucleocapsid cytotoxic T-lymphocyte epitope that is also presented by HLA-B51. *J Virol*, 75(8), 3984-3987. doi:10.1128/JVI.75.8.3984-3987.2001



- Thomas, E., Gonzalez, V. D., Li, Q., Modi, A. A., Chen, W., Noureddin, M., . . . Liang, T. J. (2012). HCV infection induces a unique hepatic innate immune response associated with robust production of type III interferons. *Gastroenterology*, 142(4), 978-988. doi:10.1053/j.gastro.2011.12.055
- Thomson, M., Nascimbeni, M., Havert, M. B., Major, M., Gonzales, S., Alter, H., . . . Liang, T. J. (2003). The clearance of hepatitis C virus infection in chimpanzees may not necessarily correlate with the appearance of acquired immunity. *J Virol*, 77(2), 862-870.
- Timpe, J. M., Stamataki, Z., Jennings, A., Hu, K., Farquhar, M. J., Harris, H. J., . . . McKeating, J. A. (2008). Hepatitis C virus cell-cell transmission in hepatoma cells in the presence of neutralizing antibodies. *Hepatology*, 47(1), 17-24. doi:10.1002/hep.21959
- Tokarev, A. A., Taussig, D., Sundaram, G., Lipatova, Z., Liang, Y., Mulholland, J. W., & Segev, N. (2009). TRAPP II complex assembly requires Trs33 or Trs65. *Traffic*, 10(12), 1831-1844. doi:10.1111/j.1600-0854.2009.00988.x
- Tokita, H., Okamoto, H., Luengrojanakul, P., Vareesangthip, K., Chainuvati, T., Iizuka, H., . . . Mayumi, M. (1995). Hepatitis C virus variants from Thailand classifiable into five novel genotypes in the sixth (6b), seventh (7c, 7d) and ninth (9b, 9c) major genetic groups. *J Gen Virol*, 76 ( Pt 9), 2329-2335. doi:10.1099/0022-1317-76-9-2329
- Tomiyasu, K., Walsh, B. W., Ikewaki, K., Judge, H., & Sacks, F. M. (2001). Differential metabolism of human VLDL according to content of ApoE and ApoC-III. *Arterioscler Thromb Vasc Biol*, 21(9), 1494-1500.
- Torres, J., Aguado, J. M., San Juan, R., Andres, A., Sierra, P., Lopez-Medrano, F., & Morales, J. M. (2008). Hepatitis C virus, an important risk factor for tuberculosis in immunocompromised: experience with kidney transplantation. *Transpl Int*, 21(9), 873-878. doi:10.1111/j.1432-2277.2008.00694.x
- Trahey, M., Oh, H. S., Cameron, C. E., & Hay, J. C. (2012). Poliovirus infection transiently increases COPII vesicle budding. *Journal of virology*, 86(18), 9675-9682. doi:10.1128/JVI.01159-12
- Tsuiki, E., Fujita, A., Ohsaki, Y., Cheng, J., Irie, T., Yoshikawa, K., . . . Fujimoto, T. (2007). All-trans-retinol generated by rhodopsin photobleaching induces rapid recruitment of TIP47 to lipid droplets in the retinal pigment epithelium. *Invest Ophthalmol Vis Sci*, 48(6), 2858-2867. doi:10.1167/iovs.06-0768
- Tsutsumi, H., Kojima, T., Hirakawa, S., Masaki, T., Okabayashi, T., Yokota, S., . . . Sawada, N. (2011). Respiratory syncytial virus infection and the tight junctions of nasal epithelial cells. *Adv Otorhinolaryngol*, 72, 153-156. doi:10.1159/000324777
- Tsutsumi, M., Urashima, S., Takada, A., Date, T., & Tanaka, Y. (1994). Detection of antigens related to hepatitis C virus RNA encoding the NS5 region in the livers of patients with chronic type C hepatitis. *Hepatology*, 19(2), 265-272.
- Tsutsumi, T., Suzuki, T., Shimoike, T., Suzuki, R., Moriya, K., Shintani, Y., . . . Miyamura, T. (2002). Interaction of hepatitis C virus core protein with retinoid X receptor alpha modulates its transcriptional activity. *Hepatology*, 35(4), 937-946. doi:10.1053/jhep.2002.32470

- Ujino, S., Nishitsuji, H., Hishiki, T., Sugiyama, K., Takaku, H., & Shimotohno, K. (2016). Hepatitis C virus utilizes VLDLR as a novel entry pathway. *Proc Natl Acad Sci U S A*, 113(1), 188-193. doi:10.1073/pnas.1506524113
- Ulsenheimer, A., Gerlach, J. T., Gruener, N. H., Jung, M. C., Schirren, C. A., Schraut, W., . . . Diepolder, H. M. (2003). Detection of functionally altered hepatitis C virus-specific CD4 T cells in acute and chronic hepatitis C. *Hepatology*, 37(5), 1189-1198. doi:10.1053/jhep.2003.50194
- Urbani, S., Amadei, B., Fisicaro, P., Tola, D., Orlandini, A., Sacchelli, L., . . . Ferrari, C. (2006). Outcome of acute hepatitis C is related to virus-specific CD4 function and maturation of antiviral memory CD8 responses. *Hepatology*, 44(1), 126-139. doi:10.1002/hep.21242
- Valachovic, M., Garaiova, M., Holic, R., & Hapala, I. (2016). Squalene is lipotoxic to yeast cells defective in lipid droplet biogenesis. *Biochem Biophys Res Commun*, 469(4), 1123-1128. doi:10.1016/j.bbrc.2015.12.050
- Valli, M. B., Crema, A., Lanzilli, G., Serafino, A., Bertolini, L., Ravagnan, G., . . . Carloni, G. (2007). Molecular and cellular determinants of cell-to-cell transmission of HCV in vitro. *Journal of medical virology*, 79(10), 1491-1499. doi:10.1002/jmv.20947
- Valli, M. B., Serafino, A., Crema, A., Bertolini, L., Manzin, A., Lanzilli, G., . . . Carloni, G. (2006). Transmission in vitro of hepatitis C virus from persistently infected human B-cells to hepatoma cells by cell-to-cell contact. *Journal of medical virology*, 78(2), 192-201. doi:10.1002/jmv.20527
- van de Laar, T. J., van der Bij, A. K., Prins, M., Bruisten, S. M., Brinkman, K., Ruys, T. A., . . . Coutinho, R. A. (2007). Increase in HCV incidence among men who have sex with men in Amsterdam most likely caused by sexual transmission. *J Infect Dis*, 196(2), 230-238. doi:10.1086/518796
- van der Goot, F. G., & Gruenberg, J. (2006). Intra-endosomal membrane traffic. *Trends in cell biology*, 16(10), 514-521. doi:10.1016/j.tcb.2006.08.003
- Van Eck, M., Twisk, J., Hoekstra, M., Van Rij, B. T., Van der Lans, C. A., Bos, I. S., . . . Van Berkel, T. J. (2003). Differential effects of scavenger receptor BI deficiency on lipid metabolism in cells of the arterial wall and in the liver. *J Biol Chem*, 278(26), 23699-23705. doi:10.1074/jbc.M211233200
- van Leeuwen, M. S., Fernandez, M. A., van Es, H. W., Stokking, R., Dillon, E. H., & Feldberg, M. A. (1994). Variations in venous and segmental anatomy of the liver: two- and three-dimensional MR imaging in healthy volunteers. *AJR Am J Roentgenol*, 162(6), 1337-1345. doi:10.2214/ajr.162.6.8191995
- van Ooij, C., Kalman, L., van, I., Nishijima, M., Hanada, K., Mostov, K., & Engel, J. N. (2000). Host cell-derived sphingolipids are required for the intracellular growth of *Chlamydia trachomatis*. *Cell Microbiol*, 2(6), 627-637.
- Varela, G. M., Antwi, D. A., Dhir, R., Yin, X., Singhal, N. S., Graham, M. J., . . . Ahima, R. S. (2008). Inhibition of ADRP prevents diet-induced insulin resistance. *Am J Physiol Gastrointest Liver Physiol*, 295(3), G621-628. doi:10.1152/ajpgi.90204.2008
- Vauloup-Fellous, C., Pene, V., Garaud-Aunis, J., Harper, F., Bardin, S., Suire, Y., . . . Rosenberg, A. R. (2006). Signal peptide peptidase-catalyzed cleavage of hepatitis C virus core protein is dispensable for virus budding but destabilizes the viral capsid. *J Biol Chem*, 281(38), 27679-27692. doi:10.1074/jbc.M602587200

- Velazquez, V. M., Hon, H., Ibegbu, C., Knechtle, S. J., Kirk, A. D., & Grakoui, A. (2012). Hepatic enrichment and activation of myeloid dendritic cells during chronic hepatitis C virus infection. *Hepatology*, 56(6), 2071-2081. doi:10.1002/hep.25904
- Viaud, J., Zeghouf, M., Barelli, H., Zeeh, J. C., Padilla, A., Guibert, B., . . . Chavanieu, A. (2007). Structure-based discovery of an inhibitor of Arf activation by Sec7 domains through targeting of protein-protein complexes. *Proceedings of the National Academy of Sciences of the United States of America*, 104(25), 10370-10375. doi:10.1073/pnas.0700773104
- Vielemeyer, O., McIntosh, M. T., Joiner, K. A., & Coppens, I. (2004). Neutral lipid synthesis and storage in the intraerythrocytic stages of *Plasmodium falciparum*. *Mol Biochem Parasitol*, 135(2), 197-209. doi:10.1016/j.molbiopara.2003.08.017
- Vieyres, G., Welsch, K., Gerold, G., Gentzsch, J., Kahl, S., Vondran, F. W., . . . Pietschmann, T. (2016). ABHD5/CGI-58, the Chanarin-Dorfman Syndrome Protein, Mobilises Lipid Stores for Hepatitis C Virus Production. *PLoS pathogens*, 12(4), e1005568. doi:10.1371/journal.ppat.1005568
- Villanueva, C. J., Monetti, M., Shih, M., Zhou, P., Watkins, S. M., Bhanot, S., & Farese, R. V., Jr. (2009). Specific role for acyl CoA:Diacylglycerol acyltransferase 1 (Dgat1) in hepatic steatosis due to exogenous fatty acids. *Hepatology*, 50(2), 434-442. doi:10.1002/hep.22980
- Visco, C., & Finotto, S. (2014). Hepatitis C virus and diffuse large B-cell lymphoma: Pathogenesis, behavior and treatment. *World J Gastroenterol*, 20(32), 11054-11061. doi:10.3748/wjg.v20.i32.11054
- Visentini, M., Cagliuso, M., Conti, V., Carbonari, M., Cibati, M., Siciliano, G., . . . Fiorilli, M. (2012). Clonal B cells of HCV-associated mixed cryoglobulinemia patients contain exhausted marginal zone-like and CD21 low cells overexpressing Stra13. *Eur J Immunol*, 42(6), 1468-1476. doi:10.1002/eji.201142313
- Vogt, D. A., Camus, G., Herker, E., Webster, B. R., Tsou, C. L., Greene, W. C., . . . Ott, M. (2013a). Lipid droplet-binding protein TIP47 regulates hepatitis C Virus RNA replication through interaction with the viral NS5A protein. *PLoS Pathog*, 9(4), e1003302. doi:10.1371/journal.ppat.1003302
- Vogt, D. A., Camus, G., Herker, E., Webster, B. R., Tsou, C. L., Greene, W. C., . . . Ott, M. (2013b). Lipid droplet-binding protein TIP47 regulates hepatitis C Virus RNA replication through interaction with the viral NS5A protein. *PLoS pathogens*, 9(4), e1003302. doi:10.1371/journal.ppat.1003302
- Volpicelli-Daley, L. A., Li, Y., Zhang, C. J., & Kahn, R. A. (2005). Isoform-selective effects of the depletion of ADP-ribosylation factors 1-5 on membrane traffic. *Mol Biol Cell*, 16(10), 4495-4508. doi:10.1091/mbc.E04-12-1042
- Wakita, T., Pietschmann, T., Kato, T., Date, T., Miyamoto, M., Zhao, Z., . . . Liang, T. J. (2005). Production of infectious hepatitis C virus in tissue culture from a cloned viral genome. *Nature medicine*, 11(7), 791-796. doi:10.1038/nm1268
- Wang, H., Perry, J. W., Lauring, A. S., Neddermann, P., De Francesco, R., & Tai, A. W. (2014). Oxysterol-binding protein is a phosphatidylinositol 4-kinase effector required for HCV replication membrane integrity and cholesterol trafficking. *Gastroenterology*, 146(5), 1373-1385. doi:10.1053/j.gastro.2014.02.002

- Wang, H., Sreenivasan, U., Hu, H., Saladino, A., Polster, B. M., Lund, L. M., . . . Sztalryd, C. (2011). Perilipin 5, a lipid droplet-associated protein, provides physical and metabolic linkage to mitochondria. *J Lipid Res*, 52(12), 2159-2168. doi:10.1194/jlr.M017939
- Wang, L., Eng, E. T., Law, K., Gordon, R. E., Rice, W. J., & Chen, B. K. (2017). Visualization of HIV T Cell Virological Synapses and Virus-Containing Compartments by Three-Dimensional Correlative Light and Electron Microscopy. *J Virol*, 91(2). doi:10.1128/JVI.01605-16
- Wang, Z. Q., Yu, Y., Zhang, X. H., Floyd, E. Z., & Cefalu, W. T. (2010). Human adenovirus 36 decreases fatty acid oxidation and increases de novo lipogenesis in primary cultured human skeletal muscle cells by promoting Cidec/FSP27 expression. *Int J Obes (Lond)*, 34(9), 1355-1364. doi:10.1038/ijo.2010.77
- Ward, T. H. (2007). Trafficking through the early secretory pathway of mammalian cells. *Methods Mol Biol*, 390, 281-296. doi:10.1007/978-1-59745-466-7\_19
- Waris, G., Felmlee, D. J., Negro, F., & Siddiqui, A. (2007). Hepatitis C virus induces proteolytic cleavage of sterol regulatory element binding proteins and stimulates their phosphorylation via oxidative stress. *Journal of virology*, 81(15), 8122-8130. doi:10.1128/JVI.00125-07
- Washburn, M. L., Bility, M. T., Zhang, L., Kovalev, G. I., Buntzman, A., Frelinger, J. A., . . . Su, L. (2011). A humanized mouse model to study hepatitis C virus infection, immune response, and liver disease. *Gastroenterology*, 140(4), 1334-1344. doi:10.1053/j.gastro.2011.01.001
- Webb, N. R., de Beer, M. C., de Beer, F. C., & van der Westhuyzen, D. R. (2004). ApoB-containing lipoproteins in apoE-deficient mice are not metabolized by the class B scavenger receptor BI. *J Lipid Res*, 45(2), 272-280. doi:10.1194/jlr.M300319-JLR200
- Welker, M. W., Susser, S., Welsch, C., Perner, D., Fuller, C., Kronenberger, B., . . . Sarrazin, C. (2012). Modulation of replication efficacy of the hepatitis C virus replicon Con1 by site-directed mutagenesis of an NS4B aminoterminal basic leucine zipper. *J Viral Hepat*, 19(11), 775-783. doi:10.1111/j.1365-2893.2012.01605.x
- Wendel, A. A., Cooper, D. E., Ilkayeva, O. R., Muoio, D. M., & Coleman, R. A. (2013). Glycerol-3-phosphate acyltransferase (GPAT)-1, but not GPAT4, incorporates newly synthesized fatty acids into triacylglycerol and diminishes fatty acid oxidation. *J Biol Chem*, 288(38), 27299-27306. doi:10.1074/jbc.M113.485219
- Wilfling, F., Thiam, A. R., Olarte, M. J., Wang, J., Beck, R., Gould, T. J., . . . Walther, T. C. (2014). Arf1/COPI machinery acts directly on lipid droplets and enables their connection to the ER for protein targeting. *Elife*, 3, e01607. doi:10.7554/eLife.01607
- Wilfling, F., Wang, H., Haas, J. T., Krahmer, N., Gould, T. J., Uchida, A., . . . Walther, T. C. (2013). Triacylglycerol synthesis enzymes mediate lipid droplet growth by relocalizing from the ER to lipid droplets. *Developmental cell*, 24(4), 384-399. doi:10.1016/j.devcel.2013.01.013
- Witteveldt, J., Evans, M. J., Bitzegeio, J., Koutsoudakis, G., Owsianka, A. M., Angus, A. G., . . . Patel, A. H. (2009). CD81 is dispensable for hepatitis C virus cell-to-cell

- transmission in hepatoma cells. *The Journal of general virology*, 90(Pt 1), 48-58. doi:10.1099/vir.0.006700-0
- Wolins, N. E., Quaynor, B. K., Skinner, J. R., Schoenfish, M. J., Tzekov, A., & Bickel, P. E. (2005). S3-12, Adipophilin, and TIP47 package lipid in adipocytes. *J Biol Chem*, 280(19), 19146-19155. doi:10.1074/jbc.M500978200
- Wolins, N. E., Quaynor, B. K., Skinner, J. R., Tzekov, A., Croce, M. A., Gropler, M. C., . . . Bickel, P. E. (2006). OXPAT/PAT-1 is a PPAR-induced lipid droplet protein that promotes fatty acid utilization. *Diabetes*, 55(12), 3418-3428. doi:10.2337/db06-0399
- Wolins, N. E., Rubin, B., & Brasaemle, D. L. (2001). TIP47 associates with lipid droplets. *J Biol Chem*, 276(7), 5101-5108. doi:10.1074/jbc.M006775200
- Wonderlich, E. R., Leonard, J. A., Kulpa, D. A., Leopold, K. E., Norman, J. M., & Collins, K. L. (2011). ADP ribosylation factor 1 activity is required to recruit AP-1 to the major histocompatibility complex class I (MHC-I) cytoplasmic tail and disrupt MHC-I trafficking in HIV-1-infected primary T cells. *J Virol*, 85(23), 12216-12226. doi:10.1128/JVI.00056-11
- Wuensch, S. A., Pierce, R. H., & Crispe, I. N. (2006). Local intrahepatic CD8+ T cell activation by a non-self-antigen results in full functional differentiation. *J Immunol*, 177(3), 1689-1697.
- Wurie, H. R., Buckett, L., & Zammit, V. A. (2012). Diacylglycerol acyltransferase 2 acts upstream of diacylglycerol acyltransferase 1 and utilizes nascent diglycerides and de novo synthesized fatty acids in HepG2 cells. *FEBS J*, 279(17), 3033-3047. doi:10.1111/j.1742-4658.2012.08684.x
- Xiao, F., Fofana, I., Heydmann, L., Barth, H., Soulier, E., Habersetzer, F., . . . Baumert, T. F. (2014). Hepatitis C virus cell-cell transmission and resistance to direct-acting antiviral agents. *PLoS pathogens*, 10(5), e1004128. doi:10.1371/journal.ppat.1004128
- Xiao, F., Fofana, I., Thumann, C., Mailly, L., Alles, R., Robinet, E., . . . Baumert, T. F. (2015). Synergy of entry inhibitors with direct-acting antivirals uncovers novel combinations for prevention and treatment of hepatitis C. *Gut*, 64(3), 483-494. doi:10.1136/gutjnl-2013-306155
- Xie, X., Tang, S. C., Cai, Y., Pi, W., Deng, L., Wu, G., . . . Teng, Y. (2016). Suppression of breast cancer metastasis through the inactivation of ADP-ribosylation factor 1. *Oncotarget*, 7(36), 58111-58120. doi:10.18632/oncotarget.11185
- Xu, W., Wu, L., Yu, M., Chen, F. J., Arshad, M., Xia, X., . . . Zhou, L. (2016). Differential Roles of CIDE Proteins in Promoting Lipid Droplet Fusion and Growth in Subpopulations of Hepatocytes. *The Journal of biological chemistry*. doi:10.1074/jbc.M115.701094
- Yamada, G., Takahashi, M., Tsuji, T., Yoshizawa, H., & Okamoto, H. (1992). Quantitative HCV RNA and effect of interferon therapy in chronic hepatitis C. *Dig Dis Sci*, 37(12), 1926-1927.
- Yamada, S., Koji, T., Nozawa, M., Kiyosawa, K., & Nakane, P. K. (1992). Detection of hepatitis C virus (HCV) RNA in paraffin embedded tissue sections of human liver of non-A, non-B hepatitis patients by in situ hybridization. *J Clin Lab Anal*, 6(1), 40-46.

- Yanagi, M., Kaneko, S., Unoura, M., Murakami, S., Kobayashi, K., Sugihara, J., . . . Muto, Y. (1991). Hepatitis C virus in fulminant hepatic failure. *N Engl J Med*, 324(26), 1895-1896. doi:10.1056/NEJM199106273242615
- Yanagi, M., Purcell, R. H., Emerson, S. U., & Bukh, J. (1997). Transcripts from a single full-length cDNA clone of hepatitis C virus are infectious when directly transfected into the liver of a chimpanzee. *Proc Natl Acad Sci U S A*, 94(16), 8738-8743.
- Yang, G., & Huang, M. (2010). Evaluation of compound activity against hepatitis C virus in replicon systems. *Current protocols in pharmacology / editorial board, S.J. Enna, Chapter 13*, Unit 13B 11. doi:10.1002/0471141755.ph13b01s50
- Yao, X., Han, Q., Song, J., Liang, C., Wakita, T., Yang, R., & Chen, X. (2008). Baculovirus mediated production of infectious hepatitis C virus in human hepatoma cells stably expressing T7 RNA polymerase. *Mol Biotechnol*, 40(2), 186-194. doi:10.1007/s12033-008-9075-2
- Yazdanpanah, Y., De Carli, G., Miguera, B., Lot, F., Campins, M., Colombo, C., . . . Bouvet, E. (2005). Risk factors for hepatitis C virus transmission to health care workers after occupational exposure: a European case-control study. *Clin Infect Dis*, 41(10), 1423-1430. doi:10.1086/497131
- Yen, C. L., & Farese, R. V., Jr. (2006). Fat breakdown: a function for CGI-58 (ABHD5) provides a new piece of the puzzle. *Cell Metab*, 3(5), 305-307. doi:10.1016/j.cmet.2006.04.001
- YUTAKA TAKEBE, M. S., JUN-ICHI FUJISAWA, PAMALA HOY, KYOKO YOKOTA,, & KEN-ICHI ARAI, M. Y., AND NAOKO ARAI. (1988). SRot Promoter: an Efficient and Versatile Mammalian cDNA Expression System Composed of the Simian Virus 40 Early Promoter and the R-U5 Segment of Human T-Cell Leukemia Virus Type 1 Long Terminal Repeat. *Molecular and cellular biology*, 8(1), 466-472.
- Zakharova, L., Svetlova, M., & Fomina, A. F. (2007). T cell exosomes induce cholesterol accumulation in human monocytes via phosphatidylserine receptor. *Journal of cellular physiology*, 212(1), 174-181. doi:10.1002/jcp.21013
- Zayas, M., Long, G., Madan, V., & Bartenschlager, R. (2016). Coordination of Hepatitis C Virus Assembly by Distinct Regulatory Regions in Nonstructural Protein 5A. *PLoS Pathog*, 12(1), e1005376. doi:10.1371/journal.ppat.1005376
- Zeisel, M. B., Crouchet, E., Baumert, T. F., & Schuster, C. (2015). Host-Targeting Agents to Prevent and Cure Hepatitis C Virus Infection. *Viruses*, 7(11), 5659-5685. doi:10.3390/v7112898
- Zerial, M., & McBride, H. (2001). Rab proteins as membrane organizers. *Nat Rev Mol Cell Biol*, 2(2), 107-117. doi:10.1038/35052055
- Zhang, K., & Kaufman, R. J. (2004). Signaling the unfolded protein response from the endoplasmic reticulum. *The Journal of biological chemistry*, 279(25), 25935-25938. doi:10.1074/jbc.R400008200
- Zhang, L., Hong, Z., Lin, W., Shao, R. X., Goto, K., Hsu, V. W., & Chung, R. T. (2012). ARF1 and GBF1 generate a PI4P-enriched environment supportive of hepatitis C virus replication. *PloS one*, 7(2), e32135. doi:10.1371/journal.pone.0032135
- Zhang, N., Yin, P., Zhou, L., Li, H., & Zhang, L. (2016). ARF1 activation dissociates ADRP from lipid droplets to promote HCV assembly. *Biochemical and biophysical research communications*, 475(1), 31-36. doi:10.1016/j.bbrc.2016.05.024

- Zhang, Q., Gong, R., Qu, J., Zhou, Y., Liu, W., Chen, M., . . . Wu, J. (2012). Activation of the Ras/Raf/MEK pathway facilitates hepatitis C virus replication via attenuation of the interferon-JAK-STAT pathway. *Journal of virology*, 86(3), 1544-1554. doi:10.1128/JVI.00688-11
- Zhang, Y., Liang, Z., Zong, Y., Wang, Y., Liu, J., Chen, K., . . . Gao, C. (2016). Efficient and transgene-free genome editing in wheat through transient expression of CRISPR/Cas9 DNA or RNA. *Nat Commun*, 7, 12617. doi:10.1038/ncomms12617
- Zhao, F., Zhao, T., Deng, L., Lv, D., Zhang, X., Pan, X., . . . Long, G. (2017). Visualizing the Essential Role of Complete Virion Assembly Machinery in Efficient Hepatitis C Virus Cell-to-Cell Transmission by a Viral Infection-Activated Split-Intein-Mediated Reporter System. *Journal of virology*, 91(2). doi:10.1128/JVI.01720-16
- Zhong, J., Gastaminza, P., Cheng, G., Kapadia, S., Kato, T., Burton, D. R., . . . Chisari, F. V. (2005). Robust hepatitis C virus infection in vitro. *Proceedings of the National Academy of Sciences of the United States of America*, 102(26), 9294-9299. doi:10.1073/pnas.0503596102
- Zhong, J., Gastaminza, P., Chung, J., Stamataki, Z., Isogawa, M., Cheng, G., . . . Chisari, F. V. (2006). Persistent hepatitis C virus infection in vitro: coevolution of virus and host. *J Virol*, 80(22), 11082-11093. doi:10.1128/JVI.01307-06
- Zhong, P., Agosto, L. M., Munro, J. B., & Mothes, W. (2013). Cell-to-cell transmission of viruses. *Curr Opin Virol*, 3(1), 44-50. doi:10.1016/j.coviro.2012.11.004
- Zhu, M., Ji, G., Jin, G., & Yuan, Z. (2009). Different responsiveness to a high-fat/cholesterol diet in two inbred mice and underlying genetic factors: a whole genome microarray analysis. *Nutr Metab (Lond)*, 6, 43. doi:10.1186/1743-7075-6-43
- Zhu, Y., Drake, M. T., & Kornfeld, S. (1999). ADP-ribosylation factor 1 dependent clathrin-coat assembly on synthetic liposomes. *Proc Natl Acad Sci U S A*, 96(9), 5013-5018.
- Zybert, I. A., van der Ende-Metselaar, H., Wilschut, J., & Smit, J. M. (2008). Functional importance of dengue virus maturation: infectious properties of immature virions. *J Gen Virol*, 89(Pt 12), 3047-3051. doi:10.1099/vir.0.2008/002535-0